Electronic Supplementary Information

Dibenzocyclooctatetraene Based Poly-Lewis-Acids: Flapping Hosts for Multidentate Guest

Maximilian J. Klingsiek,[a] Julian Buth,[a] Pia Trapp,[a] Jan-Hendrik Lamm,[a] Beate Neumann,[a] Hans-Georg Stammler,[a] and Norbert W. Mitzel[a]*

[a] Universität Bielefeld, Fakultät für Chemie, Lehrstuhl für Anorganische Chemie und Strukturchemie, Center for Molecular Materials CM_2, Universitätsstraße 25, D-33615 Bielefeld,
E-Mail: mitzel@uni-bielefeld.de; FAX: +49 521 106 6020; Tel; +495211066128.

Table of contents

General Information

1,2-Dibromo-4,5-bis(dibromomethyl)benzene (**1**),[1] dimethylaminotrimethylstannane,[2] dicyclohexylborane,[3] $[(SiMe_3)_2HC]_2AlH$ (Bis_2AlH),[4] chlorodiethylborane,[5] bis((dimethylphosphanyl)methyl)-dimethylsilane (BisPhos),[6] Bis[BisPhos] [6] di(1*H*-imidazol-1-yl)methane (N-1),[7] 1,2-di(1*H*-1,2,4-triazol-1-yl)ethane (N-2),[7] and 1,2-di(1*H*-1,2,4-triazol-1-yl)butane (N-4),[7] were synthesized according to modified literature protocols. All operations with air and moisture sensitive compounds were performed under conventional Schlenk technique or in gloveboxes under inert nitrogen or argon atmosphere. The solvents *n*-pentane, *n*-hexane (both via $LiAlH_4$), toluene (sodium), diethyl ether ($LiAlH_4$), THF (potassium), dichlormethane (CaH_2) were dried by common methods and freshly distilled before use. Column chromatography was performed on silica gel 60 (0.04−0.063 mm mesh).

NMR spectra were recorded on a BRUKER AVANCE III 500 and BRUKER AVANCE III 300. The chemical shifts (δ) were measured in ppm (parts per million) and the spectra were referenced to the residual signal of proton-containing solvents ($CDCl_3$: ^{1}H NMR, δ = 7.26 ppm, ^{13}C NMR, δ = 77.16 ppm; C_6D_6: ^{1}H NMR, δ = 7.16 ppm, ^{13}C NMR, δ = 128.06 ppm) or external standards (^{11}B: $BF_3{\cdot}Et_2O$, ^{29}Si: $SiMe_4$, ^{31}P: 85% H_3PO_4, ^{119}Sn: $SnMe_4$).

ESI accurate mass measurements are acquired using an Agilent 6220 time-of-flight mass spectrometer (Agilent Technologies, Santa Clara, CA, USA) in extended dynamic range mode equipped with a Dual-ESI source, operating with a spray voltage of 2.5 kV. Nitrogen served both as nebulizer gas and dry gas. Nitrogen was generated by a nitrogen generator NGM 11. Samples were dissolved in acetonitrile and introduced with a 1200 HPLC system consisting of an auto sampler, degasser, binary pump, column oven and diode array detector (Agilent Technologies, Santa Clara, CA, USA) using a C18 Hypersil Gold column (length: 50 mm, diameter: 2.1 mm, particle size: 1,9 µm) with a short gradient (in 4 min from 0% B to 98% B, back to 0% B in 0.2 min, total run time 7.5 min) at a flow rate of 250 µL/min and column oven temperature of 40°C. HPLC solvent A consists of 94.9% water, 5% acetonitrile and 0.1% formic acid, solvent B of 5% water, 94.9% acetonitrile and 0.1% formic acid.

Elemental analyses were performed with *HEKAtech EURO EA* instrument (too low carbon values due to the formation of silicon, boron or aluminum carbide).

The melting points were determined using the BÜCHI Melting Point B-545 device. The samples were prepared in capillaries in a glove box under an argon atmosphere, sealed and melted outside the glove box. All values determined correspond to the averaged value from a triple determination of the melting or decomposition point.

The numbering schema for NMR spectroscopic assignments is shown in Scheme S1.

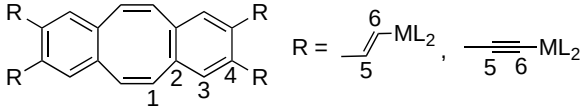

Scheme S1. Numbering scheme for NMR spectroscopic assignments

Experimental

2,3,8,9-Tetrabromodibenzo[*a*,*e*][8]annulene (2)

NaI (26.08 g, 173.7 mmol, 10.0 eq.) was placed in a two-necked Schlenk flask with reflux condenser and heated to 250 °C for 2 h in a vacuum, before DMF (120 mL) was added after cooling to rt. The mixture was stirred at 180 °C for 1.5 h so that all the NaI was dissolved before 1,2-dibromo-4,5-bis(dibromomethyl)benzene (**1**, 20.0 g, 34.6 mmol, 2.0 eq.) was added as a solid, whereby the solution abruptly turned deep black. The mixture was stirred at 180 °C for 18 h before the hot solution was poured onto an ice-water mixture (400 mL). After cooling, a saturated Na_2SO_3 solution (750 mL) was added. The resulting persimmon-colored solution was filtered and the residue was washed with KOH solution (5 N, 2 × 50 mL) and H_2O (3 × 100 mL). After column chromatographic (solvent: n-pentane) purification, 2,3,8,9-tetrabromodibenzo[a,e][8]annulene (**2**, 7.05 g, 15.5 mmol, 78%) was obtained as a yellow powder. Single yellow crystals suitable for X-ray diffraction experiments could be obtained by slow evaporation of a $CHCl_3$ solution.
^{1}H NMR (500 MHz, C_6D_6): δ = 6.93 (s, 4H, **H**^{3}), 6.03 (s, 4H, **H**^{1}) ppm. – ^{13}C{^{1}H} NMR (125 MHz, C_6D_6): δ = 137.4 (**C**^{2}), 134.0 (**C**^{3}), 132.4 (**C**^{1}), 124.0 (**C**^{4}) ppm. Elemental analysis calcd (%) for $C_{16}H_8Br_4$ (M_r = 519.86): C 36.97, H 1.55; found: C 37.53, H 1.51. – HRMS (ESI): calculated for $C_{16}H_8Br_4^+$: 515.73539; measured: 515.7363. – M.p. 278 °C.

2,3,8,9-Tetrakis((trimethylsilyl)ethynyl)dibenzo[a,e][8]annulene (3)

2,3,8,9-Tetrabromodibenzo-[a,e][8]annulene (**2**, 5.00 g, 9.6 mmol, 1.0 eq.) was placed with PPh_3 (2.02 g, 7.7 mmol, 0.8 eq.) in NEt_3 (350 mL) and degassed. $Pd(PPh_3)_2Cl_2$ (1.34 g, 1.91 mmol, 20 mol%) and CuI (0.36 g, 1.90 mmol, 20 mol%) were then added before ethynyltrimethylsilane (8.45 g, 86.0 mmol, 8.9 eq.) was added and stirred for 6 d at 100 °C. Saturated NH_4Cl solution (250 mL) was added to the dark reaction mixture and extracted with DCM (3 × 250 mL). The combined organic phases were washed with H_2O (100 mL), dried over $MgSO_4$, filtered and the solvent removed under reduced pressure. The crude product was purified by column chromatography (6 × 17 cm, solvent: *n*-pentane/DCM 20:1). 2,3,8,9-Tetrakis((trimethylsilyl)ethynyl)dibenzo[a,e][8]annulene (**3**, 2.43 g, 4.12 mmol, 43%) was isolated as an orange solid. Single colorless crystals suitable for X-ray diffraction experiments could be obtained by slow evaporation of a DCM/*n*-hexane solution.
^{1}H NMR (500 MHz, C_6D_6): δ = 7.07 (s, 4H, **H**^{3}), 6.16 (s, 4H, **H**^{1}), 0.30 (s, 9H, Si(C**H**$_3$)$_3$) ppm. – ^{1}H NMR (500 MHz, $CDCl_3$): δ = 7.13 (s, 4H, **H**^{3}), 6.65 (s, 4H, **H**^{1}), 0.23 (s, 9H, Si(C**H**$_3$)$_3$) ppm. – ^{13}C{^{1}H} NMR (125 MHz, $CDCl_3$): δ = 136.8 (**C**^{2}), 133.0 (**C**^{3}), 133.0 (**C**^{1}), 124.5 (**C**^{4}), 102.9 (**C**^{5}), 98.9 (**C**^{6}), 0.1 (Si(**C**H$_3$)$_3$) ppm. – ^{29}Si{^{1}H} NMR (99 MHz, $CDCl_3$): −17.5 ppm. Elemental analysis calcd (%) for $C_{36}H_{44}Si_4$ (M_r = 589.088): C 73.40, H 7.53; found: C 72.82, H 7.69. – HRMS (ESI): calculated for $C_{36}H_{44}Si_4Na^+$: 611.24123; measured: 611.2410. – M.p. 118 °C

2,3,8,9-Tetraethynyldibenzo[a,e][8]annulene (4)

2,3,8,9-Tetrakis((trimethylsilyl)ethynyl)dibenzo[a,e][8]annulene (**3**, 2.43 g, 4.12 mmol,1.0 eq.) was dissolved in THF (100 mL). aq. KOH solution (1 M, 100 mL) was added to the reaction mixture. After stirring at rt for 16 h than Et_2O (100 mL) was added to the resulting suspension, the phases were separated, and the aqueous phase was extracted with Et_2O (2 × 100 mL). The combined organic phases were dried over $MgSO_4$, filtered and the solvent removed under reduced pressure. The crude product was dissolved in DCM (60 mL), adsorbed on silica gel and purified by automated column chromatography (Ecoflex® Silica 25 g, solvent: *n*-pentane/DCM, 4:1). After washing the yellowish solid with MeOH (3 × 15 mL), 2,3,8,9-tetraethynyldibenzo[a,e][8]annulene (4, 1.13 g, 3.76 mmol, 90%) was isolated as a colorless solid. Single brown crystals to determine the solid state structure could be obtained by slow cooling of a concentrated boiling toluene solution.
^{1}H NMR (500 MHz, C_6D_6): δ = 6.99 (s, 4H, **H**^{3}), 6.14 (s, 4H, **H**^{1}), 2.92 (s, 4H, CC**H**) ppm. – ^{13}C{^{1}H} NMR (125 MHz, C_6D_6): δ = 137.3 (**C**^{2}), 133.8 (**C**^{3}), 133.0 (**C**^{1}), 124.4 (**C**^{4}), 82.1 (C**C**H), 81.7 (**C**CH) ppm. – Elemental analysis calcd (%) for $C_{24}H_{12}$ (M_r = 300.36): C 95.97, H 4.03; found: C 95.98, H 4.03. – HRMS (ESI): calculated for $C_{24}H_{12}^+$: 300.09335; measured: 300.0936. – M.p. 158 °C (decomposition). – Spontaneous decomposition at 150 °C under vacuum.

2,3,8,9-Tetrakis((trimethylstannyl)ethynyl)dibenzo[a,e][8]annulene (5)

2,3,8,9-Tetraethinyldibenzo[a,e]-[8]annulene (**4**, 635 mg, 2.11 mmol, 1.0 eq) was placed in a PTFE sealed tube in toluene (25 mL). Trimethylstannyldimethylamine (2.96 g, 12.3 mmol, 5.8 eq) was added to the suspension under ice bath cooling. The slightly yellow solution was stirred for 4 d at rt and then the volatile components were removed under reduced pressure. 2,3,8,9-Tetrakis((trimethylstannyl)-ethynyl)dibenzo[a,e][8]annulene (**5**, 2.00 g, 2.10 mmol, 99%) was obtained as a colorless crystalline

solid. By recrystallisation from *n*-hexane, single crystals were obtained which were suitable for X-ray diffraction experiments.
^{1}H NMR (500 MHz, C_6D_6): δ = 7.18 (s, 4H, **H**^{3}), 6.21 (s, 4H, **H**^{1}), 0.26 (s, 9H, Sn(C**H**$_3$)$_3$) ppm. – ^{13}C{^{1}H} NMR (125 MHz, C_6D_6): δ = 136.8 (**C**^{2}), 133.6 (**C**^{3}), 133.1 (**C**^{1}), 125.6 (**C**^{4}), 108.0 (C**C**H), 98.2 (**C**CH), −7.9 (Sn(**C**H$_3$)$_3$ ppm. – ^{119}Sn{^{1}H} NMR (186 MHz, C_6D_6): δ = −67.1 ppm. – Elemental analysis calcd (%) for $C_{36}H_{44}Sn_4$ (M_r = 951.588): C 45.44, H 4.66; found: C 45.44, H 4.67. – HRMS (ESI): calculated for $C_{36}H_{44}Sn_4Na^+$: 978.94229; measured: 978.9454. – M.p. 232 °C (turns dark).

[Cy$_2$BCHCH]$_4$-dbCOT (6)

2,3,8,9-Tetraethynyldibenzo[a,e][8]annulene (**4**, 47.5 mg, 158 µmol, 1.0 eq) was placed in toluene (3 mL) together with HBCy$_2$ (113 mg, 632 µmol, 4.0 eq). The reaction mixture was stirred at rt for 30 min and the solvent was removed under reduced pressure to give [Cy$_2$BCHCH]$_4$-dbCOT (**6**, 160 mg, 158 µmol, quant.) as a slightly yellowish solid. Crystals suitable for X-ray diffraction experiments were obtained from a concentrated benzene solution at room temperature.
^{1}H NMR (500 MHz, C_6D_6): δ = 7.94 (d, $^{3}J_{H,H}$ = 17.9 Hz, 4H, **H**^{5}), 7.49 (s, 4H, **H**^{3}), 6.94 (d, $^{3}J_{H,H}$ = 17.9 Hz, 4H, **H**^{6}), 6.72 (s, 4H, **H**^{1}), 1.89–1.77 (m, 24H, **H**^{Cy}), 1.77–1.68 (m, 8H, CHCHBC**H**^{Cy}), 1.68–1.57 (m, 16H, **H**^{Cy}), 1.50–1.22 (m, 40H, **H**^{Cy}) ppm. – ^{11}B{^{1}H} NMR (160 MHz, C_6D_6): δ = 77.8 ppm. – ^{13}C{^{1}H} NMR (125 MHz, C_6D_6): δ = 145.8 (**C**^{5}), 138.2 (**C**^{2}), 136.9 (**C**^{4}), 135.3 (**C**^{6}), 133.8 (**C**^{1}), 128.6 (**C**^{3}), 35.2 (B**C**^{Cy}), 28.1 (**C**^{Cy}), 28.0 (**C**^{Cy}), 27.4 (**C**^{Cy}) ppm. – Elemental analysis calcd (%) for $C_{72}H_{104}B_4$ (M_r = 1012.284): C 85.38, H 10.35; found: C 83.58, H 10.36. – Mp. 215 °C (turns dark).

[Bis$_2$AlCHCH]$_4$-dbCOT (7)

2,3,8,9-Tetraethynyldibenzo[a,e][8]annulene (**4**, 15.6 mg, 51.9 µmol, 1.0 eq) was placed in benzene (1 mL) together with HAlBis$_2$ (72.0 mg, 208 µmol, 4.0 eq). The reaction mixture was stirred at 50 °C for 2 h and the solvent was removed under reduced pressure to give [Bis$_2$AlCHCH]$_4$-dbCOT (**7**, 87.6 mg, 51.9 µmol, quant.) as a slightly yellowish solid.
^{1}H NMR (500 MHz, C_6D_6): δ = 7.77 (d, $^{3}J_{H,H}$ = 20.2 Hz, 4H, **H**^{5}), 7.45 (s, 4H, **H**^{3}), 6.84 (d, $^{3}J_{H,H}$ = 20.3 Hz, 4H, **H**^{6}), 6.63 (s, 4H, **H**^{1}), 0.28 (s, 144H, Si(C**H**$_3$)$_3$), −0.21 (s, 8H, AlC**H**) ppm. – ^{13}C{^{1}H} NMR (125 MHz, C_6D_6): δ = 147.2 (**C**^{5}), 141.5 (**C**^{6}), 137.7 (**C**$^{2/4}$), 137.6 (**C**$^{2/4}$), 133.6 (**C**^{1}), 127.7 (**C**^{3}), 10.5 (Al**C**H), 4.5 (Si**C**H$_3$) ppm. – ^{29}Si{^{1}H} NMR (99 MHz, C_6D_6): δ = −3.6 ppm. – Elemental analysis calcd (%) for $C_{80}H_{168}Al_4Si_{16}$ (M_r = 1687.510): C 56.94, H 10.04; found: C 56.94, H 9.64. – M.p. 266 °C (slightly yellowish).

[Et$_2$BCC]$_4$-dbCOT (8)

2,3,8,9-Tetrakis((trimethylstannyl)ethynyl)dibenzo[a,e][8]annulene (**5**, 50.0 mg, 52.5 µmol, 1.0 eq.) was dissolved in benzene and a solution of diethylchloroborane in DCM (Et$_2$BCl/DCM 1:2 mol ratio, 60 mg, 0.22 mmol, 4.2 eq.) was added with stirring and the solution immediately turned an intense yellow color. The mixture was stirred for 3 h at rt. The resulting, amber-colored solution contained few particles of an insoluble solid. After filtration and removal of all volatile components in vacuum at 80 °C, [Et$_2$BCC]4-dbCOT (**8**, 28.8 mg, 50.4 µmol, 96%) was obtained as a brownish solid.
^{1}H NMR (500 MHz, C_6D_6): δ = 7.17 (s, 4H, **H**^{3}), 6.24 (s, 4H, **H**^{1}), 1.38–1.28 (m, 16H, BC**H**$_2$), 1.25–1.17 (m, 24H, BCH$_2$C**H**$_3$) ppm. – ^{11}B{^{1}H} NMR (160 MHz, C_6D_6): 74.6 ppm. – ^{13}C{^{1}H} NMR (125 MHz, C_6D_6): δ = 137.9 (**C**^{2}), 133.7 (**C**^{4}), 133.2 (**C**^{1}), 124.9 (**C**^{3}), 118.9 (**C**^{5}), 21.9 (B**C**H$_2$), 9.6 (BCH$_2$**C**H$_3$) ppm, No signal for **C**^{6} was observed. – Elemental analysis calcd (%) for $C_{72}H_{104}B_4$ (M_r = 572.04): C 83.98, H 8.46; found: C 82.73, H 7.72. – M.p. 128 °C (decomposition).

[Bis$_2$AlCC]$_4$-dbCOT (9)

2,3,8,9-Tetrakis((trimethylstannyl)ethynyl)dibenzo[a,e][8]annulene (**5**, 45.0 mg, 43.2 µmol, 1.0 eq) was placed in benzene (0.5 mL) together with HAlBis$_2$ (62 mg, 173 µmol, 4.0 eq). The reaction mixture was stirred at 50 °C for 2 h and the solvent as well as HSnMe$_3$ was removed under reduced pressure to give [Bis$_2$AlCC]$_4$-dbCOT (**9**, 68.2 mg, 43.0 µmol, 99%) as a slightly yellowish solid.
^{1}H NMR (500 MHz, C_6D_6): δ = 7.28 (s, 4H, **H**^{3}), 6.26 (s, 4H, **H**^{1}), 0.35 (s, 144H, SiC**H**$_3$), −0.33 (s, 8H, AlC**H**) ppm. – ^{13}C{^{1}H} NMR (125 MHz, C_6D_6): δ = 136.8 (**C**^{2}), 134.3 (**C**^{1}), 132.7 (**C**^{4}), 124.1 (**C**^{3}), 110.6 (**C**^{6}), 108.1 (**C**^{5}), 10.9 (Al**C**H), 4.0 (Si**C**H$_3$) ppm. – ^{29}Si{^{1}H} NMR (99 MHz, C_6D_6): δ = −3.1 ppm. – Elemental analysis calcd (%) for $C_{80}H_{166}Al_4Si_{16}$ (M_r = 1679.45): C 56.94, H 9.62; found: C 58.16, H 8.80. – M.p. 217 °C (turns dark).

Other tin element exchange reactions investigated

Analogous to the tin element exchange reactions described above, the exchange with other Lewis acidic units was also investigated (Table S1). However, apart from the exchange with $ClSb(C_2F_5)_2$, these exchange reactions either did not occur at all or were less selective, so that the use of these PLAs for further investigation was not pursued further. $[(C_2F_5)_2SbCC]_4$-dbCOT was isolated on a large scale (200 mg) but showed very little interaction with the tested bases in the initial reactivity studies and was therefore also not investigated on a large scale.

Table S1. All tested tin element exchange reactions including conditions and resulting conclusions.

XML_2	Temperature / °C	solvent	conclusion
$ClBPh_2$	25	C_6H_6	insoluble solid
$ClBPh_2$	25	$CHCl_3$	insoluble solid
$ClBCy_2$	25	C_6H_6	Conversion complete + a lot of non-removable decomposition product
$ClBCy_2$	−15	C_6H_6	Conversion complete + a lot of non-removable decomposition product
$ClBBis_2$	25	C_6H_6	no conversion
$ClBBis_2$	60	C_6H_6	no conversion
ClBCat	25	C_6H_6	insoluble solid
ClBCat	25	$CHCl_3$	insoluble solid
HAl^tBu	25	C_6H_6	insoluble solid
$ClGa^tBu_2$	25	C_6H_6	incomplete reaction
$BrGaBis_2$	25	C_6H_6	incomplete reaction
$ClIn^tBu_2$	25 to 70	C_6H_6	no conversion
$ClIn^tBu_2$	25 to 70	$CHCl_3$	no conversion
$ClSb(C_2F_5)_2$	25	toluene	complete exchange

General procedure for NMR experiments to explore the complexation behavior of PLAs

For the complexation experiments, the respective PLAs were dissolved in C_6D_6 and combined with different equivalents of the corresponding bases. The solutions obtained were analyzed by NMR spectroscopy immediately after addition. If the adduct formation resulted in an insoluble solid, the solvent was removed and the solid dissolved in THF-d_8. After complete characterization of the adducts by NMR spectroscopy, the solutions were stored at rt for crystallization and successively concentrated or *n*-hexane was added as required. For some adducts, the solvent was also completely exchanged for *n*-hexane, $CHCl_3$ or *o*-difluorobenzene in order to obtain single crystals for the subsequent X-ray diffraction experiments.

The results of the complexation tests are summarized in Table S2. The color code used provides an indication of the strength of the interaction between the respective base and the PLA compared to the other PLAs. Yellow stands for a very weak interaction, so that it was experimentally possible to remove the base again in a vacuum if it was volatile. Orange stands for an interaction that is moderately strong, so the bases cannot be removed in a vacuum, but it is also not possible to distinguish between free and bound base using NMR spectroscopic investigations at room temperature in solution if an excess of base is used. Instead, the base signals average out due to the rapid exchange in solution. Red thus stands for a strong interaction which makes it possible to distinguish between the free and completed base molecules in solution at room temperature, since no or only a very slow exchange takes place.

Table S2. Results of the complexation experiments.

LB	BCy$_2$ **6**	AlBis$_2$ **7**	BEt$_2$ **8**	AlBis$_2$ **9**
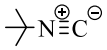 ^{t}BuNC	decomposition	1:4-Ad.	1:4-Ad.	1:4-Ad.
 Pyridin	1:4-Ad.	1:4-Ad.	1:4-Ad.	1:4-Ad.
 NMe$_3$	no interaction	1:4-Ad.	1:4-Ad.	1:4-Ad.
 PMe$_3$	1:4-Ad.	1:4-Ad.	1:4-Ad.	1:4-Ad.
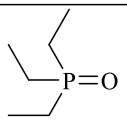 Et$_3$PO	1:4-Ad.	1:4-Ad.	1:4-Ad.	1:4-Ad.
 THF	no interaction	1:4-Ad.	1:4-Ad.	1:4-Ad.
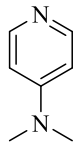 DMAP	1:4-Ad.	1:4-Ad.	1:4-Ad.	1:4-Ad.
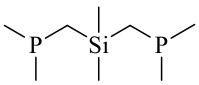 BisPhos	1:2-Ad.	weak interaction	1:2-Ad.	1:2-Ad.
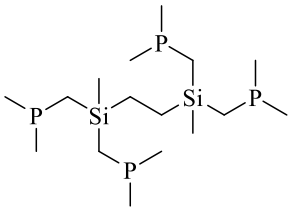 Bis[BisPhos]	non-selective	no interaction	non-selective	1:2-Ad.-Polymer
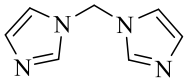 Bisimidazolylmethane (N-1)	non-selective	1:2-Ad.	non-selective	1:2-Ad.
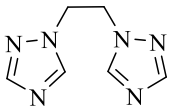 Bistriazolylethane (N-2)	non-selective	1:2-Ad.	1:2-Ad.	1:2-Ad.

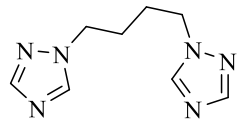 Bistriazolylbutan (N-4)	non-selective	1:2-Ad.	non-selective	1:2-Ad.-Polymer
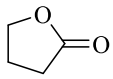 GBL	untested	no interaction	decomposition	1:4-Ad.
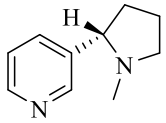 L-Nicotine (Nico)	untested	1:4-Ad.	non-selective	1:4-Ad.
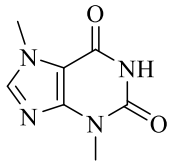 Theobromine (Theo)	no interaction	decomposition	no interaction	decomposition
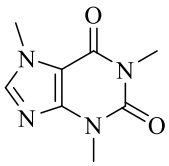 Caffein (Caff)	no interaction	1:2-Ad.	1:2-Ad.	1:2-Ad.

7·4^{t}BuNC:

^{1}H NMR (500 MHz, C_6D_6): δ = 7.65 (d, $^{3}J_{H,H}$ = 20.0 Hz, 4H, **H**^{5}), 7.52 (s, 4H, **H**^{3}), 7.01 (d, $^{3}J_{H,H}$ = 19.9 Hz, 4H, **H**^{6}), 6.70 (s, 4H, **H**^{1}), 0.96 (s, 36H, ^{t}**Bu**NC), 0.42 (s, 144H, Si(C**H**$_3$)$_3$), −0.79 (s, 8H, AlC**H**) ppm. – ^{13}C{^{1}H} NMR (125 MHz, C_6D_6): δ = 146.0 (**C**^{5}), 142.6 (**C**^{6}), 138.5 (**C**^{2}), 136.3 (**C**^{4}), 133.5 (C^{1}), 28.9 (^{t}**Bu**NC), 5.1 (Si**C**H$_3$), −0.3 (Al**C**H) ppm, no signal for ^{t}BuN**C** and **C**^{3} was observed. – ^{29}Si{^{1}H} NMR (99 MHz, C_6D_6): δ = −1.6 ppm.

8·4 ^{t}BuNC:

^{1}H NMR (500 MHz, C_6D_6): δ = 7.32 (s, 4H, **H**^{3}), 6.30 (s, 4H, **H**^{1}), 1.63–1.37 (m, 24H, CH$_2$C**H**$_3$), 1.29–1.10 (m, 16H, BC**H**$_2$), 0.78 (s, 36H, ^{t}**Bu**NC) ppm. – ^{11}B{^{1}H} NMR (160 MHz, C_6D_6): δ = −18.9 ppm. No interpretable ^{13}C{^{1}H} NMR spectrum could be obtained.

9·4 ^{t}BuNC:

^{1}H NMR (500 MHz, C_6D_6): δ = 7.37 (s, 4H, **H**^{3}), 6.47 (s, 4H, **H**^{1}), 0.97 (s, 36H, ^{t}**Bu**NC), 0.48 (s, 144H, Si(C**H**$_3$)$_3$), −0.88 (s, 8H, AlC**H**) ppm. – ^{13}C{^{1}H} NMR (125 MHz, C_6D_6): δ = 135.7 (**C**^{2}), 135.6 (**C**^{1}), 133.1 (**C**^{4}), 126.0 (**C**^{3}), 114.7 (**C**^{6}), 108.9 (**C**^{5}), 29.0 (^{t}**Bu**NC), 4.8 (Si**C**H$_3$), −0.1 (Al**C**H) ppm. – ^{29}Si{^{1}H} NMR (99 MHz, C_6D_6): δ = −1.3 ppm.

6·4Py:

^{1}H NMR (500 MHz, C_6D_6): δ = 8.51–8.14 (m, 8H, Py–**H**^{o}), 7.67 (s, 4H, **H**^{3}), 7.33 (d, $^{3}J_{H,H}$ = 18.1 Hz, 4H, **H**^{6}), 6.95 (s, 4H, **H**^{1}), 6.93–6.75 (m, 4H, Py–**H**^{p}), 6.72–6.43 (m, 12H, Py–**H**^{m}, **H**^{5}), 2.20–1.45 (m, 48H, **H**^{Cy}), 1.42–1.07 (m, 16H, **H**^{Cy}), 1.08–0.49 (m, 12H, **H**^{Cy}) ppm. – ^{11}B{^{1}H} NMR (160 MHz, C_6D_6): 0.8 ppm. No interpretable ^{13}C{^{1}H} NMR spectrum could be obtained.

7·4Py:

^{1}H NMR (500 MHz, C_6D_6): δ = 8.74–8.69 (m, 8H, Py–**H**^{o}), 7.69 (s, 4H, **H**^{3}), 7.55 (d, $^{3}J_{H,H}$ = 20.1 Hz, 4H, **H**^{6}), 7.21 (d, $^{3}J_{H,H}$ = 20.1 Hz, 4H, **H**^{5}), 6.96–6.90 (m, 4H, Py–**H**^{p}), 6.83 (s, 4H, **H**^{1}), 6.70–6.65 (m, 8H, Py–**H**^{m}), 0.32 (s, 72H, SiC**H**$_3$), 0.13 (s, 72H, SiC**H**$_3$), −0.70 (s, 8H, AlC**H**) ppm – ^{13}C{^{1}H} NMR (125 MHz, C_6D_6): δ = 149.2 (Py–**C**^{o}), 146.8 (**C**^{5}), 142.0 (**C**^{6}), 141.2 (Py–**C**^{p}), 138.1 (**C**^{2}), 136.6 (**C**^{4}), 133.7 (**C**^{1}), 125.2 (Py–**C**^{m}), 5.5 (Si**C**H$_3$), 5.3 (Si**C**H$_3$), 0.6 (Al**C**H) ppm – ^{29}Si{^{1}H} NMR (99 MHz, C_6D_6): δ = −1.8, −2.2 ppm.

8·4Py:

^{1}H NMR (500 MHz, C_6D_6): δ = 8.83–8.78 (m, 8H, Py–**H**^{o}), 7.50 (s, 4H, **H**^{3}), 6.72–6.64 (m, 4H, Py–**H**^{p}), 6.52 (t, $^{3}J_{H,H}$ = 6.9 Hz, 8H, Py–**H**^{m}), 6.43 (s, 4H, **H**^{1}), 1.28–1.13 (m, 32H, BC**H**$_2$C**H**$_3$), 0.96–0.87 (m, 8H, BC**H**$_2$C**H**$_3$) ppm. – ^{11}B{^{1}H} NMR (160 MHz, C_6D_6): δ = −0.7 ppm – ^{13}C{^{1}H} NMR (125 MHz, C_6D_6): δ = 145.6 (Py–**C**^{o}), 138.7 (**C**^{2}), 135.8 (**C**^{4}), 133.8 (**C**^{3}), 133.2 (**C**^{1}), 127.4 (Py–**C**^{p}), 124.7 (Py–**C**^{m}), 100.1 (**C**^{5}), 19.3 (B**C**H$_2$CH$_3$), 11.4 (BCH$_2$**C**H$_3$) ppm, no signal for **C**^{6} was observed.

9·4Py:

^{1}H NMR (500 MHz, C_6D_6): δ = 9.15–8.97 (m, 8H, Py–**H**^{o}), 7.51 (s, 4H, **H**^{3}), 6.96–6.91 (m, 4H, Py–**H**^{p}), 6.76–6.70 (m, 8H, Py–**H**^{m}), 6.52 (s, 4H, **H**^{1}), 0.44 (s, 72H, SiC**H**$_3$), 0.18 (s, 72H, SiC**H**$_3$), −0.74 (s, 8H, AlC**H**) ppm. – ^{13}C{^{1}H} NMR (125 MHz, C_6D_6): δ = 149.4 (Py–**C**^{o}), 141.2 (Py–**C**^{p}), 136.3 (**C**^{2}), 135.5 (**C**^{3}), 133.2 (**C**^{1}), 125.7 (**C**^{4}), 125.2 (Py–**C**^{m}),115.4 (**C**^{6}), 110.3 (**C**^{5}), 5.2 (Si**C**H$_3$), 5.1 (Si**C**H$_3$), 1.1 (Al**C**H) ppm. – ^{29}Si{^{1}H} NMR (99 MHz, C_6D_6): δ = −1.3, −2.0 ppm.

7·4NMe$_3$:

^{1}H NMR (500 MHz, C_6D_6): δ = 7.75 (d, $^{3}J_{H,H}$ = 20.2 Hz, 4H, **H**^{6}), 7.46 (s, 4H, **H**^{3}), 6.85 (d, $^{3}J_{H,H}$ = 20.2 Hz, 4H, **H**^{5}), 6.67 (s, 4H, **H**^{1}), 2.04 (s, 36H, N(C**H**$_3$)$_3$), 0.30 (s, 144H, SiC**H**$_3$), −0.32 (s, 8H, AlC**H**) ppm. – ^{13}C{^{1}H} NMR (125 MHz, C_6D_6): δ = 147.2 (**C**^{5}), 141.6 (**C**^{6}), 137.7 (**C**^{2}), 137.6 (**C**^{4}), 133.6 (**C**^{1}), 48.3 (N(**C**H$_3$)$_3$), 10.4 (Al**C**H), 4.5 (Si**C**H$_3$) ppm, no signal for **C**^{3} was observed. – ^{29}Si{^{1}H} NMR (99 MHz, C_6D_6): δ = −3.6 ppm.

8·4NMe_3:

^{1}H NMR (500 MHz, C_6D_6): δ = 7.37 (s, 4H, **H**^{3}), 6.43 (s, 4H, **H**^{1}), 2.01 (s, 36H, N(C**H**$_3$)$_3$), 1.39 (t, $^3J_{H,H}$ = 7.7 Hz, 25H, BCH$_2$C**H**$_3$), 0.64 (q, $^3J_{H,H}$ = 7.7 Hz, 16H, BC**H**$_2$) ppm – ^{11}B{^{1}H} NMR (160 MHz, C_6D_6): δ = −0.3 ppm. – ^{13}C{^{1}H} NMR (125 MHz, C_6D_6): δ = 135.5 (**C**^{2}), 133.9 (**C**^{4}), 133.1 (**C**^{1}), 127.2 (**C**^{3}), 98.8 (**C**^{5}), 49.0 (N(**C**H$_3$)$_3$), 47.8 (free N(**C**H$_3$)$_3$), 12.8 (BCH$_2$**C**H$_3$), −1.2 (B**C**H$_2$) ppm. No signal for **C**^{6} was observed.

9·4NMe_3:

^{1}H NMR (500 MHz, C_6D_6): δ = 7.40 (s, 4H, **H**^{3}), 6.54 (s, 4H, **H**^{1}), 2.20 (s, 36H, N(C**H**$_3$)$_3$), 0.43 (s, 144H, SiC**H**$_3$), −1.17 (s, 8H, AlC**H**) ppm. No interpretable ^{13}C{^{1}H} NMR spectrum could be obtained. – The ^{29}Si{^{1}H} NMR experiment showed no signals.

6·4PMe_3:

^{1}H NMR (500 MHz, C_6D_6): δ = 7.50 (s, 4H, **H**^{3}), 7.11 (d, $^3J_{H,H}$ = 18.0 Hz, 4H, **H**^{6}), 6.79 (s, 4H, **H**^{1}), 6.40 (d, $^3J_{H,H}$ = 17.9 Hz, 4H, **H**^{5}), 2.07–1.74 (m, 40H, **H**^{Cy}), 1.59–1.32 (m, 40H, **H**^{Cy}), 1.00–0.88 (m, 8H, **H**^{Cy}), 0.68 (d, $^2J_{P,H}$ = 7.6 Hz, 36H, P(C**H**$_3$)$_3$) ppm. – ^{11}B{^{1}H} NMR (160 MHz, C_6D_6): δ = −11.4 ppm. – ^{13}C{^{1}H} NMR (125 MHz, C_6D_6): δ = 144.2 (**C**^{5}), 137.6 (**C**^{2}), 135.8 (**C**^{4}), 133.7 (**C**^{6}), 133.1 (**C**^{1}), 126.9 (**C**^{3}), 33.0 (**C**^{Cy}), 32.1 (B**C**^{Cy}), 30.2 (**C**^{Cy}), 28.4 (**C**^{Cy}), 12.0 (d, $^1J_{P,C}$ = 20.2 Hz, P(**C**H$_3$)$_3$) ppm. – ^{31}P{^{1}H} NMR (202 MHz, C_6D_6) δ = −19.5 ppm.

7·4PMe_3:

^{1}H NMR (500 MHz, C_6D_6): δ = 7.72 (d, $^3J_{H,H}$ = 20.1 Hz, 4H, **H**^{6}), 7.47 (s, 4H, **H**^{3}), 6.87 (d, $^3J_{H,H}$ = 20.1 Hz, 4H, **H**^{5}), 6.68 (s, 4H, **H**^{1}), 0.80 (d, $^2J_{P,H}$ = 2.0 Hz, 36H, P(C**H**$_3$)$_3$), 0.31 (s, 144H, SiC**H**$_3$), −0.38 (s, 8H, AlC**H**) ppm. – ^{13}C{^{1}H} NMR (125 MHz, C_6D_6): δ = 146.9 (**C**^{5}), 141.9 (**C**^{6}), 137.7 (**C**^{2}), 137.7 (**C**^{4}), 133.6 (**C**^{1}), 9.9 (Al**C**H), 4.6 (Si**C**H$_3$) ppm, no signal for **C**^{3} and P(**C**H$_3$)$_3$ was observed. – ^{29}Si{^{1}H} NMR (99 MHz, C_6D_6): δ = −3.5 ppm. – ^{31}P{^{1}H} NMR (202 MHz, C_6D_6) δ = −57.5 ppm.

8·4PMe_3:

^{1}H NMR (500 MHz, C_6D_6): δ = 7.32 (s, 4H, **H**^{3}), 6.43 (s, 4H, **H**^{1}), 1.38–1.31 (m, 24H, CH$_2$C**H**$_3$), 0.81–0.76 (m, 52H, P(C**H**$_3$)$_3$ + BC**H**$_2$) – ^{11}B{^{1}H} NMR (160 MHz, C_6D_6): δ = −17.6 ppm. – ^{13}C{^{1}H} NMR (125 MHz, C_6D_6): δ = 135.3 (**C**^{2}), 134.0 (d, $^4J_{P,C}$ = 4.0 Hz, **C**^{4}), 133.1 (**C**^{1}), 127.3 (**C**^{3}), 98.25 (d, $^3J_{P,C}$ = 8.6 Hz, **C**^{5}), 12.5 (d, $^3J_{P,C}$ = 11.6 Hz, CH$_2$**C**H$_3$), 11.9 (br s, B**C**H$_2$), 8.3 (d, $^1J_{P,C}$ = 31.9 Hz, P(**C**H$_3$)$_3$) ppm, no signal for **C**^{6} was observed. – ^{31}P{^{1}H} NMR (202 MHz, C_6D_6) δ = −10.5 ppm.

9·4PMe_3:

^{1}H NMR (500 MHz, C_6D_6): δ = 7.43 (s, 4H, **H**^{3}), 6.53 (s, 4H, **H**^{1}), 1.02 (d, $^2J_{P,H}$ = 6.2 Hz, 36H, P(C**H**$_3$)$_3$), 0.40 (s, 144H, SiC**H**$_3$), −0.91 (s, 8H, AlC**H**) ppm. – ^{13}C{^{1}H} NMR (125 MHz, C_6D_6): δ = 136.4 (**C**^{2}), 135.8 (**C**^{3}), 133.1 (**C**^{1}), 124.9 (**C**^{4}), 12.76 (d, $^1J_{P,C}$ = 15.6 Hz, P(**C**H$_3$)$_3$), 5.15 (Si**C**H$_3$) ppm, no signal for Al**C**H(SiMe$_3$)$_2$ and **C**$^{5/6}$ was observed. – ^{29}Si{^{1}H} NMR (99 MHz, C_6D_6): δ = −1.6 ppm –^{31}P{^{1}H} NMR (202 MHz, C_6D_6) δ = −51.1 ppm.

6·4$OPEt_3$:

^{1}H NMR (500 MHz, C_6D_6): δ = 7.80 (d, $^3J_{H,H}$ = 17.9 Hz, 4H, **H**^{6}), 7.52 (s, 4H, **H**^{3}), 6.90 (d, $^3J_{H,H}$ = 17.9 Hz, 4H, **H**^{5}), 6.73 (s, 4H, **H**^{1}), 1.95–1.70 (m, 44H, **H**^{Cy}), 1.61–1.29 (m, 44H, **H**^{Cy}), 1.16 (dq, $^2J_{P,H}$ = 11.7 Hz, $^3J_{H,H}$ = 7.7 Hz, 24H, PC**H**$_2$), 0.80 (dt, $^3J_{P,H}$ = 15.6 Hz, $^3J_{H,H}$ = 7.7 Hz, 36H, PCH$_2$C**H**$_3$) ppm. – ^{11}B{^{1}H} NMR (160 MHz, C_6D_6): δ = 70.0–48.1 ppm. – ^{13}C{^{1}H} NMR (125 MHz, C_6D_6): δ = 142.4 (**C**^{5}), 138.7 (**C**^{6}), 137.5 (**C**^{2}), 137.4 (**C**^{1}), 133.8 (**C**^{4}), 115.9 (**C**^{3}), 34.8 (**C**^{Cy}), 29.0 (**C**^{Cy}), 28.5 (**C**^{Cy}), 27.8 (**C**^{Cy}), 19.9 (d, $^1J_{P,C}$ = 65.9 Hz, P**C**), 5.9 (d, $^2J_{P,C}$ = 4.9 Hz, PCH$_2$**C**) ppm. – ^{31}P{^{1}H} NMR (202 MHz, C_6D_6) δ = 29.7 ppm.

7·4OPEt$_3$:

^{1}H NMR (500 MHz, C_6D_6): δ = 7.66 (s, 4H, **H**^{3}), 7.61 (d, $^3J_{H,H}$ = 20.0 Hz, 4H, **H**^{6}), 7.19 (d, $^3J_{H,H}$ = 20.1 Hz, 4H, **H**^{5}), 6.89 (s, 4H, **H**^{1}), 1.45 (dq, $^2J_{P,H}$ = 13.0, $^3J_{H,H}$ = 7.7 Hz, 24H, PC**H**$_2$), 0.67 (dt, $^3J_{P,H}$ = 18.1, $^3J_{H,H}$ = 7.7 Hz, 9H, PCH$_2$C**H**$_3$), 0.52 (s, 72H, SiC**H**$_3$), 0.48 (s, 72H, SiC**H**$_3$), −0.85 (s, 8H, AlC**H**) ppm. – ^{13}C{^{1}H} NMR (125 MHz, C_6D_6): δ = 152.6 (**C**^{5}), 138.7 (**C**^{6}), 138.4 (**C**^{2}), 135.9 (**C**^{4}), 133.6 (**C**^{1}),18.9 (d, $^1J_{P,C}$ = 66.5 Hz, P**C**), 6.0 (Si**C**H$_3$), 6.0 (Si**C**H$_3$), 5.1 (d, $^2J_{P,C}$ = 4.9 Hz, PCH$_2$**C**), 2.6 (Al**C**H) ppm. – ^{29}Si{^{1}H} NMR (99 MHz, C_6D_6): δ = −2.0, −2.1 ppm – ^{31}P{^{1}H} NMR (202 MHz, C_6D_6) δ = 70.3 ppm.

8·4OPEt$_3$:

^{1}H NMR (500 MHz, C_6D_6): δ = 7.38 (s, 4H, **H**^{3}), 6.49 (s, 4H, **H**^{1}), 1.55–1.43 (m, 48H, PC**H**$_2$ + BCH$_2$C**H**$_3$), 1.09 (p, $^3J_{H,H}$ = 8.4 Hz, 16H, BC**H**$_2$), 0.73 (dt, $^2J_{P,H}$ = 17.3, $^3J_{H,H}$ = 7.7 Hz, 36H, PCH$_2$C**H**$_3$) ppm. – ^{11}B{^{1}H} NMR (160 MHz, C_6D_6): δ = 8.3 ppm. – ^{13}C{^{1}H} NMR (125 MHz, C_6D_6): δ = 135.7 (**C**^{2}), 134.2 (**C**^{4}), 133.2 (**C**^{1}), 127.4 (**C**^{3}), 17.9 (d, $^1J_{P,C}$ = 66.2 Hz, P**C**), 11.3 (BCH$_2$**C**H$_3$), 5.6 (d, $^2J_{P,C}$ = 4.6 Hz, PCH$_2$**C**) ppm, no signal for **C**$^{5/6}$ was observed. – ^{31}P{^{1}H} NMR (202 MHz, C_6D_6) δ = 68.3 ppm.

9·4OPEt$_3$:

^{1}H NMR (500 MHz, C_6D_6): δ = 7.55 (s, 4H, **H**^{3}), 6.61 (s, 4H, **H**^{1}), 1.67 (dq, $^2J_{P,H}$ = 15.3, $^3J_{H,H}$ = 7.9 Hz, 24H, PC**H**$_2$), 0.76 (dt, $^3J_{P,H}$ = 18.3, 7.7 Hz, 36H, PCH$_2$C**H**$_3$), 0.56 (s, 72H, SiC**H**$_3$), 0.51 (s, 72H, SiC**H**$_3$), −0.94 (s, 8H, AlC**H**) ppm. – ^{13}C{^{1}H} NMR (125 MHz, C_6D_6): δ = 136.4 (**C**^{2}), 135.7 (**C**^{3}), 133.0 (**C**^{1}), 125.8 (**C**^{4}), 106.9 (**C**^{5}), 18.6 (d, $^1J_{P,C}$ = 66.2 Hz, P**C**), 6.1 (d, $^2J_{P,C}$ = 4.2 Hz, PCH$_2$**C**), 5.8 (Si**C**H$_3$), 5.7 (Si**C**H$_3$), 2.9 (Al**C**H) ppm, no signals for B–**C**'s was observed. – ^{29}Si{^{1}H} NMR (99 MHz, C_6D_6): δ = −1.7, −1.9 ppm. – ^{31}P{^{1}H} NMR (202 MHz, C_6D_6) δ = 72.7 ppm.

7·4THF:

^{1}H NMR (500 MHz, C_6D_6): δ = 7.59 (d, $^3J_{H,H}$ = 20.5 Hz, 4H, **H**^{6}), 7.56 (s, 4H, **H**^{3}), 6.91–6.82 (m, 8H, **H**$^{5/1}$), 3.84 (br s, 16H, THF), 1.38 (br s, 16H, THF), 0.33 (s, 144H, Si(C**H**$_3$)$_3$), –0.85 (s, 8H, AlC**H**) ppm. – ^{13}C{^{1}H} NMR (125 MHz, C_6D_6): δ = 146.3 (**C**^{5}), 141.7 (**C**^{6}), 138.2 (**C**^{2}), 136.5 (**C**^{4}), 133.7 (**C**^{1}), 71.1 (THF), 25.3 (THF), 5.5 (Si**C**H$_3$), 2.1 (Al**C**H) ppm. – ^{29}Si{^{1}H} NMR (99 MHz, C_6D_6): δ = −2.3 ppm.

8·4THF:

^{1}H NMR (500 MHz, C_6D_6): δ = 7.10 (s, 4H, **H**^{3}), 6.64 (s, 4H, **H**^{3}), 3.92–3.38 (m, 4H, THF), 1.75 (br s, 4H, THF), 0.86 (t, $^3J_{H,H}$ = 7.7 Hz, 24H, BCH$_2$C**H**$_3$), 0.54 (q, $^3J_{H,H}$ = 7.7 Hz, 16H, BC**H**$_2$) ppm. – ^{11}B{^{1}H} NMR (160 MHz, C_6D_6): δ = 69.7 ppm. – ^{13}C{^{1}H} NMR (125 MHz, C_6D_6): 137.8 (**C**^{2}), 133.7 (**C**^{4}), 133.2 (**C**^{1}), 124.9 (**C**^{3}), 118.6 (**C**^{5}), 69.6 (THF), 25.2 (THF), 21.8 (B**C**H$_2$CH$_3$), 9.7 (BCH$_2$**C**H$_3$) ppm, no signal for **C**^{6} was observed.

9·4THF:

^{1}H NMR (500 MHz, C_6D_6): δ = 7.37 (s, 4H, **H**^{3}), 6.52 (s, 4H, **H**^{1}), 4.12 (s, 16H, THF), 1.42 (s, 16H, THF), 0.46 (s, 72H, Si(C**H**$_3$)$_3$), 0.32 (s, 72H, Si(C**H**$_3$)$_3$), −0.99 (s, 8H, Al**C**H) ppm. – ^{13}C{^{1}H} NMR (125 MHz, C_6D_6): δ = 136.1 (**C**^{2}), 135.7 (**C**^{3}), 133.2 (**C**^{1}), 125.3 (**C**^{4}), 109.5 (**C**^{5}), 73.2 (THF), 25.2 (THF), 5.2 (Si**C**H$_3$), 1.8 (Al**C**H) ppm, no signal for **C**^{6} was observed. – ^{29}Si{^{1}H} NMR (99 MHz, C_6D_6): δ = −1.6, −2.0 ppm.

[**6**·2BisPhos]$_2$:

^{1}H NMR (500 MHz, C_6D_6): δ = 7.56 (s, 4H, **H**^{3}), 7.37 (d, $^3J_{H,H}$ = 18.0 Hz, 4H, **H**^{6}), 6.86 (s, 4H, **H**^{1}), 6.58 (d, $^3J_{H,H}$ = 17.6 Hz, 4H, **H**^{5}), 2.17–1.82 (m, 44H, **H**^{Cy}), 1.59–1.48 (m, 36H, **H**^{Cy}), 1.22–1.09 (m, 8H, **H**^{Cy}), 0.92 (d, $^2J_{P,H}$ = 10.4 Hz, 24H, PC**H**$_3$), 0.64 (d, $^2J_{P,H}$ = 10.4 Hz, 8H, SiC**H**$_2$P), −0.13 (s, 12H, SiC**H**$_3$) ppm – ^{11}B{^{1}H} NMR (160 MHz, C_6D_6): δ = −6.5 (br s) ppm. – ^{13}C{^{1}H} NMR (125 MHz, C_6D_6): δ = 143.5 (**C**^{5}), 137.2 (**C**^{2}), 136.4 (**C**^{1}), 135.2 (**C**^{6}), 133.7 (**C**^{4}), 126.5 (**C**^{3}), 32.8 (**C**^{Cy}), 32.5 (**C**^{Cy}), 30.0 (**C**^{Cy}), 28.5 (d, $^1J_{P,C}$ = 22.1 Hz, Si**C**P), 28.3 (**C**^{Cy}), 12.08 (d, $^1J_{P,C}$ = 22.1 Hz, P**C**H$_3$), 1.5 (Si**C**H$_3$) ppm. – ^{29}Si{^{1}H} NMR (99 MHz, C_6D_6): δ = 1.9 (t, $^2J_{Si,P}$ = 11.0 Hz) ppm. – ^{31}P{^{1}H} NMR (202 MHz, C_6D_6) δ = −9.9 ppm.

8·2BisPhos:

^{1}H NMR (500 MHz, C_6D_6): δ = 7.31 (s, 4H, **H**^{3}), 6.28 (s, 4H, **H**^{1}), 1.41 (q, $^{3}J_{H,H}$ = 7.5 Hz, 24H, $BCH_2C\mathbf{H}_3$), 1.03 (d, $^{2}J_{P,H}$ = 13.8 Hz, 8H, $SiC\mathbf{H}_2P$), 0.88–0.79 (m, 40H, $PC\mathbf{H}_3$ + $BC\mathbf{H}_2$), 0.02 (s, 12H, $SiC\mathbf{H}_3$) ppm. – ^{11}B{^{1}H} NMR (160 MHz, C_6D_6): −17.9 ppm. – ^{31}P{^{1}H} NMR (202 MHz, C_6D_6) δ = −3.3 ppm. – No interpretable ^{13}C{^{1}H} NMR spectrum could be obtained.

9·2BisPhos:

^{1}H NMR (500 MHz, C_6D_6): δ = 7.45 (s, 4H, **H**^{3}), 6.50 (s, 4H, **H**^{1}), 1.29 (d, $^{2}J_{P,H}$ = 7.1 Hz, 8H, $SiC\mathbf{H}_2P$), 1.12 (d, $^{2}J_{P,H}$ = 6.4 Hz, 24H, $PC\mathbf{H}_3$), 0.43 (s, 144H, $AlCSi(C\mathbf{H}_3)_3$), −0.01 (s, 12H, $PCSi(C\mathbf{H}_3)_2$), −0.98 (s, 8H, Al**C**H) ppm – ^{29}Si{^{1}H} NMR (99 MHz, C_6D_6): δ = −1.4 ppm. – ^{31}P{^{1}H} NMR (202 MHz, C_6D_6) δ = −40.3 ppm. – No interpretable ^{13}C{^{1}H} NMR spectrum could be obtained.

9·2Bis[BisPhos]:

^{1}H NMR (500 MHz, C_6D_6): δ = 7.43 (s, 4H, **H**^{3}), 6.49 (s, 4H, **H**^{1}), 1.18–1.14 (m, 32H, $SiC\mathbf{H}_2P$ + $PC\mathbf{H}_3$), 0.77 (br s, 4H, $SiC\mathbf{H}_2$), 0.44 (s, 144H, $AlCSi(C\mathbf{H}_3)_3$), 0.22 (s, 6H, $SiC\mathbf{H}_3$), −0.91 (br s, 8H, Al**C**H). – ^{29}Si{^{1}H} NMR (99 MHz, C_6D_6): δ = −1.5 ppm. – ^{31}P{^{1}H} NMR (202 MHz, C_6D_6) δ = −39.4 ppm. – No interpretable ^{13}C{^{1}H} NMR spectrum could be obtained.

7·2N-1:

7·2N-1 rapidly formed microcrystalline crystals in C_6D_6 which could not be redissolved by heating (80 °C) and could not be dissolved in $CDCl_3$. Only in THF-d_8 the adduct was soluble.

^{1}H NMR (500 MHz, THF-d_8): δ = 8.61 (s, 4H, N-1: NC**H**N), 7.70–7.65 (m, 4H, N-1:$CH_2NC\mathbf{H}$), 7.45–7.41 (m, 4H, N-1: $CH_2NCHC\mathbf{H}N$), 7.32 (s, 4H, **H**^{3}), 7.04 (d, $^{3}J_{H,H}$ = 2.6 Hz, 8H, **H**^{5} + **H**^{6}), 6.71 (s, 4H, **H**^{1}), 6.58 (s, 4H, N-1: $NC\mathbf{H}_2N$), 0.10 (s, 72H, $SiC\mathbf{H}_3$), 0.13 (s, 72H, $SiC\mathbf{H}_3$), −1.03 (s, 8H, Al**C**H) ppm. – ^{13}C{^{1}H} NMR (125 MHz, THF-d_8): δ = 148.8 (**C**^{5}), 141.3 (N-1: N**C**HN), 140.6 (**C**^{6}), 137.3 (**C**^{2}), 136.8 (**C**^{4}), 134.0 (**C**^{1}), 130.4 (N-1: N**C**HCHNCH_2), 126.9 (**C**^{3}), 121.7 (N-1: NCH**C**HNCH_2), 58.1 (N-1: N**C**H_2N), 5.5 ($SiC\mathbf{H}_3$), 5.4 ($SiC\mathbf{H}_3$), 1.6 (Al**C**H) ppm. – ^{29}Si{^{1}H} NMR (99 MHz, THF-d_8): δ = −1.8, −2.3 ppm.

9·2N-1:

9·2N-1 rapidly formed microcrystalline crystals in C_6D_6 which could not be redissolved by heating (80 °C) and could not be dissolved in $CDCl_3$. Only in THF-d_8 the adduct was soluble for a short time, but it always crystallized too quickly to obtain meaningful ^{13}C or ^{29} Si spectra.

^{1}H NMR (500 MHz, THF-d_8): δ = 9.10 (s, 4H, N-1: NC**H**N), 7.60 (s, 4H, N-1:$CH_2NC\mathbf{H}$), 7.32 (s, 4H, N-1: $CH_2NCHC\mathbf{H}N$), 7.23 (s, 4H, **H**^{3}), 6.68 (s, 4H, **H**^{1}), 6.59 (s, 4H, $NC\mathbf{H}_2N$), 0.17 (s, 72H, $SiC\mathbf{H}_3$), −0.07 (s, 73H, $SiC\mathbf{H}_3$), −1.14 (s, 8H, Al**C**H) ppm.

7·2N-2:

7·2N-2 rapidly formed microcrystalline crystals in C_6D_6 which could not be redissolved by heating (80 °C) and could not be dissolved in $CDCl_3$. Only in THF-d_8 the adduct was soluble.

^{1}H NMR (500 MHz, THF-d_8): δ = 9.00 (s, 4H, N-2: NC**H**N), 8.33 (s, 4H, N-2: NC**H**NCH_2), 7.25 (s, 4H, **H**^{3}), 6.87 (d, $^{3}J_{H,H}$ = 20.3 Hz, 4H, **H**^{6}), 6.70 (d, $^{3}J_{H,H}$ = 20.4 Hz, 4H, **H**^{5}), 6.65 (s, 4H, **H**^{1}), 5.10 (s, 8H, N-2: $NC\mathbf{H}_2$), 0.15 (s, 72H, $SiC\mathbf{H}_3$), −0.12 (s, 72H, $SiC\mathbf{H}_3$), −1.02 (s, 8H, Al**C**H) ppm. – ^{13}C{^{1}H} NMR (125 MHz, THF-d_8): δ = 151.5 (N-2: N**C**N), 147.3 (**C**^{5}), 139.3 (**C**^{6}), 137.0 (**C**^{2}), 136.7 (**C**^{4}), 134.0 (**C**^{1}), 126.8 (**C**^{3}), 49.1 (N-2: N**C**H_2), 5.4 ($SiC\mathbf{H}_3$), 5.1 ($SiC\mathbf{H}_3$), 1.0 (Al**C**H) ppm. – ^{29}Si{^{1}H} NMR (99 MHz, THF-d_8): δ = −1.5, −2.2 ppm.

8·2N-2:

8·2N-2 rapidly formed microcrystalline crystals in C_6D_6 which could not be redissolved by heating (80 °C) and could not be dissolved in $CDCl_3$. Only in THF-d_8 the adduct was soluble.

^{1}H NMR (500 MHz, THF-d_8): δ = 8.83 (s, 4H, N-2: NC**H**N), 8.38 (s, 4H, NC**H**NCH$_2$), 7.01 (s, 4H, **H**^{3}), 6.68 (s, 4H, **H**^{3}), 4.89 (s, 8H, N-2: NC**H**$_2$), 0.76 (t, $^{3}J_{H,H}$ = 7.6 Hz, 24H, BCH$_2$C**H**$_3$), 0.55 – 0.45 (m, 16H, BC**H**$_2$) ppm. – ^{11}B{^{1}H} NMR (160 MHz, C_6D_6): δ = –6.8 ppm.

9·2N-2:

9·2N-2 rapidly formed microcrystalline crystals in C_6D_6 which could not be redissolved by heating (80 °C) and could not be dissolved in $CDCl_3$. Only in THF-d_8 the adduct was soluble.

^{1}H NMR (500 MHz, THF-d_8): δ = 8.78 (s, 4H, N-2: NC**H**N), 8.63 (s, 4H, N-2: NC**H**NCH$_2$), 7.11 (s, 4H, **H**^{3}), 6.57 (s, 4H, **H**^{1}), 4.91 (s, 8H, N-2: NC**H**$_2$), 0.21 (s, 72H, SiC**H**$_3$), –0.07 (s, 72H, SiC**H**$_3$), –1.05 (s, 8H, AlC**H**) ppm. – ^{13}C{^{1}H} NMR (125 MHz, THF-d_8): δ = 152.2 (N-2: N**C**N), 146.5 (N-2: N**C**N), 136.6 (**C**^{2}), 135.6 (**C**^{3}), 133.8 (**C**^{1}), 126.1 (**C**^{4}), 115.6 (**C**^{6}), 109.8 (**C**^{5}), 51.1 (N-2: N**C**H$_2$**C**H$_2$N), 5.2 (Si**C**H$_3$), 4.9 (Si**C**H$_3$), 1.7 (Al**C**H), 0.9 (Al**C**H). – ^{29}Si{^{1}H} NMR (99 MHz, THF-d_8): δ = –1.1, – 1.9 ppm.

7·2N-4:

Crystallized so quickly from C_6D_6 that only a ^{1}H NMR spectrum could be recorded.
^{1}H NMR (500 MHz, C_6D_6): δ = 8.40 (s, 4H, N-4: NC**H**N), 8.38 (s, 4H, N-4: NC**H**N), 7.69 (s, 4H **H**^{3}), 7.32 (d, $^{3}J_{H,H}$ = 20.2 Hz, 4H, **H**^{6}), 7.22 (d, $^{3}J_{H,H}$ = 20.3 Hz, 4H, **H**^{5}), 6.76 (s, 4H, **H**^{1}), 3.07 (s, 8H, NC**H**$_2$C), 1.03 (s, 8H, NCH$_2$C**H**$_2$), 0.40 (s, 72H, SiC**H**$_3$), 0.14 (s, 72H, SiC**H**$_3$), –0.79 (s, 8H, AlC**H**) ppm.

[**9**·2N-4]$_n$:

^{1}H NMR (500 MHz, C_6D_6): δ = 9.21 (s, 2H, N-4: NC**H**N), 8.88 (s, 2H, N-4: NC**H**N), 8.45 (s, 2H, N-4: NC**H**N), 8.31 (s, 2H, N-4: NC**H**N), 7.56 (s, 2H, **H**^{3}), 7.31 (s, 2, **H**^{3}), 6.48 (s, 4H, **H**^{1}), 2.86 (s, 8H, NC**H**$_2$C), 1.13 (s, 8H, NCH$_2$C**H**$_2$), 0.47 (s, 36H, SiC**H**$_3$), 0.36 (s, 36H, SiC**H**$_3$), 0.18 (s, 72H, SiC**H**$_3$), −0.65 (s, 2H, AlC**H**), −0.72 (s, 2H, AlC**H**), −0.82 (s, 4H, AlC**H**) ppm. – No interpretable ^{13}C{^{1}H} NMR spectrum could be obtained. – ^{29}Si{^{1}H} NMR (99 MHz, C_6D_6): δ = −1.2, −2.1 ppm.

9·4GBL:

^{1}H NMR (500 MHz, C_6D_6): δ = 7.41 (s, 4H, **H**^{3}), 6.53 (s, 4H, **H**^{1}), 3.54 (br s, 8H, GBL: C**H**$_2$CH$_2$CH$_2$OC=O), 2.82 (br s, 8H, GBL: CH$_2$CH$_2$C**H**$_2$OC=O), 1.44 (br s, 8H, GBL: CH$_2$C**H**$_2$CH$_2$OC=O), 0.52–0.37 (m, 144H, SiC**H**$_3$), −0.81 (s, 8H, AlC**H**). – No interpretable ^{13}C{^{1}H} NMR spectrum could be obtained. – ^{29}Si{^{1}H} NMR (99 MHz, C_6D_6): δ = −1.6 ppm.

7·4Nico:

^{1}H NMR (500 MHz, C_6D_6): δ = 8.82 (d, $^{3}J_{H,H}$ = 2.0 Hz, 4H, Nico: NC**H**C–pyrrolidine), 8.60 (d, $^{3}J_{H,H}$ = 5.5, Hz, 4H, Nico: **H**CN), 7.52 (s, 4H, **H**^{3}), 7.45 (d, $^{3}J_{H,H}$ = 20.1 Hz, 4H, **H**^{5}), 7.20 (dt, $^{3}J_{H,H}$ = 8.0, 1.7 Hz, 4H, Nico: **H**CHCN), 7.12 (d, $^{3}J_{H,H}$ = 20.1 Hz, 4H, **H**^{6}), 6.71 (dd, ^{3}J = 7.9, 5.5 Hz, 4H, Nico: **H**CHCHCN), 6.67 (s, 4H, **H**^{1}), 2.89 (t, $^{3}J_{H,H}$ = 8.3 Hz, 4H, Nico: pyrrolidine-**H**), 2.75 (t, $^{3}J_{H,H}$ = 8.0 Hz, 4H, Nico: pyrrolidine-**H**), 1.99–1.84 (m, 16H, Nico: pyrrolidine-**H** + Nico-C**H**$_3$), 1.80–1.71 (m, 4H, Nico: pyrrolidine-**H**), 1.62–1.50 (m, 4H, Nico: pyrrolidine-**H**), 1.35–1.23 (m, 36H, Nico: pyrrolidine-**H**), 0.19 (s, 36H, SiC**H**$_3$), 0.16 (s, 36H, SiC**H**$_3$), 0.02 (s, 36H, SiC**H**$_3$), 0.00 (s, 36H, SiC**H**$_3$), −0.80 (overlapping s, 8H, AlC**H**) ppm. – ^{13}C{^{1}H} NMR (125 MHz, C_6D_6): δ = 149.2 (Nico-**C**), 147.7 (Nico-**C**), 143.0 (**C**^{5}), 142.2 (**C**^{6}), 140.4 (Nico-**C**), 138.4 (**C**^{2}), 136.4 (**C**^{4}), 133.8 (**C**^{1}), 125.2 (**C**^{3}), 68.2 (Nico-**C**), 56.9 (Nico-**C**), 40.7 (Nico-**C**), 36.0 (Nico-**C**), 23.4 (Nico-**C**), 5.6 (Si**C**H$_3$), 5.3 (Si**C**H$_3$), 5.3 (Si**C**H$_3$), 0.7 (Al**C**H), 0.5 (Al**C**H). – ^{29}Si{^{1}H} NMR (99 MHz, C_6D_6): δ = −1.8, −2.2, −2.1 ppm.

9·4Nico:

^{1}H NMR (500 MHz, C_6D_6): δ = 9.38–9.10 (m, 8H, Nico: NC**H**), 7.56 (s, 4H, **H**^{3}), 7.39 (dt, $^{3}J_{H,H}$ = 9.5, 2.8 Hz, 4H, Nico: **H**CHCN), 7.09 (dd, $^{3}J_{H,H}$ = 7.9, 5.5 Hz, 4H, Nico: **H**CHCHCN), 6.55 (s, 4H, **H**^{1}), 3.11–3.05 (m, 4H, Nico: pyrrolidine-**H**), 2.92 (t, $^{3}J_{H,H}$ = 8.1 Hz, 4H, Nico: pyrrolidine-**H**), 2.13 (td, $^{3}J_{H,H}$ = 9.3, 7.7 Hz, 4H, Nico: pyrrolidine-**H**), 2.05 (s, 12H, Nico-C**H**$_3$), 1.97–1.88 (m, 4H, pyrrolidine-**H**), 1.77–1.66 (m, 4H, pyrrolidine-**H**), 1.54–1.41 (m, 8H, pyrrolidine-**H**), 0.50 (s, 36H, SiC**H**$_3$), 0.48 (s, 36H, SiC**H**$_3$), 0.25 (s, 36H, SiC**H**$_3$), 0.23 (s, 36H, SiC**H**$_3$), −0.66 (s, 4H, AlC**H**), −0.68 (s, 4H, AlC**H**) ppm. – ^{13}C{^{1}H} NMR (125 MHz, C_6D_6): δ = ^{13}C NMR (126 MHz, C_6D_6) 148.6 (Nico-**C**), 147.7 (Nico-**C**), 142.6 (Nico-**C**), 140.2

(Nico-**C**), 135.7 (**C**^{2}), 135.2 (**C**^{3}), 133.0 (**C**^{1}), 125.6 (**C**^{4}), 125.1 (**C**^{6}), 109.7 (**C**^{5}), 68.0 (Nico-**C**), 56.6 (Nico-**C**), 40.3 (Nico-**C**), 35.6 (Nico-**C**), 23.0 (Nico-**C**), 5.0 (Si**C**H$_3$), 4.8 (Si**C**H$_3$), 4.7 (Si**C**H$_3$), 0.8 (Al**C**H) ppm. – ^{29}Si{^{1}H} NMR (99 MHz, C_6D_6): δ = −1.3, −1.9 ppm.

7·2Caff:

^{1}H NMR (500 MHz, C_6D_6): δ = 7.47 (s, 4H, **H**^{3}), 7.44 (d, $^{3}J_{H,H}$ = 21.6 Hz, 4H, **H**^{5}), 6.98 (d, $^{3}J_{H,H}$ = 20.3 Hz, 4H, **H**^{6}), 6.65 (s, 4H, **H**^{1}), 6.39 (s, 4H, Caff: NC**H**N), 3.79 (s, 12H, Caff: C**H**$_3$), 3.62 (s, 12H, Caff: C**H**$_3$), 3.07 (s, 12H, Caff: C**H**$_3$), 0.32 (s, 144H, SiC**H**$_3$), −0.62 (s, 8H, AlC**H**) ppm. No interpretable ^{13}C{^{1}H} NMR spectrum could be obtained. – ^{29}Si{^{1}H} NMR (99 MHz, C_6D_6): δ = −2.32 ppm.

8·2Caff:

^{1}H NMR (500 MHz, C_6D_6): δ = 7.19 (s, 4H, **H**^{3}), 6.84 (s, 2H, Caff: NC**H**N), 6.25 (s, 4H, **H**^{1}), 3.63 (s, 6H, Caff: C**H**$_3$), 3.25 (s, 6H, Caff: C**H**$_3$), 2.93 (s, 6H, Caff: C**H**$_3$), 1.31–1.22 (m, 10H, BC**H**$_2$C**H**$_3$) – ^{11}B{^{1}H} NMR (160 MHz, C_6D_6): δ = 66.5 ppm. – ^{13}C{^{1}H} NMR (125 MHz, C_6D_6): δ = 154.4 (Caff: C(N)**C**=O), 151.0 (Caff: N(N)**C**=O), 146.5 (Caff: N**C**N), 139.7 (Caff: N**C**N), 137.3 (**C**^{2}), 133.3 (**C**^{4}), 132.8 (**C**^{1}), 124.7 (**C**^{3}), 116.6 (**C**CB), 107.7 (C**C**B), 32.6 (Caff: **C**H$_3$), 27.4 (Caff: **C**H$_3$), 21.0 (Caff: **C**H$_3$), 9.5 (BCH$_2$**C**H$_3$).

9·2Caff:

^{1}H NMR (500 MHz, C_6D_6): δ = 7.30 (s, 1H, **H**^{3}), 7.29 (s, 1H, **H**^{3}), 7.27 (s, 1H, **H**^{3}), 7.25 (s, 1H, **H**^{3}), 6.21–6.10 (m, 20H, **H**^{1} + Caff: NC**H**N), 4.78 (s, 6H, Caff: C**H**$_3$), 3.48 (s, 6H, Caff: C**H**$_3$), 3.32 (s, 6H, Caff: C**H**$_3$), 0.53 (br s, 72H, SiC**H**$_3$), 0.45–0.27 (m, 36H, SiC**H**$_3$), 0.26–(−0.01) (m, 36H, SiC**H**$_3$), −0.51–(−0.77) (m, 4H, AlC**H**), −1.02–(−1.31) (m, 4H, AlC**H**) ppm. – No interpretable ^{13}C{^{1}H} NMR spectrum could be obtained. – ^{29}Si{^{1}H} NMR (99 MHz, C_6D_6): δ = −1.6 ppm.

NMR Spectra

Compound 2

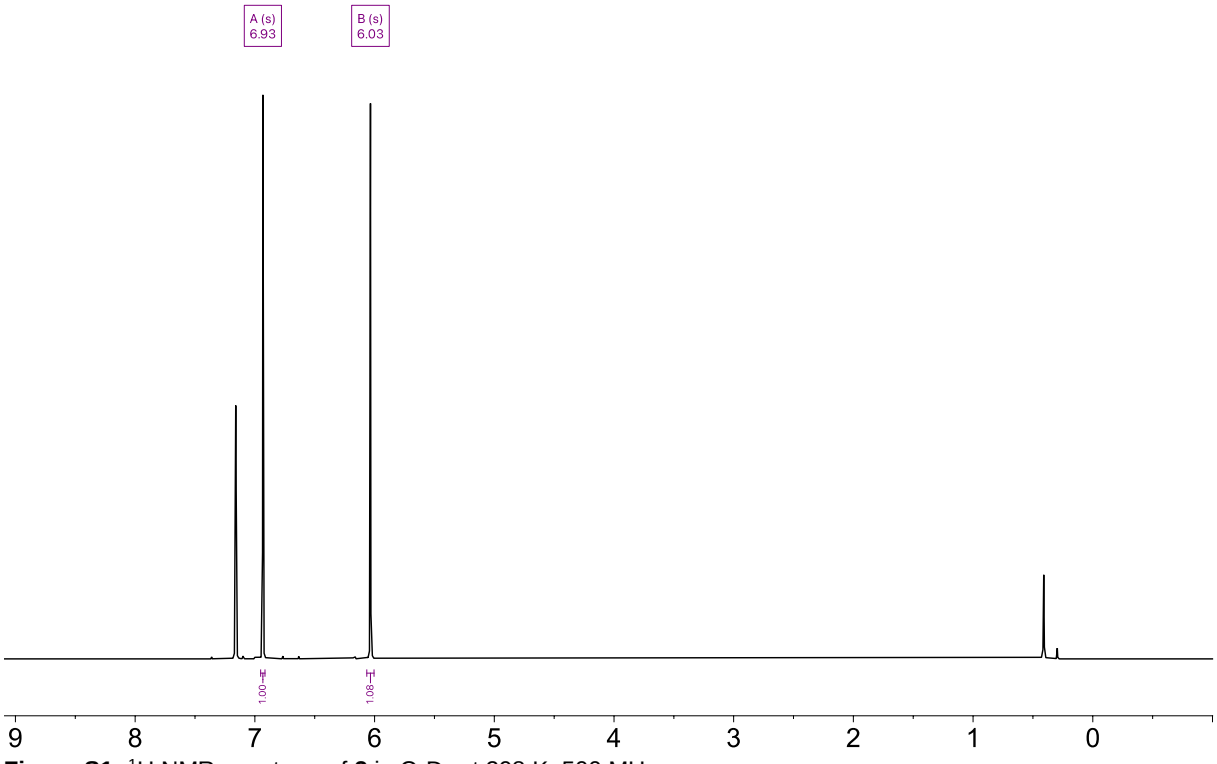

Figure S1: ^{1}H NMR spectrum of **2** in C_6D_6 at 298 K, 500 MHz.

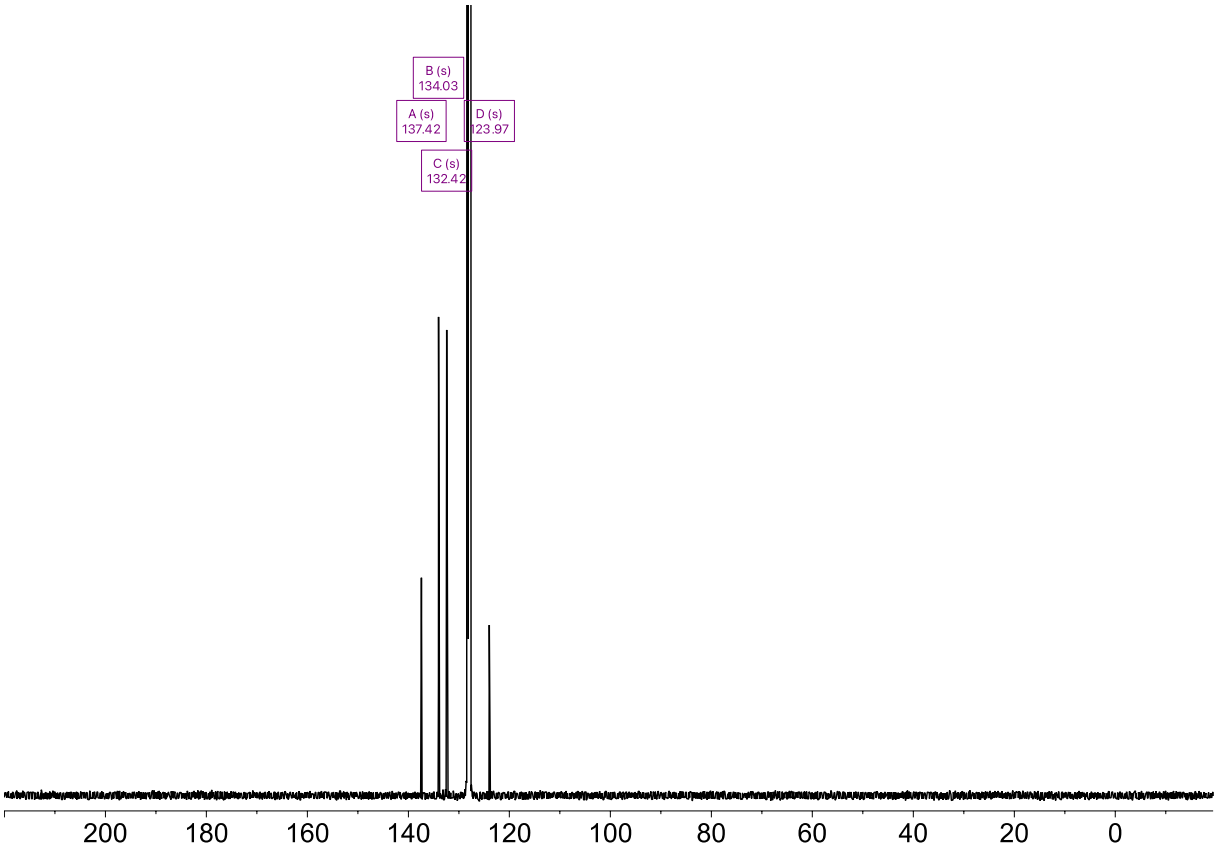

Figure S2: $^{13}C\{^{1}H\}$ NMR spectrum of **2** in C_6D_6 at 298 K, 125 MHz.

Compound 3

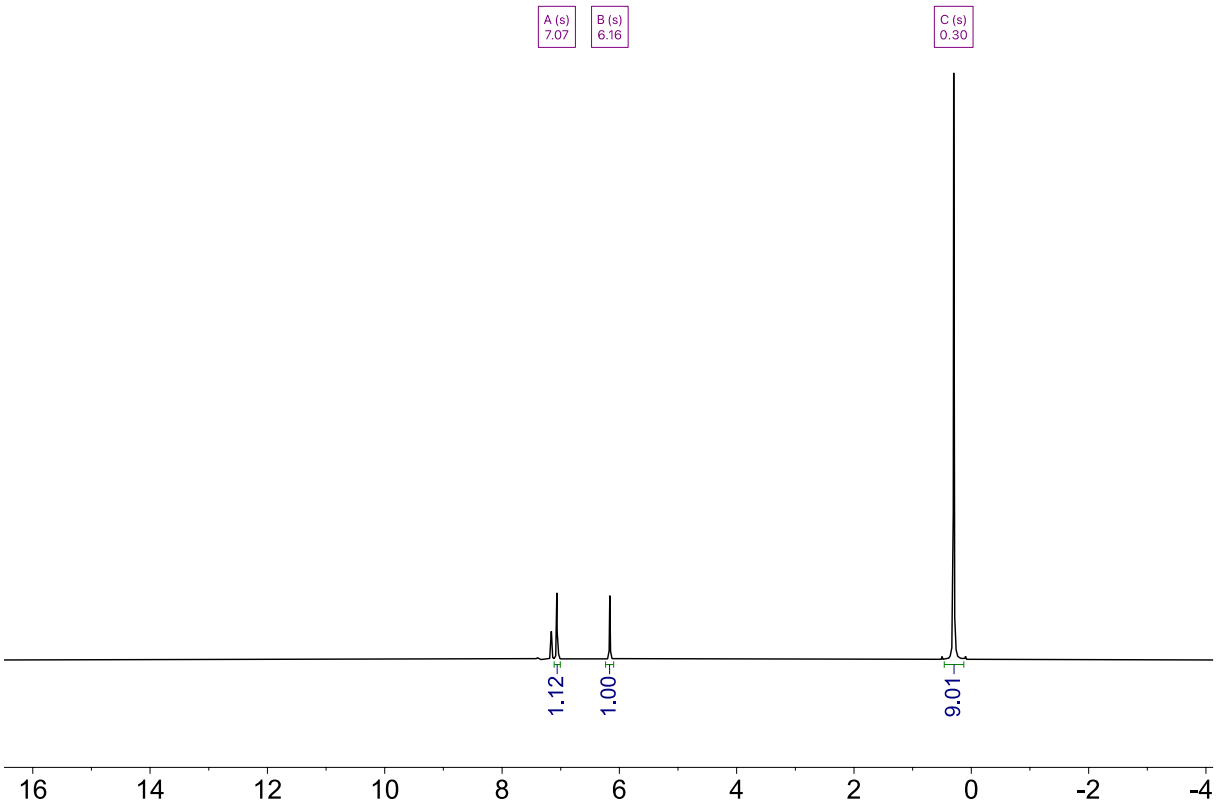

Figure S3: ^{1}H NMR spectrum of **3** in C_6D_6 at 298 K, 500 MHz.

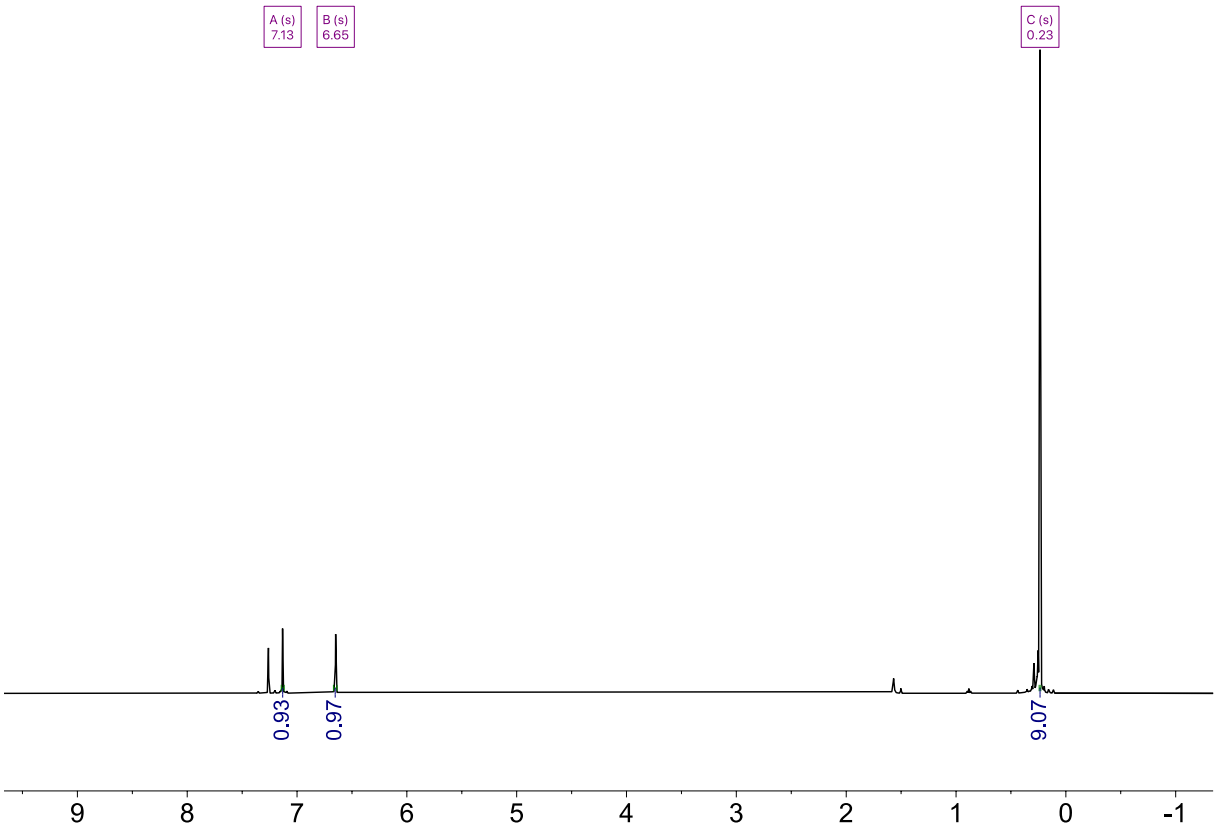

Figure S4: ^{1}H NMR spectrum of **3** in $CDCl_3$ at 298 K, 500 MHz.

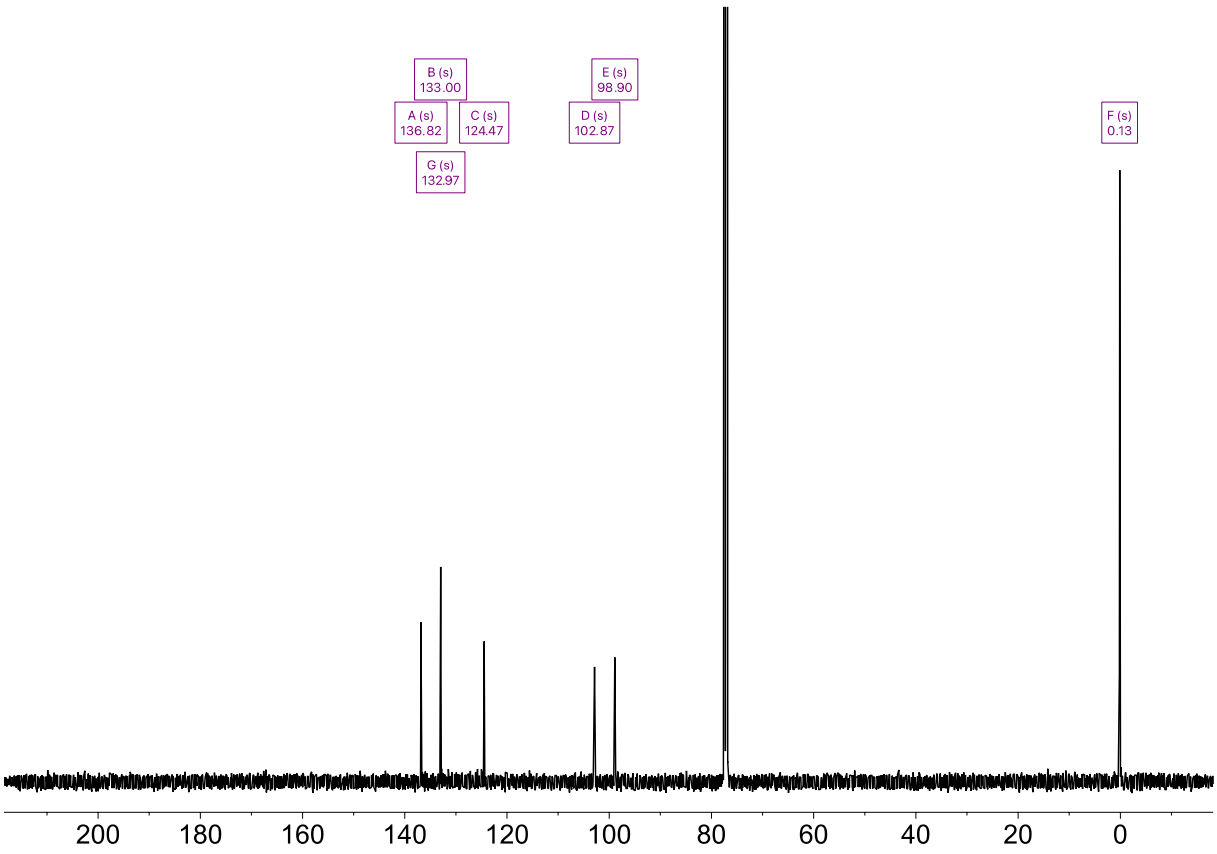

Figure S5: $^{13}C\{^{1}H\}$ NMR spectrum of **3** in $CDCl_3$ at 298 K, 125 MHz.

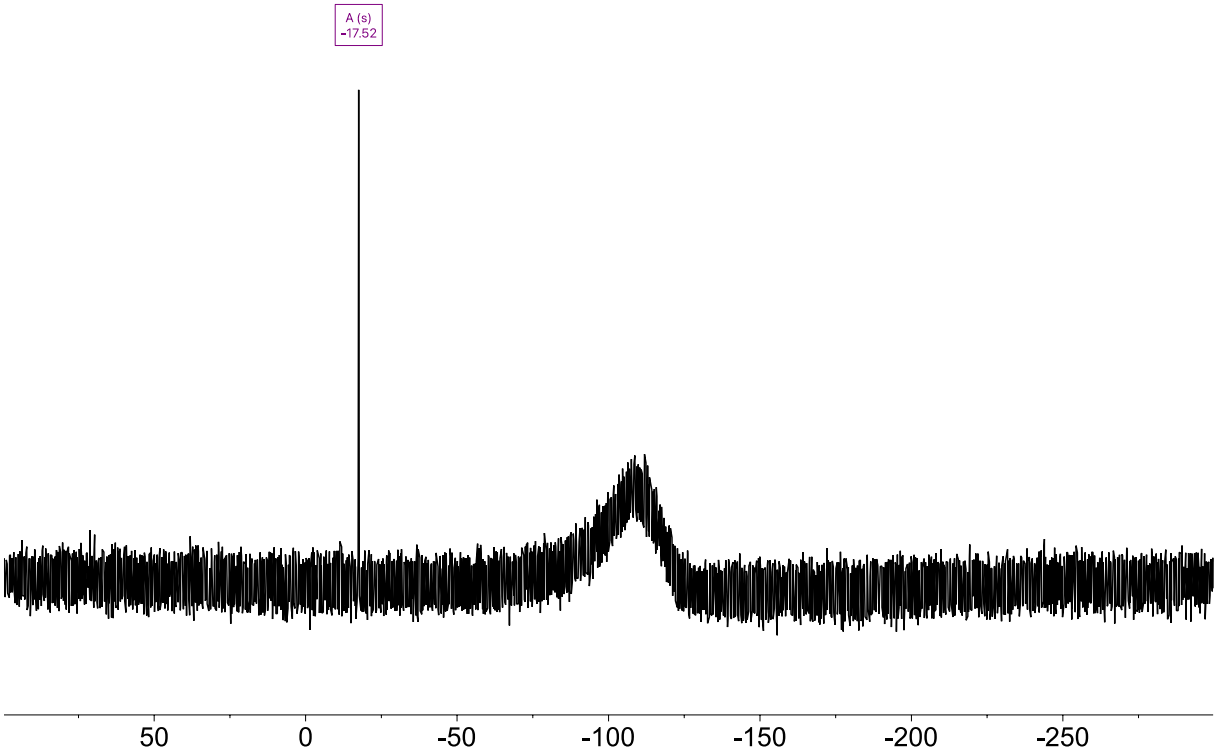

Figure S6: $^{29}Si\{^{1}H\}$ NMR spectrum of **3** in $CDCl_3$ at 298 K, 99 MHz. The peak at 0–100 ppm is due to the silicon atoms in the glass.

Compound 4

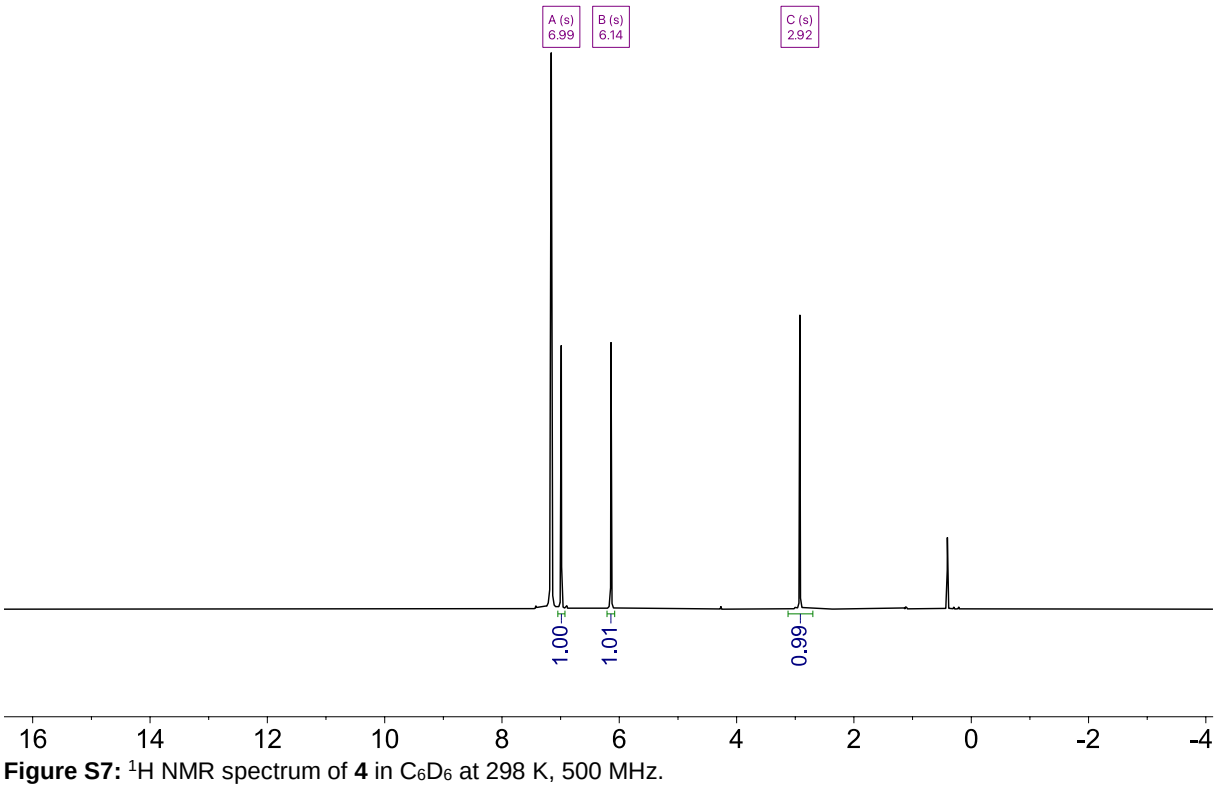

Figure S7: ^{1}H NMR spectrum of **4** in C_6D_6 at 298 K, 500 MHz.

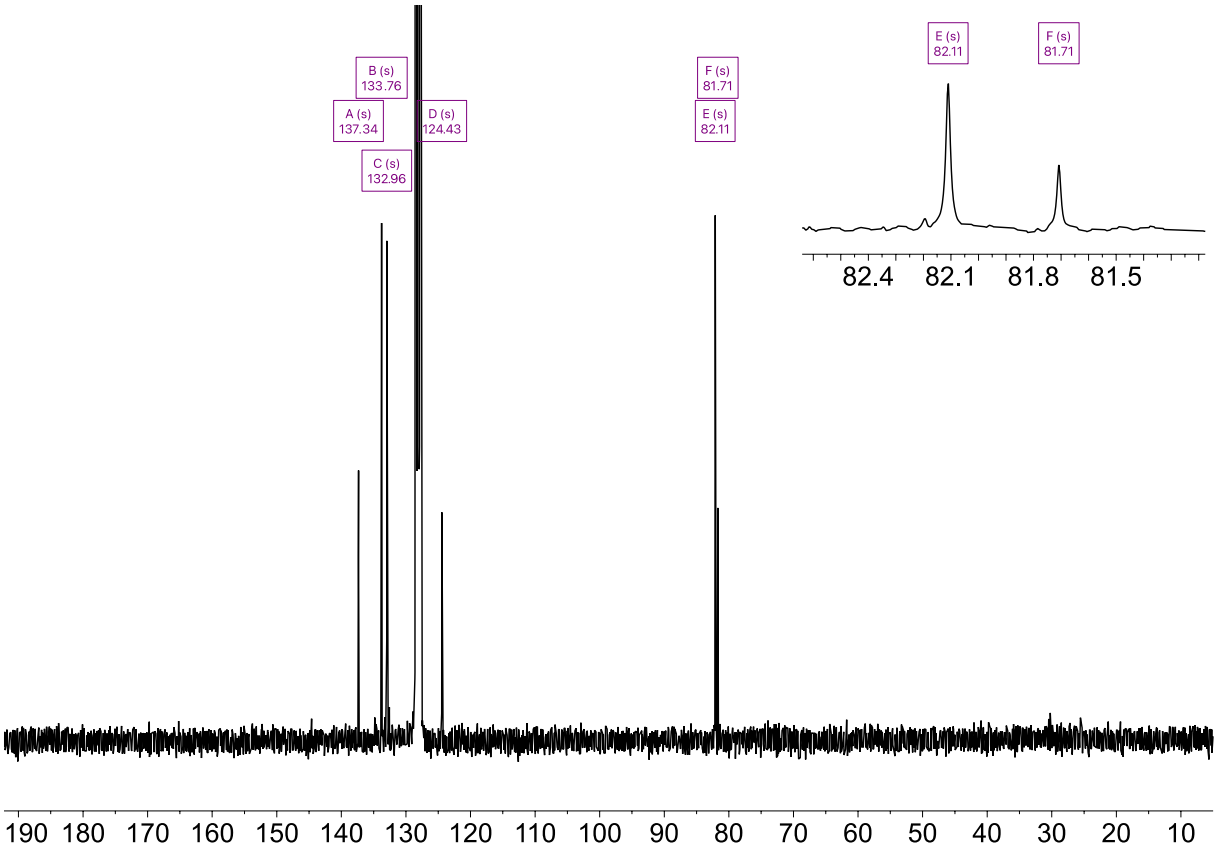

Figure S8: $^{13}C\{^{1}H\}$ NMR spectrum of **4** in C_6D_6 at 298 K, 125 MHz.

Compound 5

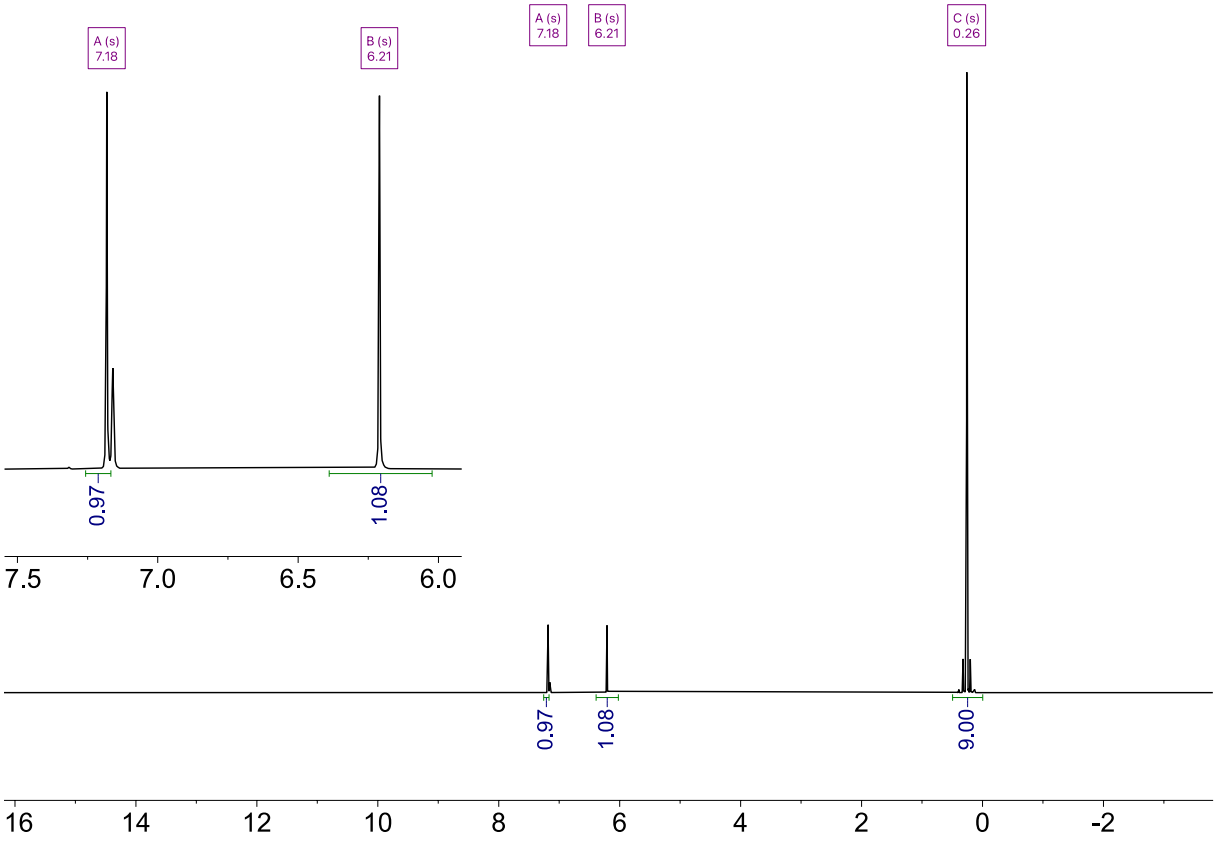

Figure S9: ^{1}H NMR spectrum of **5** in C_6D_6 at 298 K, 500 MHz.

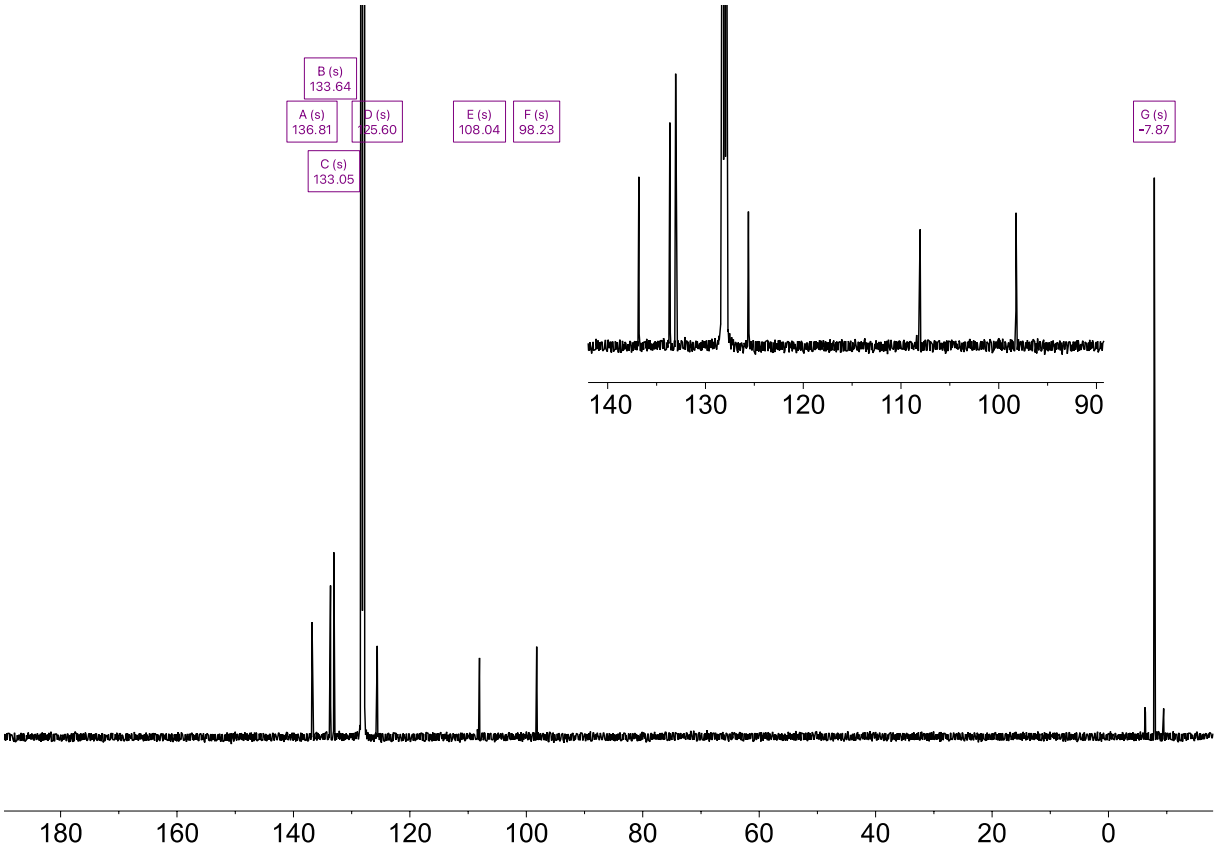

Figure S10: $^{13}C\{^{1}H\}$ NMR spectrum of **5** in C_6D_6 at 298 K, 125 MHz.

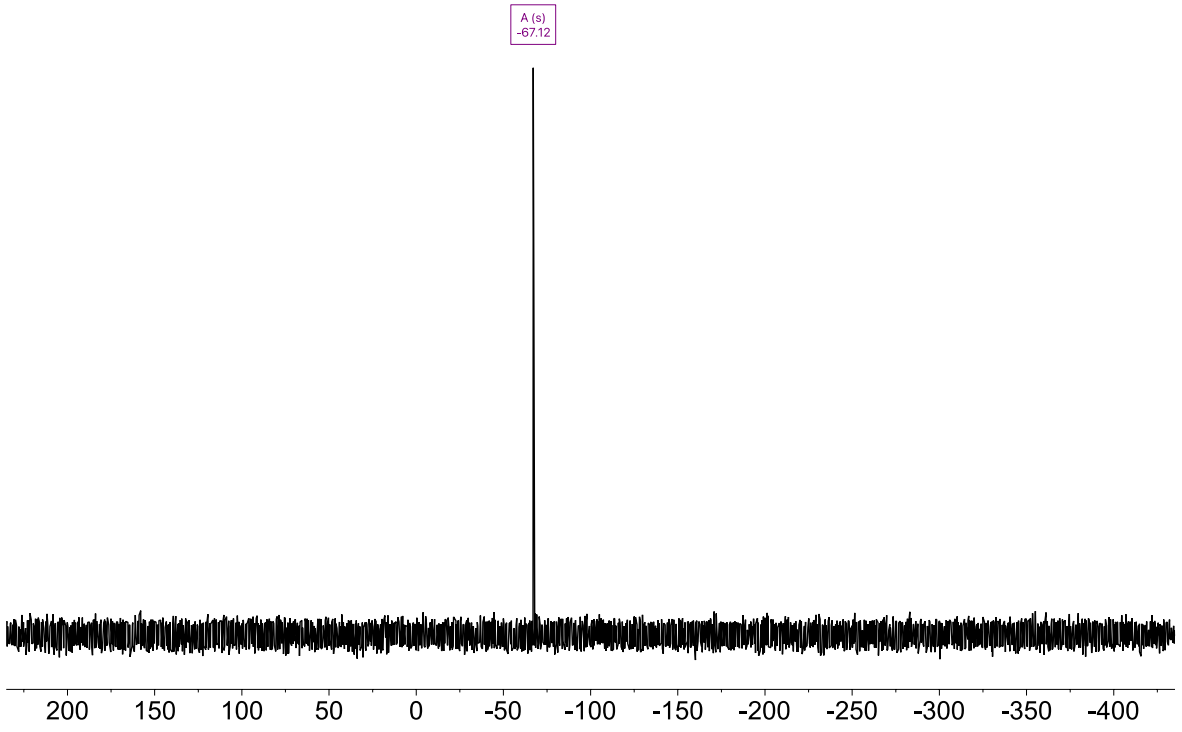

Figure S11: $^{119}Sn\{^{1}H\}$ NMR spectrum of **5** in C_6D_6 at 298 K, 186 MHz.

Compound 6

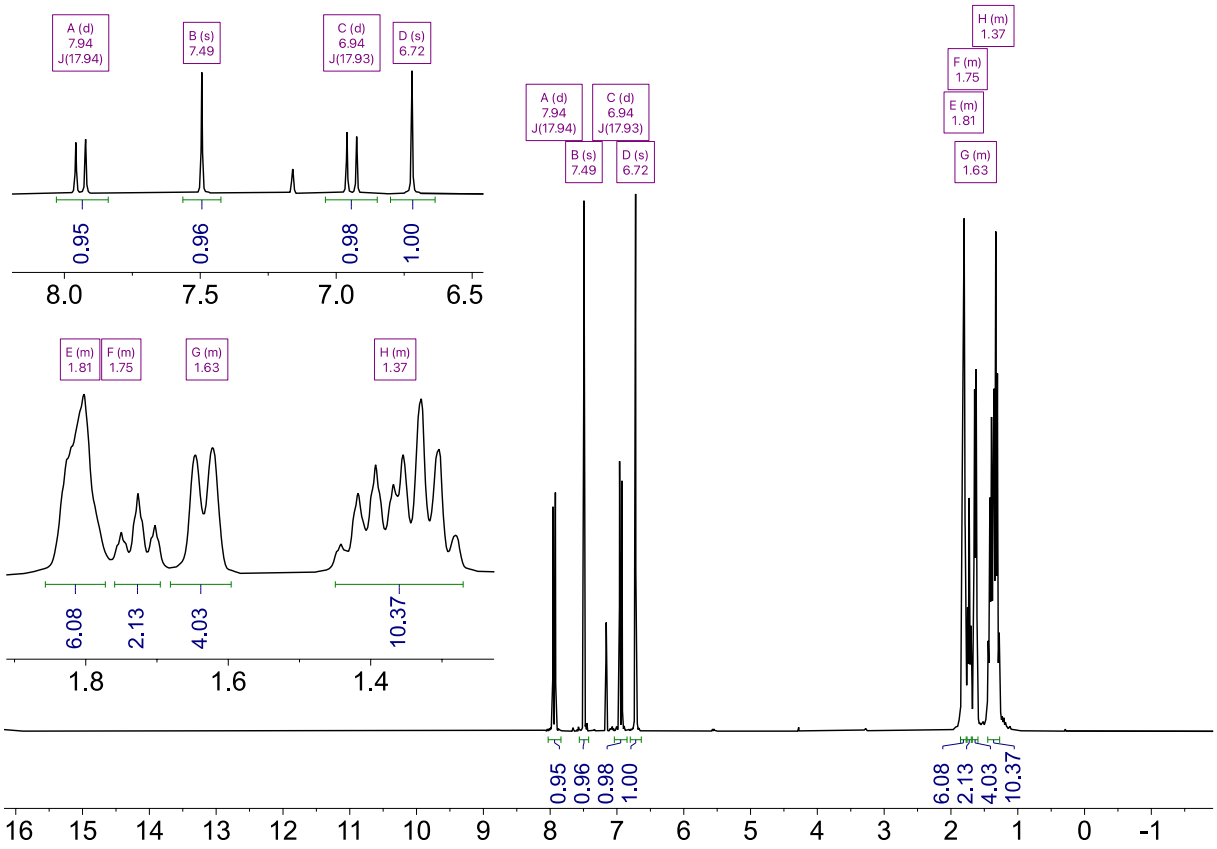

Figure S12: ^{1}H NMR spectrum of **6** in C_6D_6 at 298 K, 500 MHz.

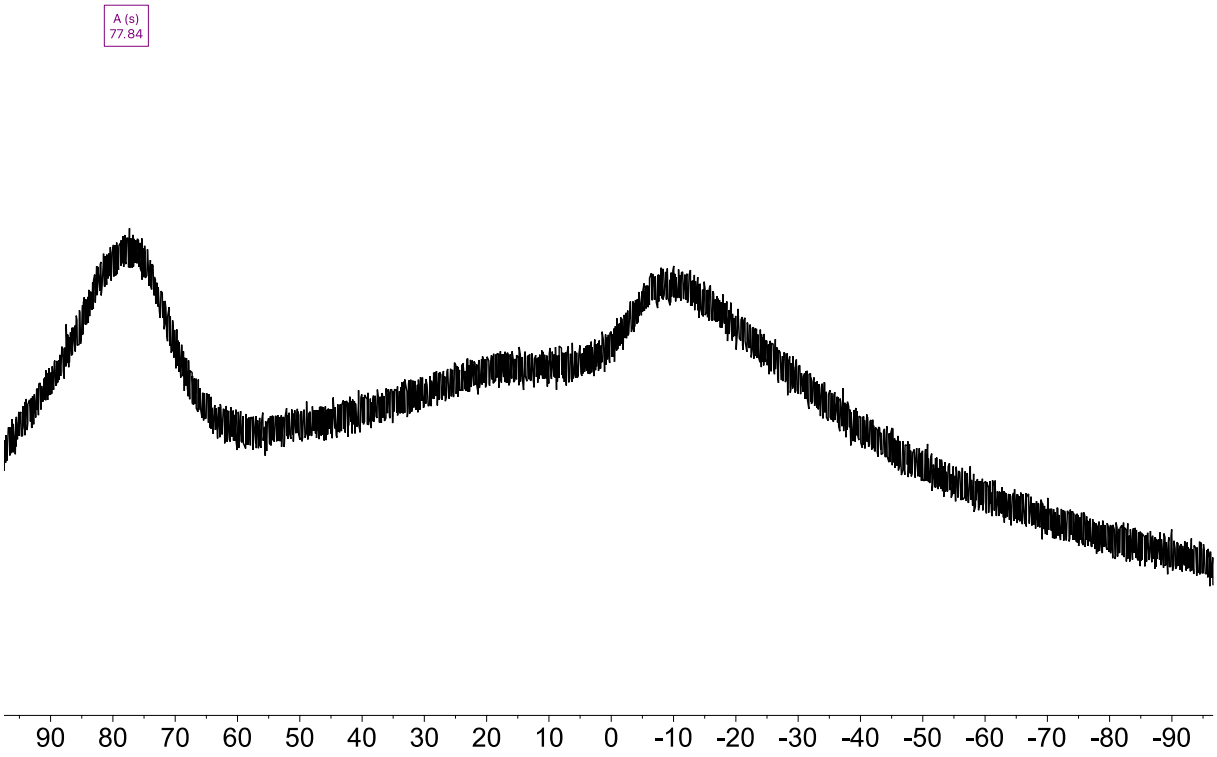

Figure S13: ^{11}B NMR spectrum of **6** in C_6D_6 at 298 K, 160 MHz. The peak at 0 to –25 ppm is due to the boron atoms in the glass.

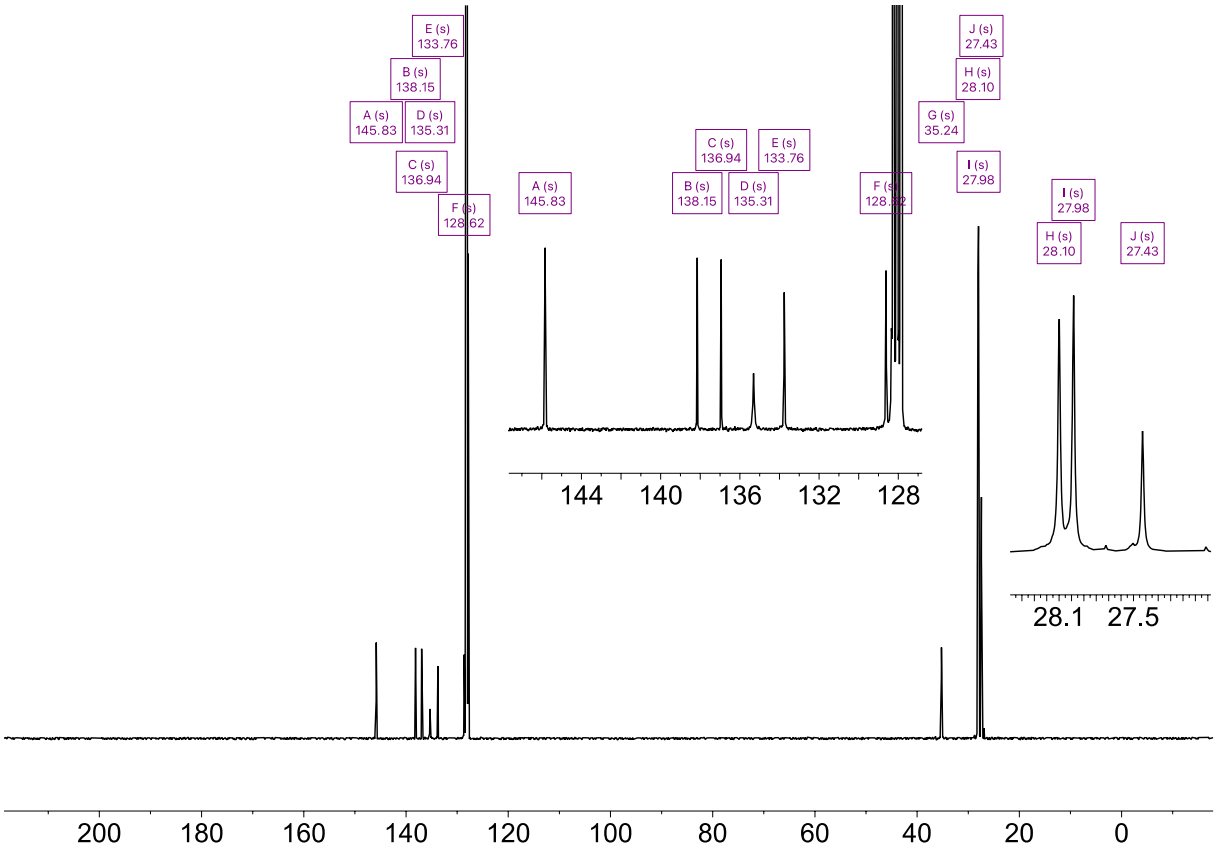

Figure S14: $^{13}C\{^{1}H\}$ NMR spectrum of **6** in C_6D_6 at 298 K, 125 MHz.

Compound 7

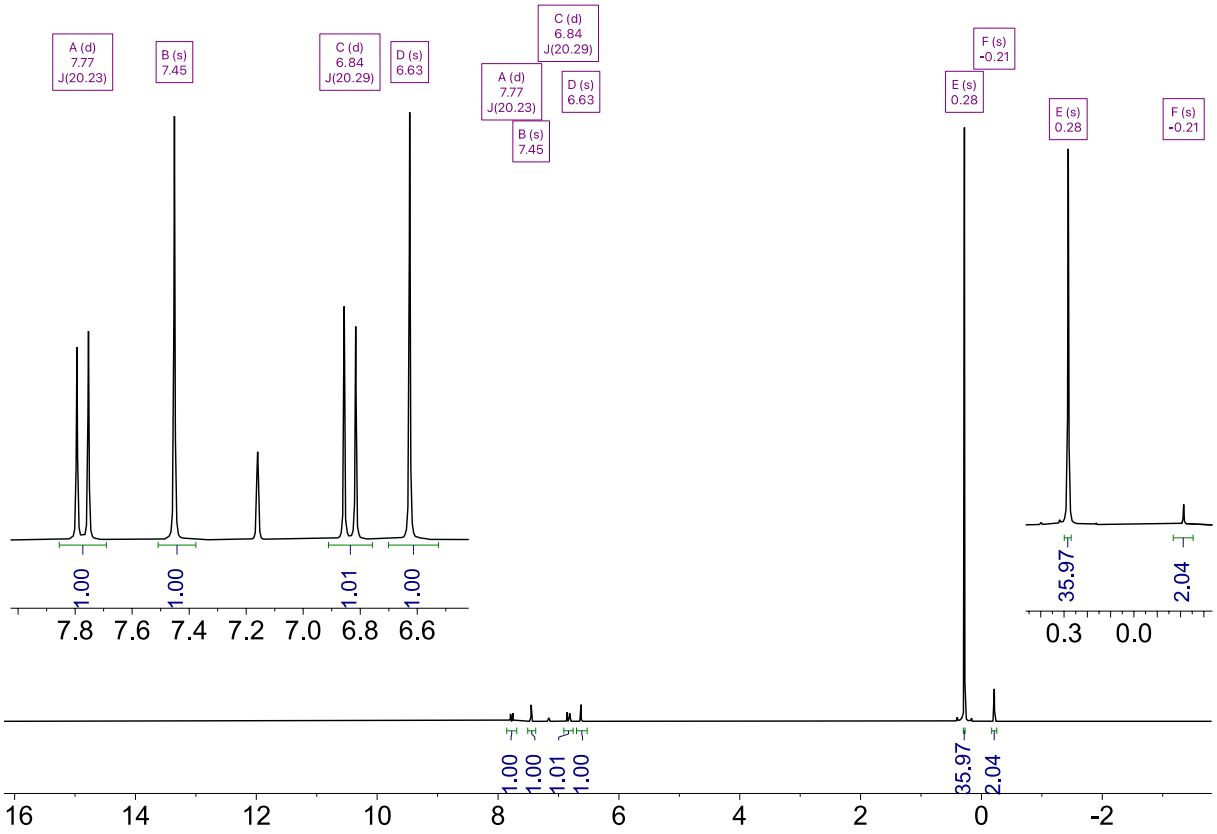

Figure S15: ^{1}H NMR spectrum of **7** in C_6D_6 at 298 K, 500 MHz.

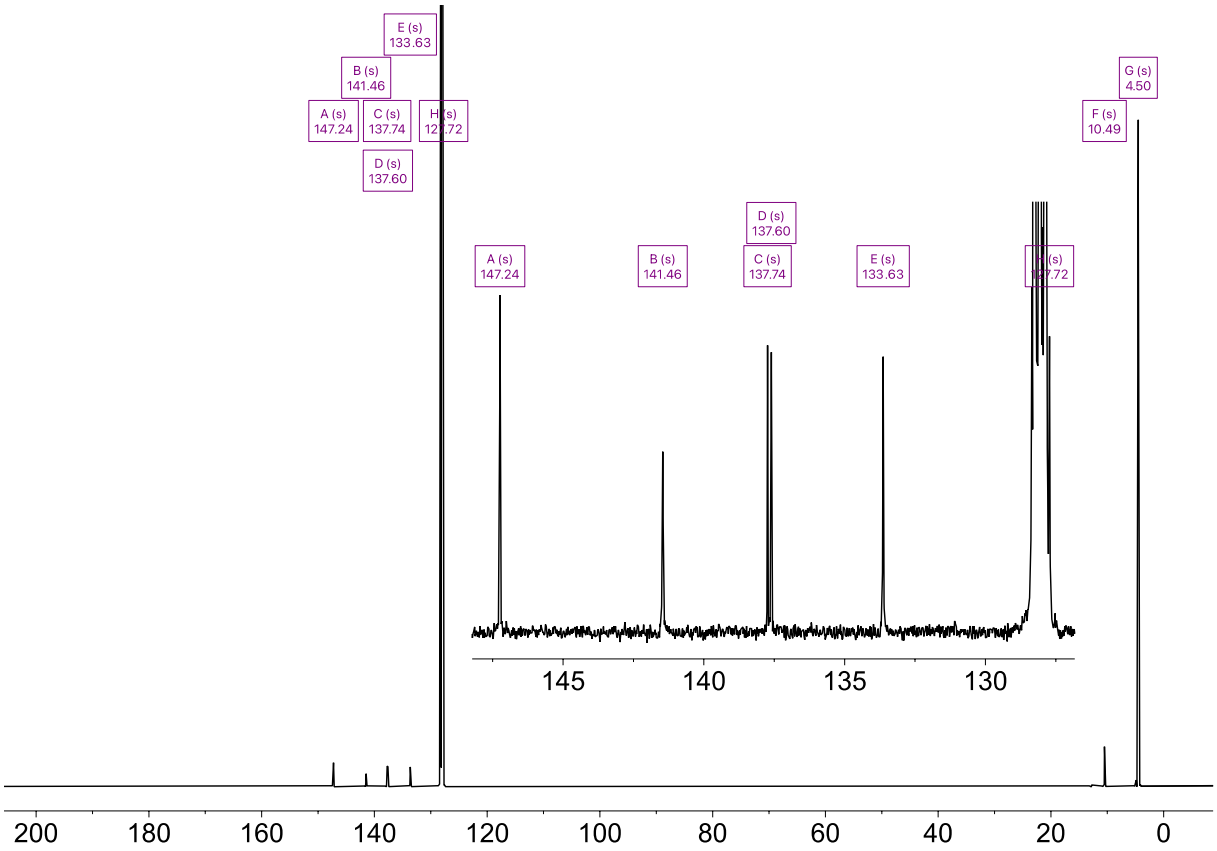

Figure S16: $^{13}C\{^{1}H\}$ NMR spectrum of **7** in C_6D_6 at 298 K, 125 MHz.

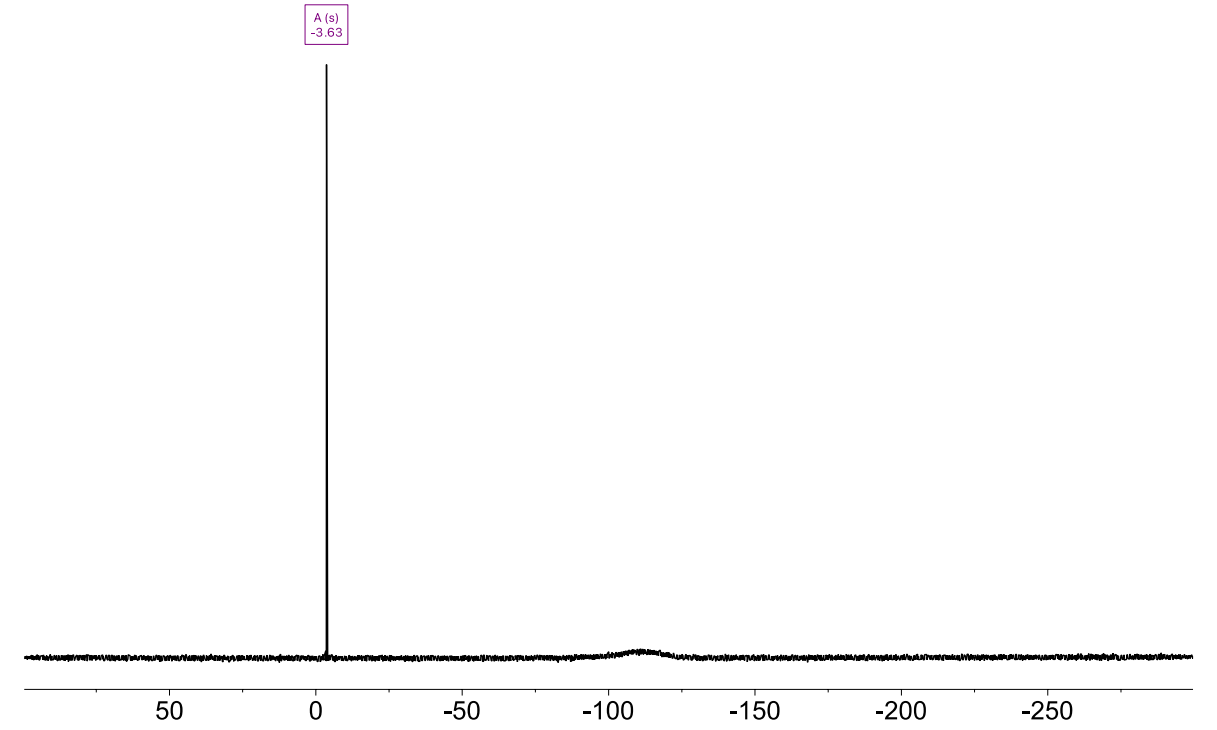

Figure S17: $^{29}Si\{^{1}H\}$ NMR spectrum of **7** in C_6D_6 at 298 K, 99 MHz. The peak at –110 ppm is due to the silicon atoms in the glass.

Compound 8

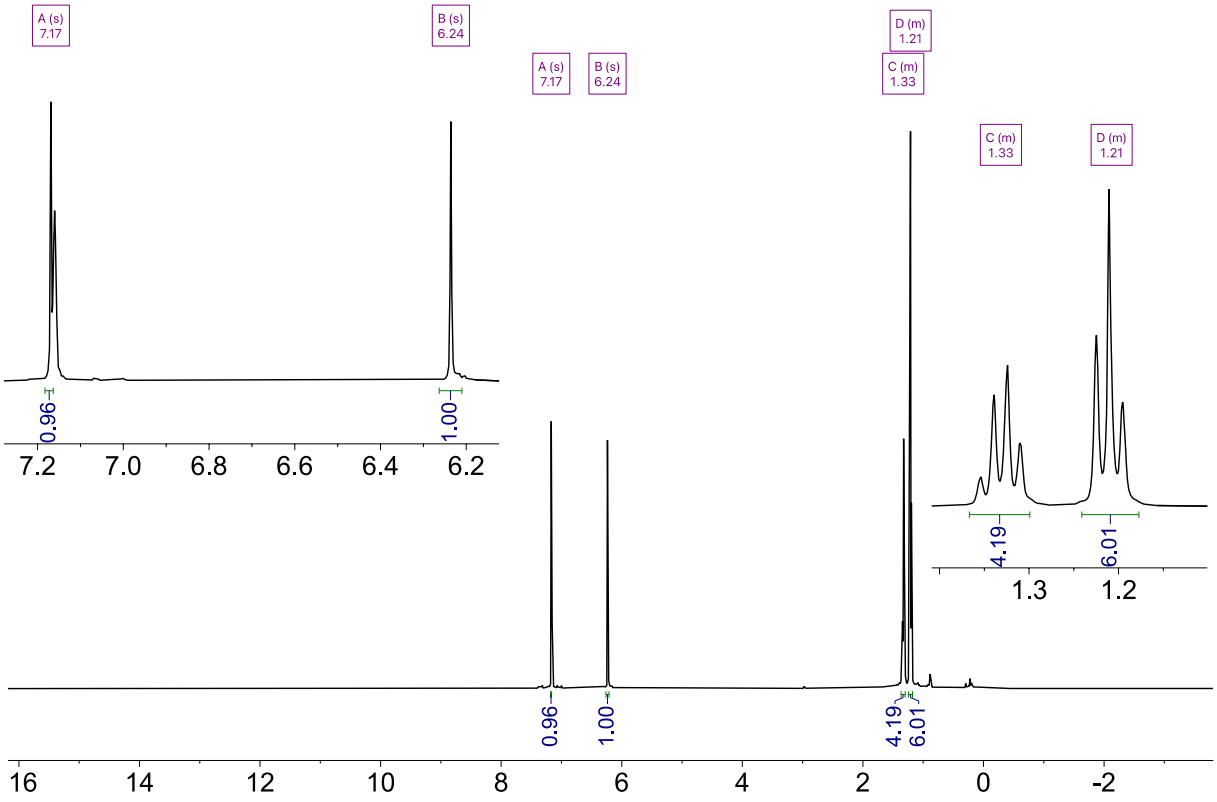

Figure S18: ^{1}H NMR spectrum of **8** in C_6D_6 at 298 K, 500 MHz.

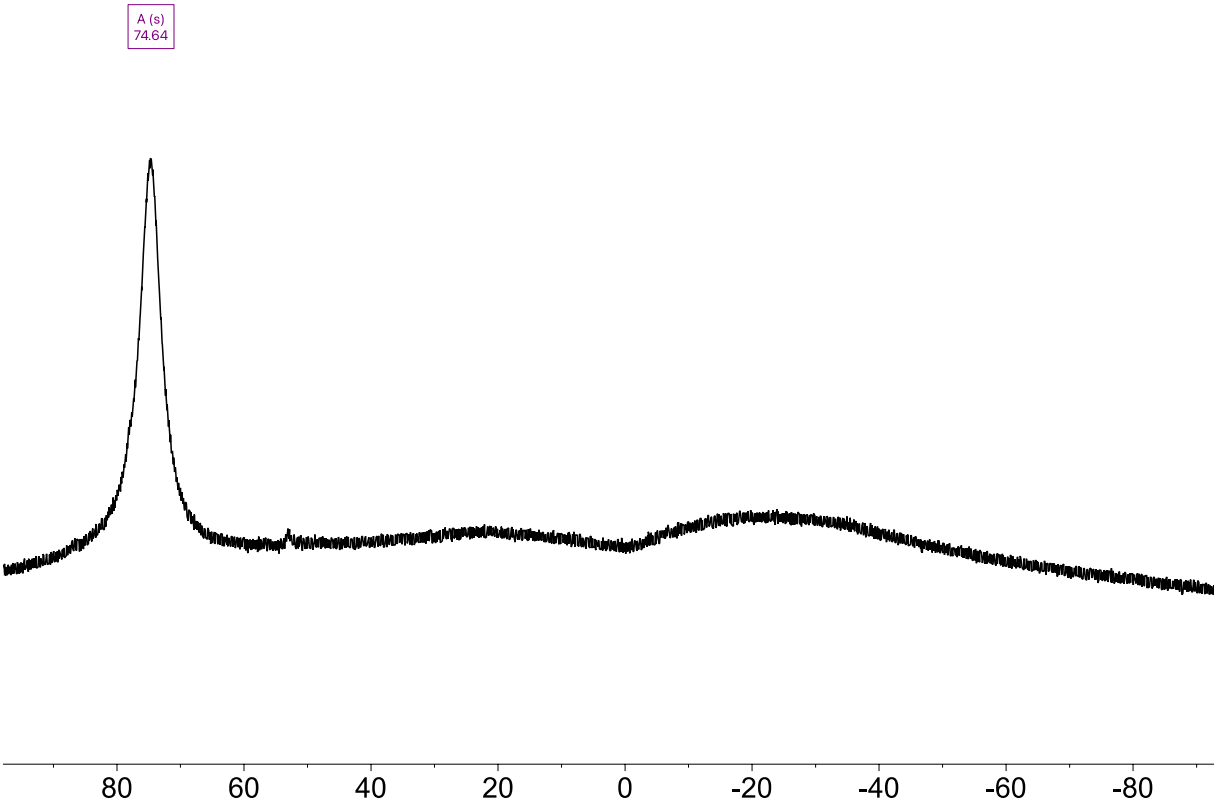

Figure S19: ^{11}B NMR spectrum of **8** in C_6D_6 at 298 K, 160 MHz. The peak at 0 to –25 ppm is due to the boron atoms in the glass.

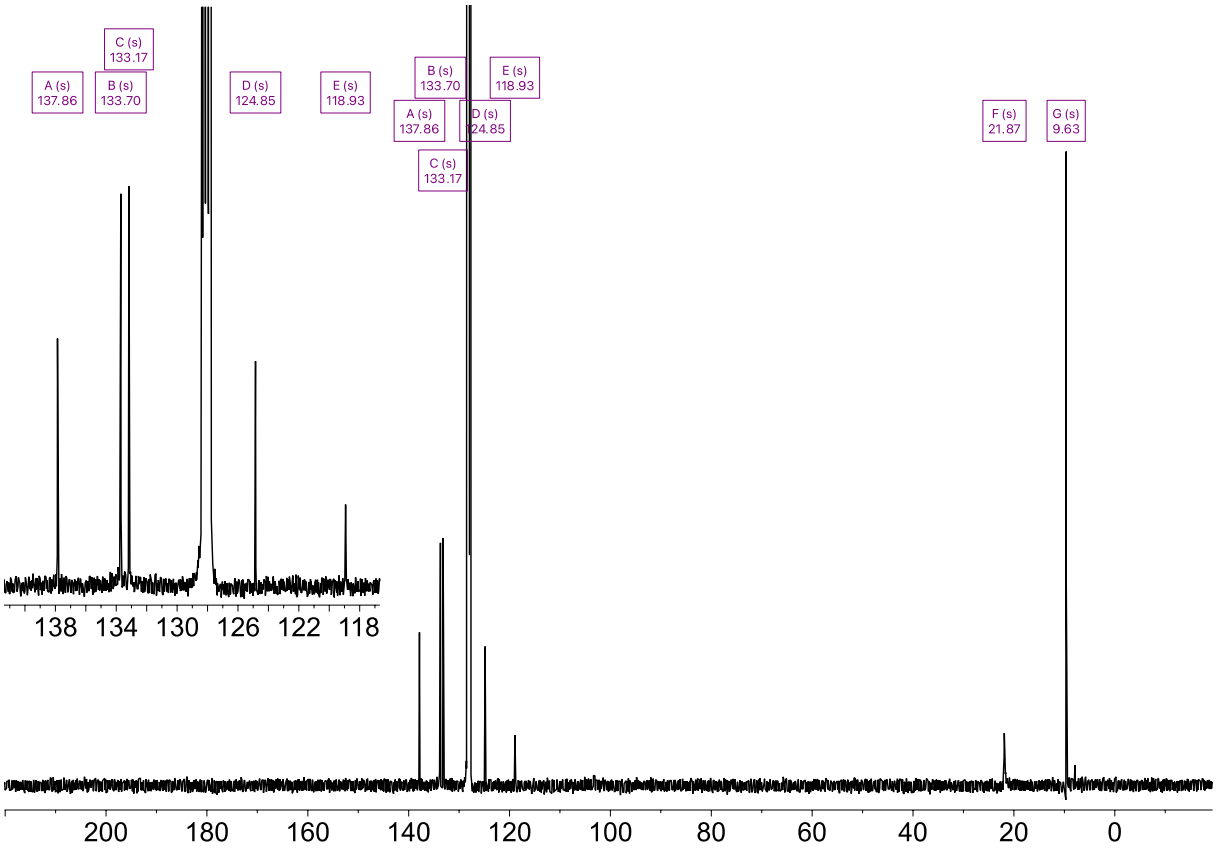

Figure S20: $^{13}C\{^{1}H\}$ NMR spectrum of **8** in C_6D_6 at 298 K, 125 MHz.

Compound 9

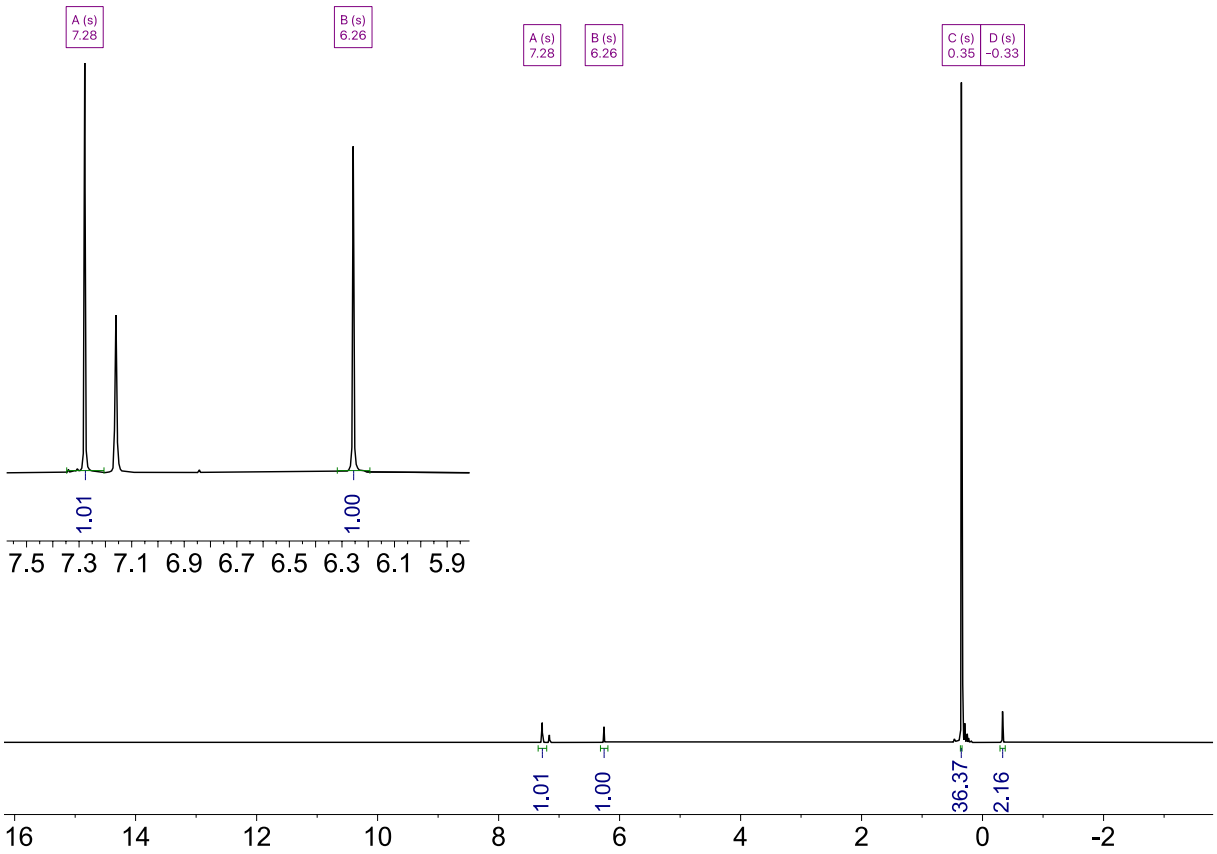

Figure S21: ^{1}H NMR spectrum of **9** in C_6D_6 at 298 K, 500 MHz.

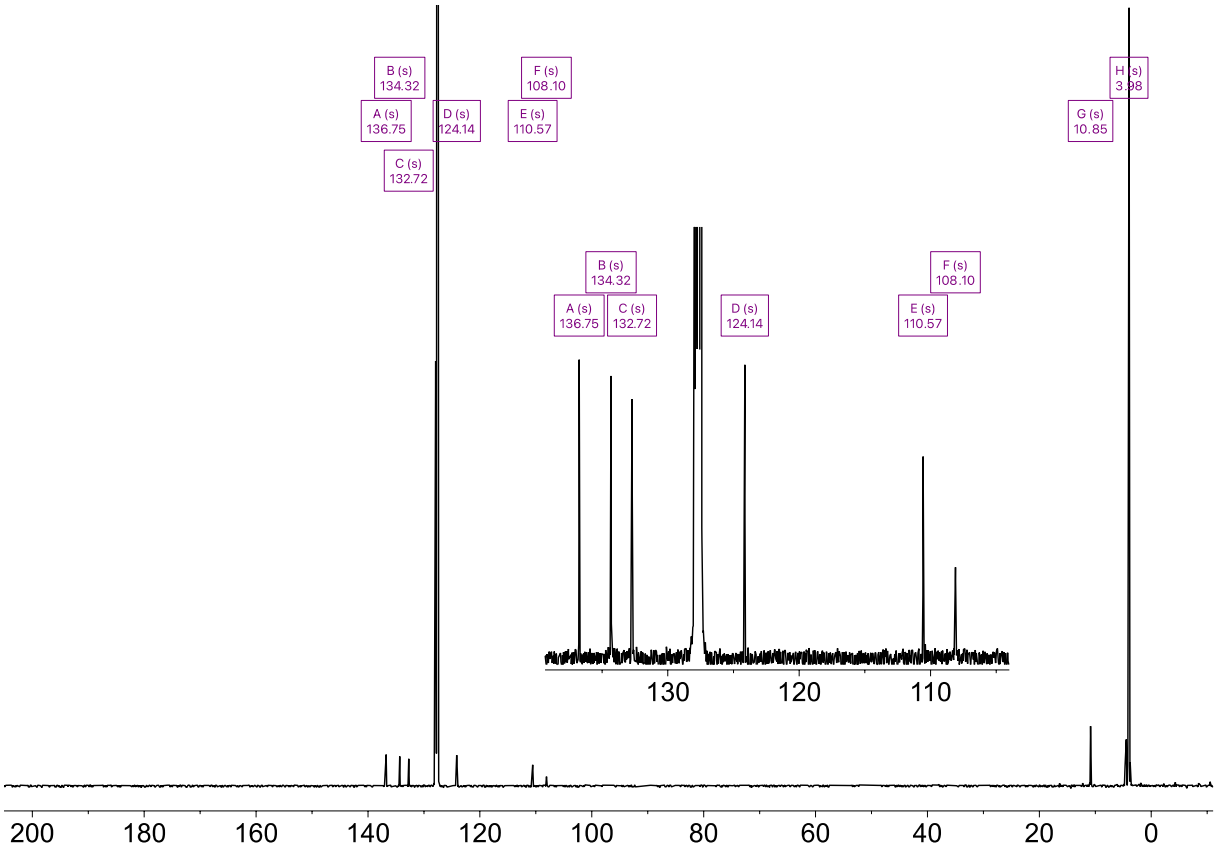

Figure S22: $^{13}C\{^{1}H\}$ NMR spectrum of **9** in C_6D_6 at 298 K, 125 MHz.

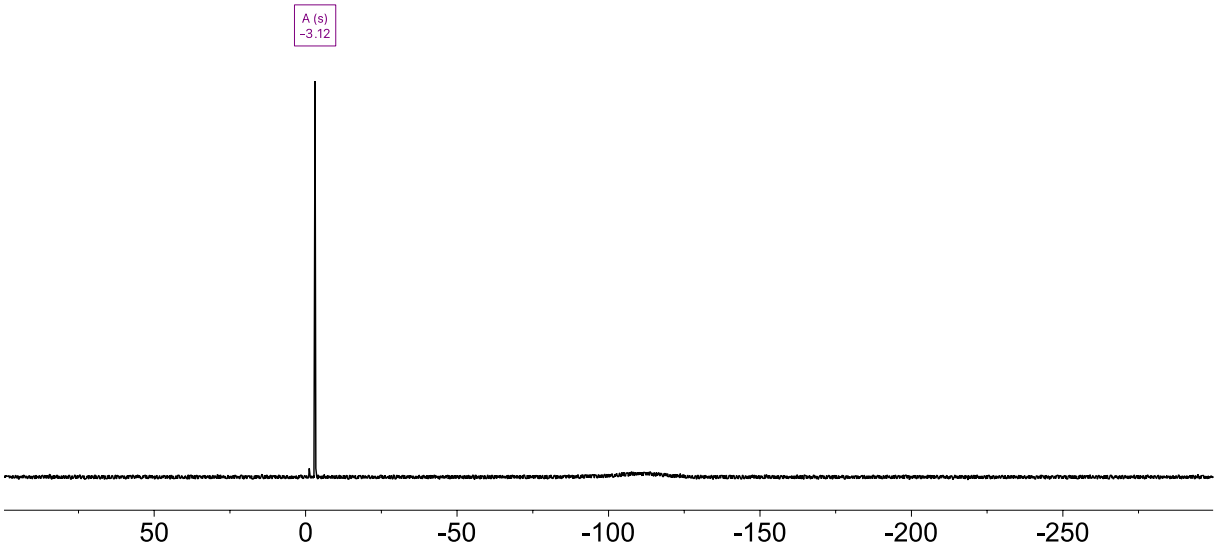

Figure S23: $^{29}Si\{^{1}H\}$ NMR spectrum of **9** in C_6D_6 at 298 K, 99 MHz. The peak at –110 ppm is due to the silicon atoms in the glass.

Adduct **7**·4^{t}BuNC

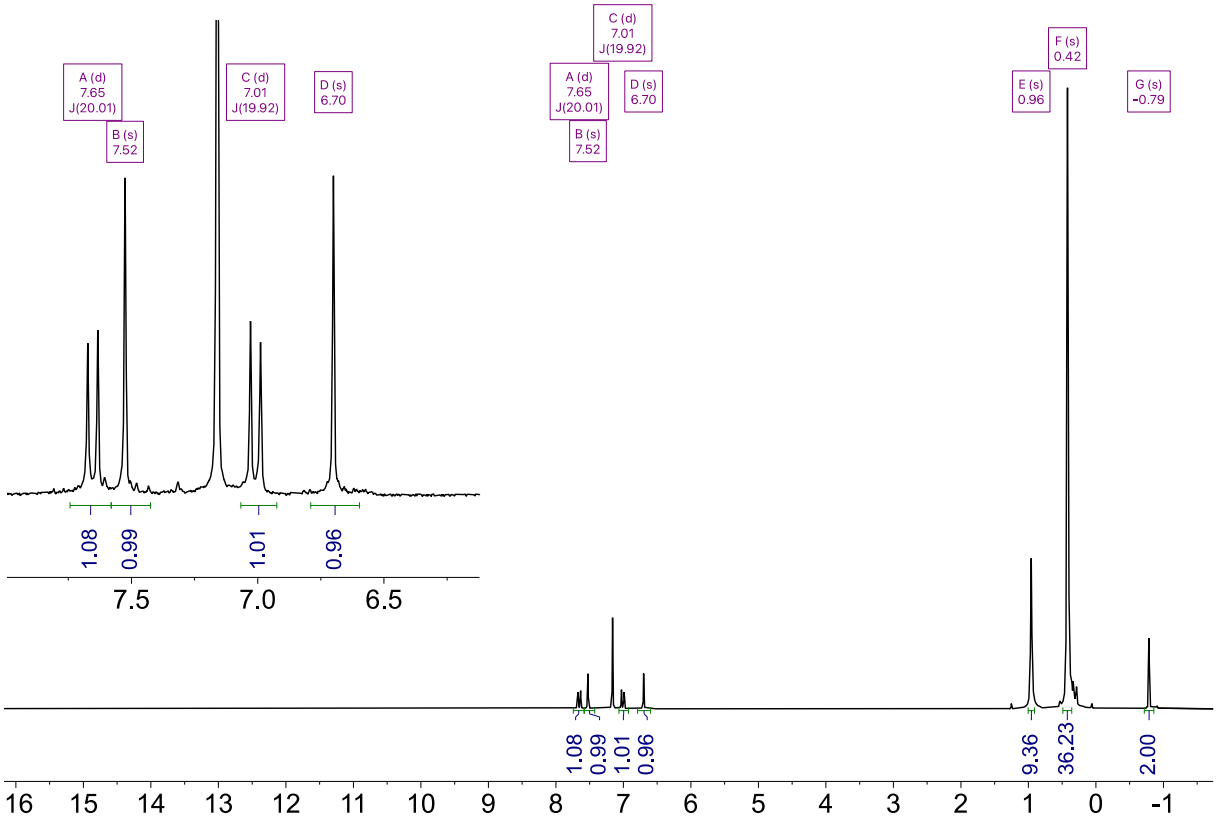

Figure S24: ^{1}H NMR spectrum of **7**·4^{t}BuNC in C_6D_6 at 298 K, 500 MHz.

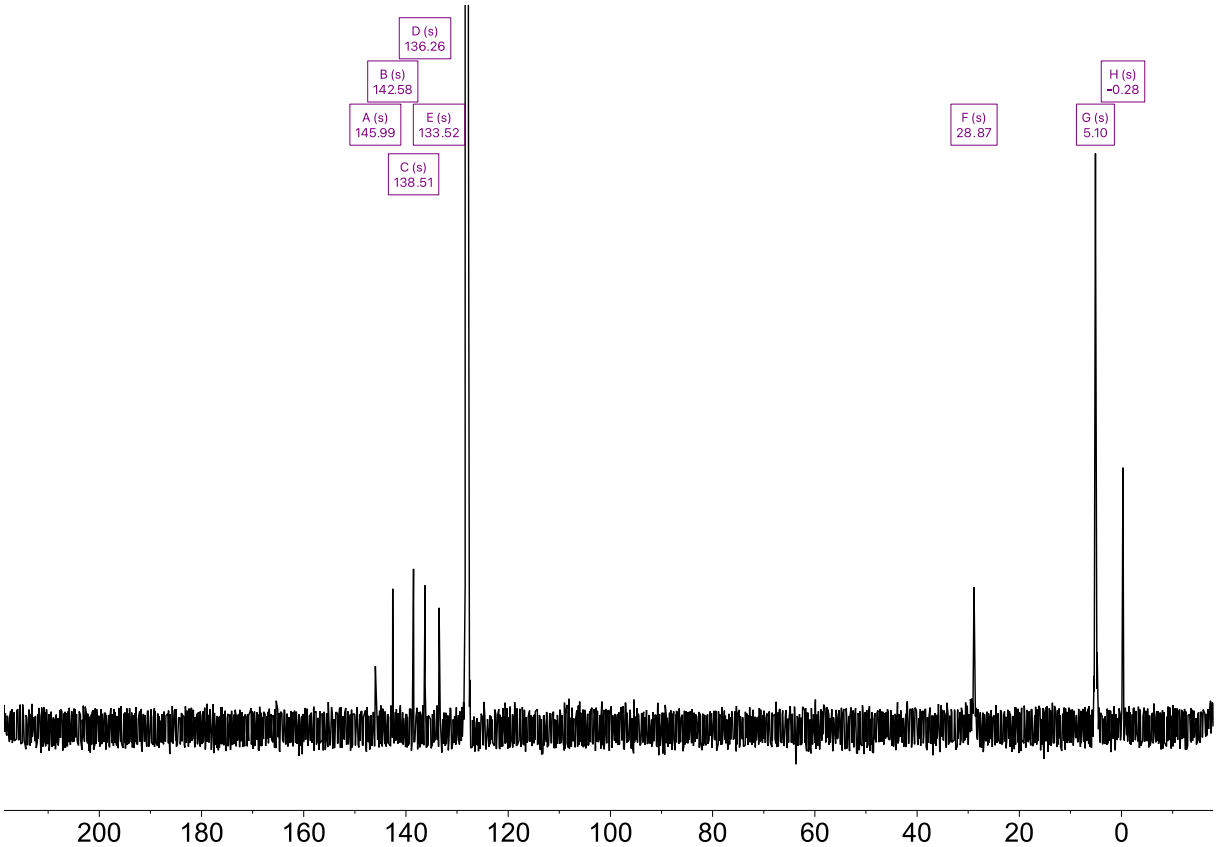

Figure S25: ^{13}C{^{1}H} NMR spectrum of **7**·4^{t}BuNC in C_6D_6 at 298 K, 125 MHz.

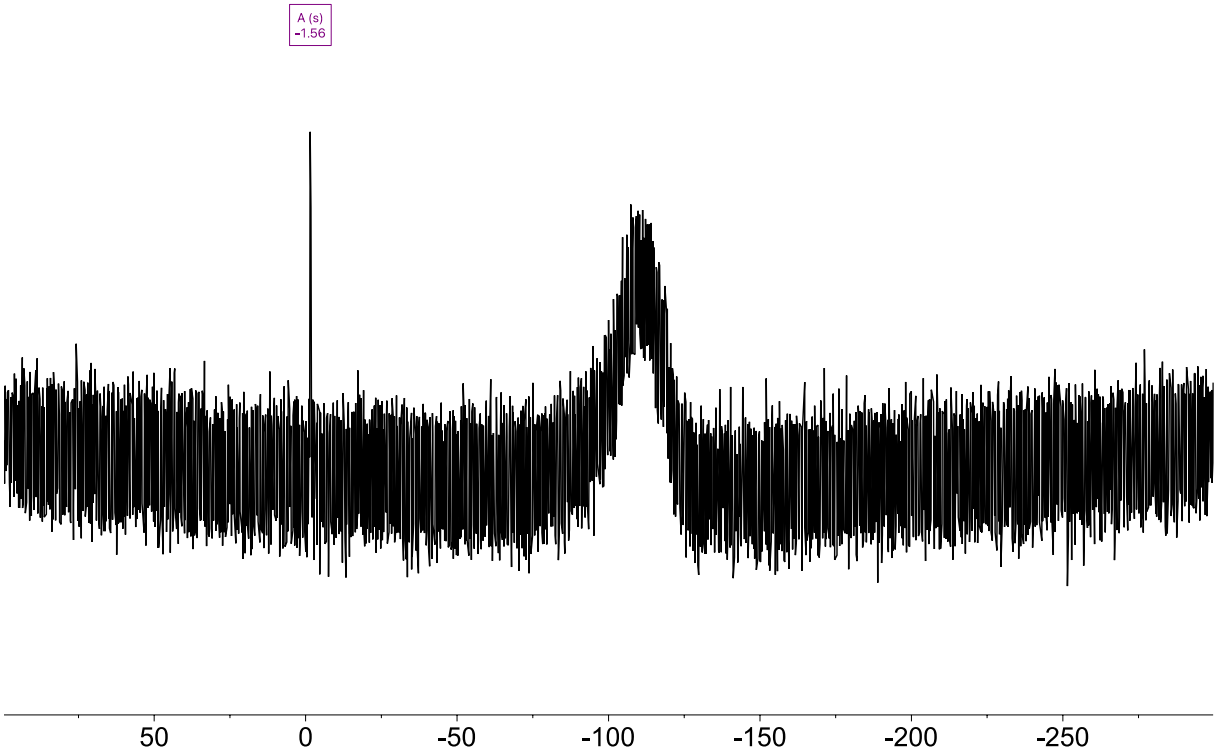

Figure S26: $^{29}Si\{^{1}H\}$ NMR spectrum of **7**·4^{t}BuNC in C_6D_6 at 298 K, 99 MHz.

Adduct **8**·4 ^{t}BuNC

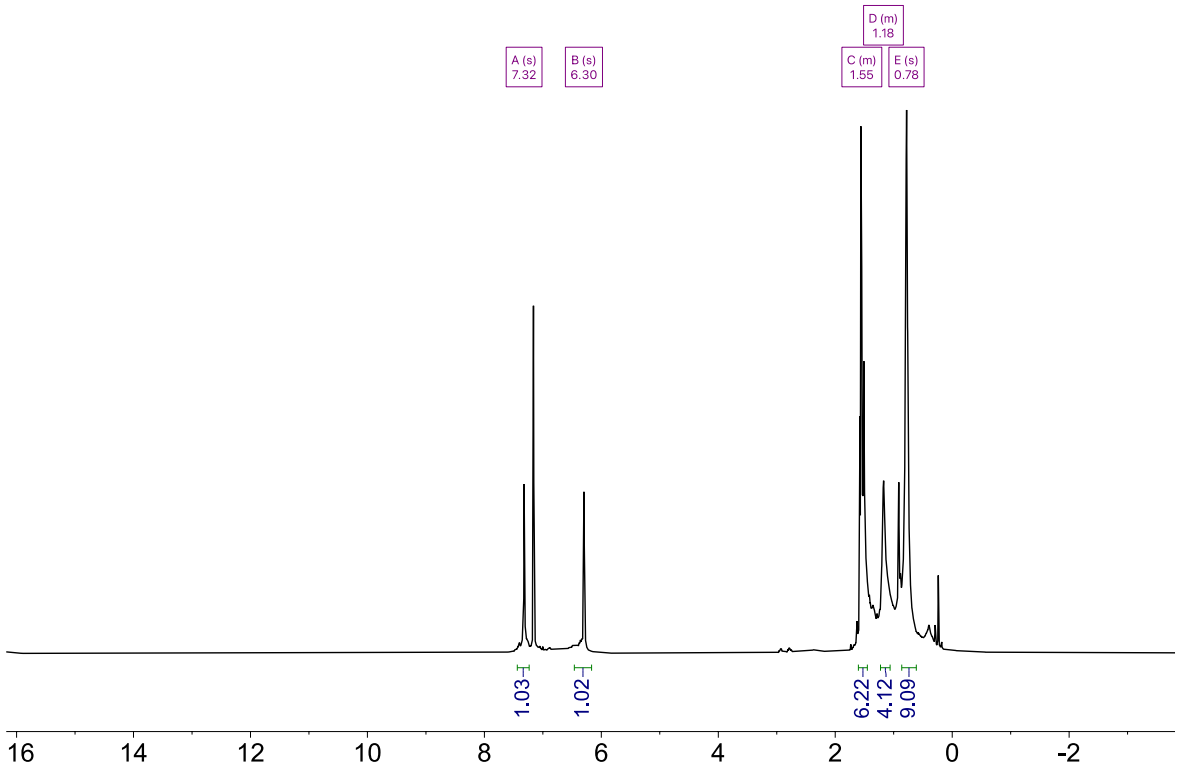

Figure S27: ^{1}H NMR spectrum of **8**·4 ^{t}BuNC in C_6D_6 at 298 K, 500 MHz.

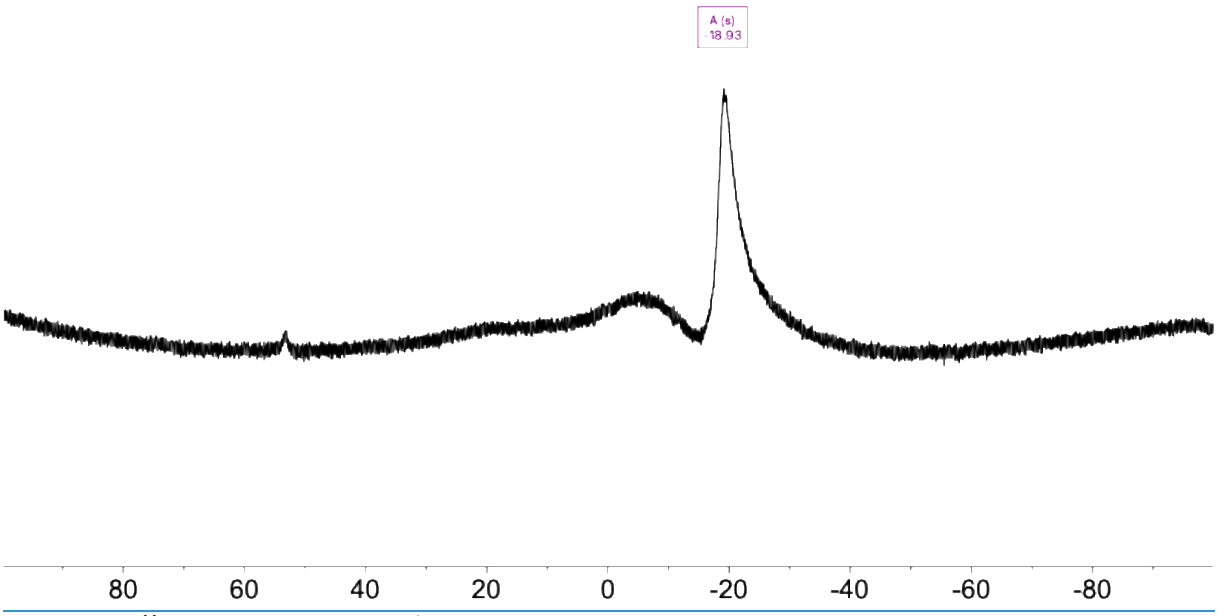

Figure S28: ^{11}B NMR spectrum of **8**·4 ^{t}BuNC in C_6D_6 at 298 K, 160 MHz. The peak at 0 to –25 ppm is due to the boron atoms in the glass.

Adduct **9**·4 ^{t}BuNC

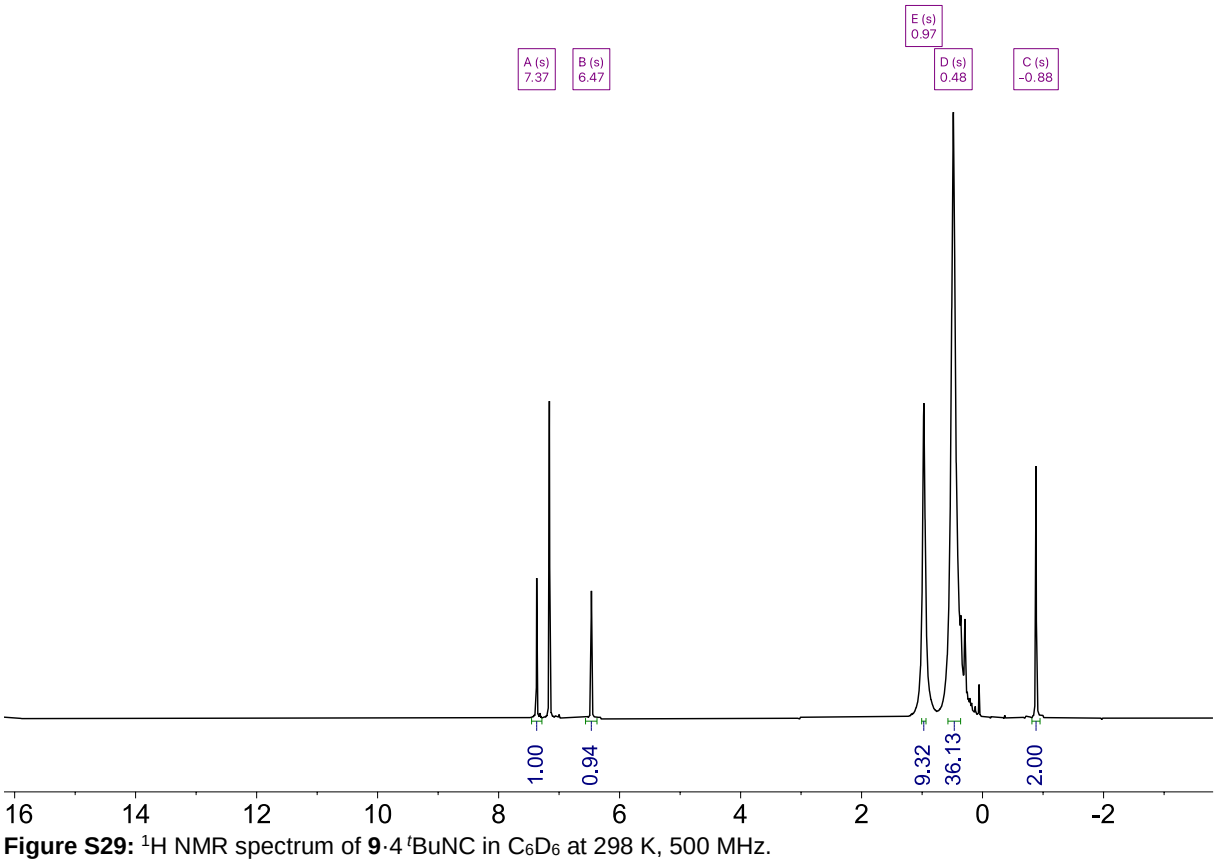

Figure S29: ^{1}H NMR spectrum of **9**·4 ^{t}BuNC in C_6D_6 at 298 K, 500 MHz.

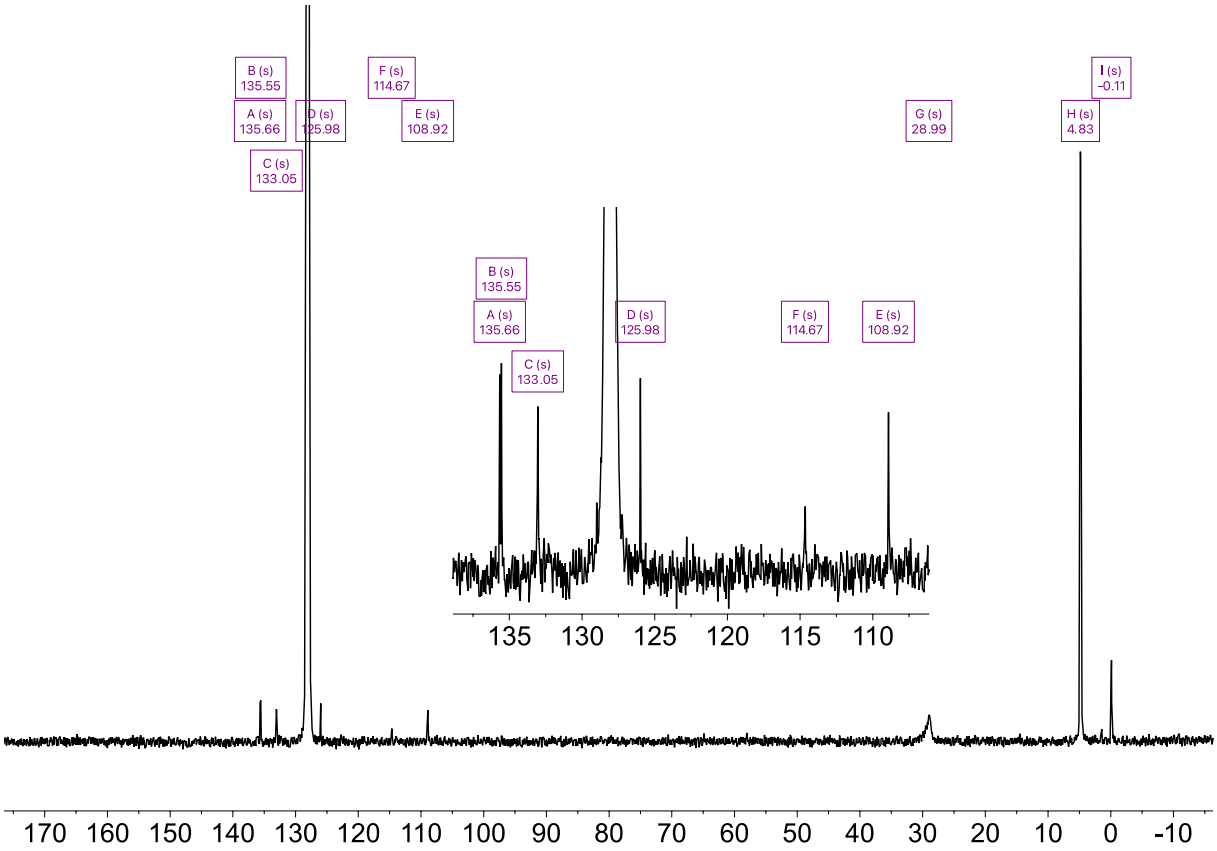

Figure S30: $^{13}C\{^{1}H\}$ NMR spectrum of **9**·4 ^{t}BuNC in C_6D_6 at 298 K, 125 MHz.

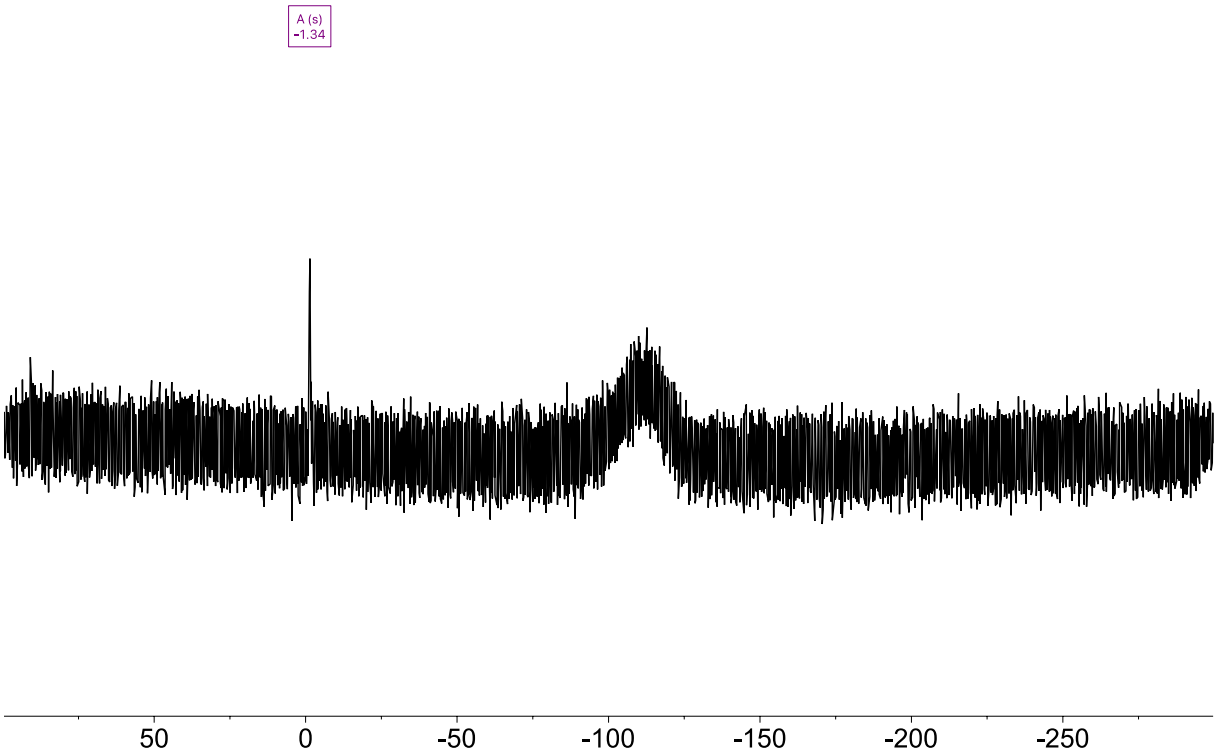

Figure S31: $^{29}Si\{^{1}H\}$ NMR spectrum of **9**·4 ^{t}BuNC in C_6D_6 at 298 K, 99 MHz. The peak at –110 ppm is due to the silicon atoms in the glass.

Adduct 6·4Py

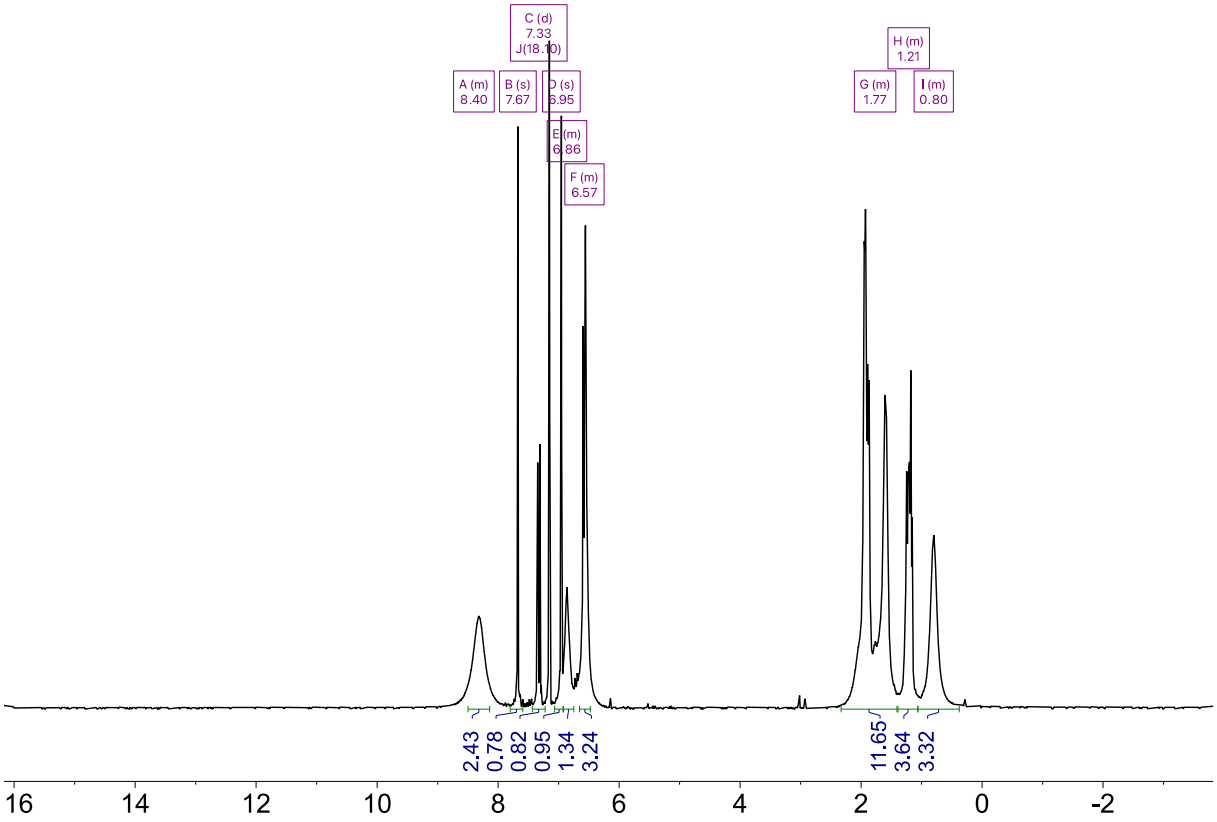

Figure S32: ^{1}H NMR spectrum of **6**·4Py in C_6D_6 at 298 K, 500 MHz.

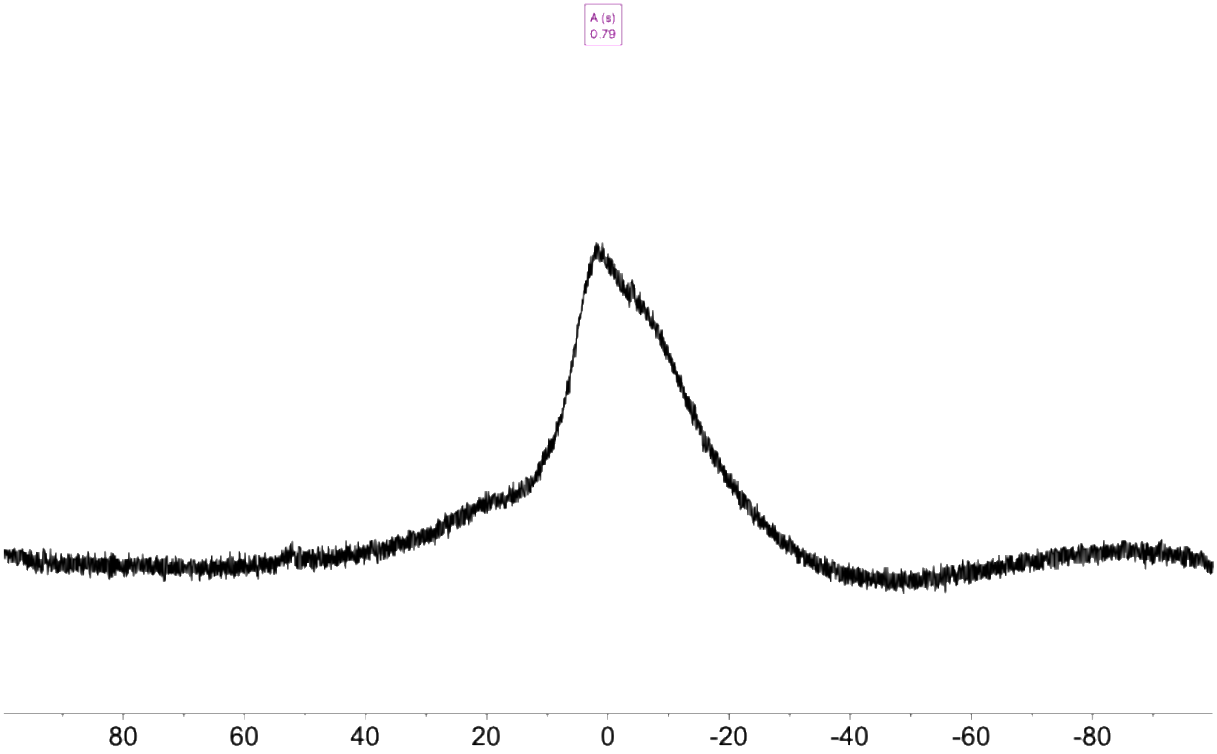

Figure S33: ^{11}B NMR spectrum of **6**·4Py in C_6D_6 at 298 K, 160 MHz. The signal is partially superimposed by the signal of the boron atoms 0 to –25 ppm contained in the glass.

Adduct **7**·4Py

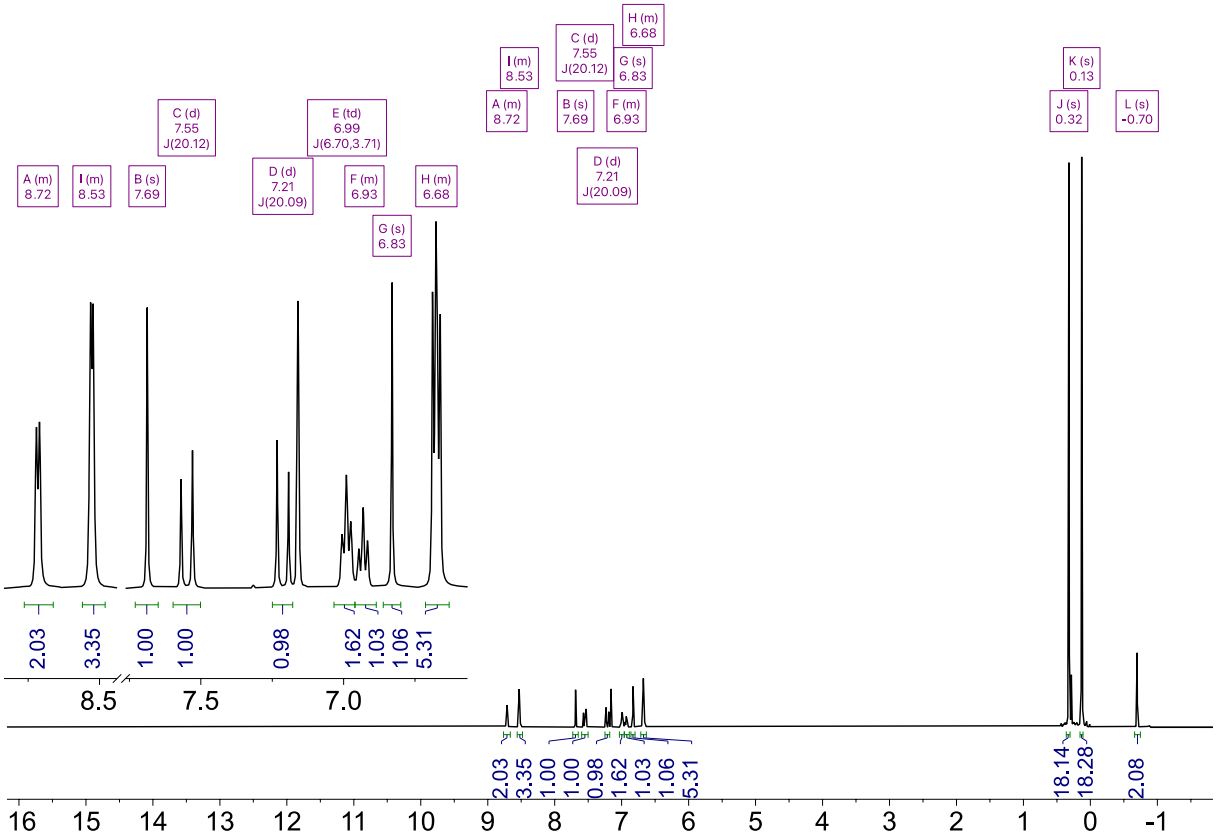

Figure S34: ^{1}H NMR spectrum of **7**·4Py in C_6D_6 at 298 K, 500 MHz. The signals at 8.53, 6.99, 6.68 (overlaid with bound pyridine) ppm come from 6.7 eq free pyridine.

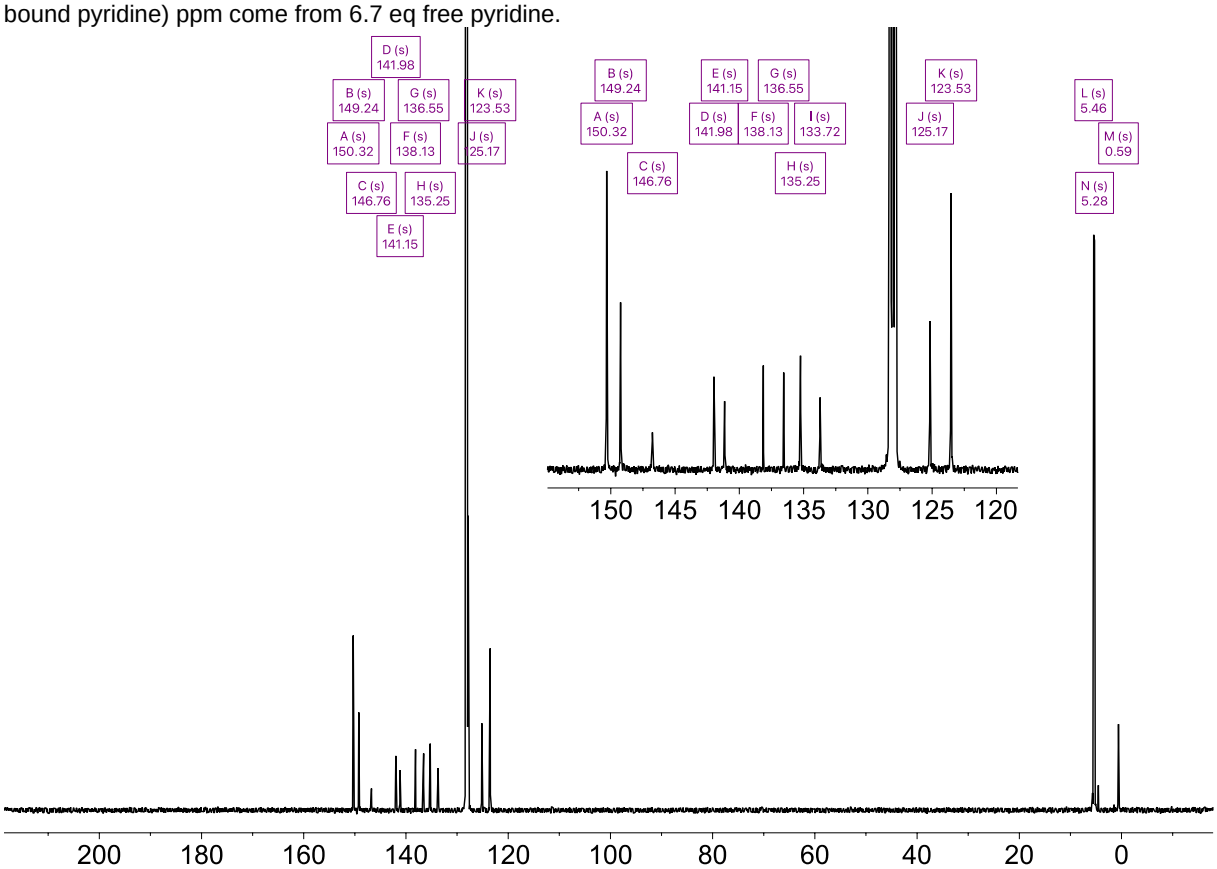

Figure S35: $^{13}C\{^{1}H\}$ NMR spectrum of **7**·4Py in C_6D_6 at 298 K, 125 MHz. The signals at 150.3, 135.3, 123.5 ppm come from 6.7 eq free pyridine.

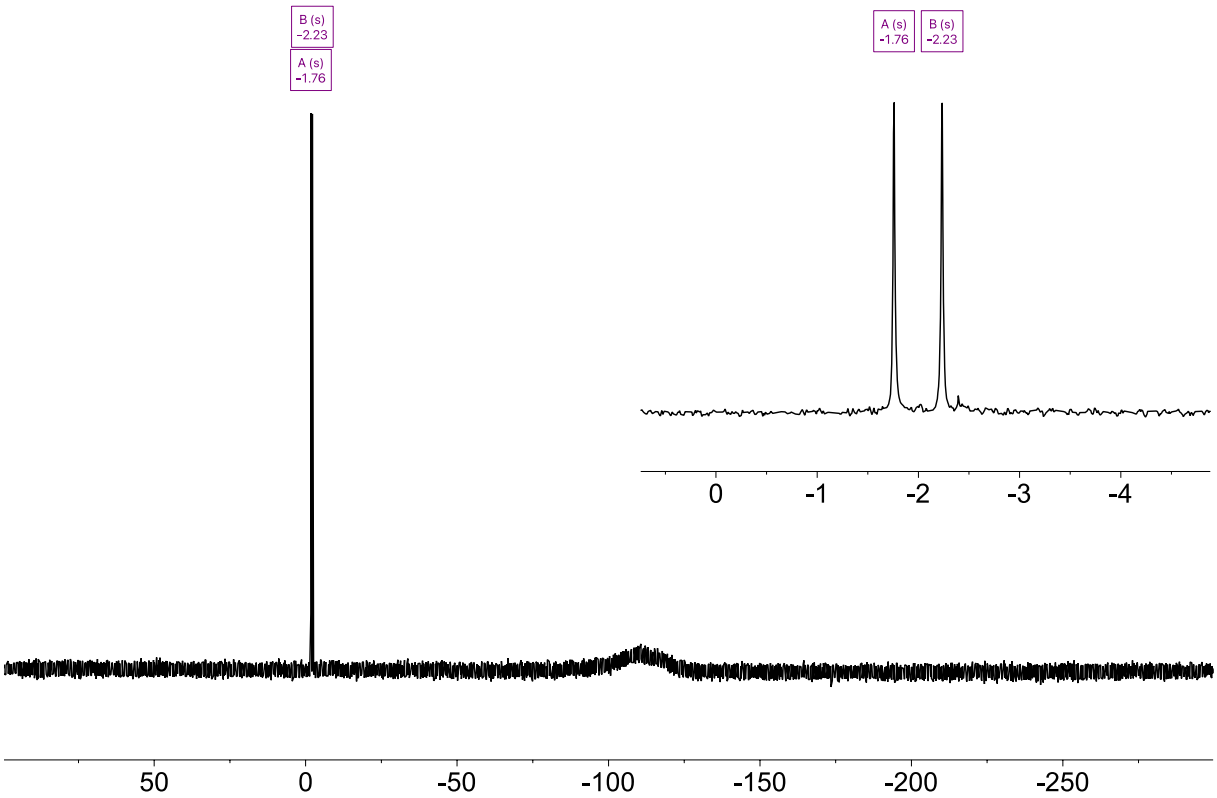

Figure S36: $^{29}Si\{^{1}H\}$ NMR spectrum of **7**·4Py in C_6D_6 at 298 K, 99 MHz. The peak at –110 ppm is due to the silicon atoms in the glass.

Adduct **8**·4Py

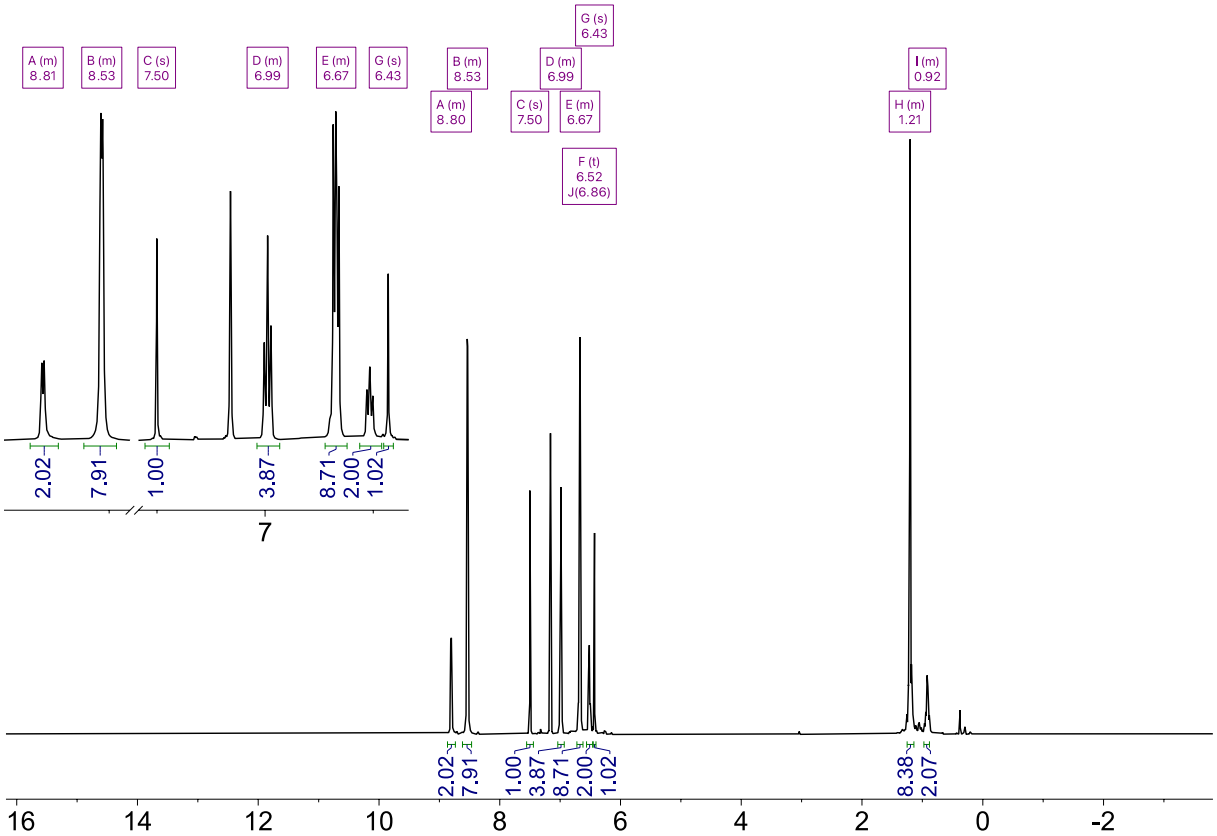

Figure S37: ^{1}H NMR spectrum of **8**·4Py in C_6D_6 at 298 K, 500 MHz. The signals at 8.53, 6.99, 6.67 (overlaid with bound pyridine) ppm come from 6.7 eq free pyridine.

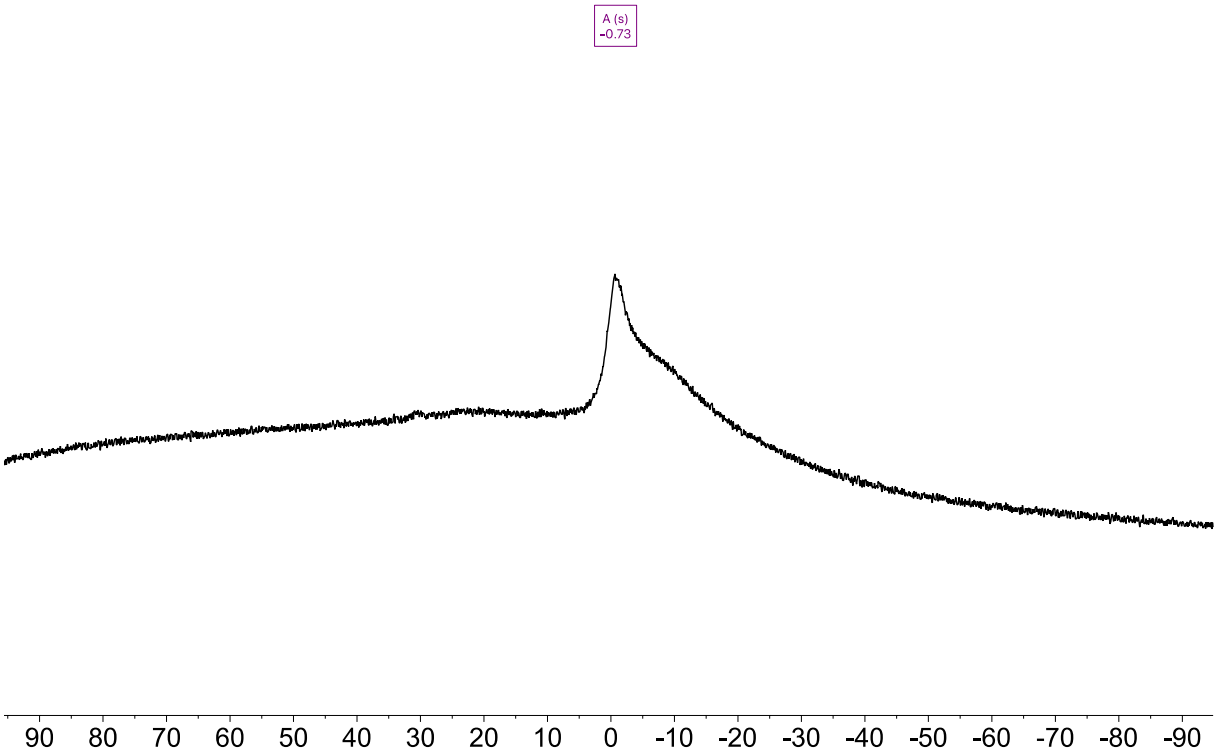

Figure S38: ^{11}B NMR spectrum of **8**·4Py in C_6D_6 at 298 K, 160 MHz. The signal is partially superimposed by the signal of the boron atoms 0 to –25 ppm contained in the glass.

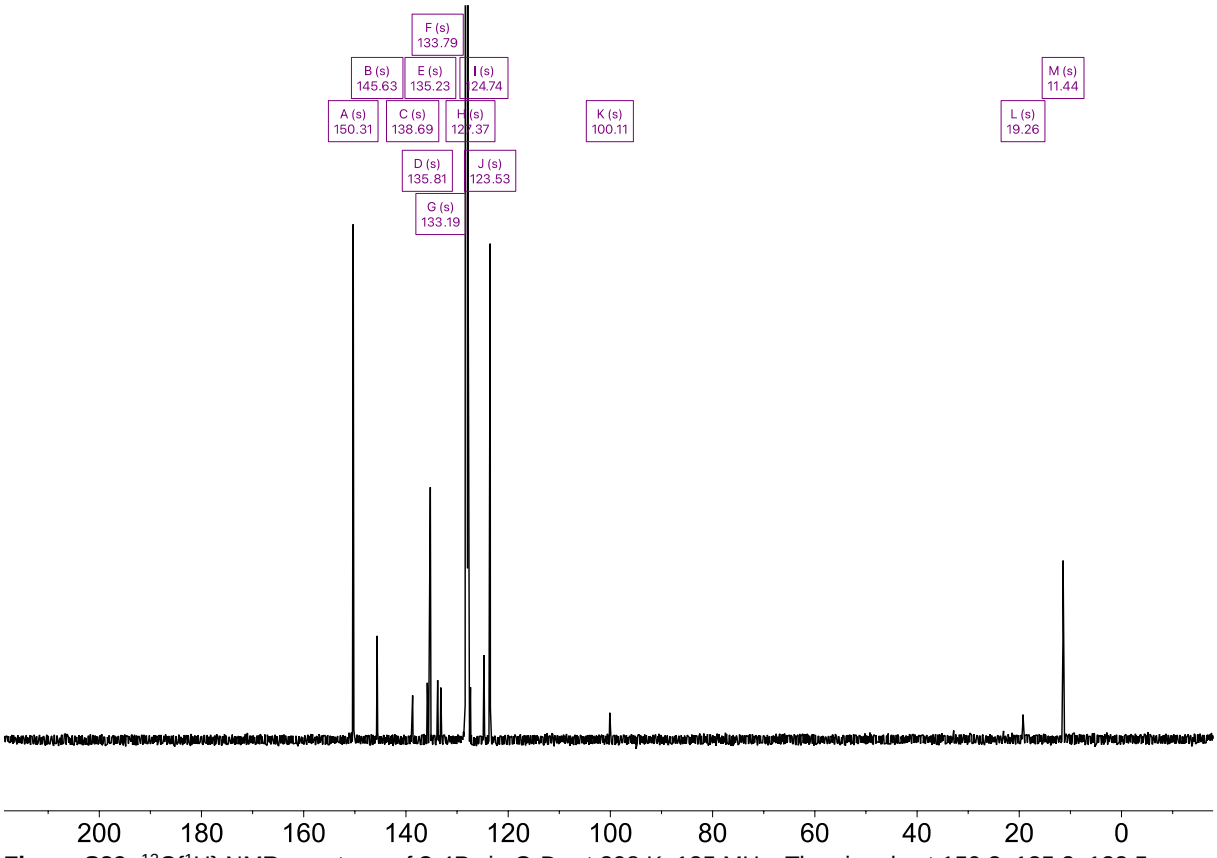

Figure S39: ^{13}C{^{1}H} NMR spectrum of **8**·4Py in C_6D_6 at 298 K, 125 MHz. The signals at 150.3, 135.2, 123.5 ppm come from 15.8 eq free pyridine.

Adduct **9**·4Py

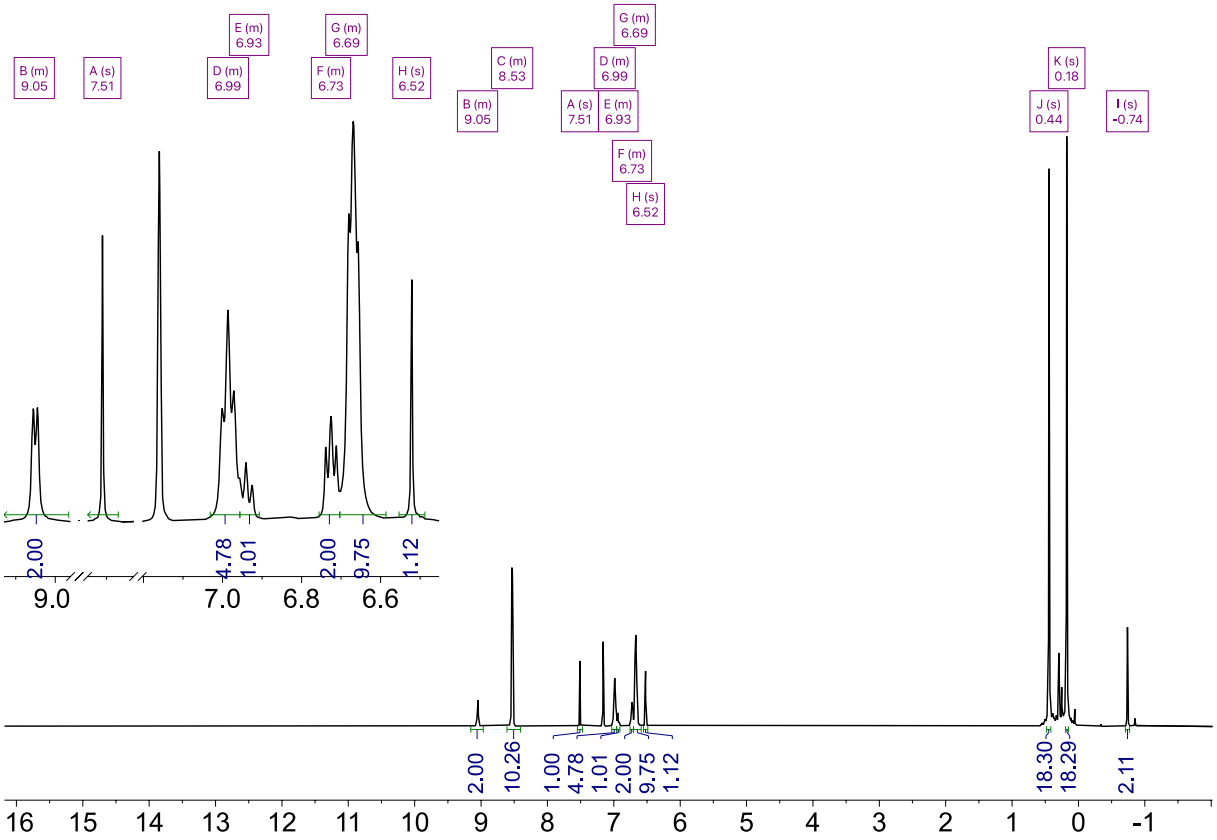

Figure S40: ^{1}H NMR spectrum of **9**·4Py in C_6D_6 at 298 K, 500 MHz. The signals at 8.53, 6.99, 6.68 ppm come from 20.5 eq free pyridine.

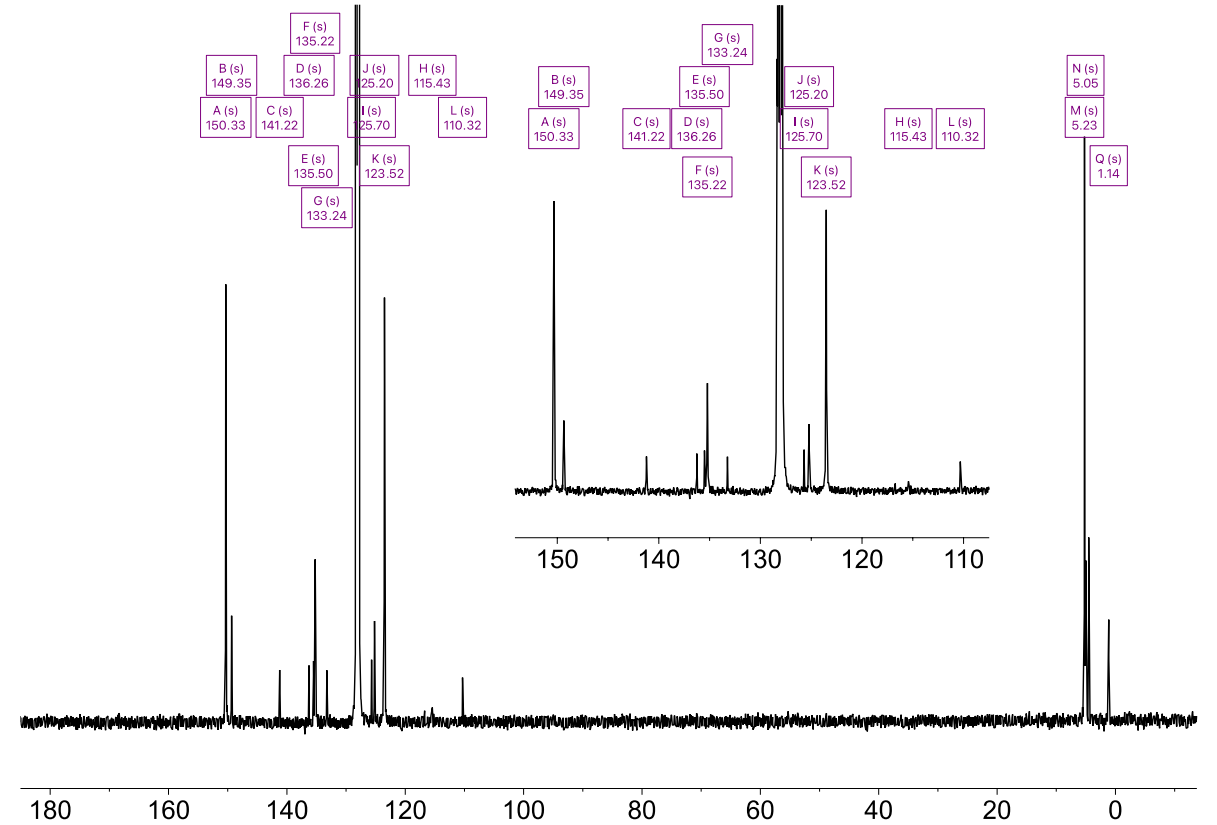

Figure S41: ^{13}C{^{1}H} NMR spectrum of **9**·4Py in C_6D_6 at 298 K, 125 MHz. The signals at 150.3, 135.2, 123.5 ppm come from 20.5 eq free pyridine.

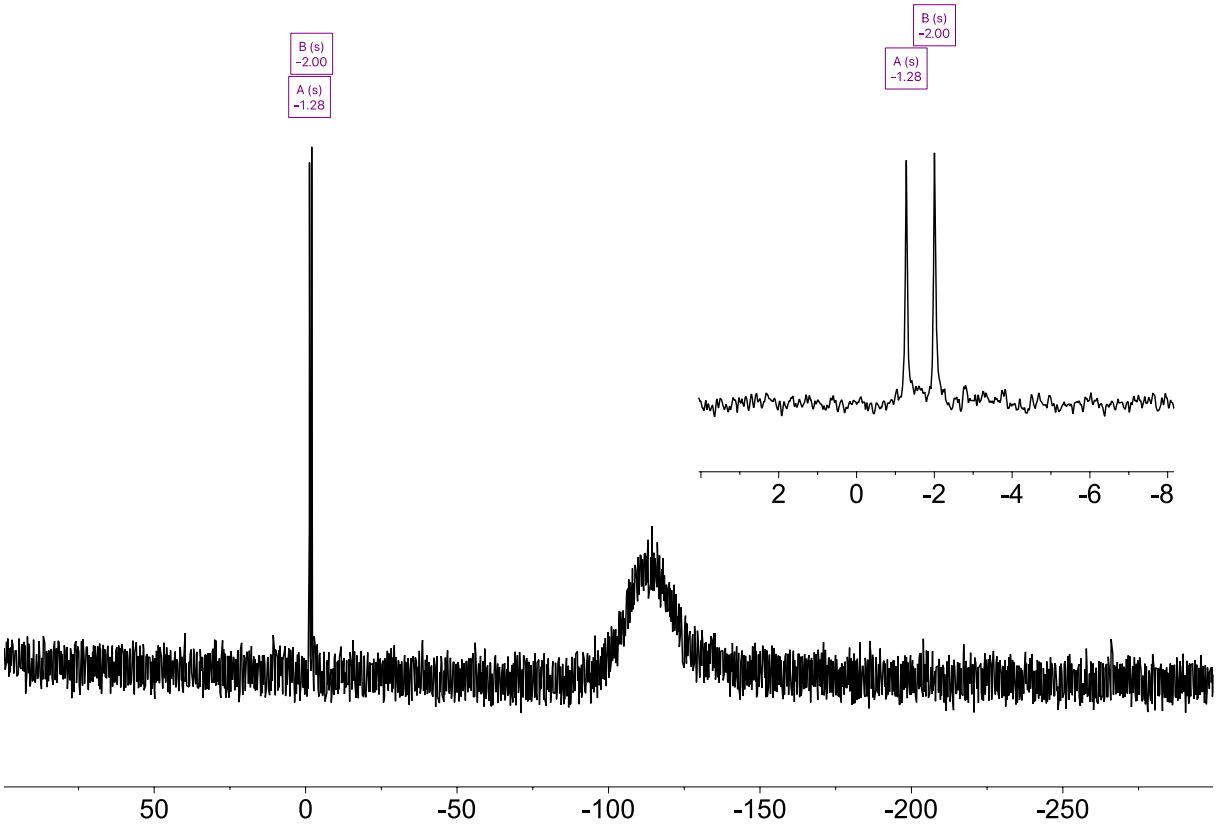

Figure S42: $^{29}Si\{^{1}H\}$ NMR spectrum of **9**·4Py in C_6D_6 at 298 K, 99 MHz. The peak at –110 ppm is due to the silicon atoms in the glass.

Adduct **7**·4NMe_3

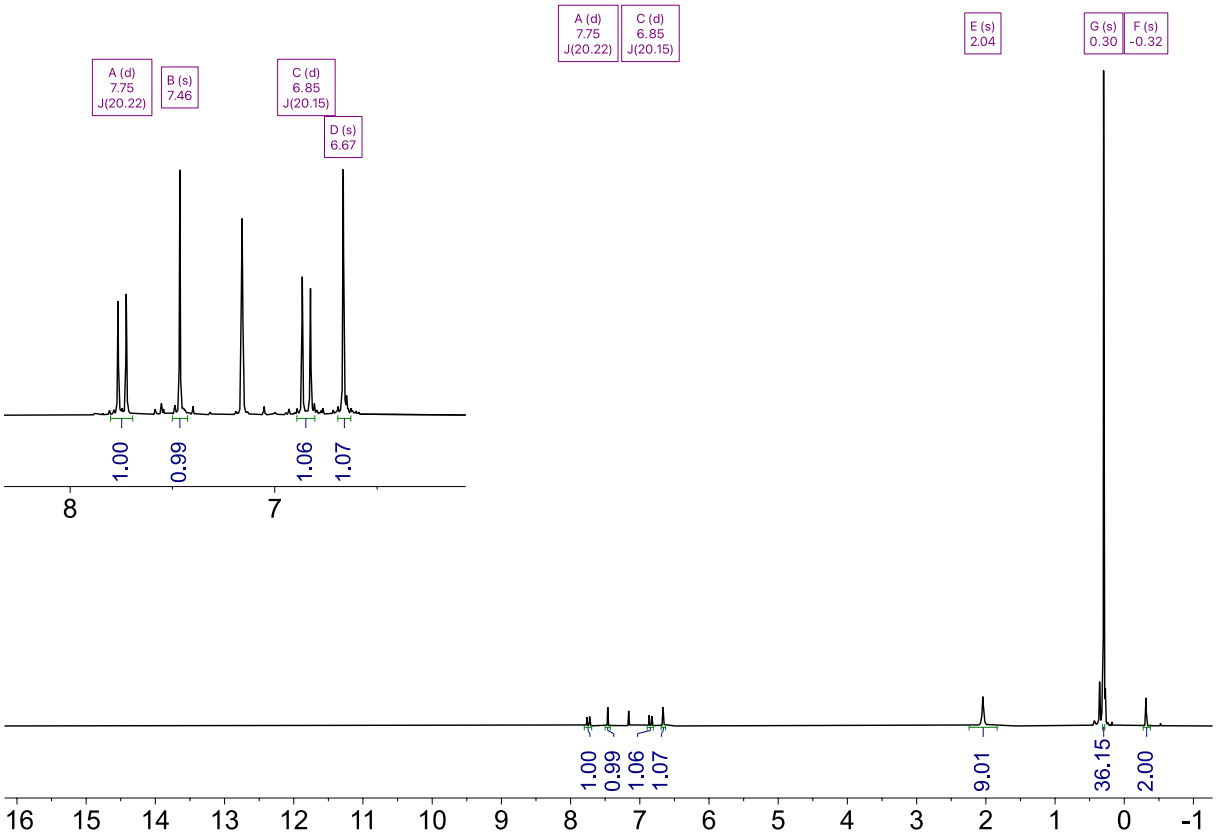

Figure S43: ^{1}H NMR spectrum of **7**·4NMe_3 in C_6D_6 at 298 K, 500 MHz.

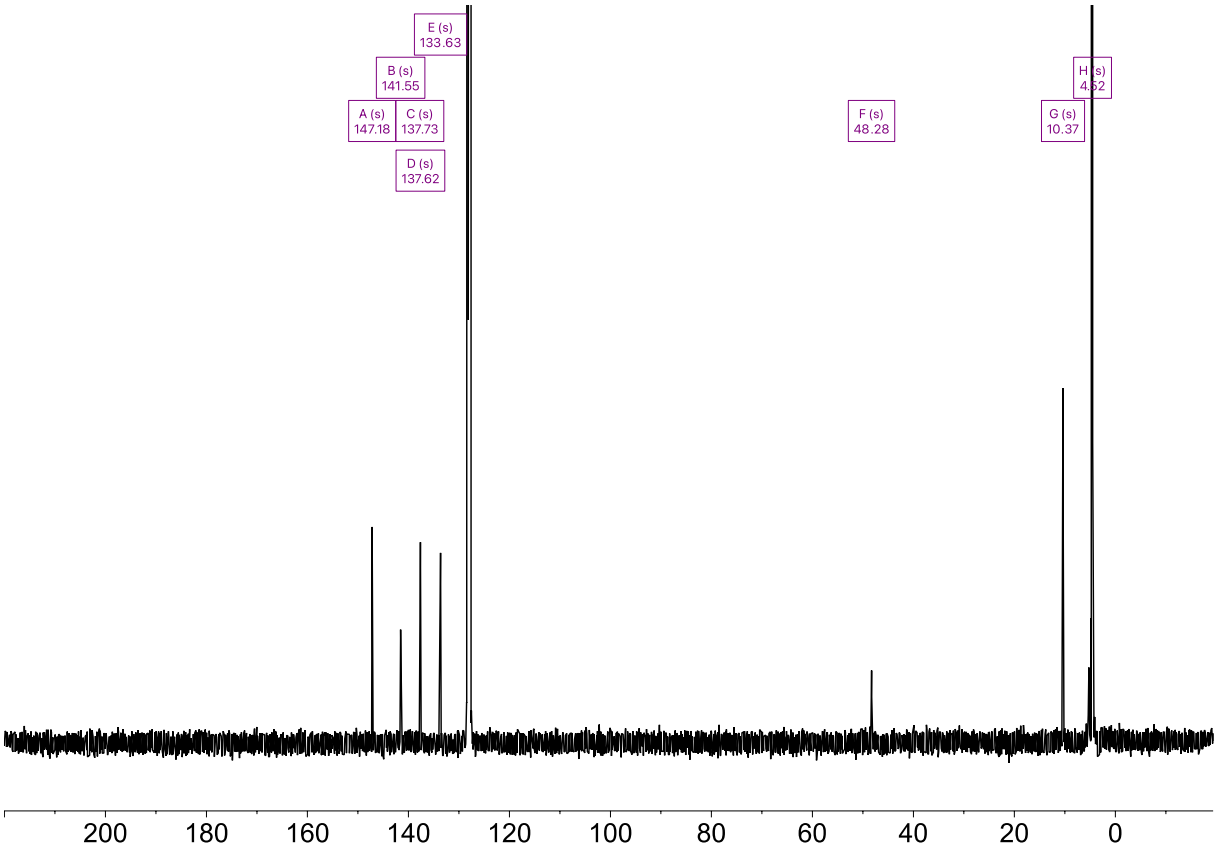

Figure S44: $^{13}C\{^{1}H\}$ NMR spectrum of **7**·4NMe_3 in C_6D_6 at 298 K, 125 MHz.

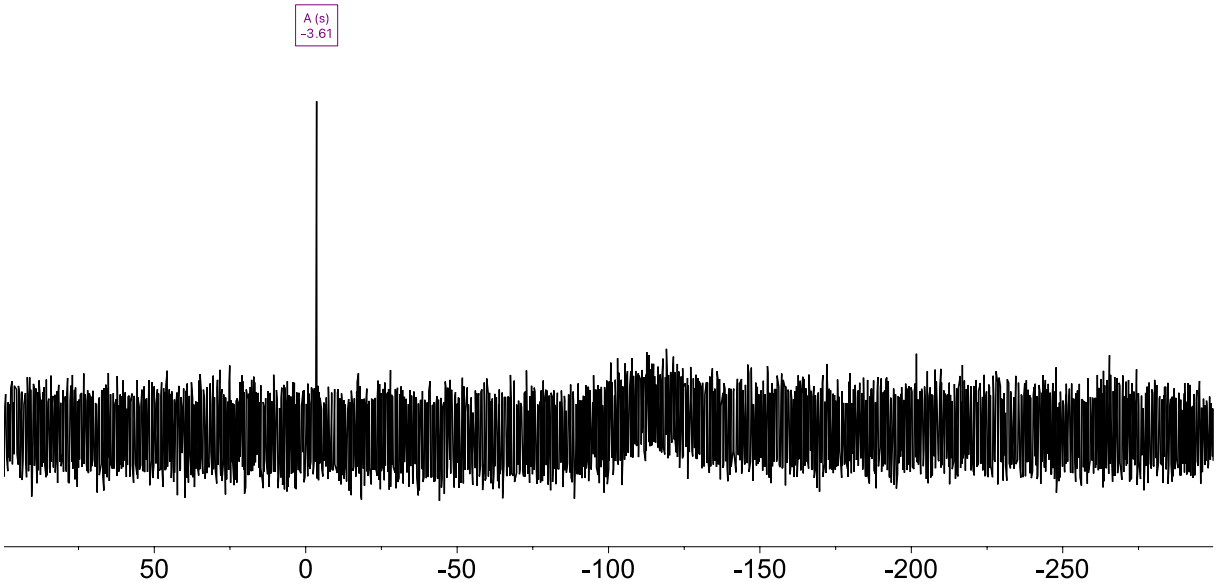

Figure S45: $^{29}Si\{^{1}H\}$ NMR spectrum of **7**·4NMe_3 C_6D_6 at 298 K, 99 MHz. The peak at –110 ppm is due to the silicon atoms in the glass.

Adduct 8·4NMe$_3$

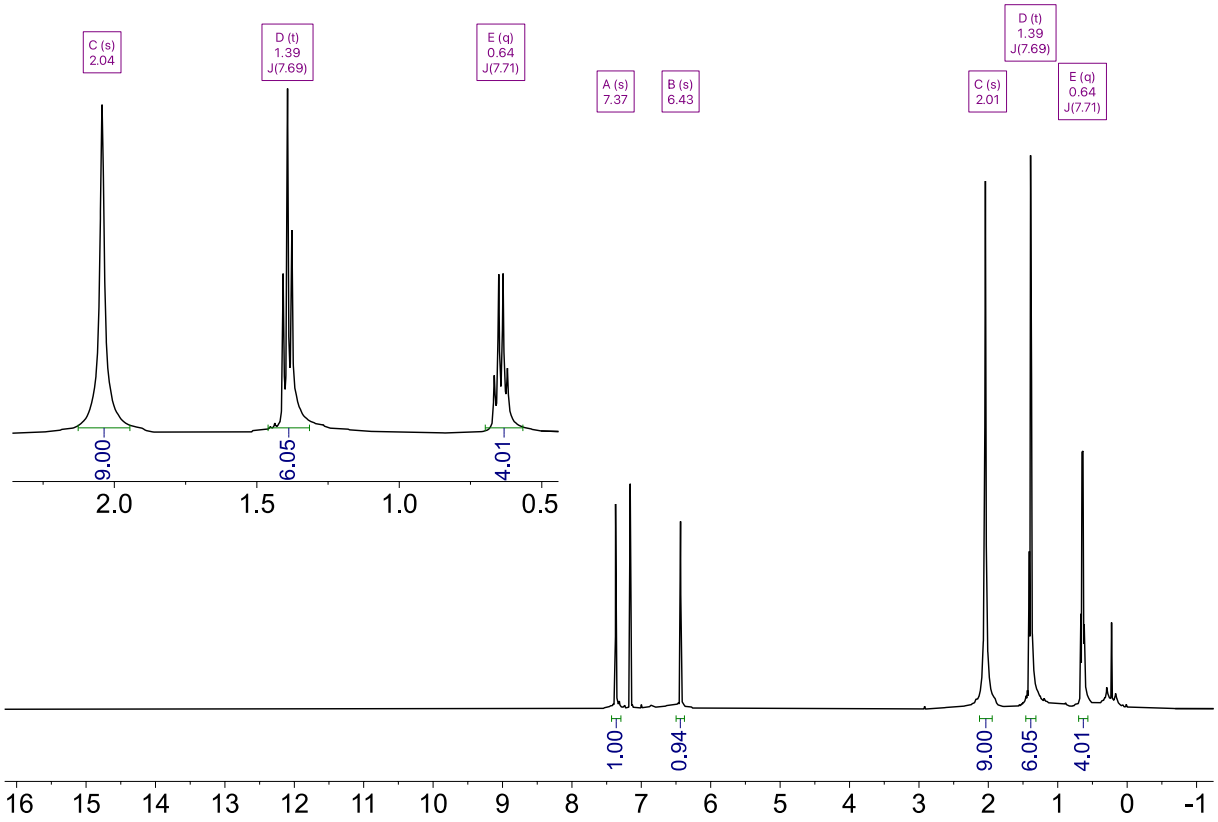

Figure S46: ^{1}H NMR spectrum of **8**·4NMe$_3$ in C_6D_6 at 298 K, 500 MHz.

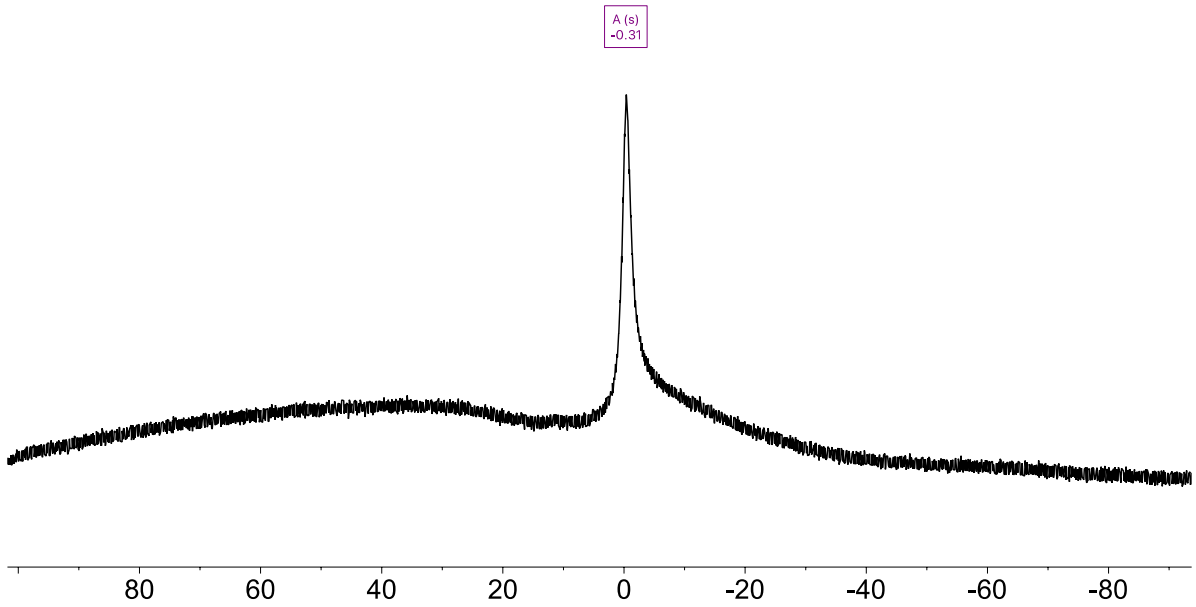

Figure S47: ^{11}B NMR spectrum of **8**·4NMe$_3$ in C_6D_6 at 298 K, 160 MHz. The signal is partially superimposed by the signal of the boron atoms 0 to –25 ppm contained in the glass.

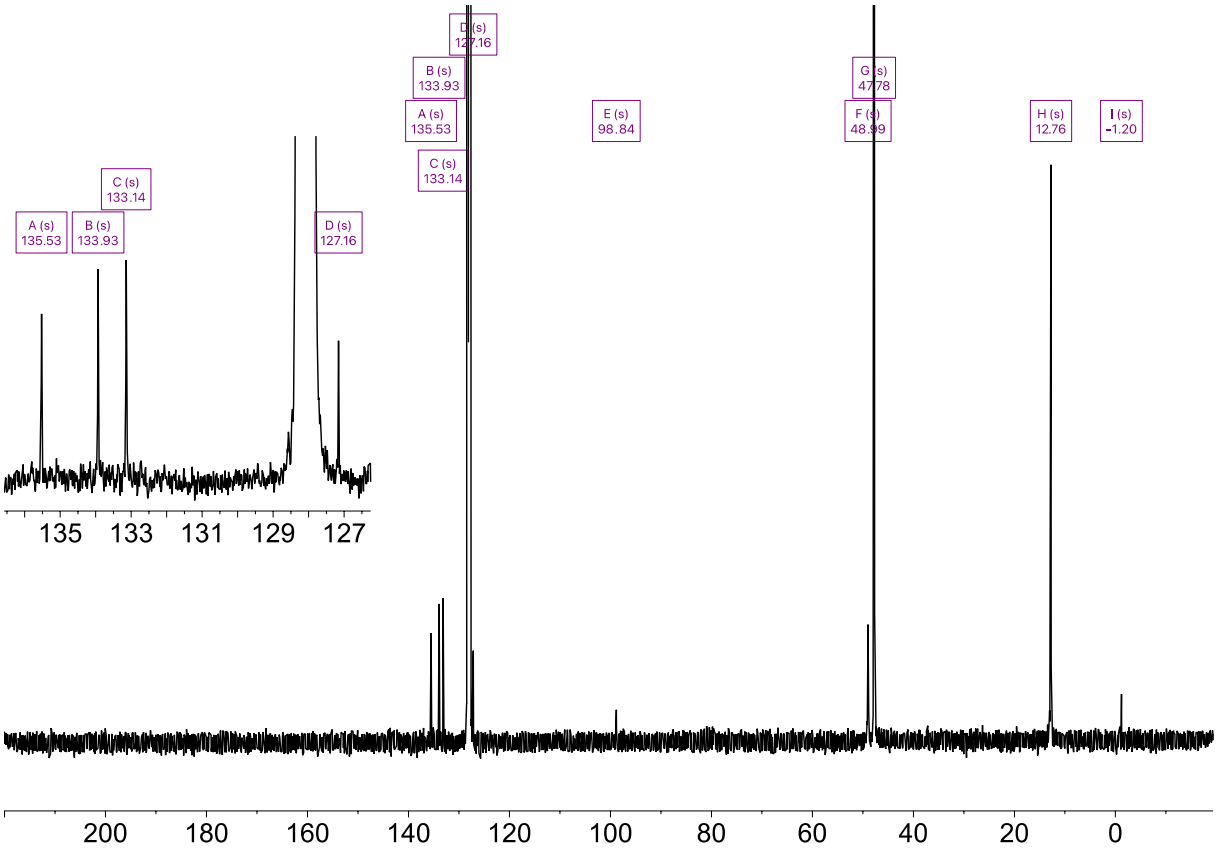

Figure S48: $^{13}C\{^{1}H\}$ NMR spectrum of **8**·4NMe_3 with ex. NMe_3 (47.8 ppm) in C_6D_6 at 298 K, 125 MHz.

Adduct **9**·4NMe_3

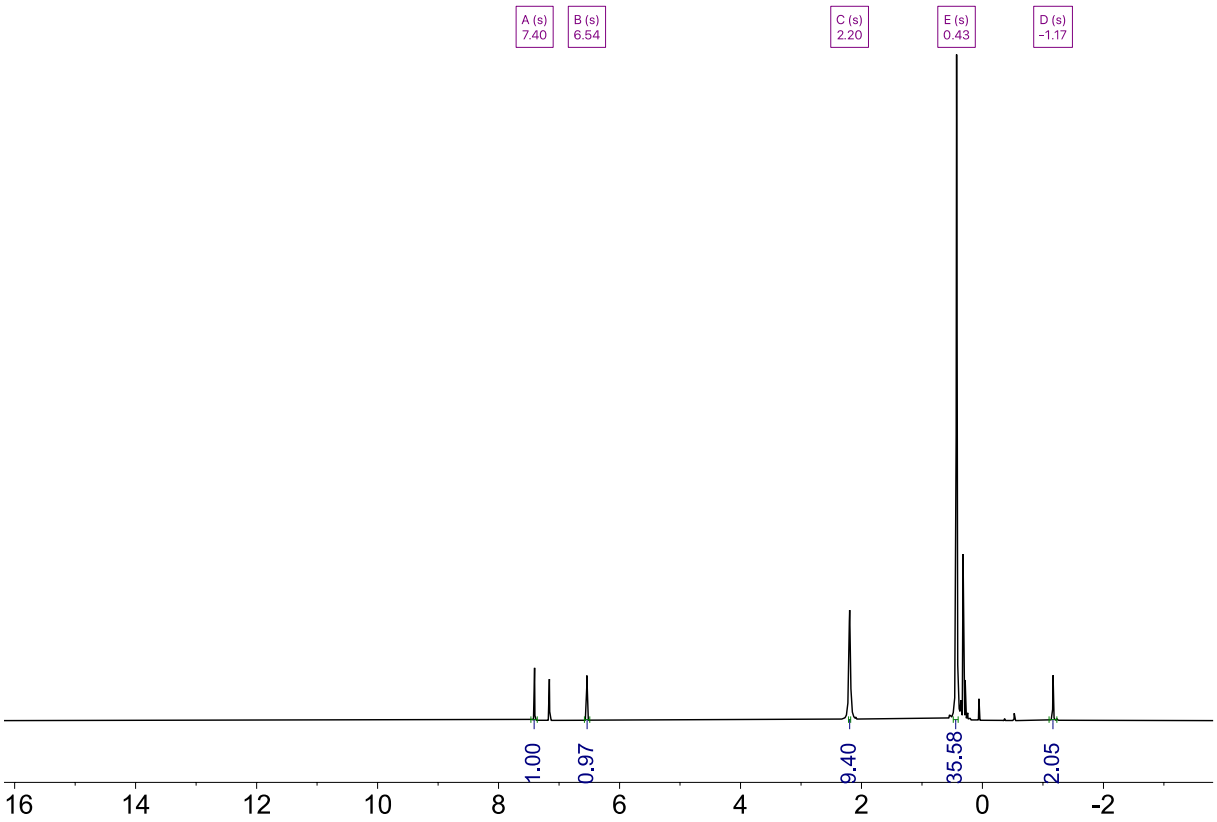

Figure S49: ^{1}H NMR spectrum of **9**·4NMe_3 in C_6D_6 at 298 K, 500 MHz.

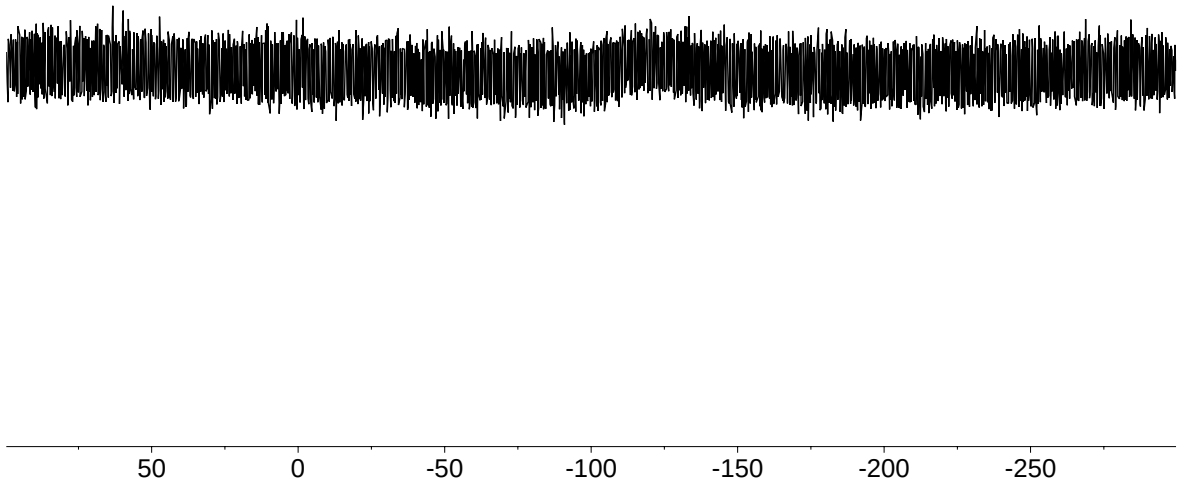

Figure S50: $^{29}Si\{^{1}H\}$ NMR spectrum of **9**·4NMe$_3$ in C_6D_6 at 298 K, 99 MHz.

Adduct **6**·4PMe$_3$

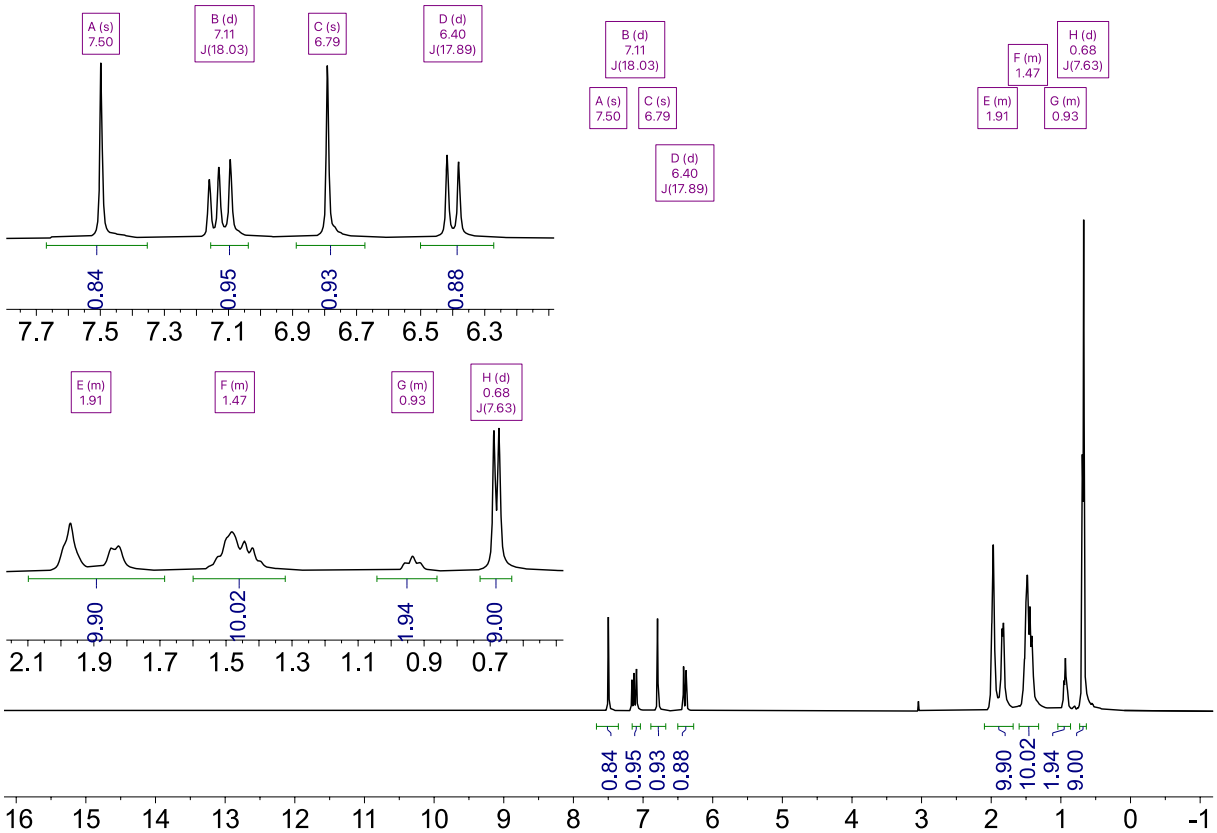

Figure S51: ^{1}H NMR spectrum of **6**·4PMe$_3$ in C_6D_6 at 298 K, 500 MHz.

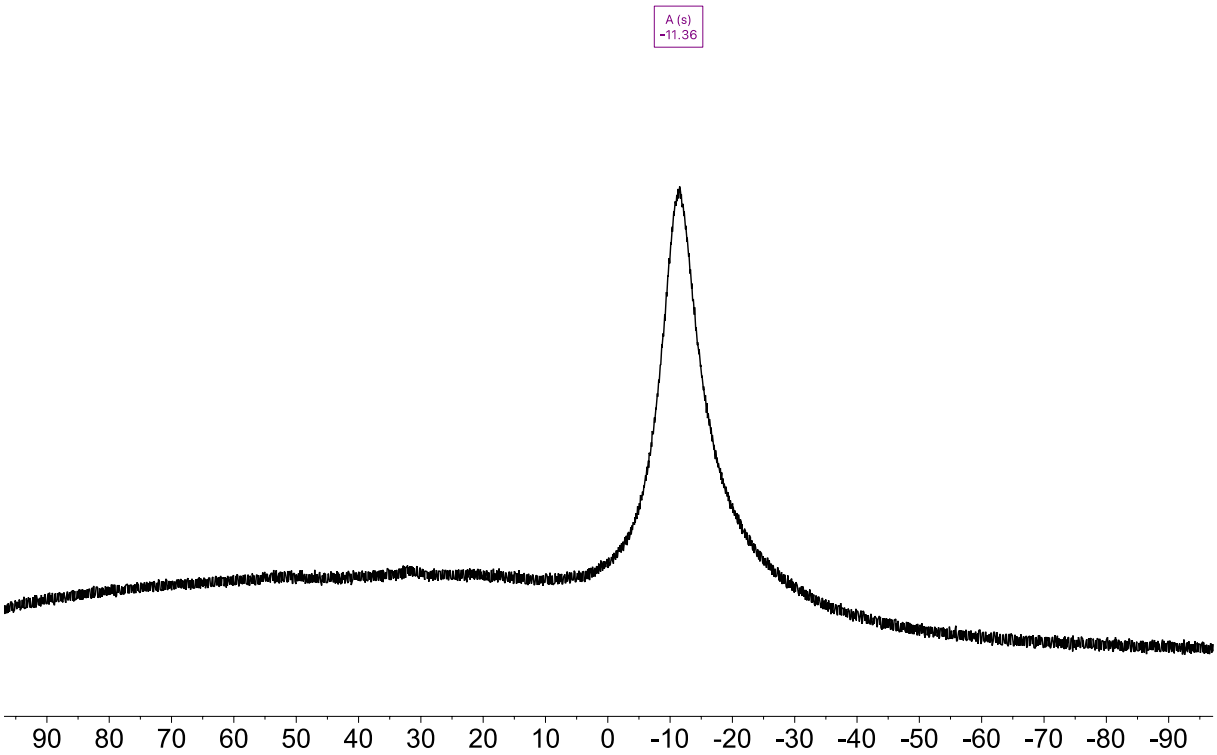

Figure S52: ^{11}B NMR spectrum of **6**·4PMe$_3$ in C_6D_6 at 298 K, 160 MHz. The signal is partially superimposed by the signal of the boron atoms 0 to –25 ppm contained in the glass.

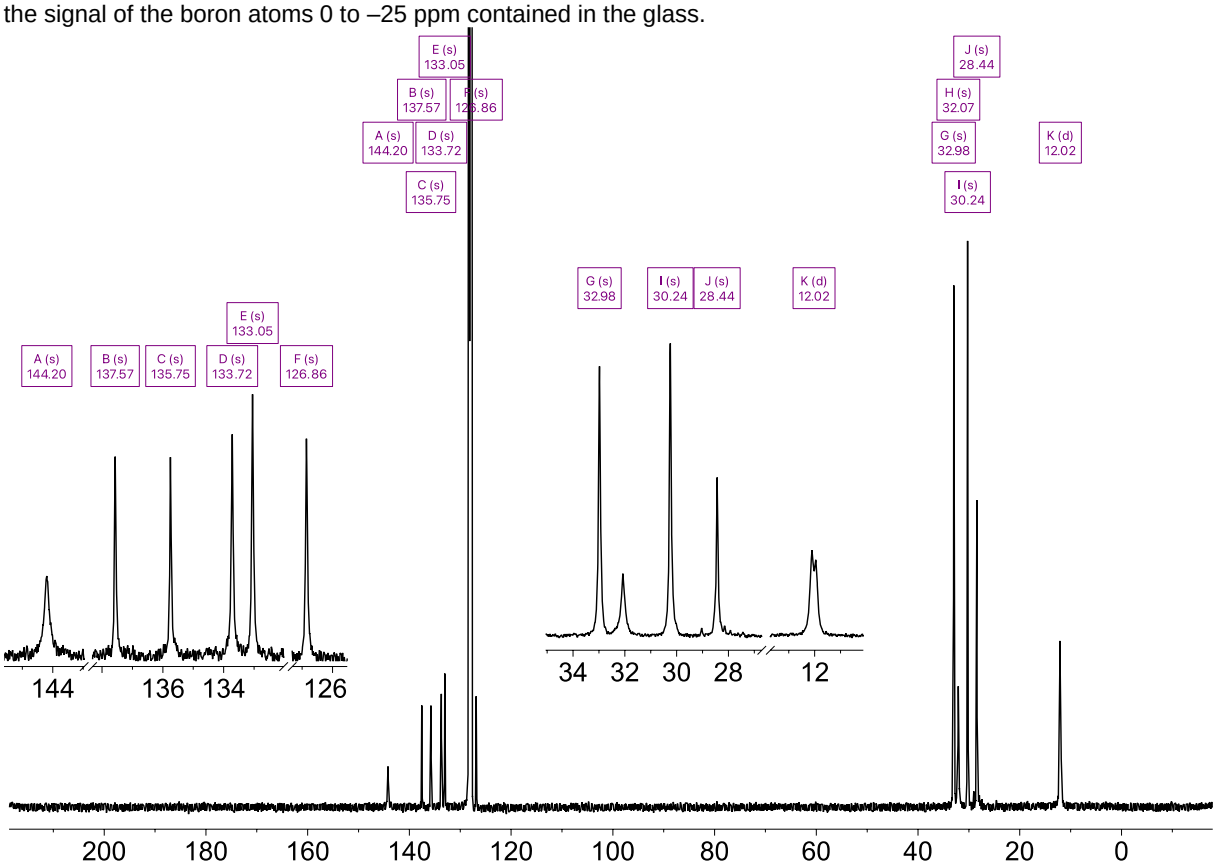

Figure S53: $^{13}C\{^1H\}$ NMR spectrum of **6**·4PMe$_3$ in C_6D_6 at 298 K, 125 MHz.

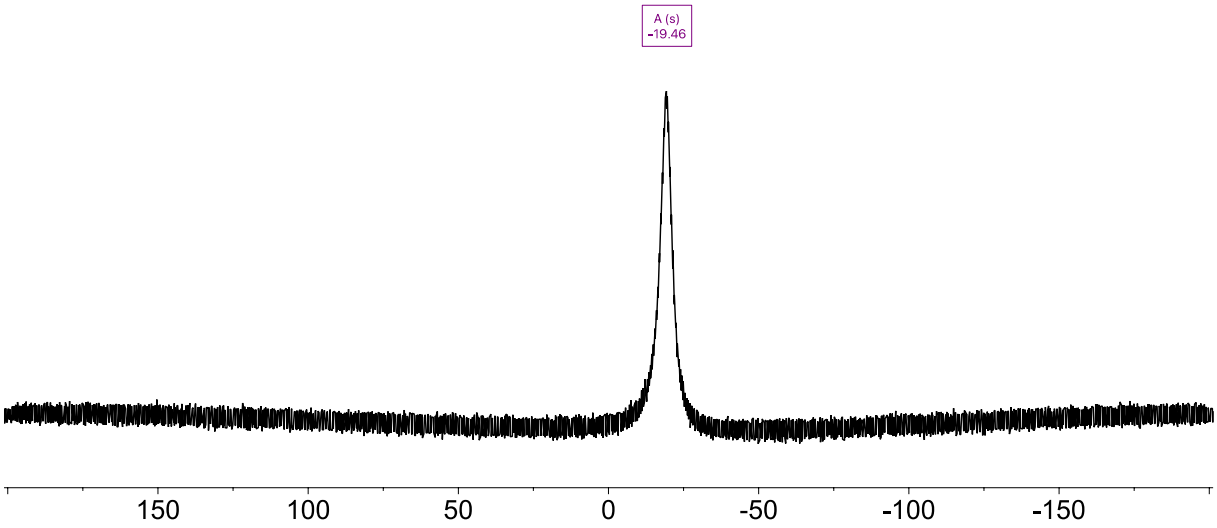

Figure S54: $^{31}P\{^{1}H\}$ NMR spectrum of **6**·4PMe$_3$ in C_6D_6 at 298 K, 202 MHz.

Adduct **7**·4PMe$_3$

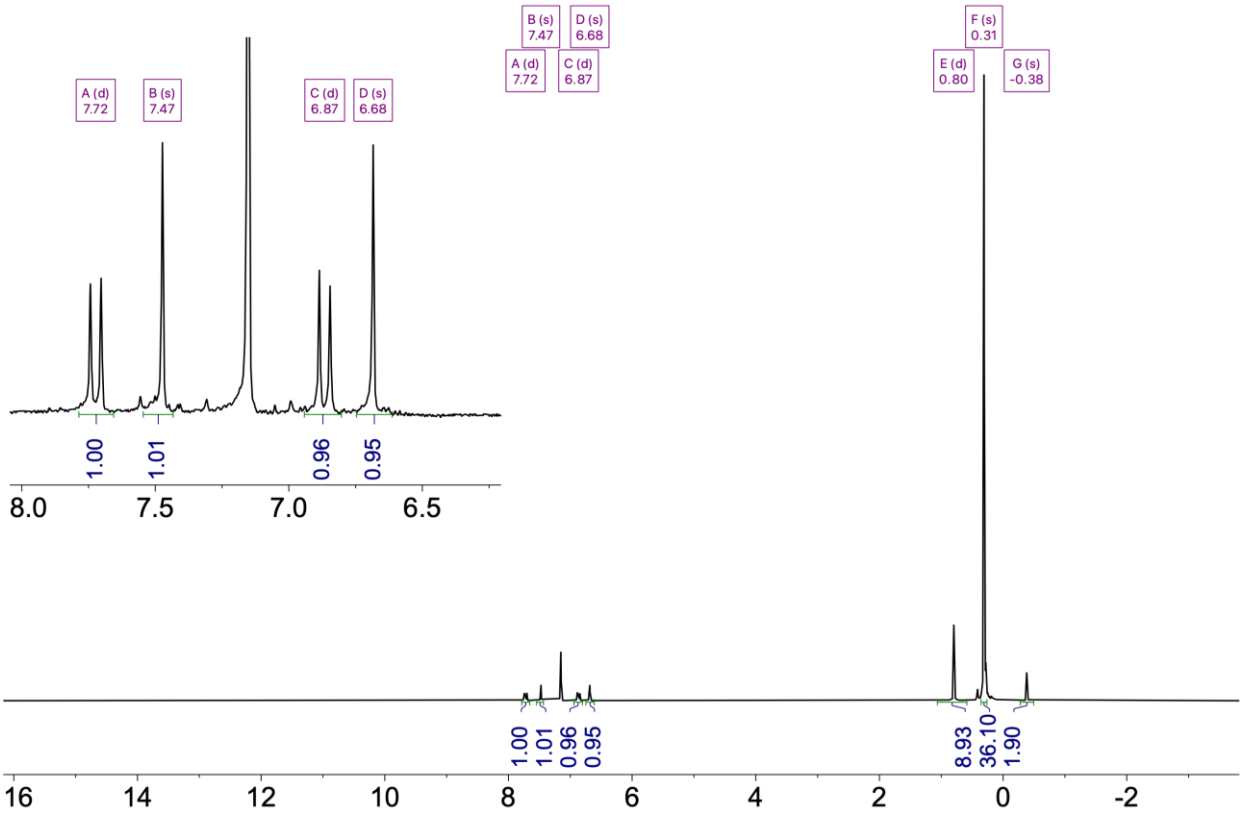

Figure S55: ^{1}H NMR spectrum of **7**·4PMe$_3$ in C_6D_6 at 298 K, 500 MHz.

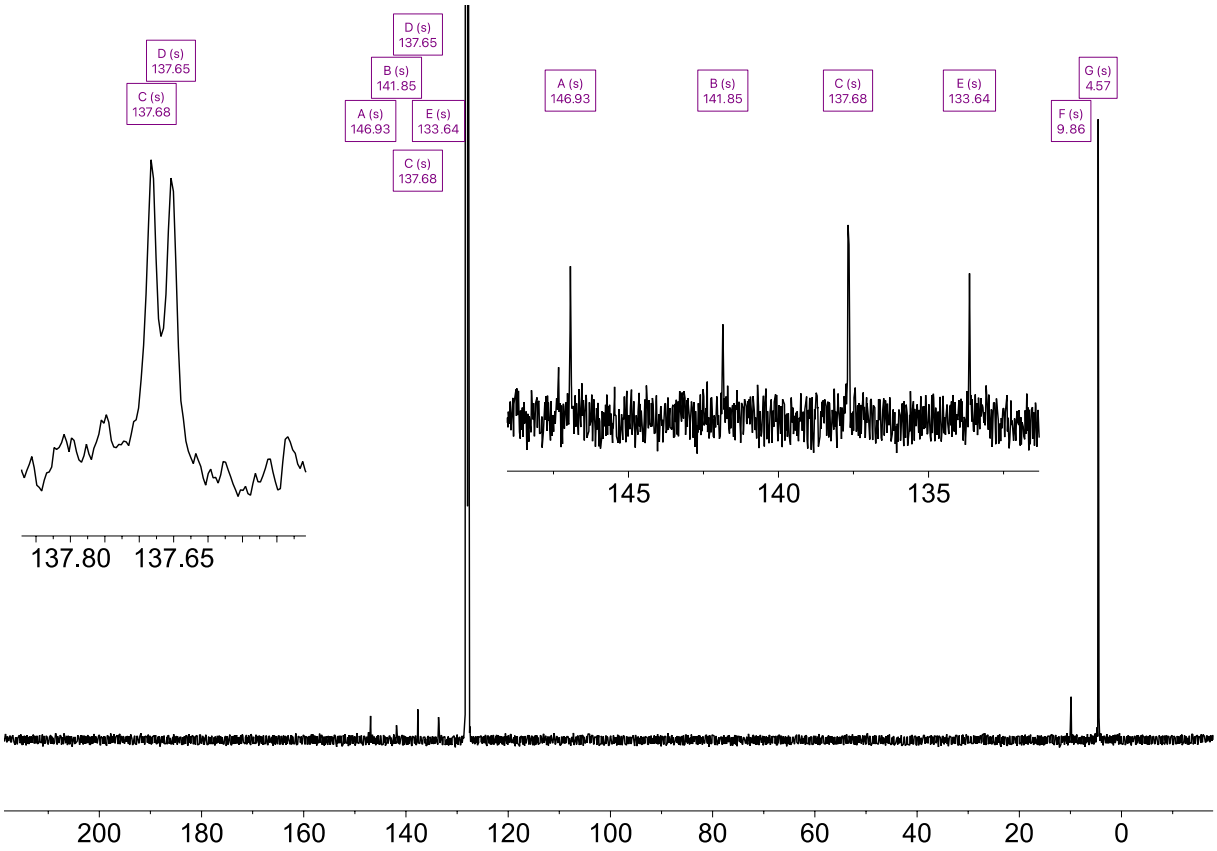

Figure S56: $^{13}C\{^{1}H\}$ NMR spectrum of **7**·4PMe$_3$ in C_6D_6 at 298 K, 125 MHz.

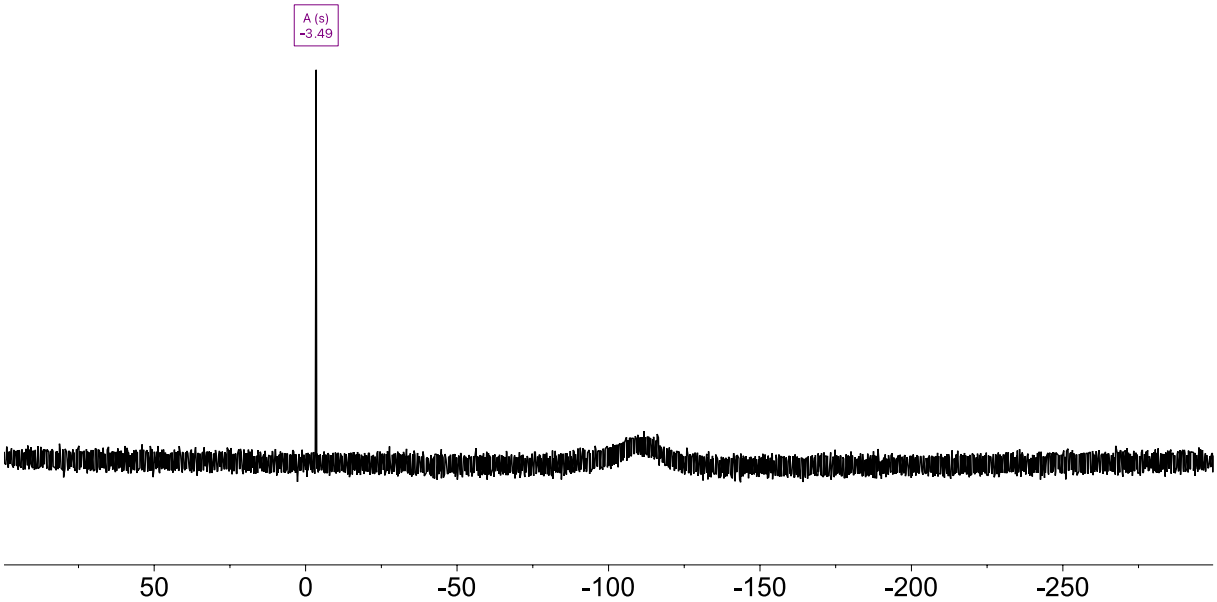

Figure S57: $^{29}Si\{^{1}H\}$ NMR spectrum of **7**·4PMe$_3$ in C_6D_6 at 298 K, 99 MHz. The peak at –110 ppm is due to the silicon atoms in the glass.

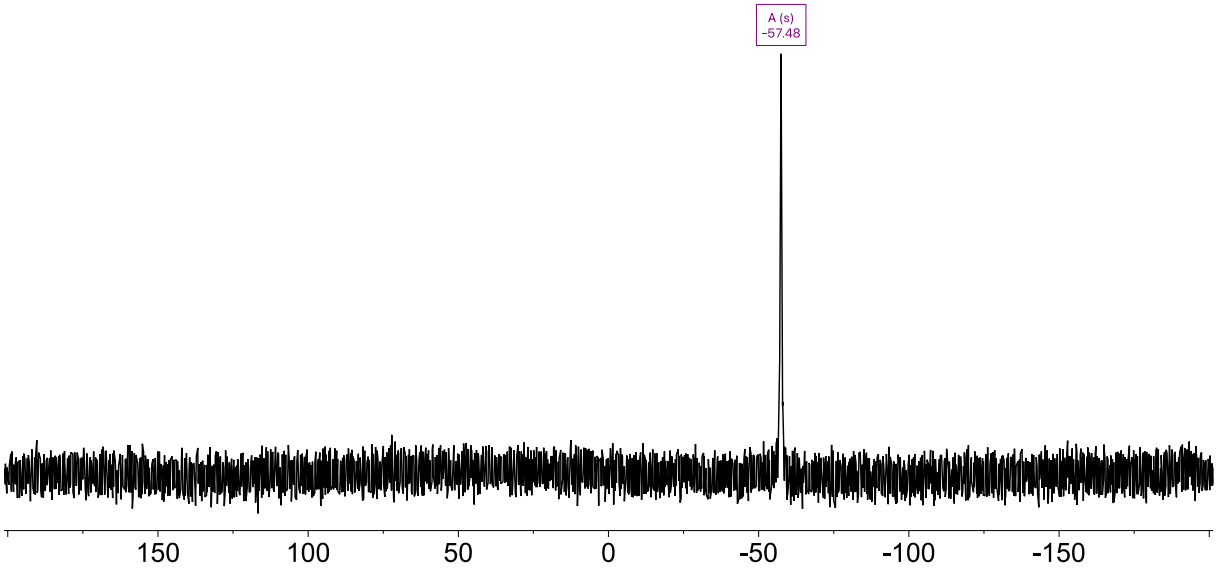

Figure S58: $^{31}P\{^{1}H\}$ NMR spectrum of **7**·4PMe$_3$ in C_6D_6 at 298 K, 202 MHz.

Adduct **8**·4PMe$_3$

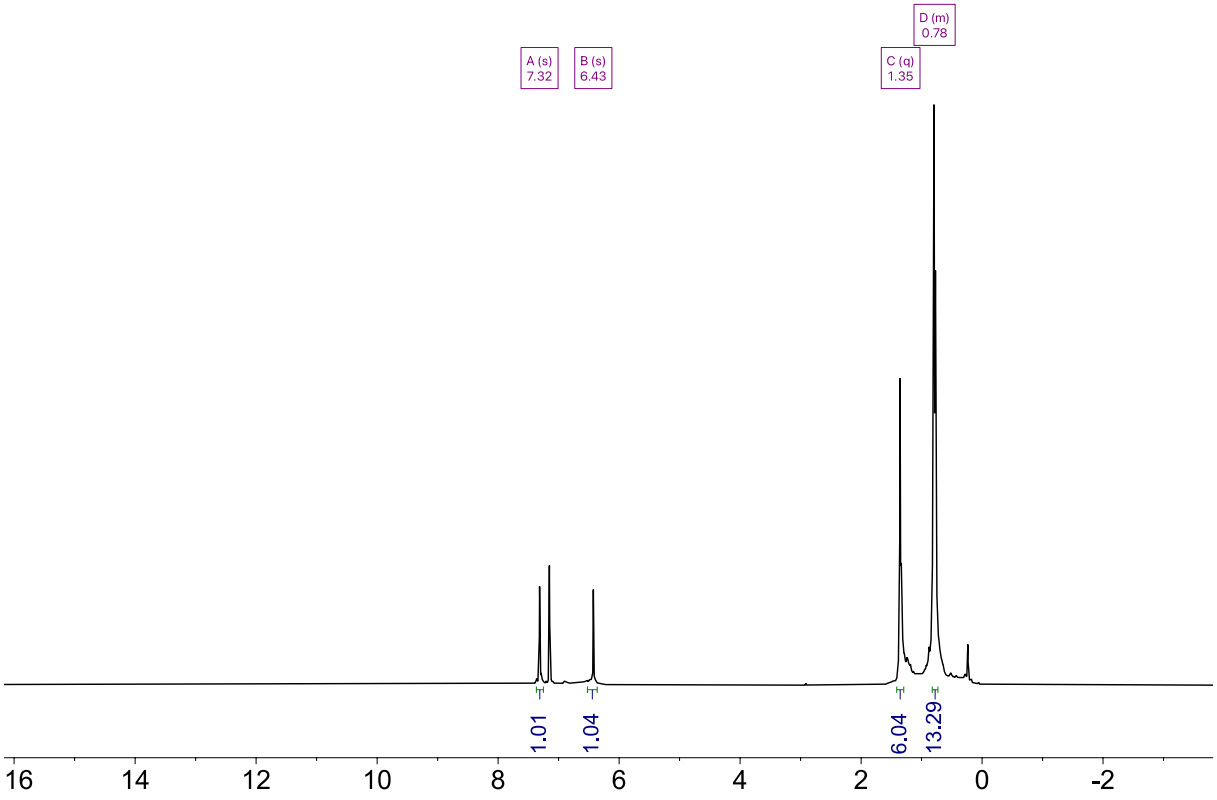

Figure S59: ^{1}H NMR spectrum of **8**·4PMe$_3$ in C_6D_6 at 298 K, 500 MHz.

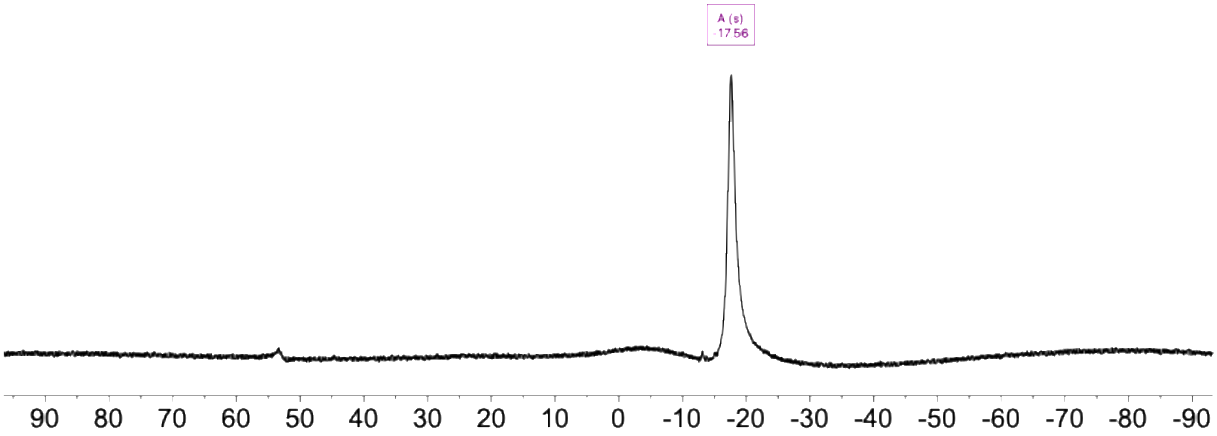

Figure S60: ^{11}B NMR spectrum of **8**·4PMe$_3$ in C_6D_6 at 298 K, 160 MHz. The signal is partially superimposed by the signal of the boron atoms 0 to –25 ppm contained in the glass.

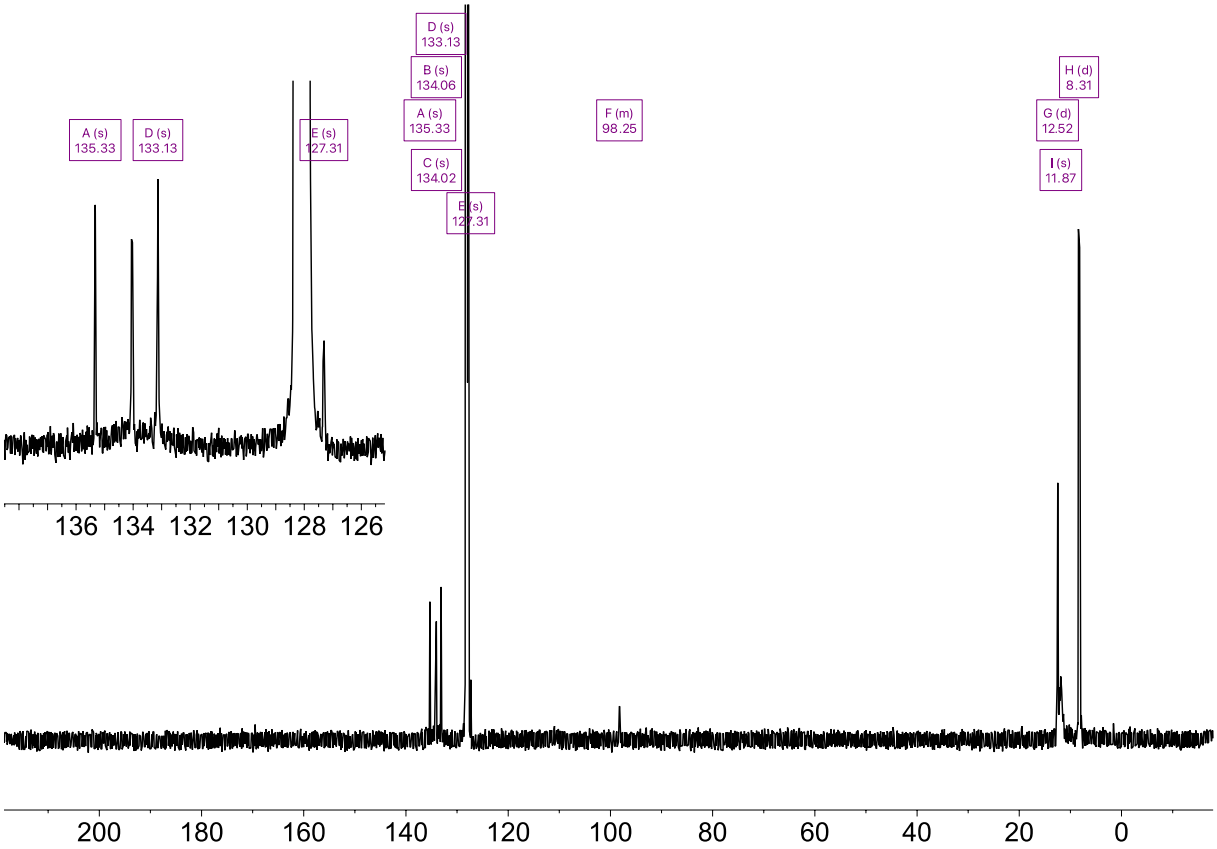

Figure S61: ^{13}C{^{1}H} NMR spectrum of **8**·4PMe$_3$ in C_6D_6 at 298 K, 125 MHz.

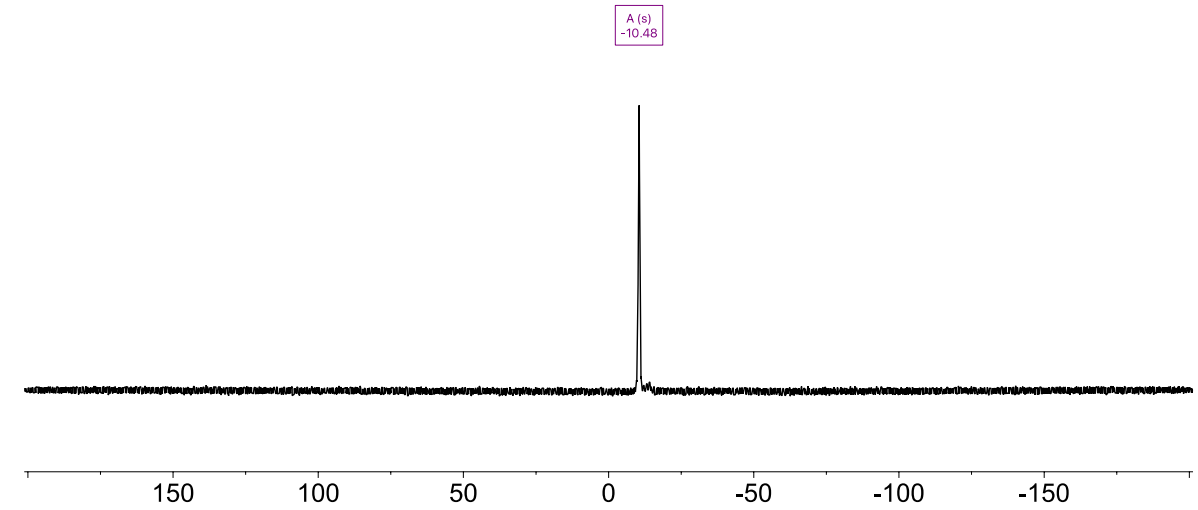

Figure S62: $^{31}P\{^{1}H\}$ NMR spectrum of **8**·4PMe$_3$ in C_6D_6 at 298 K, 202 MHz.

Adduct **9**·4PMe$_3$

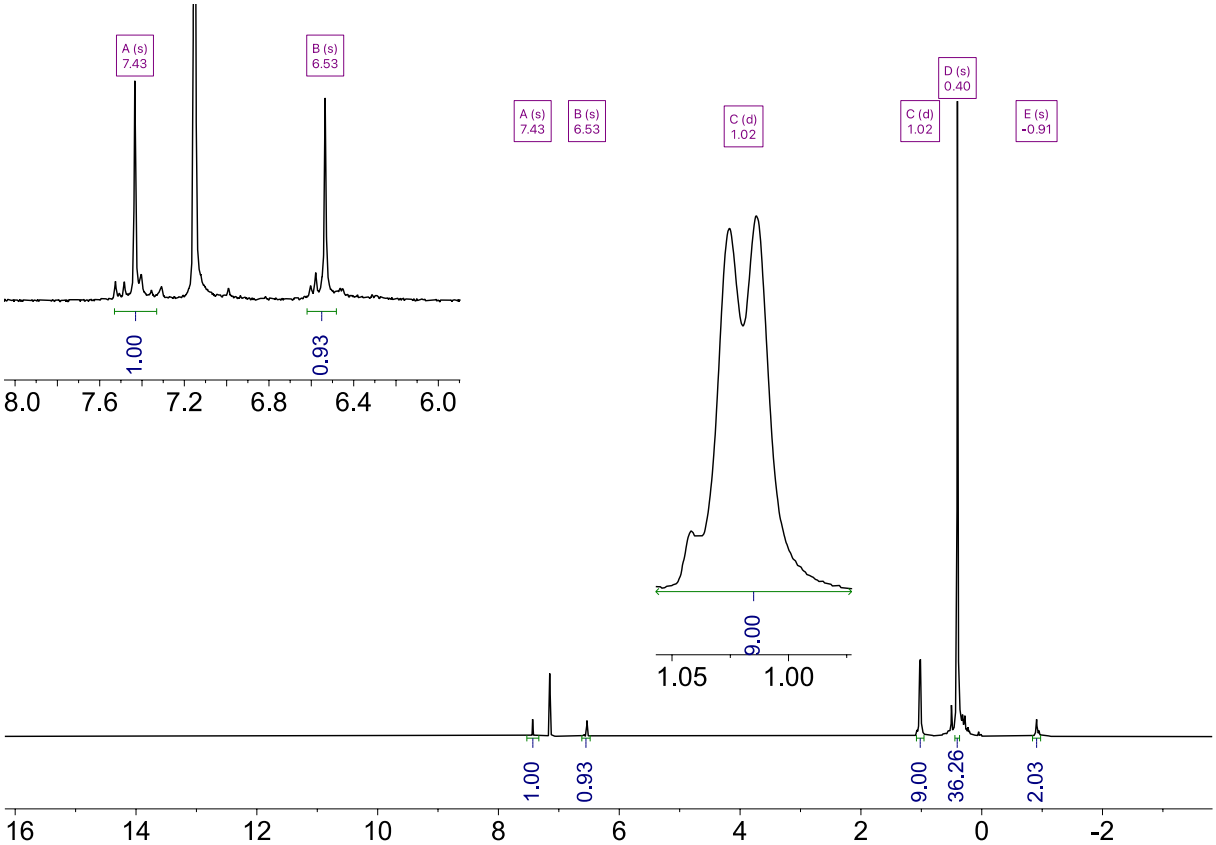

Figure S63: ^{1}H NMR spectrum of **9**·4PMe$_3$ in C_6D_6 at 298 K, 500 MHz.

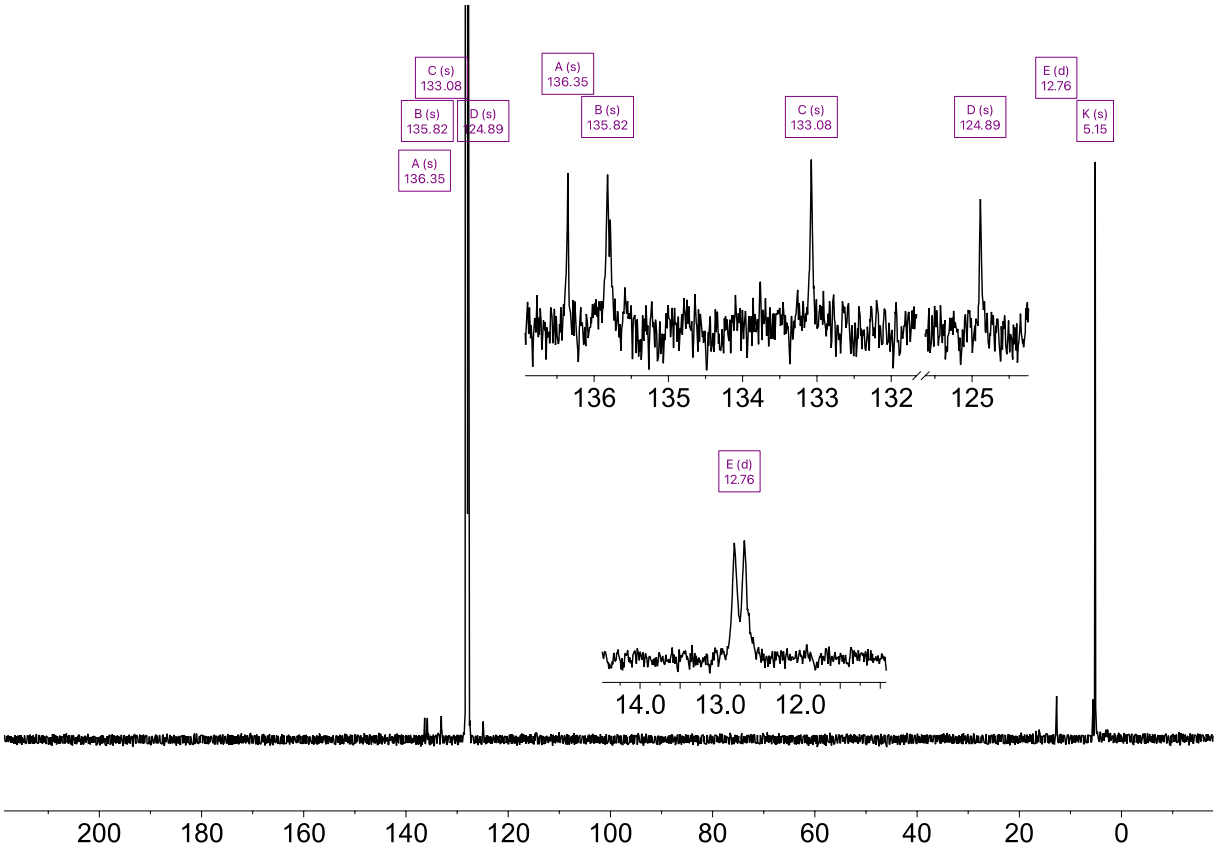

Figure S64: $^{13}C\{^{1}H\}$ NMR spectrum of **9**·4PMe$_3$ in C_6D_6 at 298 K, 125 MHz.

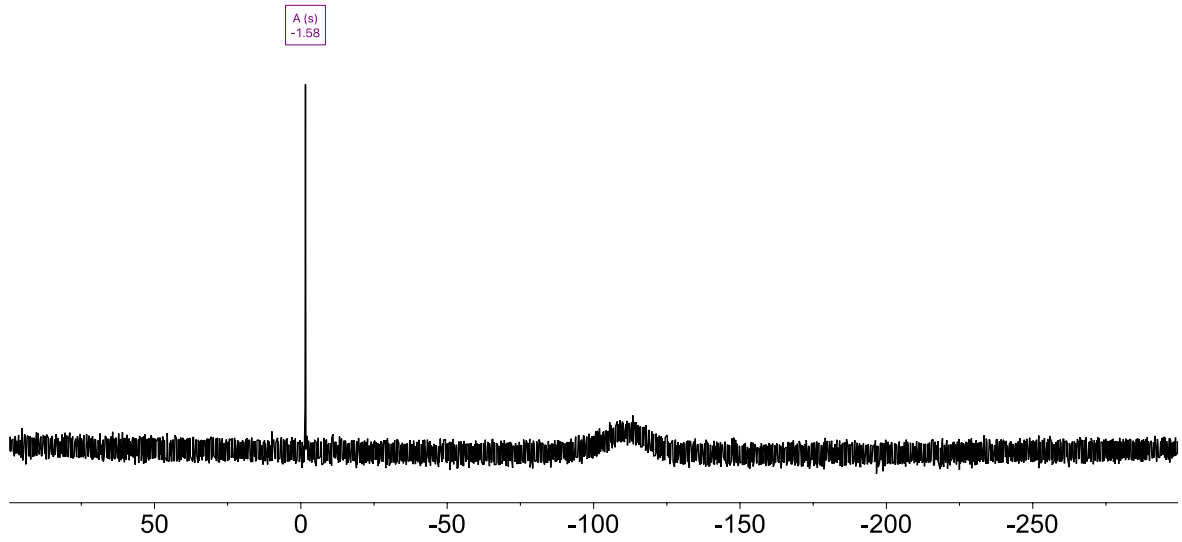

Figure S65: $^{29}Si\{^{1}H\}$ NMR spectrum of **9**·4PMe$_3$ in C_6D_6 at 298 K, 99 MHz. The peak at –110 ppm is due to the silicon atoms in the glass.

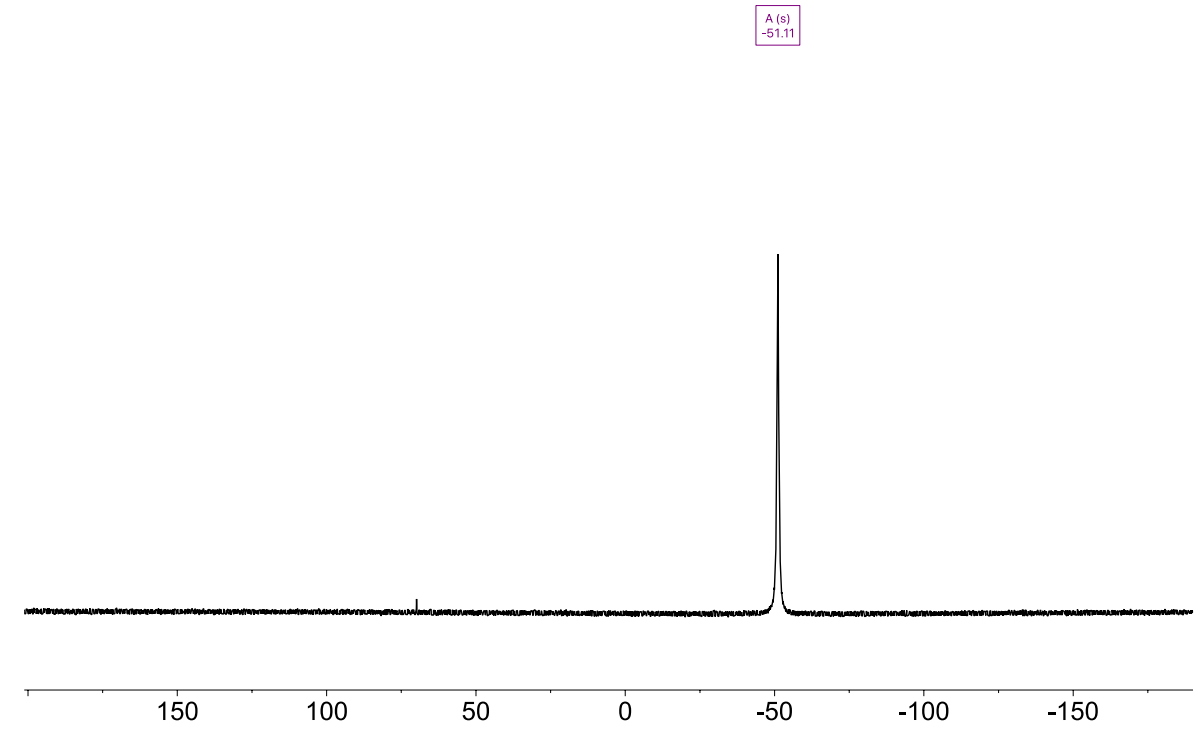

Figure S66: $^{31}P\{^{1}H\}$ NMR spectrum of **9**·4PMe$_3$ in C_6D_6 at 298 K, 202 MHz.

Adduct **6**·4OPEt$_3$

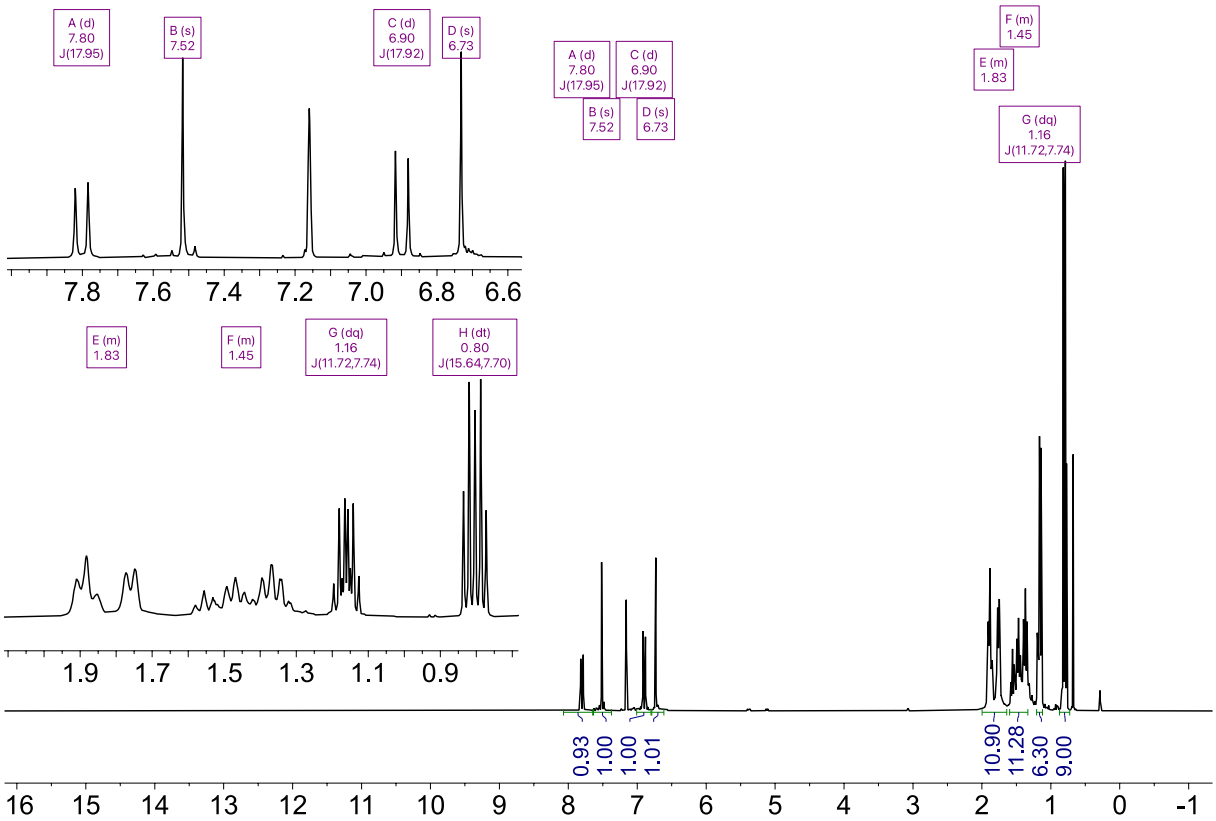

Figure S67: ^{1}H NMR spectrum of **6**·4OPEt$_3$ in C_6D_6 at 298 K, 500 MHz.

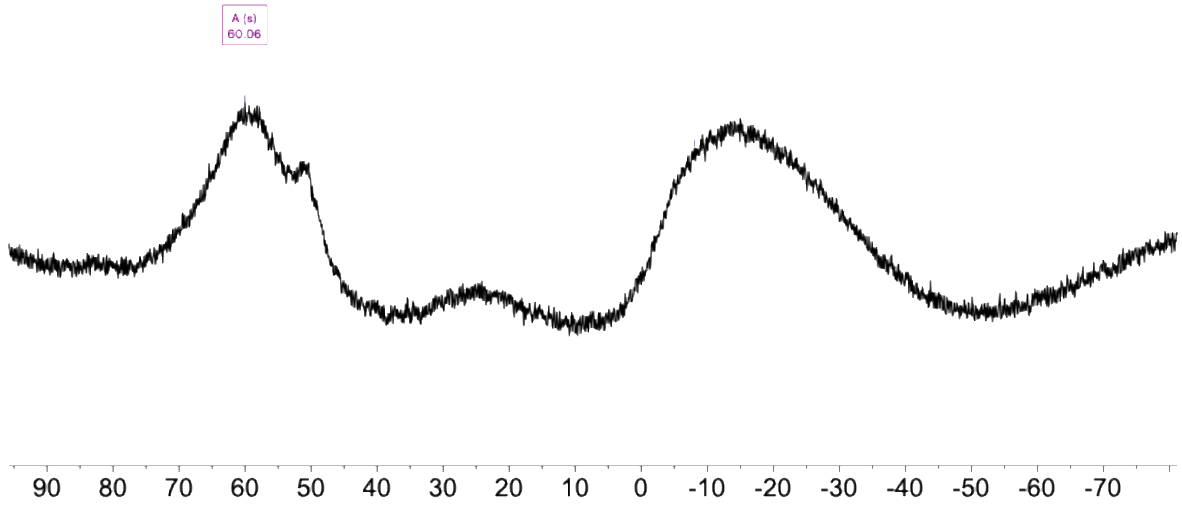

Figure S68: ^{11}B NMR spectrum of **6**·4OPEt$_3$ in C_6D_6 at 298 K, 160 MHz. The peak at 0 to –25 ppm is due to the boron atoms in the glass.

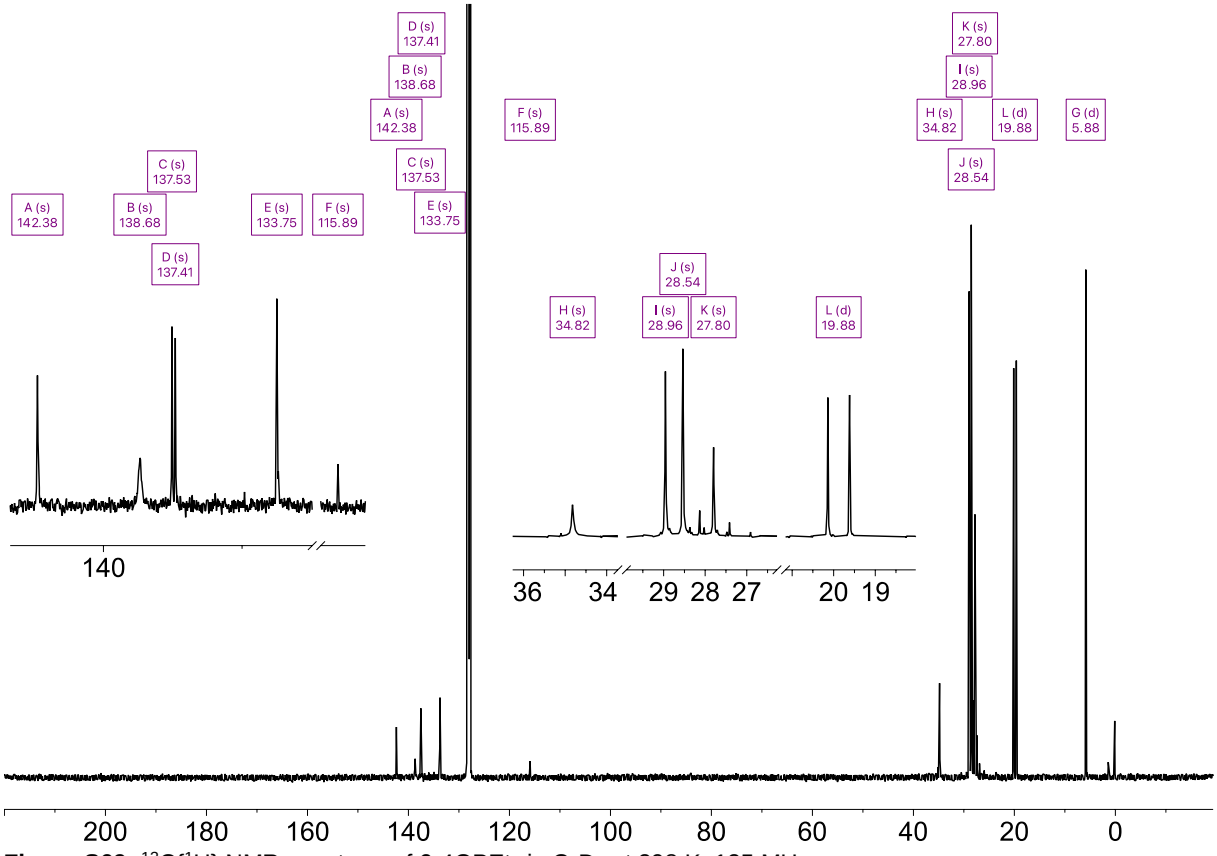

Figure S69: ^{13}C{^{1}H} NMR spectrum of **6**·4OPEt$_3$ in C_6D_6 at 298 K, 125 MHz.

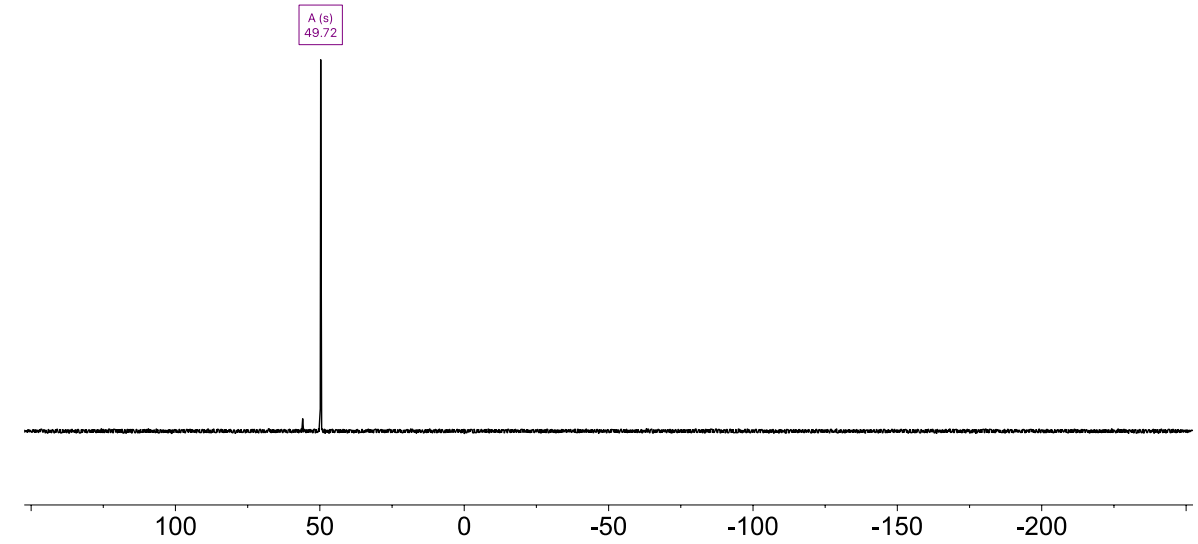

Figure S70: $^{31}P\{^{1}H\}$ NMR spectrum of **6**·4OPEt$_3$ in C_6D_6 at 298 K, 202 MHz.

Adduct **7**·4OPEt$_3$

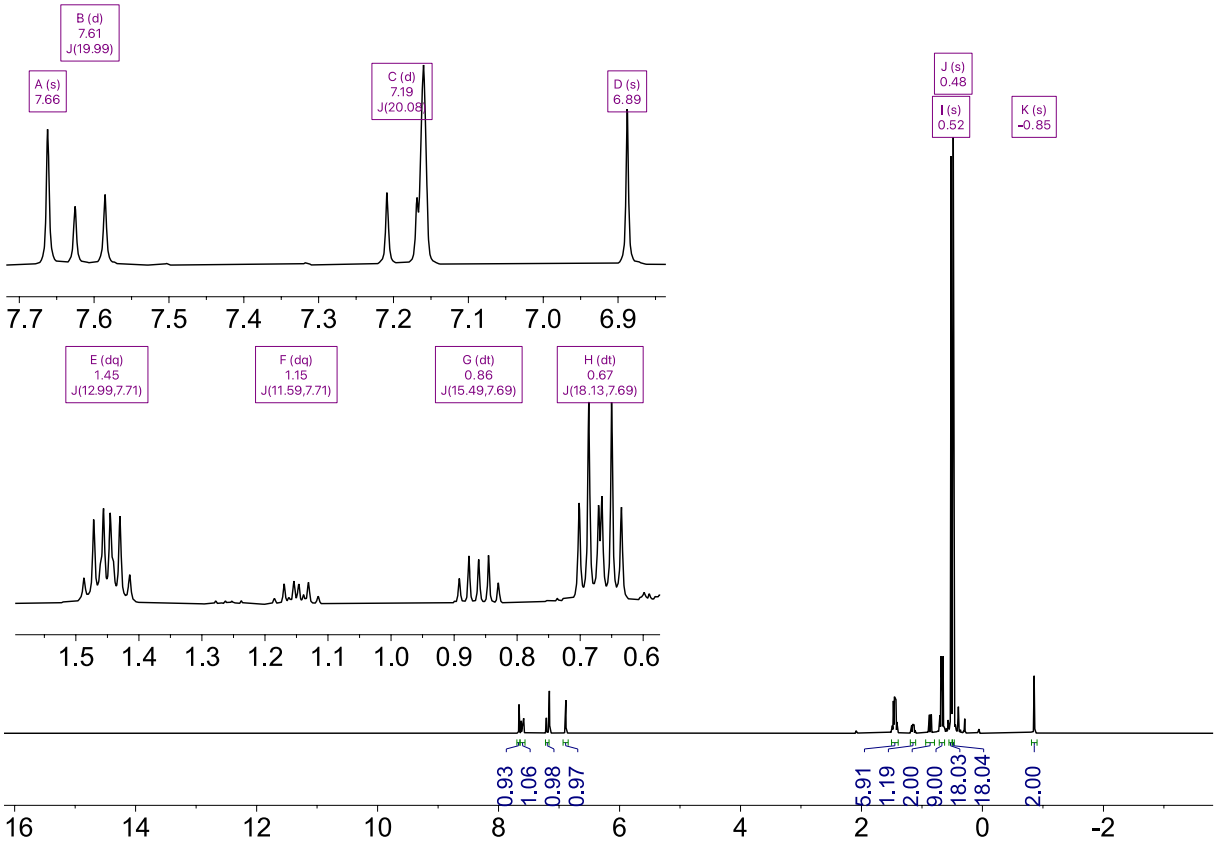

Figure S71: ^{1}H NMR spectrum of **7**·4OPEt$_3$ in C_6D_6 at 298 K, 500 MHz. The signals at 1.15 and 0.86 ppm come from 2.4 eq free OPEt$_3$.

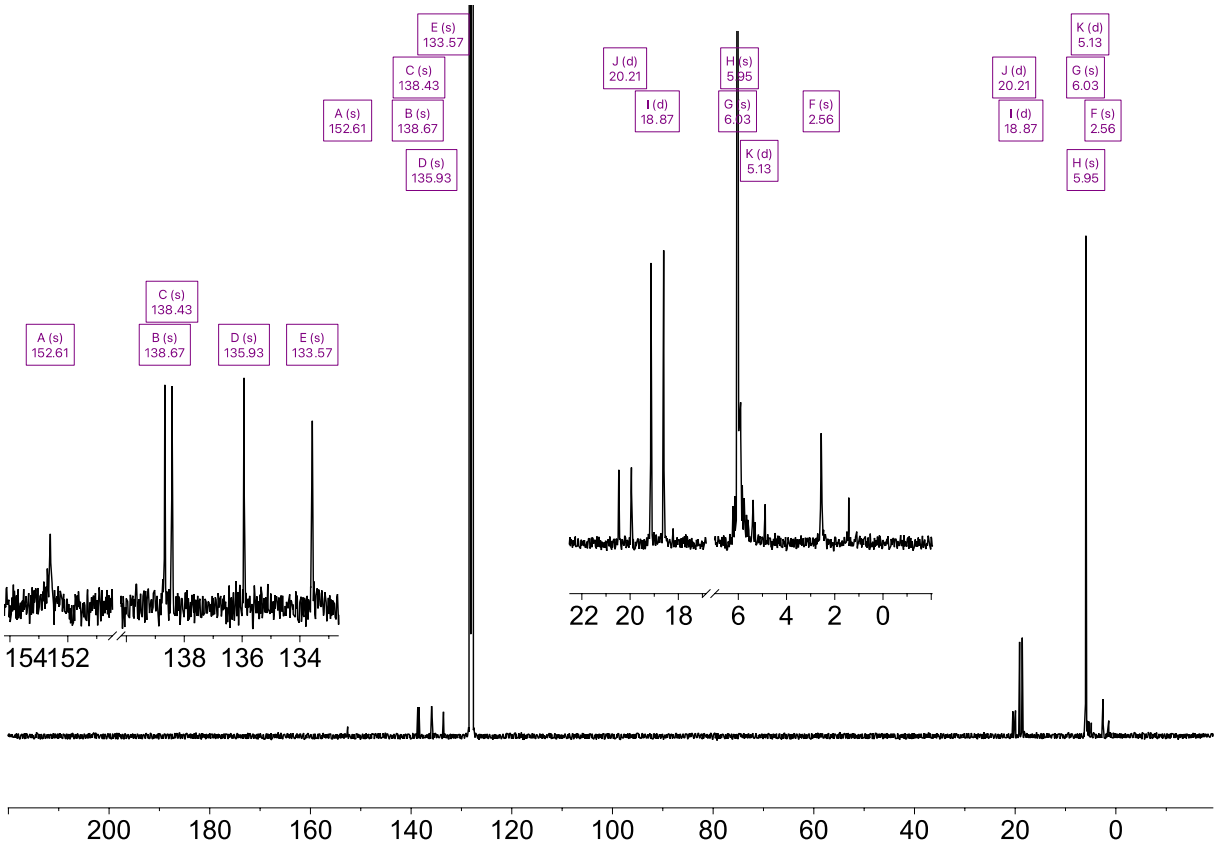

Figure S72: $^{13}C\{^{1}H\}$ NMR spectrum of **7**·4OPEt$_3$ in C_6D_6 at 298 K, 125 MHz.

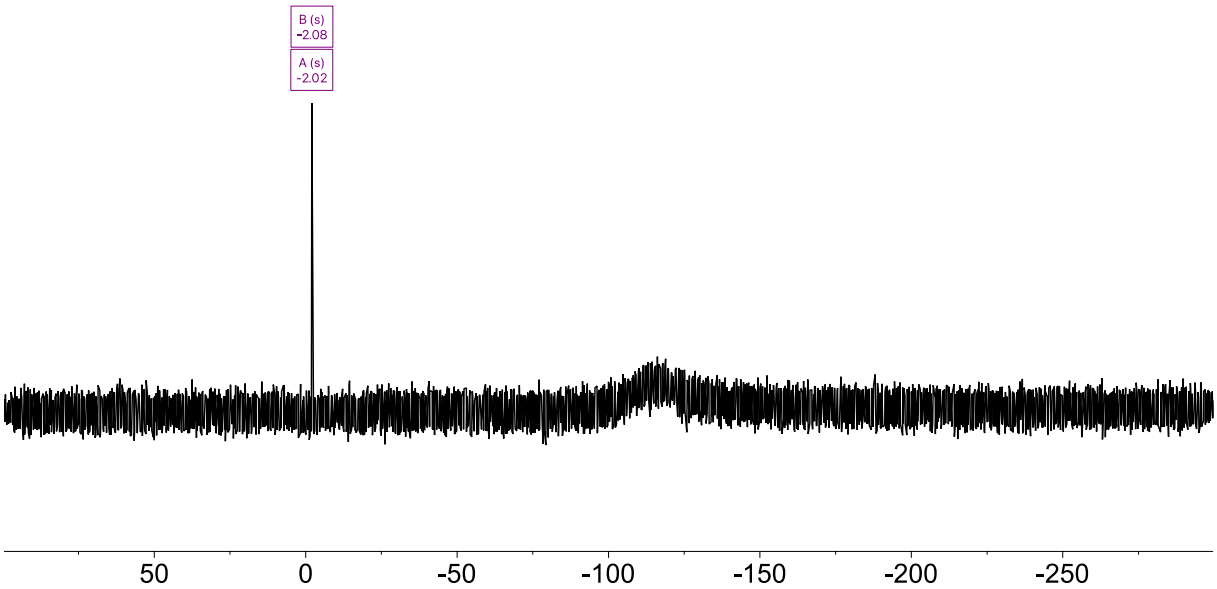

Figure S73: $^{29}Si\{^{1}H\}$ NMR spectrum of **7**·4OPEt$_3$ in C_6D_6 at 298 K, 99 MHz. The peak at –110 ppm is due to the silicon atoms in the glass.

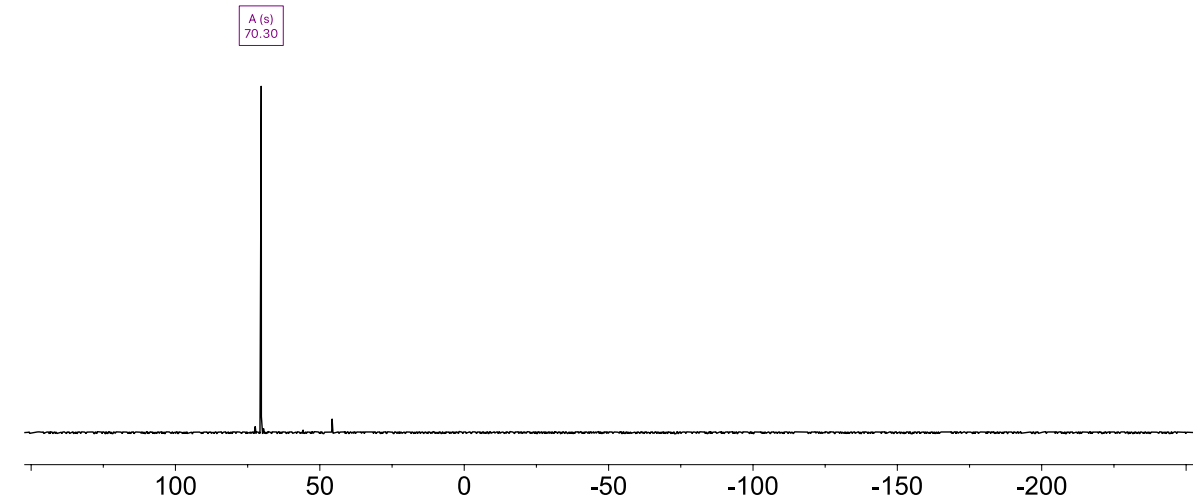

Figure S74: $^{31}P\{^{1}H\}$ NMR spectrum of **7**·4OPEt$_3$ in C_6D_6 at 298 K, 202 MHz.

Adduct **8**·4OPEt$_3$

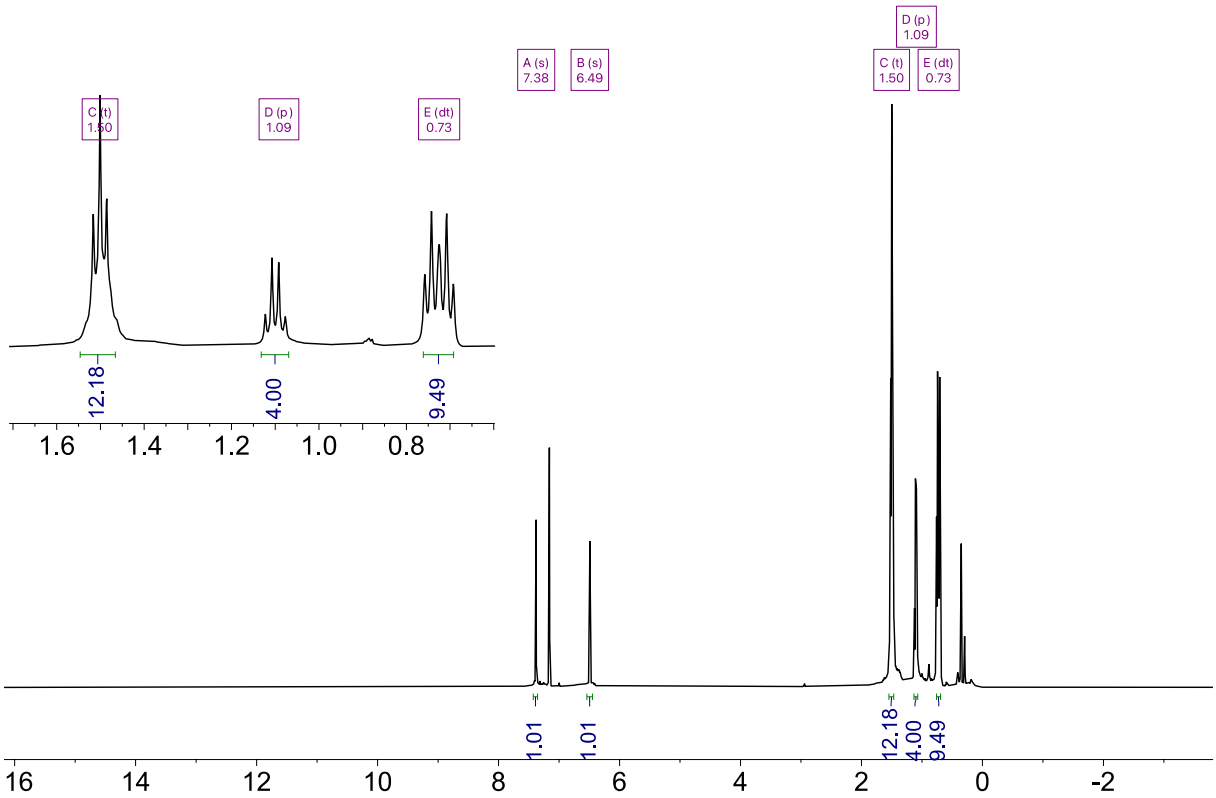

Figure S75: ^{1}H NMR spectrum of **8**·4OPEt$_3$ in C_6D_6 at 298 K, 500 MHz.

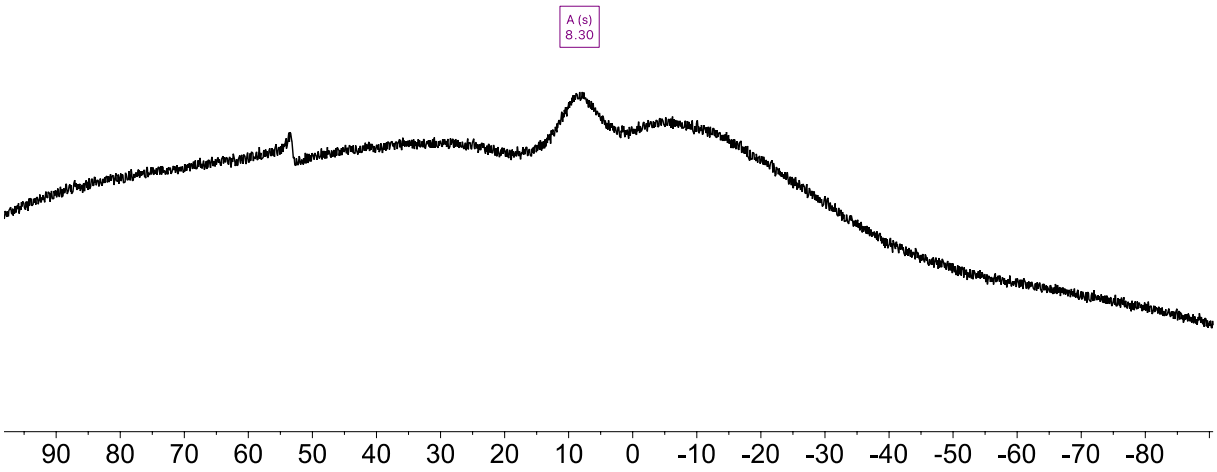

Figure S76: ^{11}B NMR spectrum of **8**·4OPEt$_3$ in C_6D_6 at 298 K, 160 MHz. The peak at 0 to –25 ppm is due to the boron atoms in the glass.

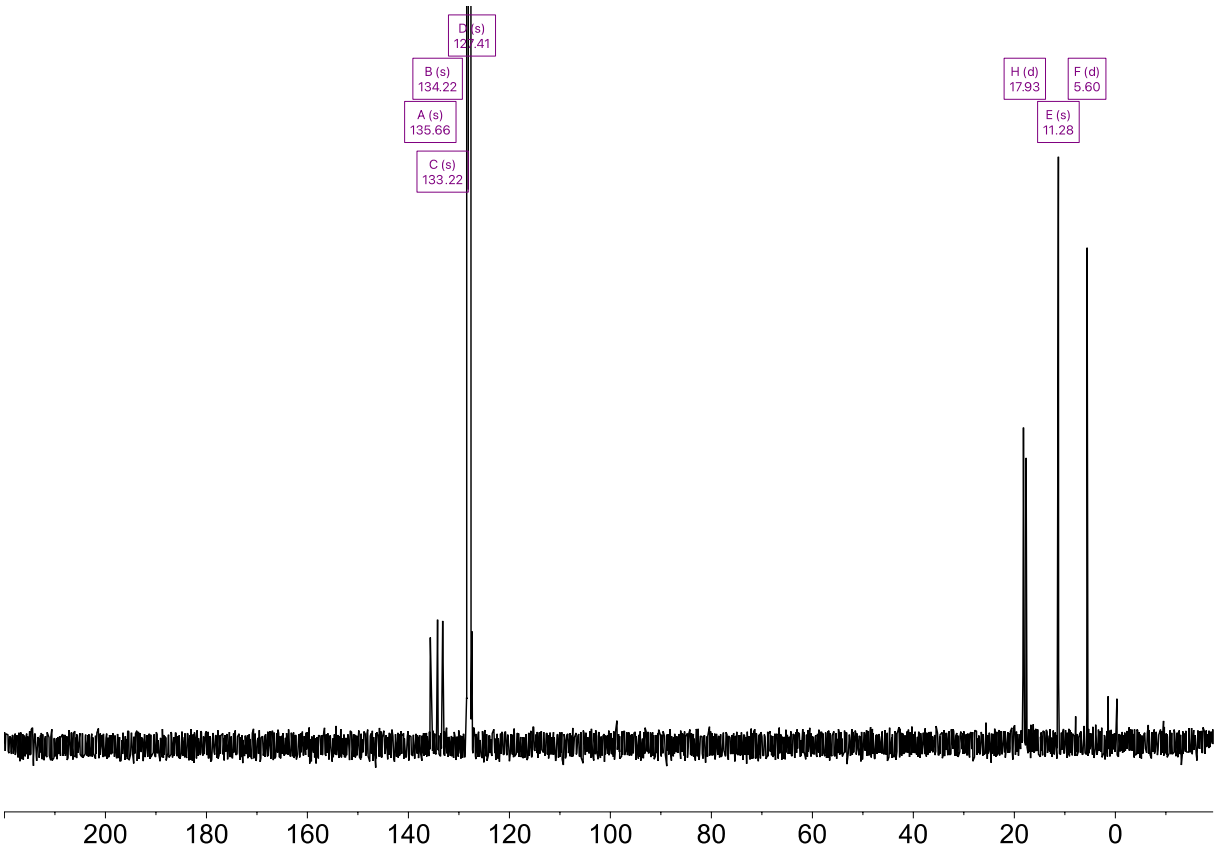

Figure S77: ^{13}C{^{1}H} NMR spectrum of **8**·4OPEt$_3$ in C_6D_6 at 298 K, 125 MHz.

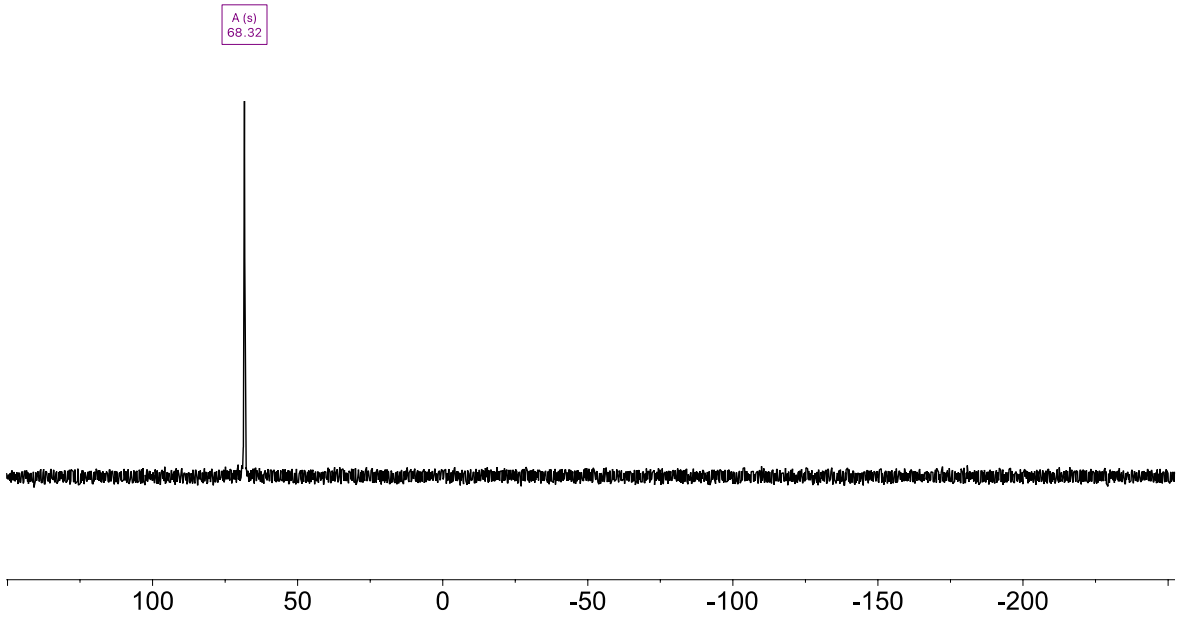

Figure S78: $^{31}P\{^{1}H\}$ NMR spectrum of **8**·4OPEt$_3$ in C_6D_6 at 298 K, 202 MHz.

Adduct **9**·4OPEt$_3$

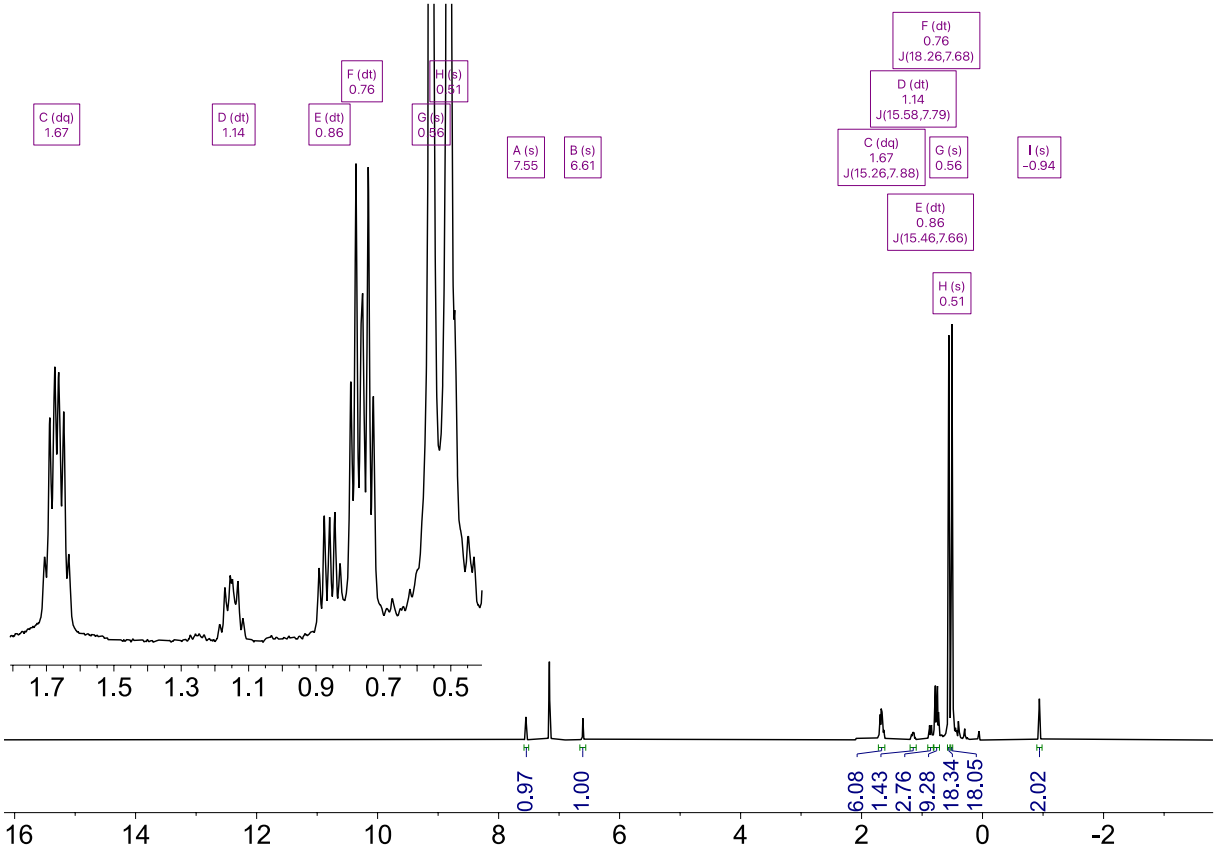

Figure S79: ^{1}H NMR spectrum of **9**·4OPEt$_3$ in C_6D_6 at 298 K, 500 MHz. The signals at 1.15 and 0.86 ppm come from 2.4 eq free OPEt$_3$.

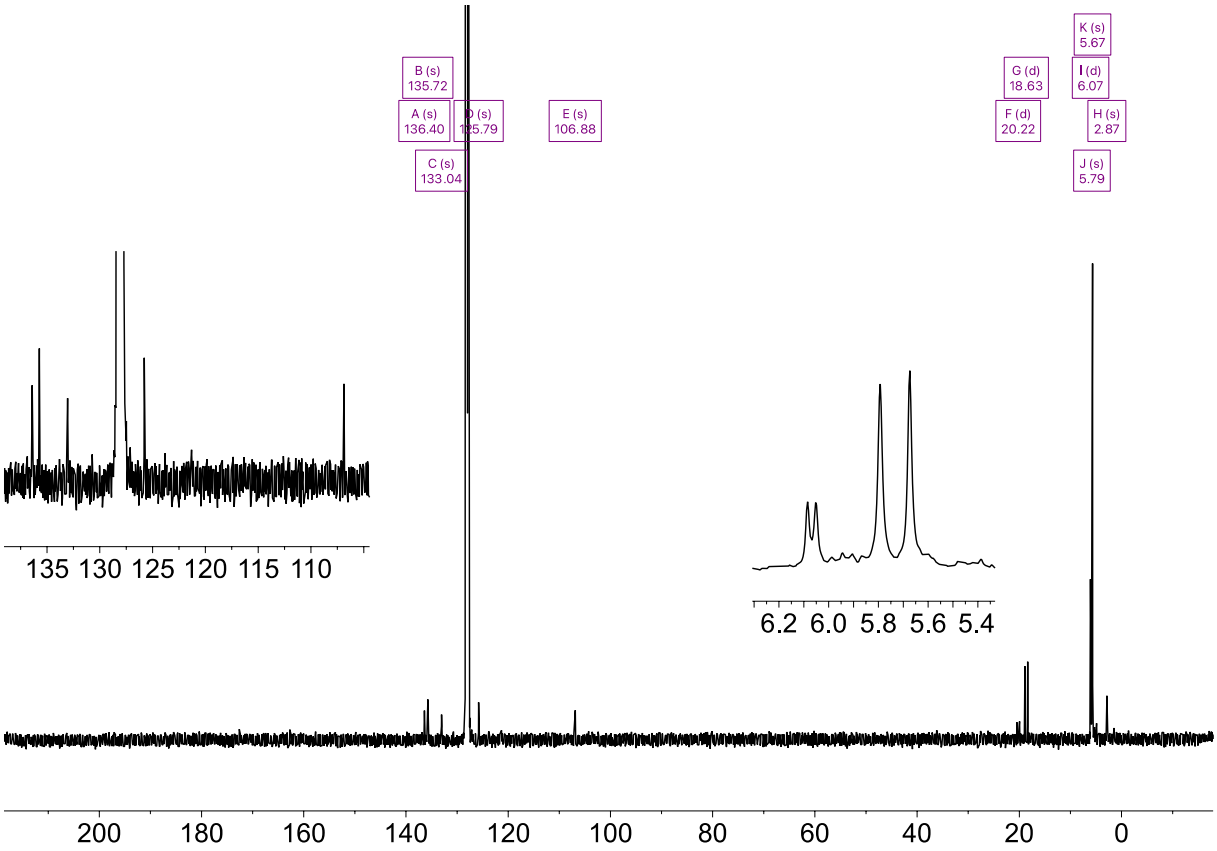

Figure S80: $^{13}C\{^{1}H\}$ NMR spectrum of **9**·4OPEt$_3$ in C_6D_6 at 298 K, 125 MHz.

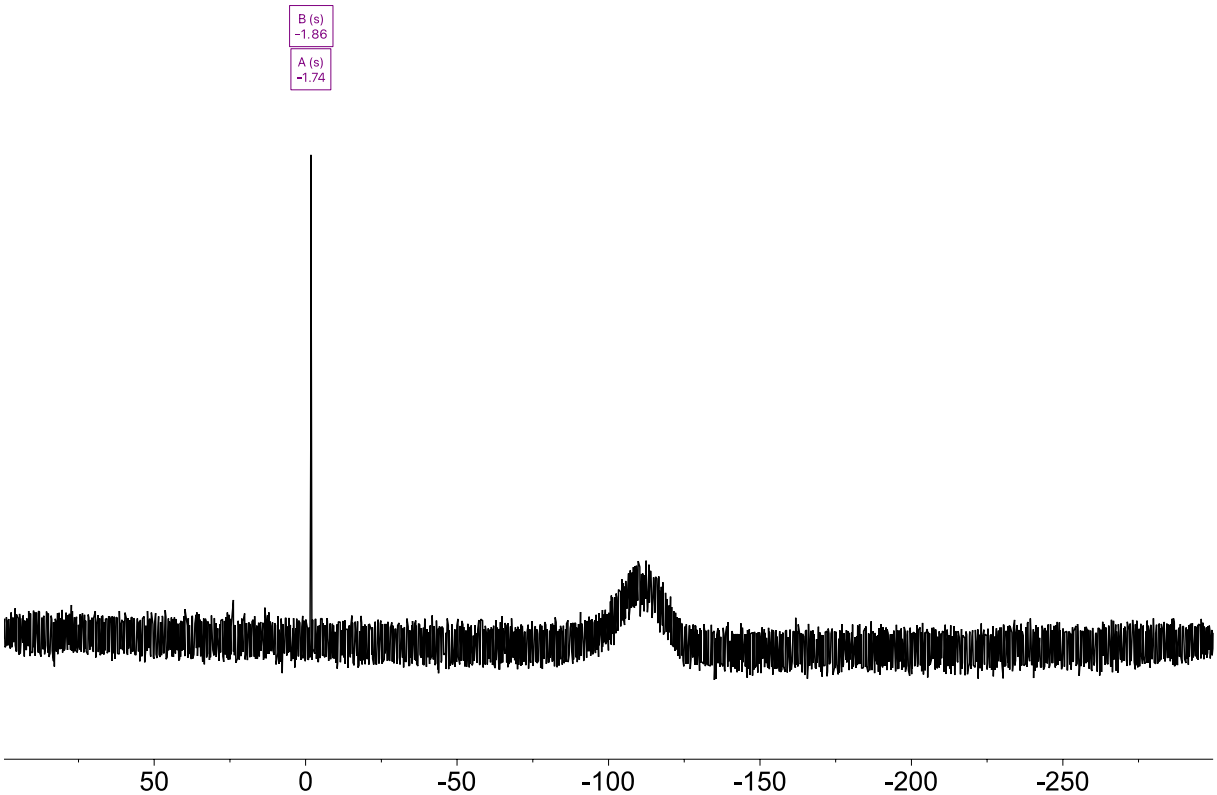

Figure S81: $^{29}Si\{^{1}H\}$ NMR spectrum of **9**·4OPEt$_3$ in C_6D_6 at 298 K, 99 MHz. The peak at –110 ppm is due to the silicon atoms in the glass.

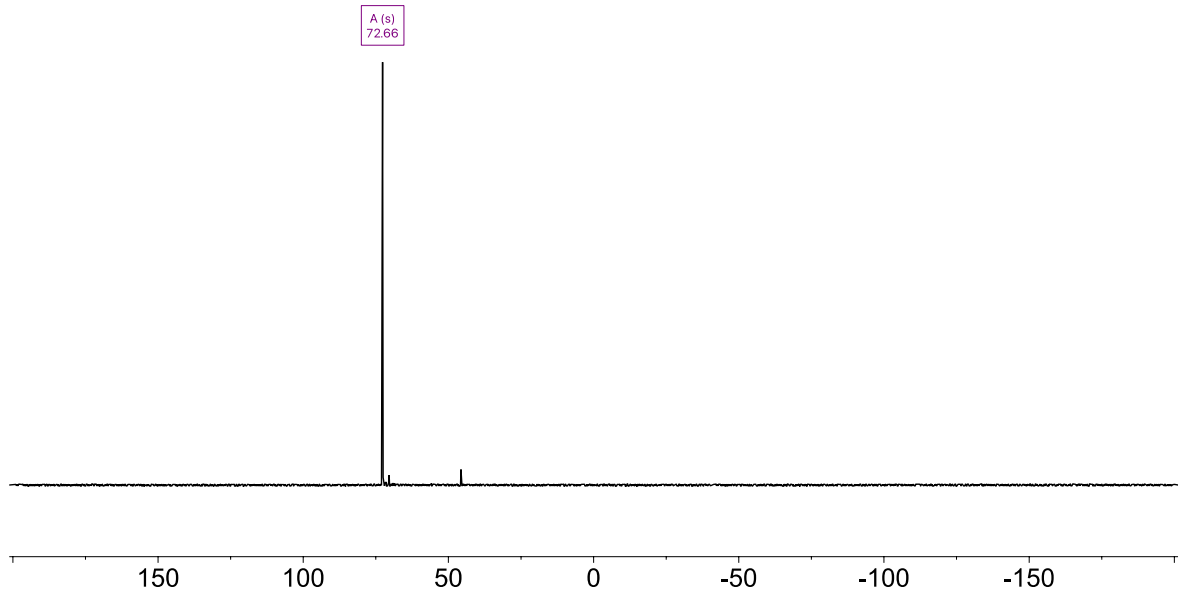

Figure S82: $^{31}P\{^{1}H\}$ NMR spectrum of **9**·4OPEt$_3$ in C_6D_6 at 298 K, 202 MHz.

Adduct **7**·4THF

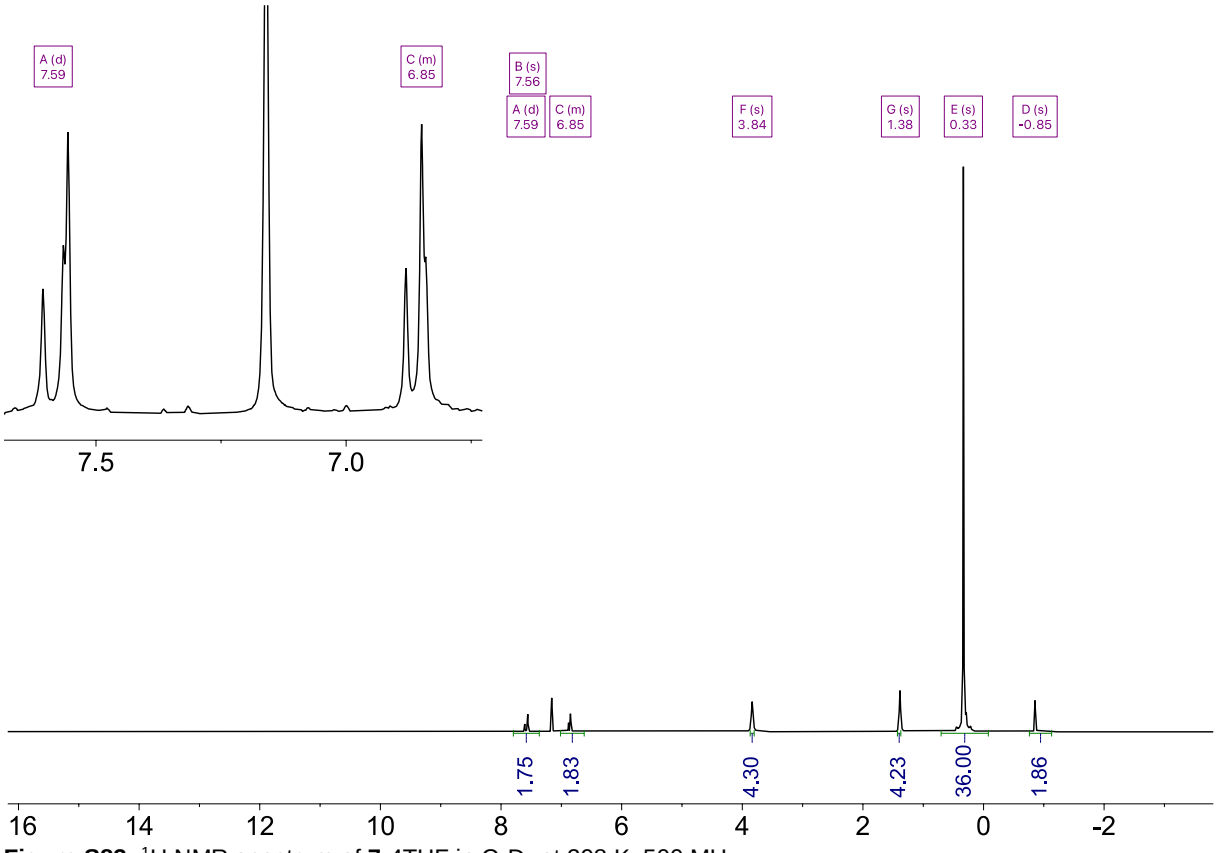

Figure S83: ^{1}H NMR spectrum of **7**·4THF in C_6D_6 at 298 K, 500 MHz.

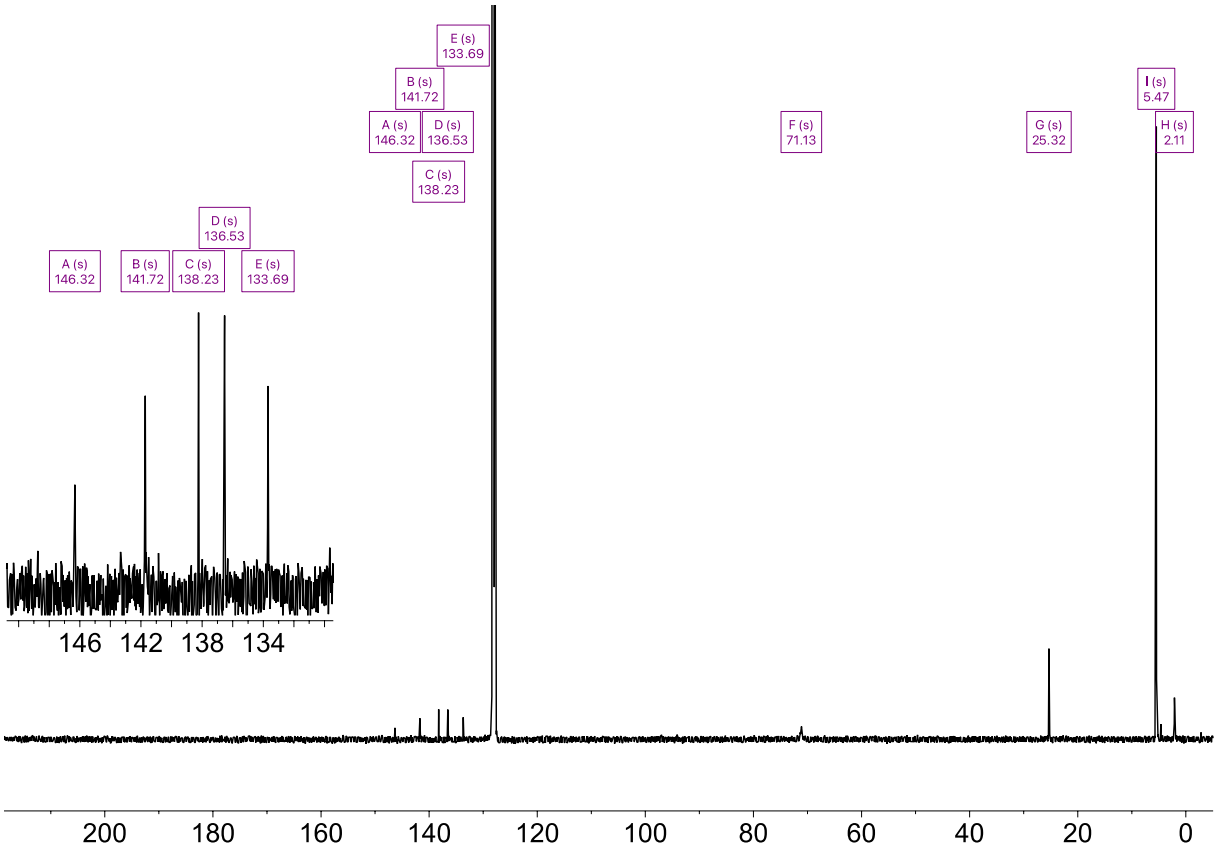

Figure S84: $^{13}C\{^{1}H\}$ NMR spectrum of **7**·4THF in C_6D_6 at 298 K, 125 MHz.

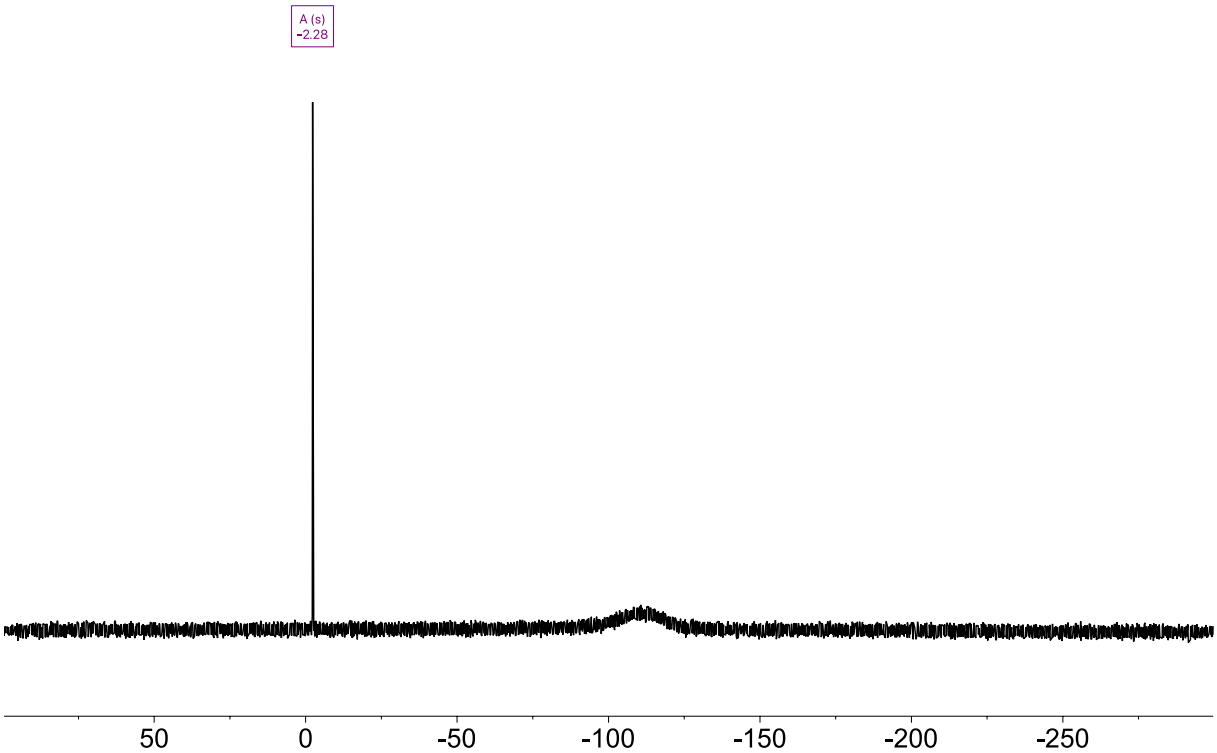

Figure S85: $^{29}Si\{^{1}H\}$ NMR spectrum of **7**·4THF in C_6D_6 at 298 K, 99 MHz. The peak at –110 ppm is due to the silicon atoms in the glass.

Adduct 8·4THF

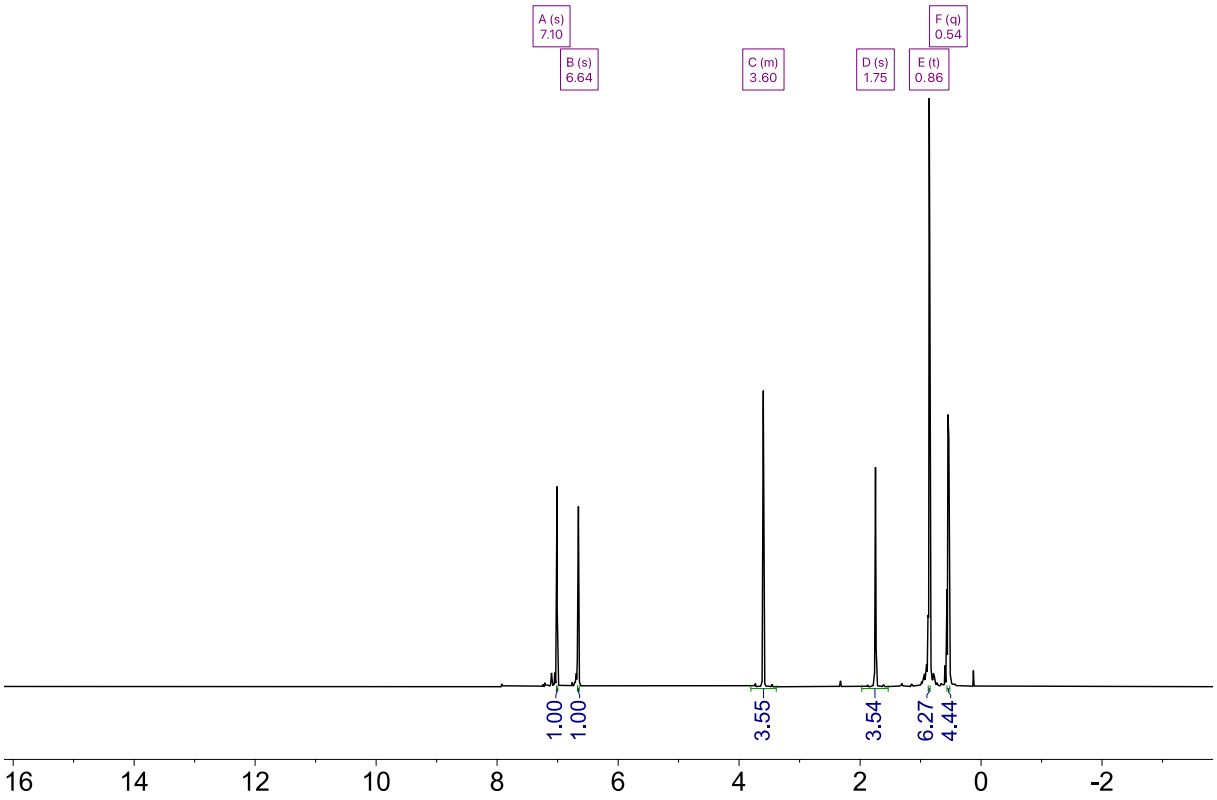

Figure S86: ^{1}H NMR spectrum of **8**·4THF in C_6D_6 at 298 K, 500 MHz.

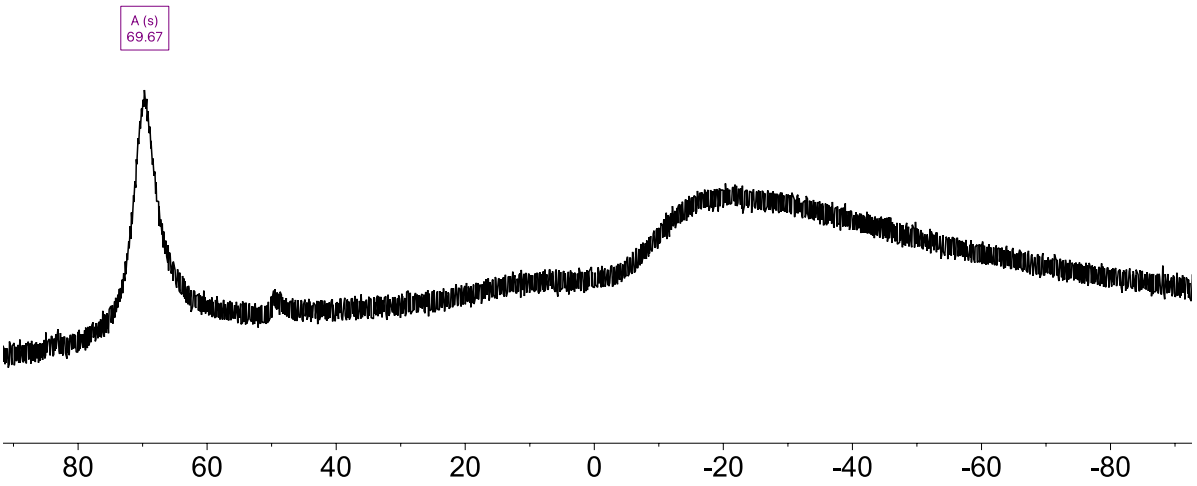

Figure S87: ^{11}B NMR spectrum of **8**·4THF in C_6D_6 at 298 K, 160 MHz. The peak at 0 to –25 ppm is due to the boron atoms in the glass.

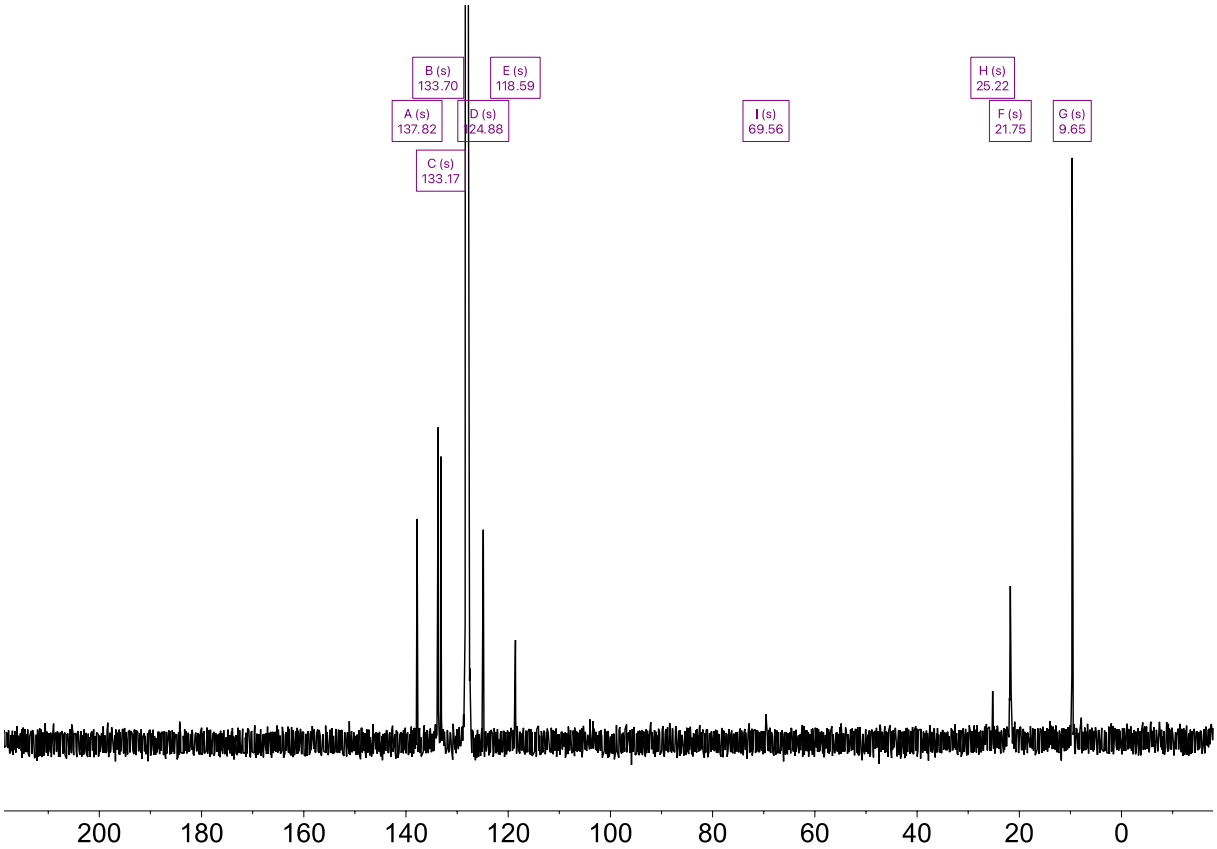

Figure S88: $^{13}C\{^{1}H\}$ NMR spectrum of **8**·4THF in C_6D_6 at 298 K, 125 MHz.

Adduct **9**·4THF

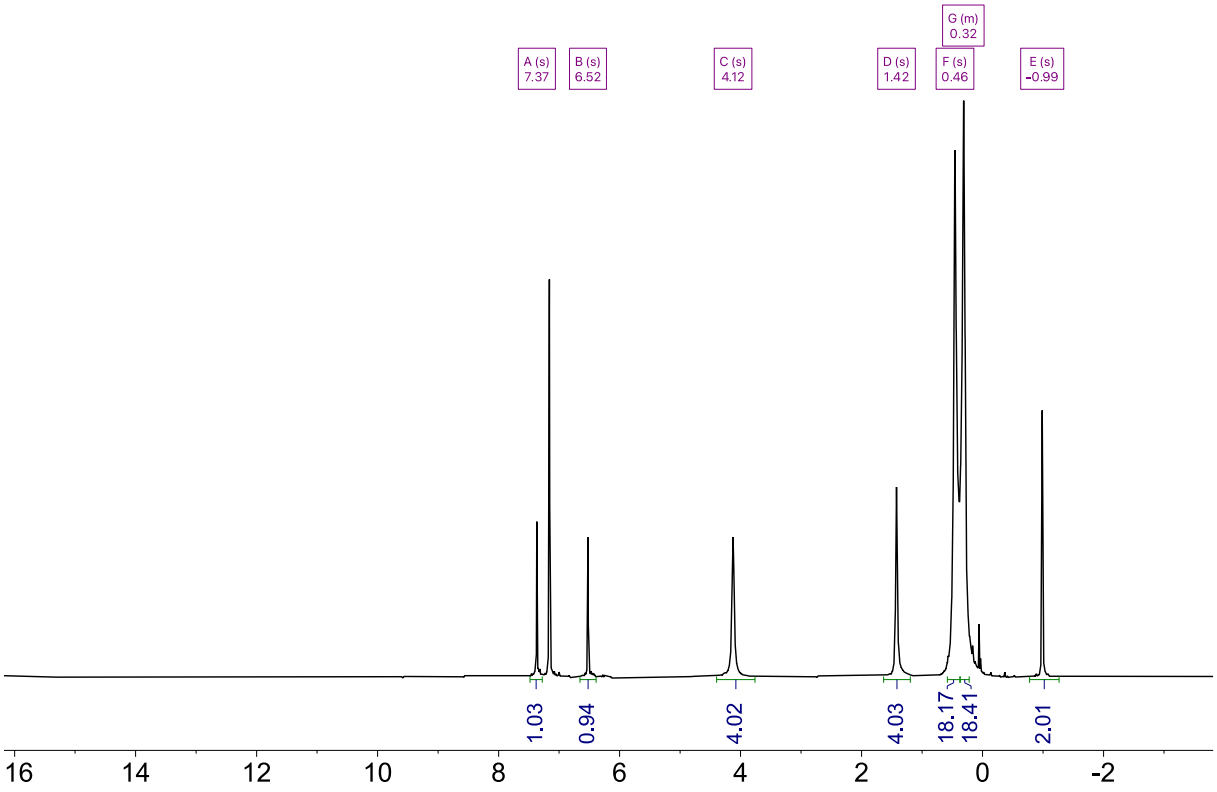

Figure S89: ^{1}H NMR spectrum of **8**·4THF in C_6D_6 at 298 K, 500 MHz.

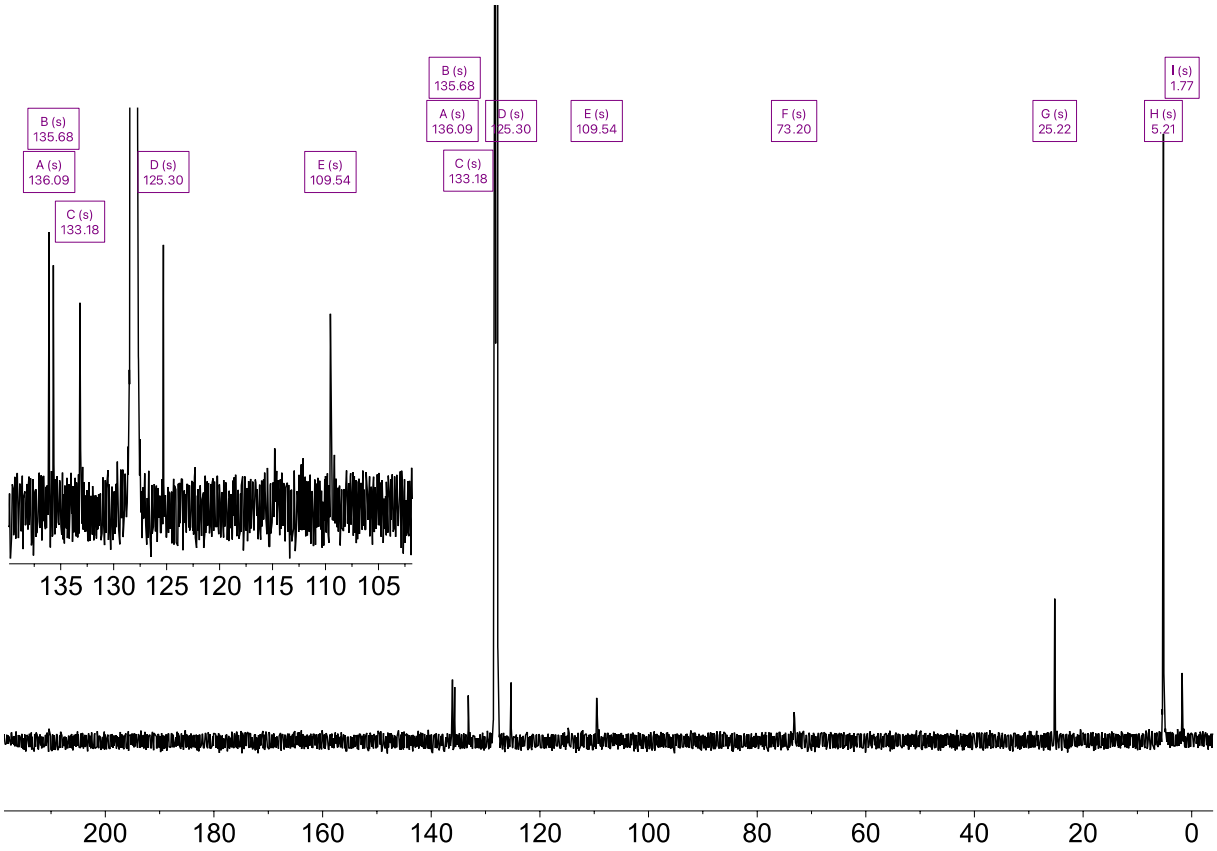

Figure S90: $^{13}C\{^{1}H\}$ NMR spectrum of **8**·4THF in C_6D_6 at 298 K, 125 MHz.

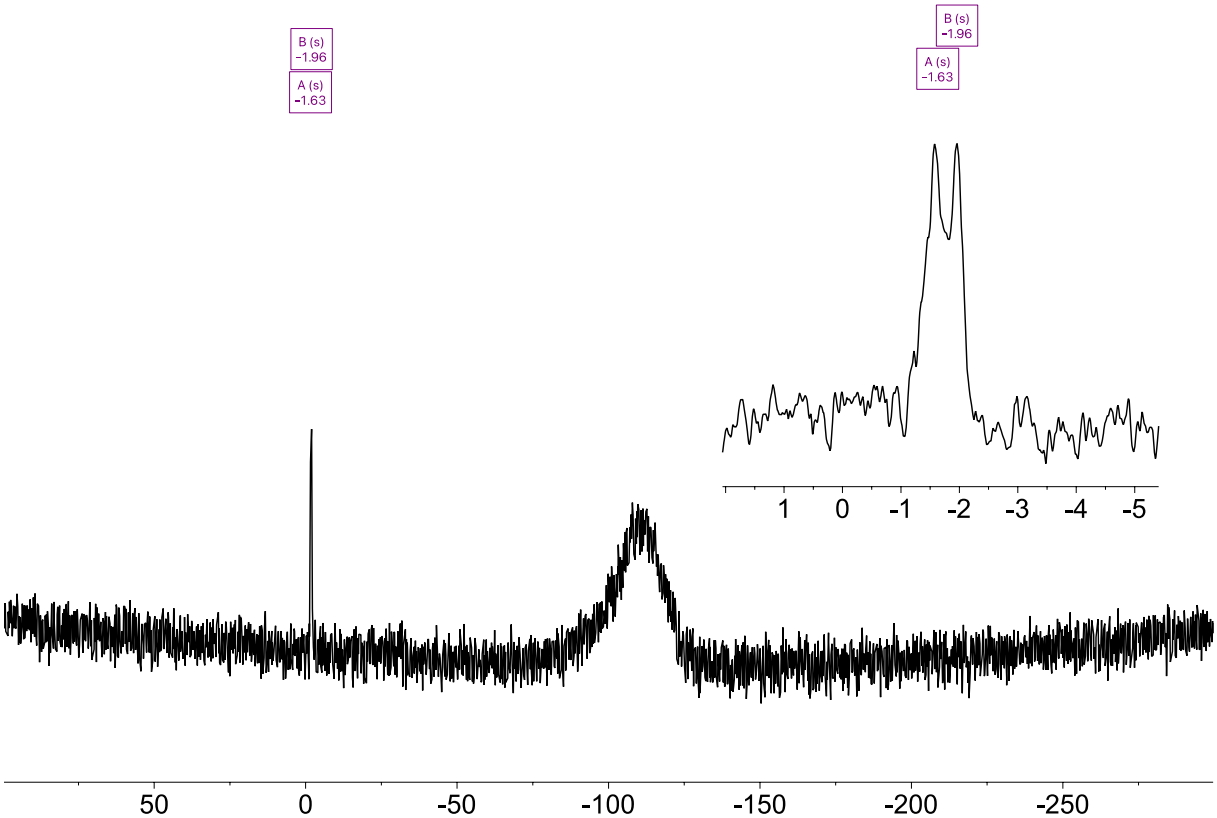

Figure S91: $^{29}Si\{^{1}H\}$ NMR spectrum of **8**·4THF in C_6D_6 at 298 K, 99 MHz. The peak at –110 ppm is due to the silicon atoms in the glass.

Adduct [6·2BisPhos]$_2$

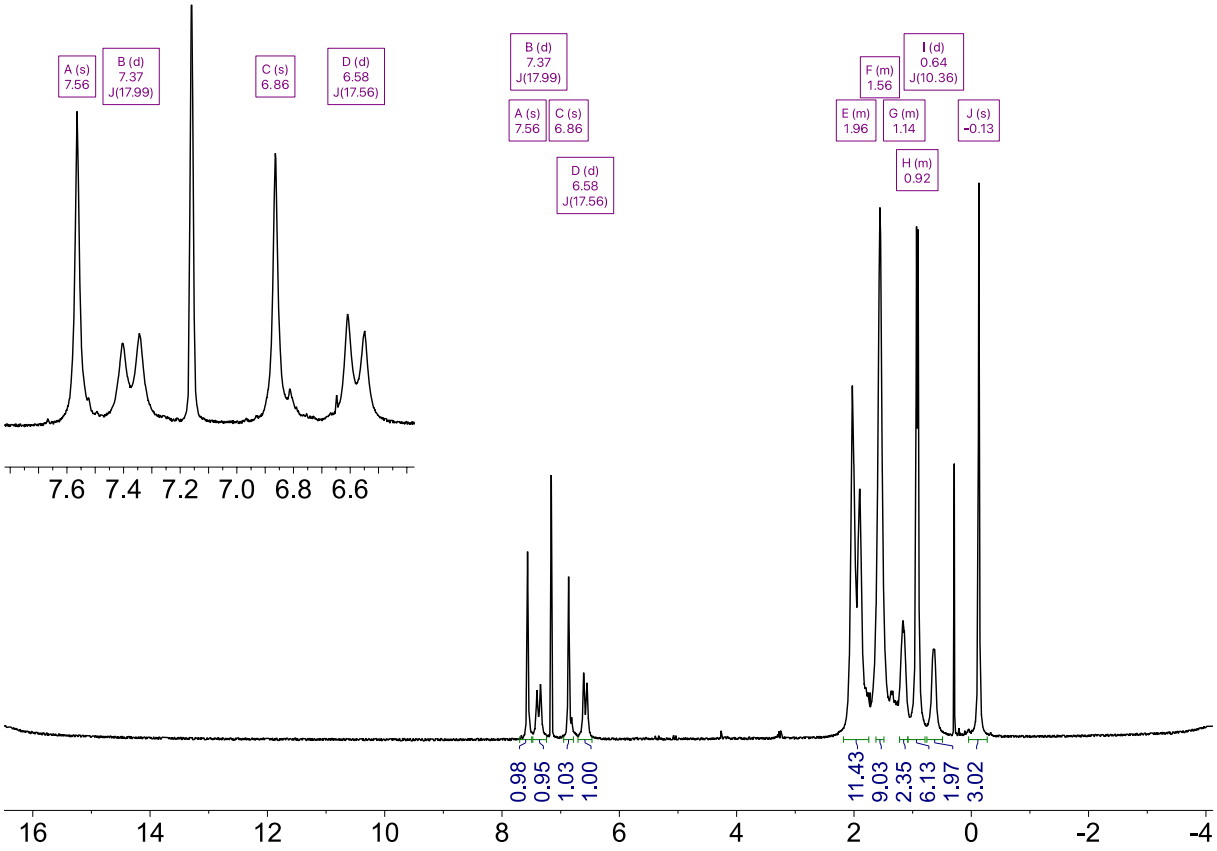

Figure S91: ^{1}H NMR spectrum of [**6**·2BisPhos]$_2$ in C_6D_6 at 298 K, 500 MHz.

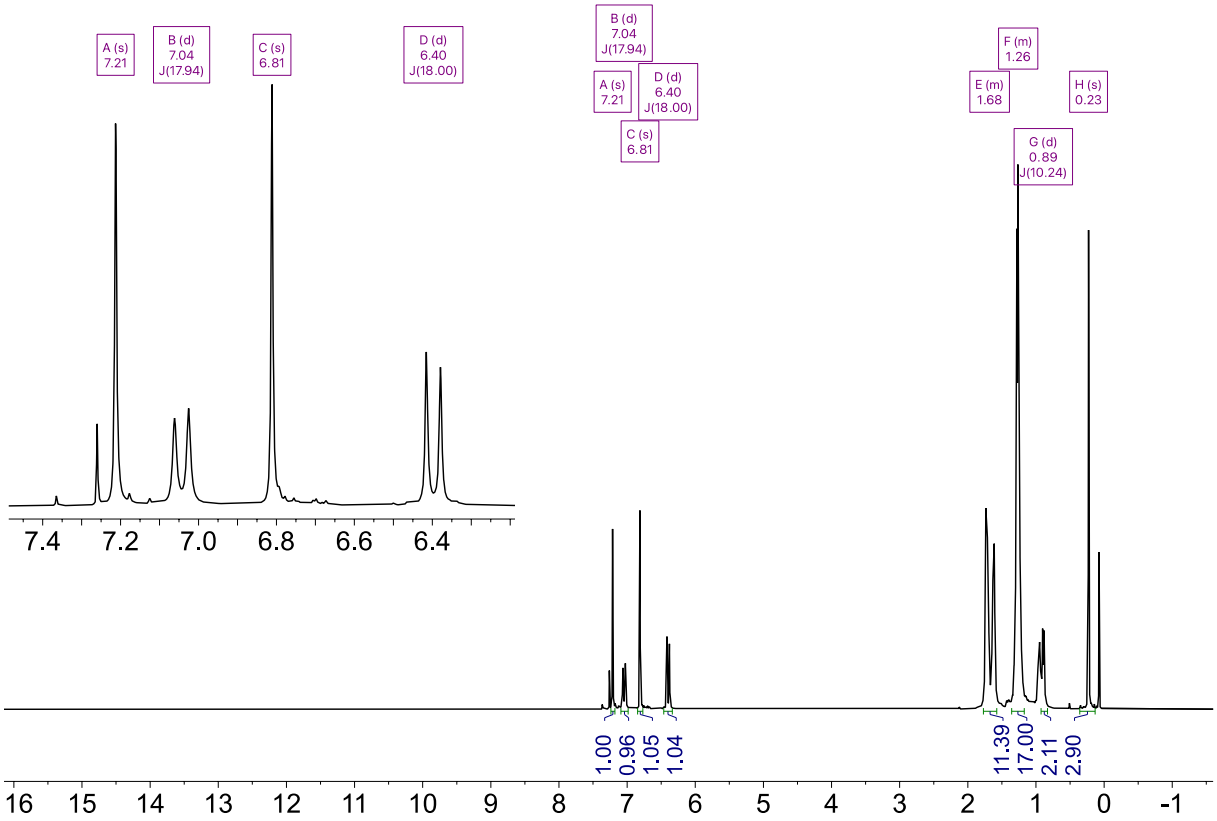

Figure S92: ^{1}H NMR spectrum of [**6**·2BisPhos]$_2$ in $CDCl_3$ at 298 K, 500 MHz.

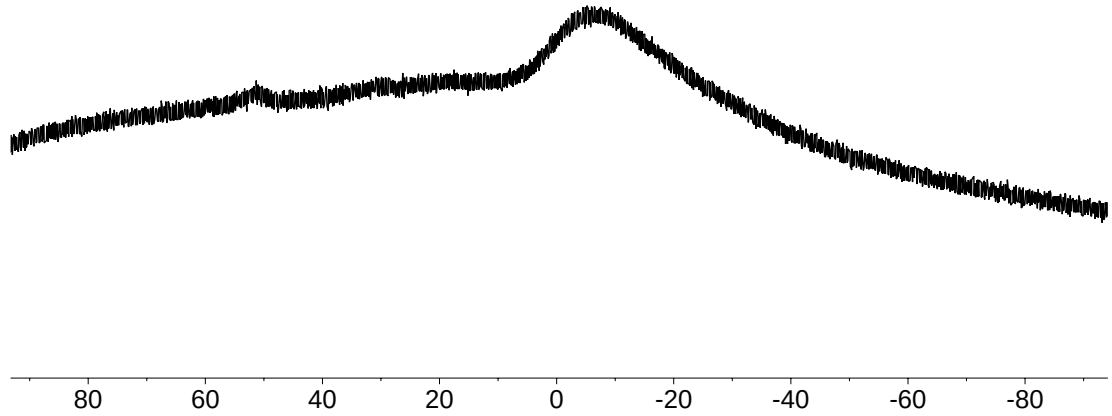

Figure S93: ^{11}B NMR spectrum of [**6**·2BisPhos]$_2$ in C_6D_6 at 298 K, 160 MHz. The signal is partially superimposed by the signal of the boron atoms 0 to –25 ppm contained in the glass.

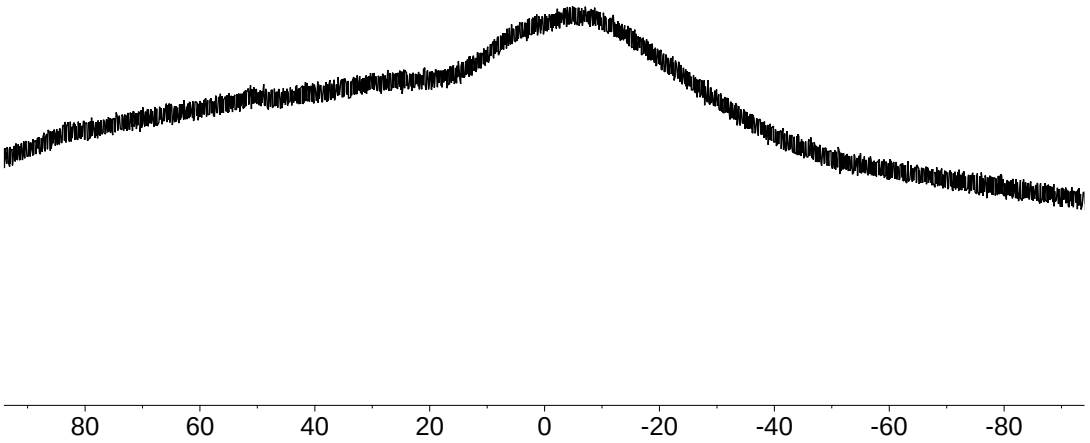

Figure S94: ^{11}B NMR spectrum of [**6**·2BisPhos]$_2$ in $CDCl_3$ at 298 K, 160 MHz. The signal is partially superimposed by the signal of the boron atoms 0 to –25 ppm contained in the glass.

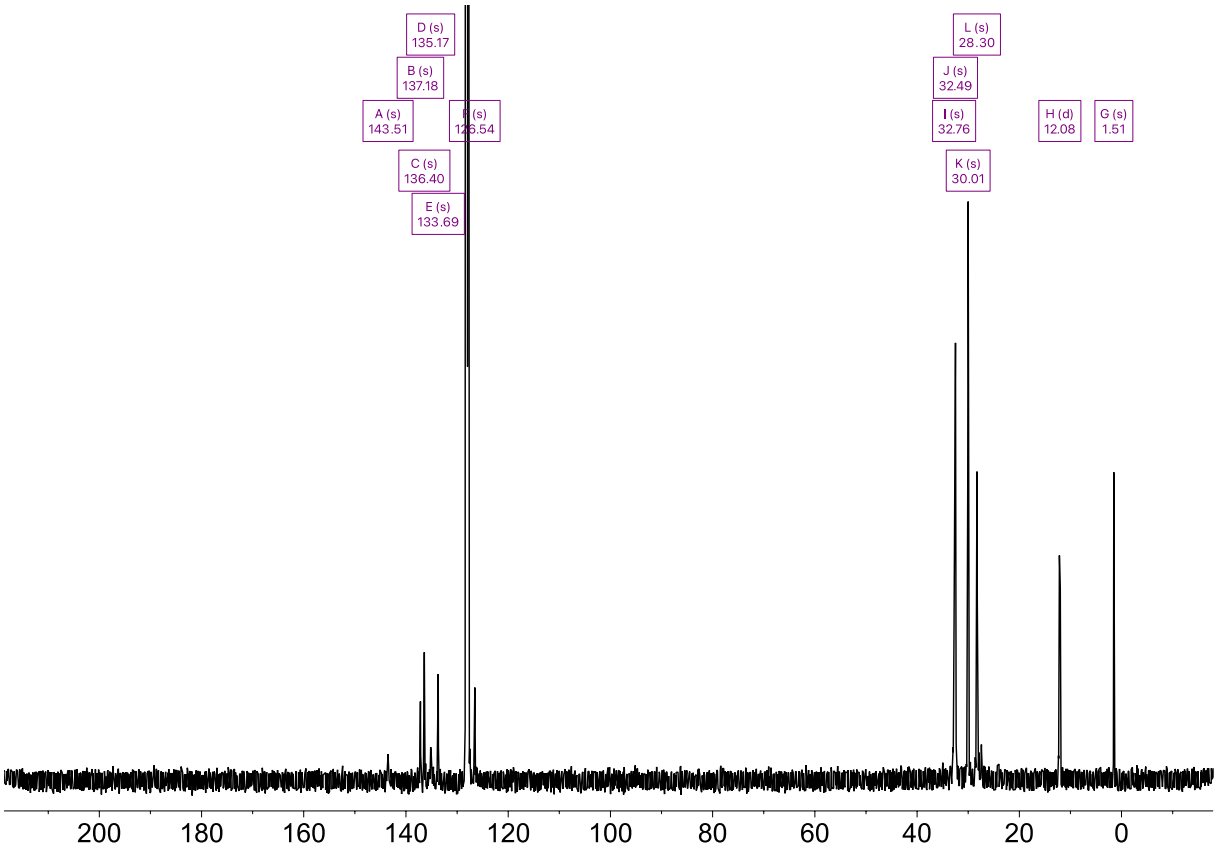

Figure S95: $^{13}C\{^{1}H\}$ NMR spectrum of [**6**·2BisPhos]$_2$ in C_6D_6 at 298 K, 125 MHz.

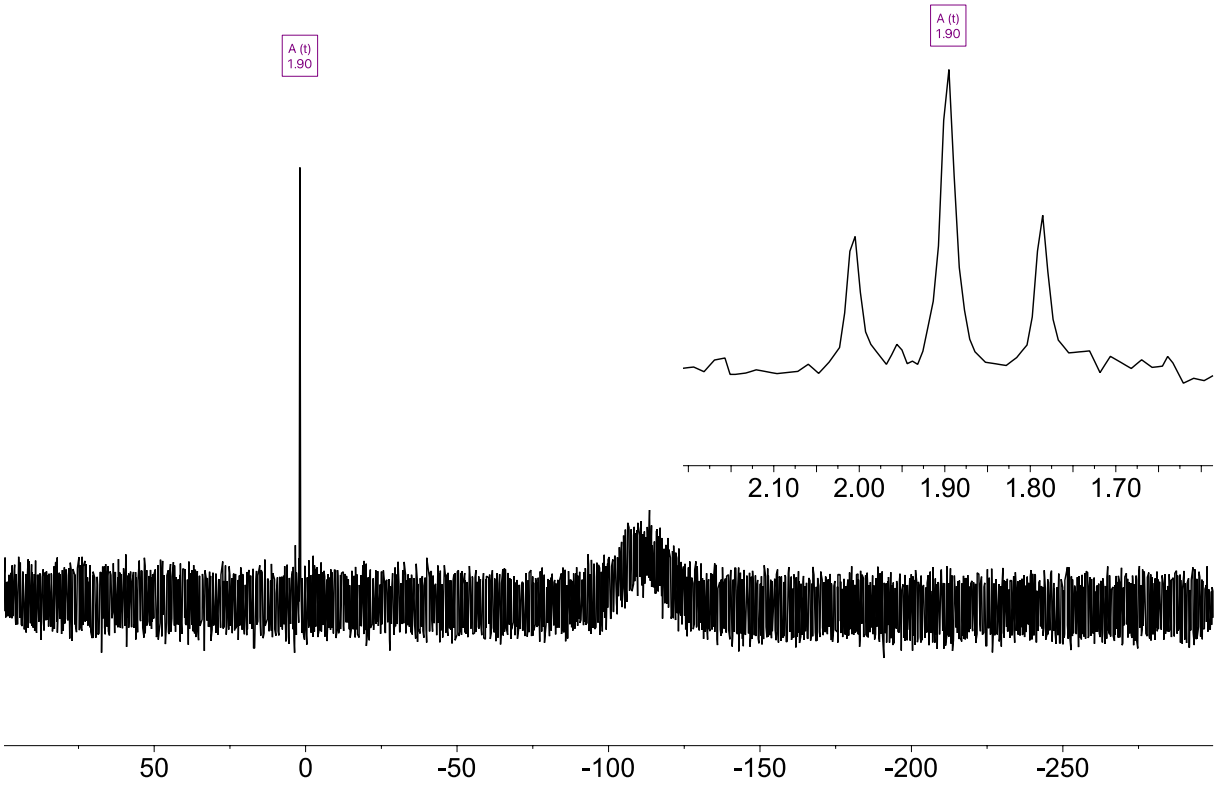

Figure S96: $^{29}Si\{^{1}H\}$ NMR spectrum of [**6**·2BisPhos]$_2$ in C_6D_6 at 298 K, 99 MHz. The peak at –110 ppm is due to the silicon atoms in the glass.

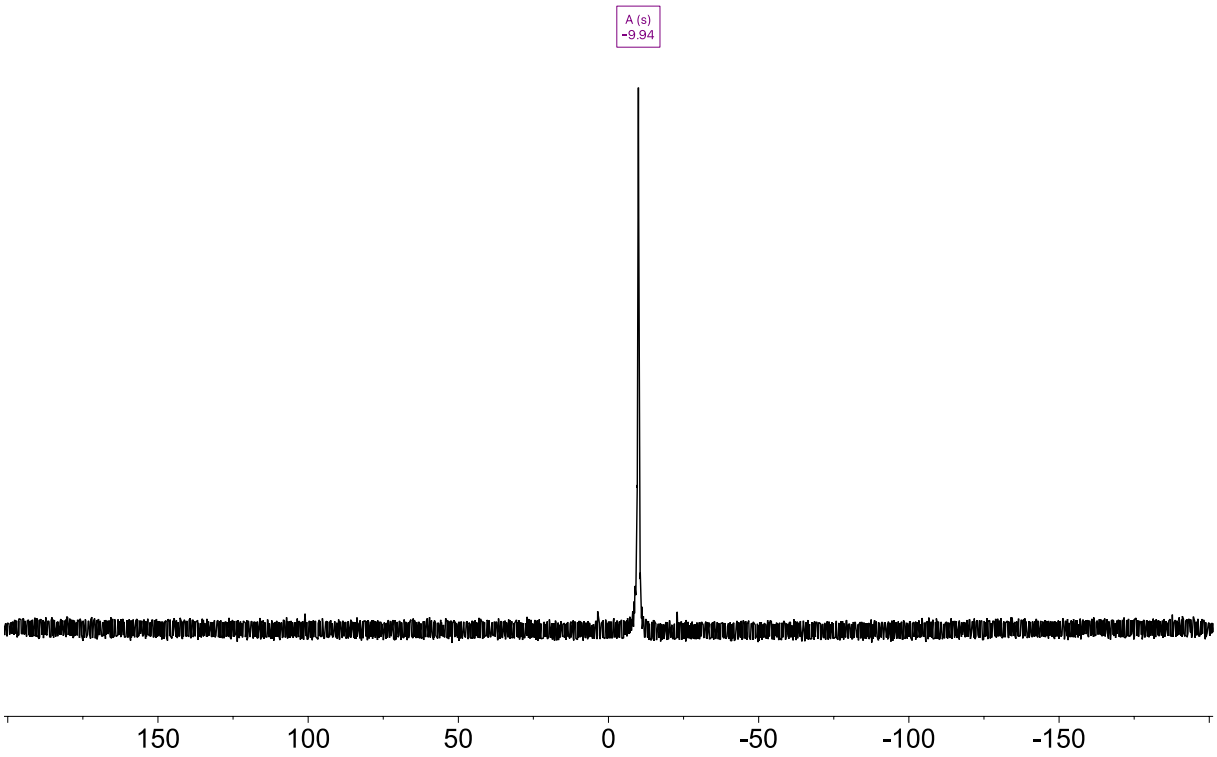

Figure S97: $^{31}P\{^{1}H\}$ NMR spectrum of [**6**·2BisPhos]$_2$ in C_6D_6 at 298 K, 202 MHz.

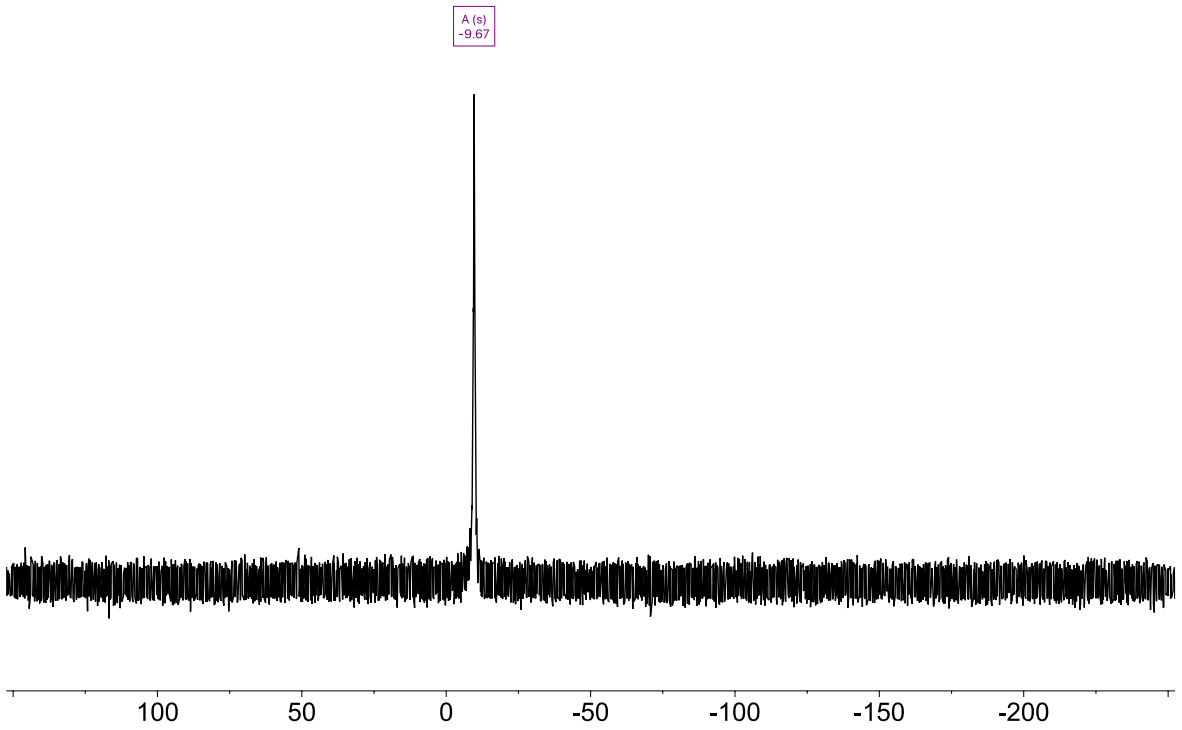

Figure S98: $^{31}P\{^{1}H\}$ NMR spectrum of [**6**·2BisPhos]$_2$ in $CDCl_3$ at 298 K, 202 MHz.

Adduct 7 + BisPhos

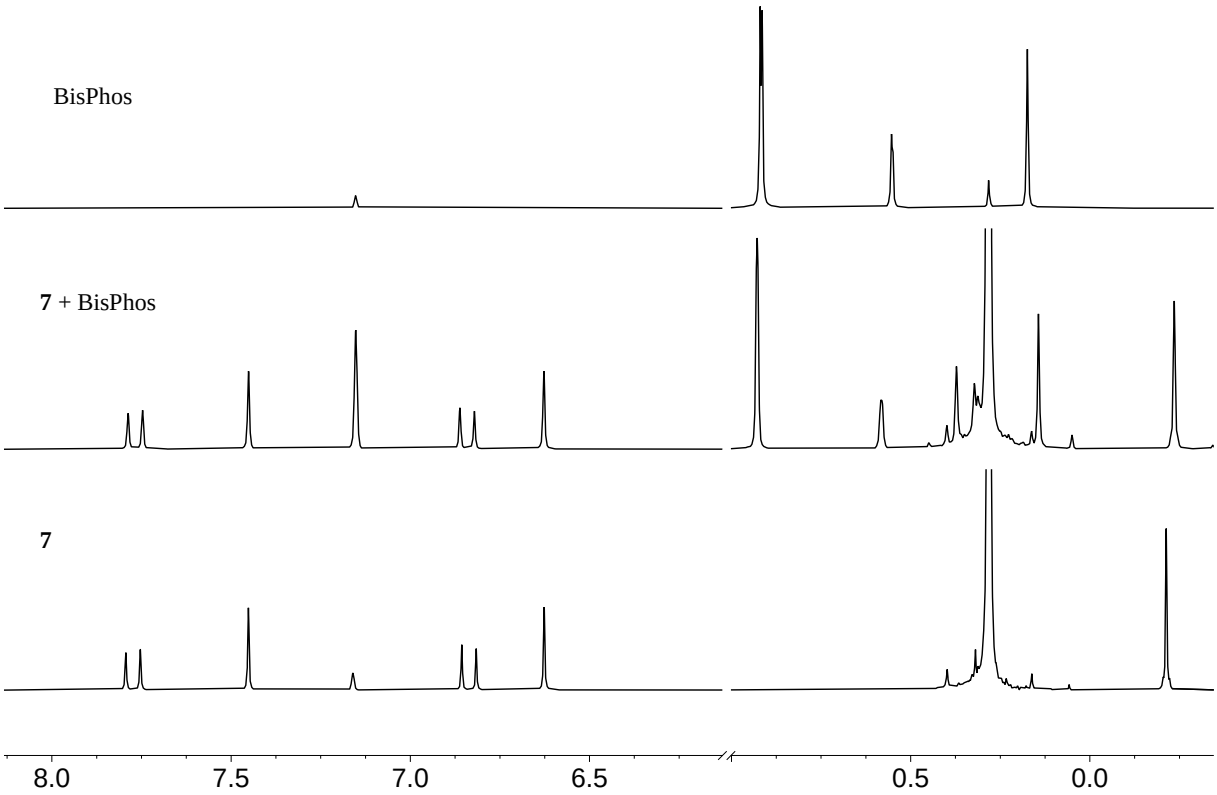

Figure S99: ^{1}H NMR spectra of BisPhos, **7** and BisPhos + **7** in C_6D_6 at 298 K, 500 MHz.

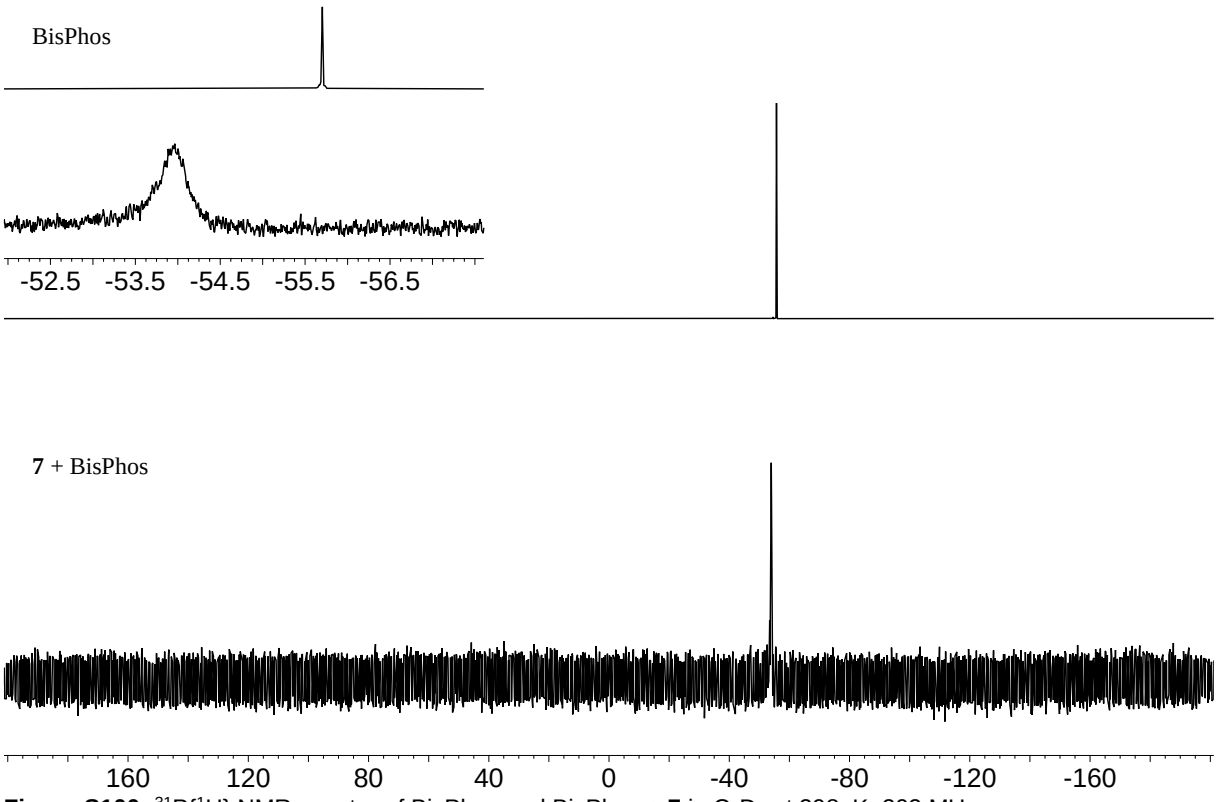

Figure S100: $^{31}P\{^{1}H\}$ NMR spectra of BisPhos and BisPhos + **7** in C_6D_6 at 298 K, 202 MHz.

Adduct 8·2BisPhos

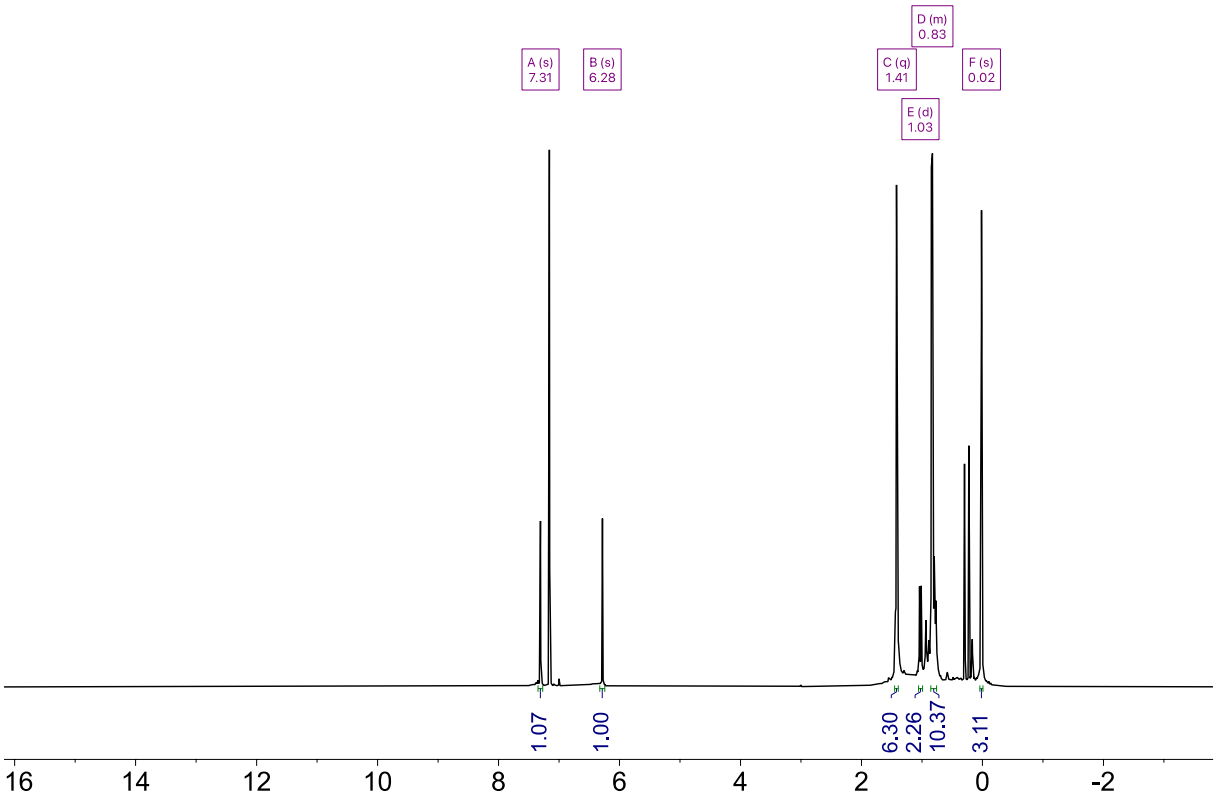

Figure S101: ^{1}H NMR spectrum of **8**·2BisPhos in C_6D_6 at 298 K, 500 MHz.

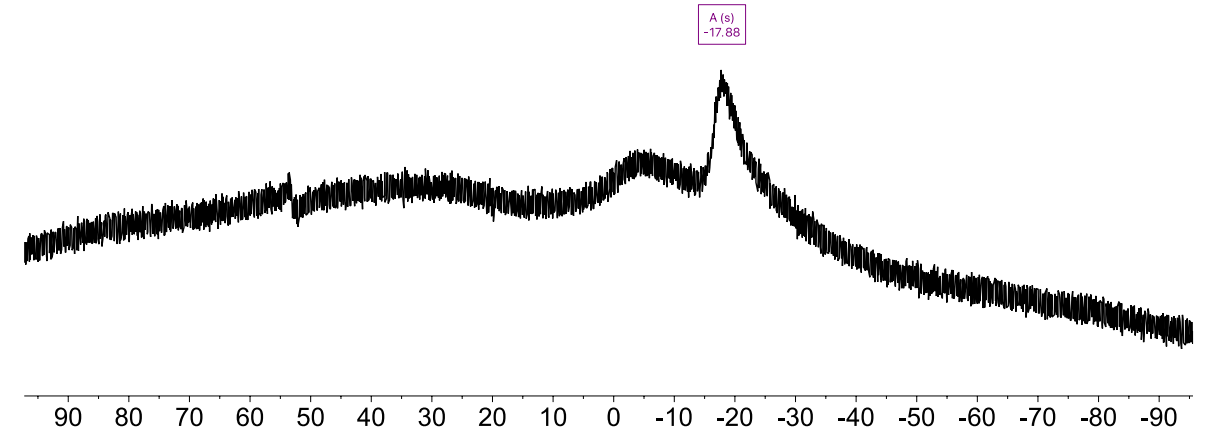

Figure S102: ^{11}B NMR spectrum of **8**·2BisPhos in C_6D_6 at 298 K, 160 MHz.

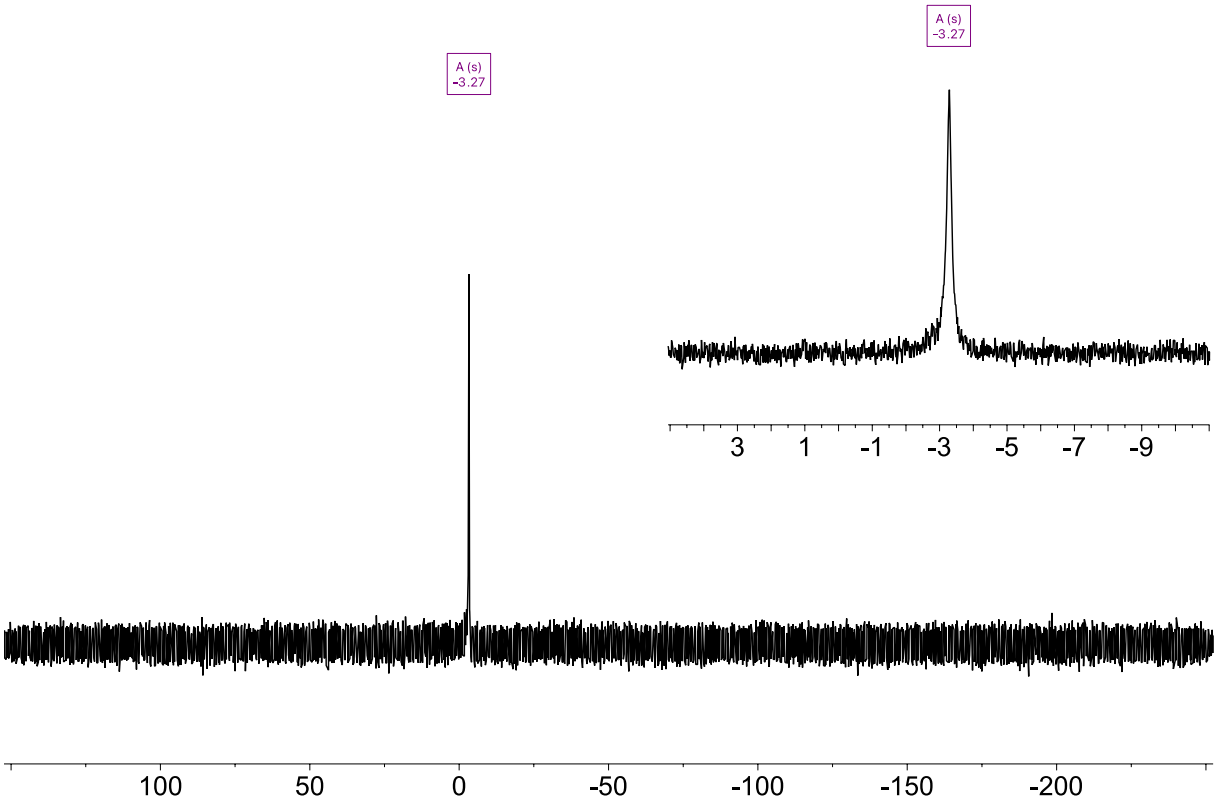

Figure S103: $^{31}P\{^{1}H\}$ NMR spectrum of 8·**2BisPhos** in C_6D_6 at 298 K, 202 MHz.

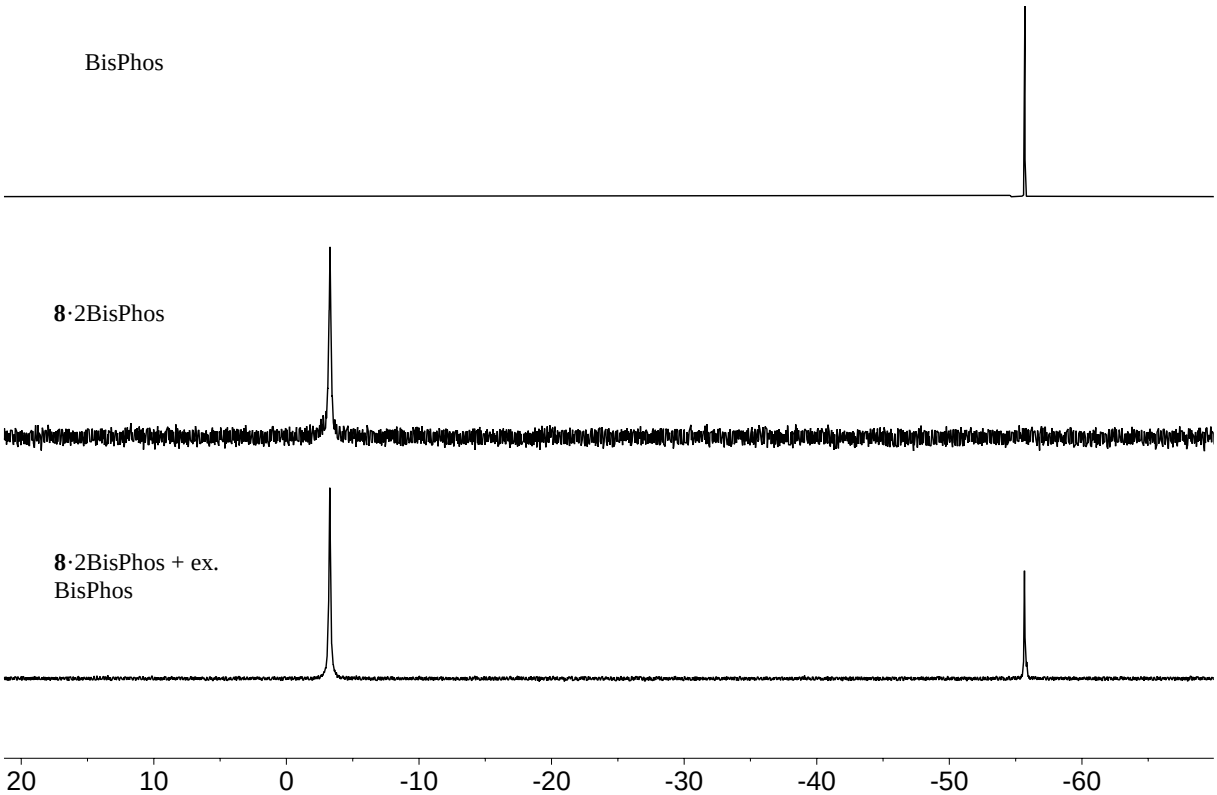

Figure S104: $^{31}P\{^{1}H\}$ NMR spectra of BisPhos, **8**·2BisPhos and **8**·2BisPhos + ex. BisPhos in C_6D_6 at 298 K, 202 MHz.

Adduct 9·2BisPhos

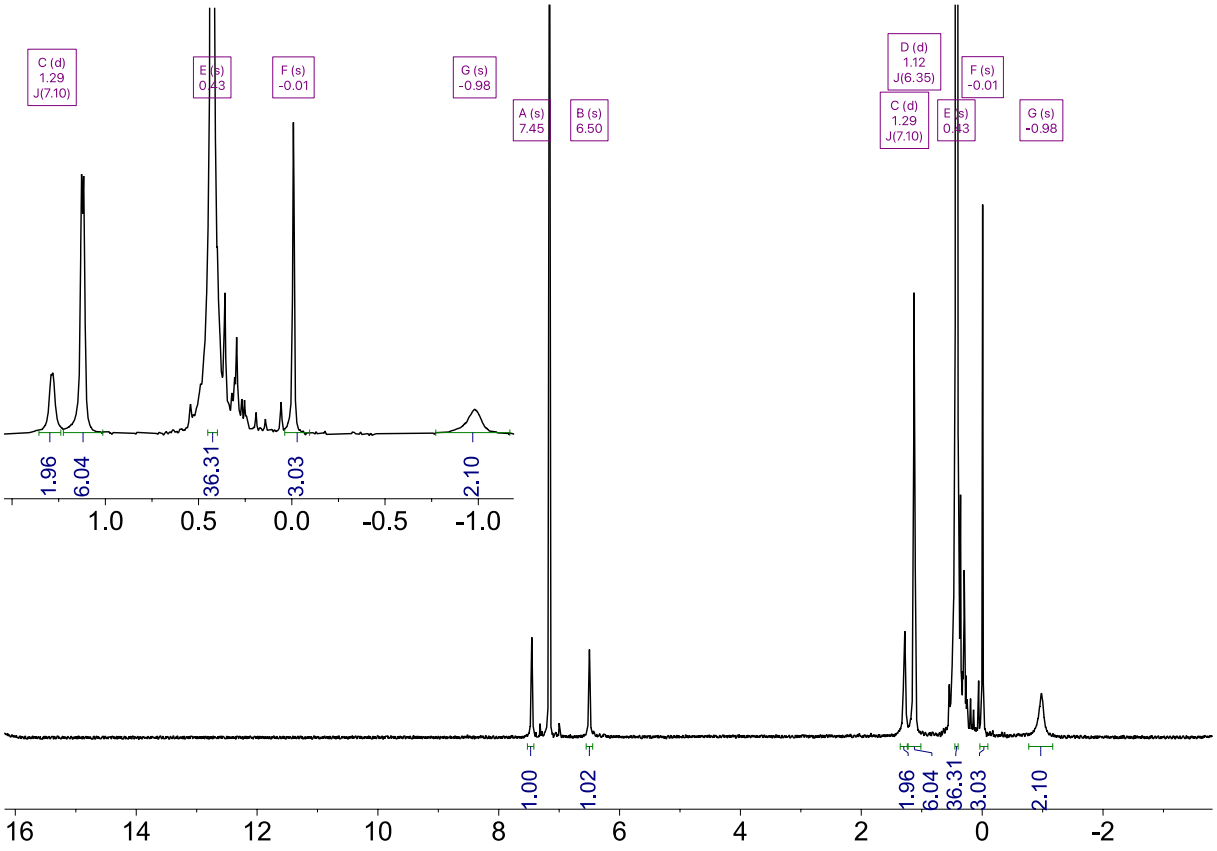

Figure S105: ^{1}H NMR spectrum of **9**·2BisPhos in C_6D_6 at 298 K, 500 MHz.

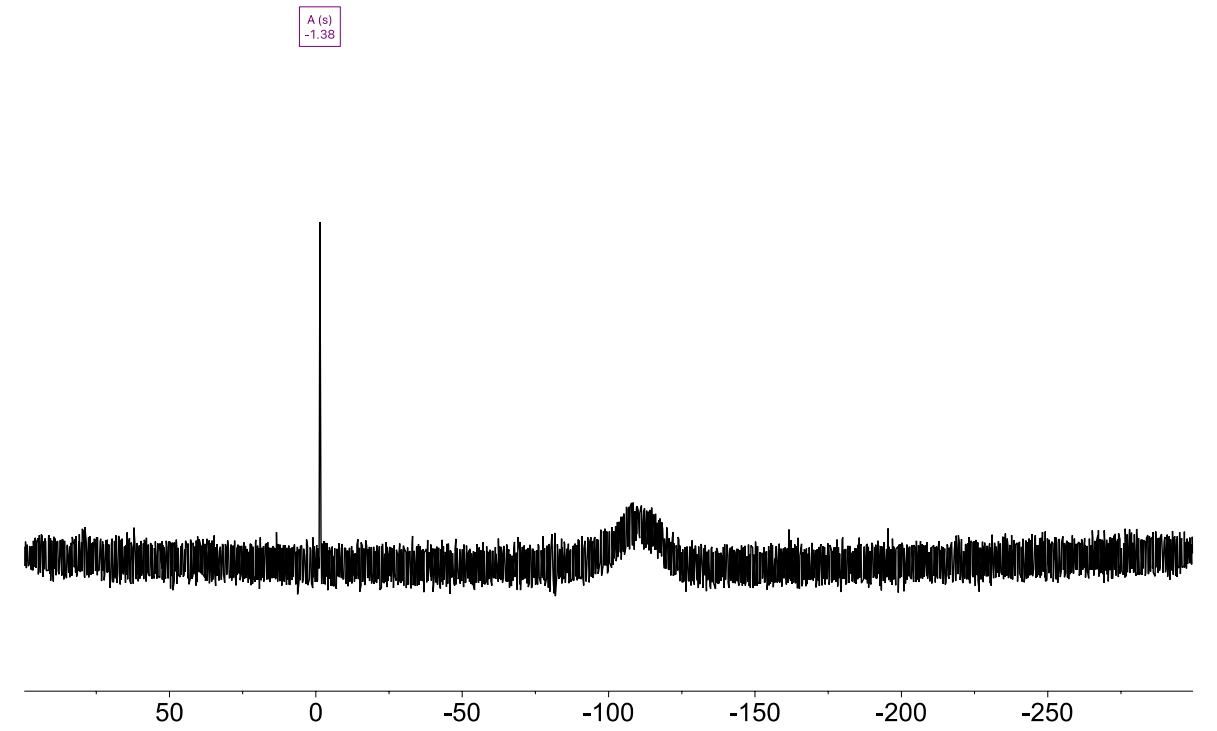

Figure S106: ^{29}Si{^{1}H} NMR spectrum of **9**·2BisPhos in C_6D_6 at 298 K, 99 MHz.

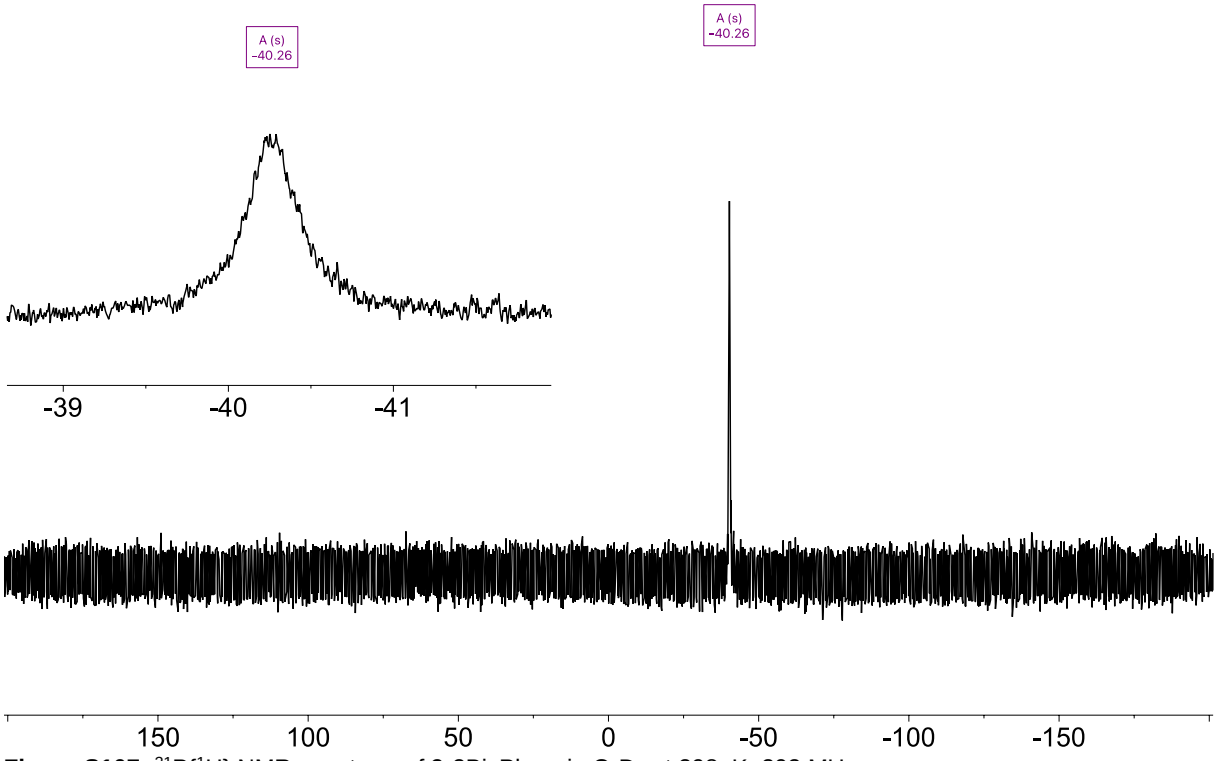

Figure S107: $^{31}P\{^{1}H\}$ NMR spectrum of **9**·2BisPhos in C_6D_6 at 298 K, 202 MHz.

Bis[BisPhos]

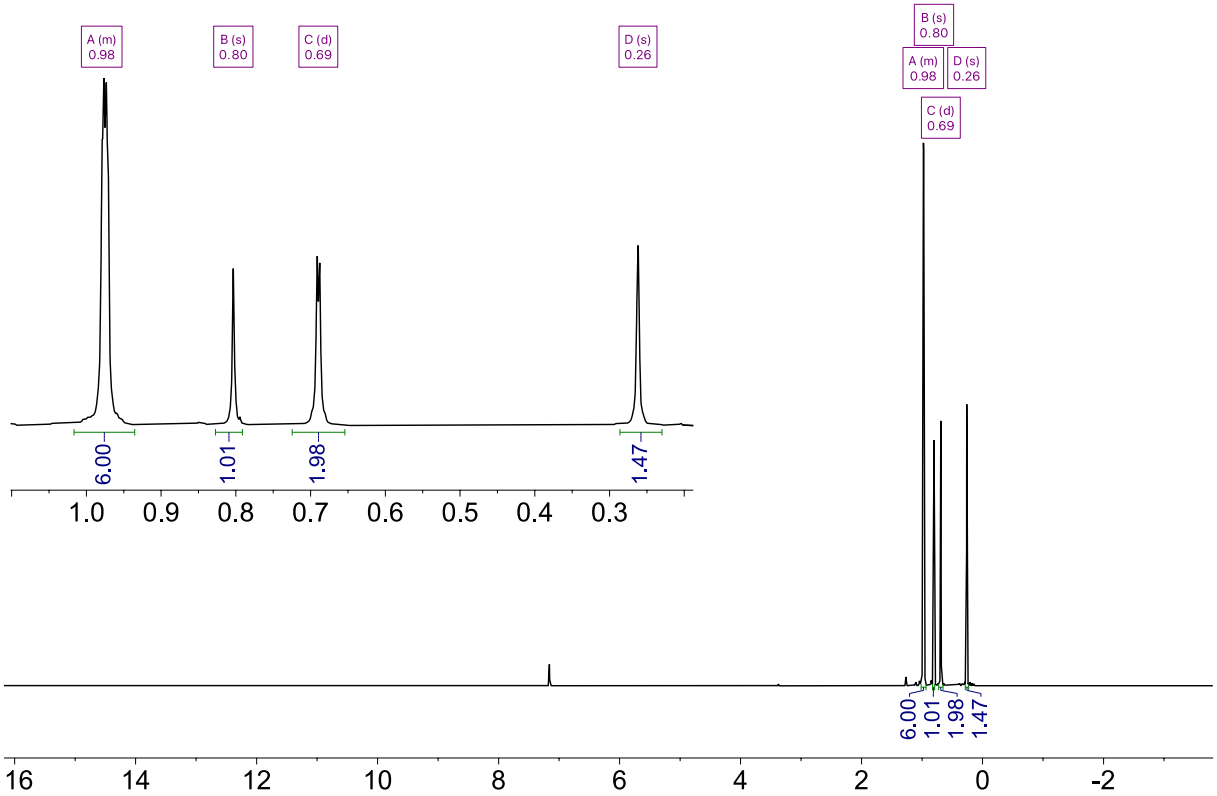

Figure S108: ^{1}H NMR spectrum of Bis[BisPhos] in C_6D_6 at 298 K, 500 MHz.

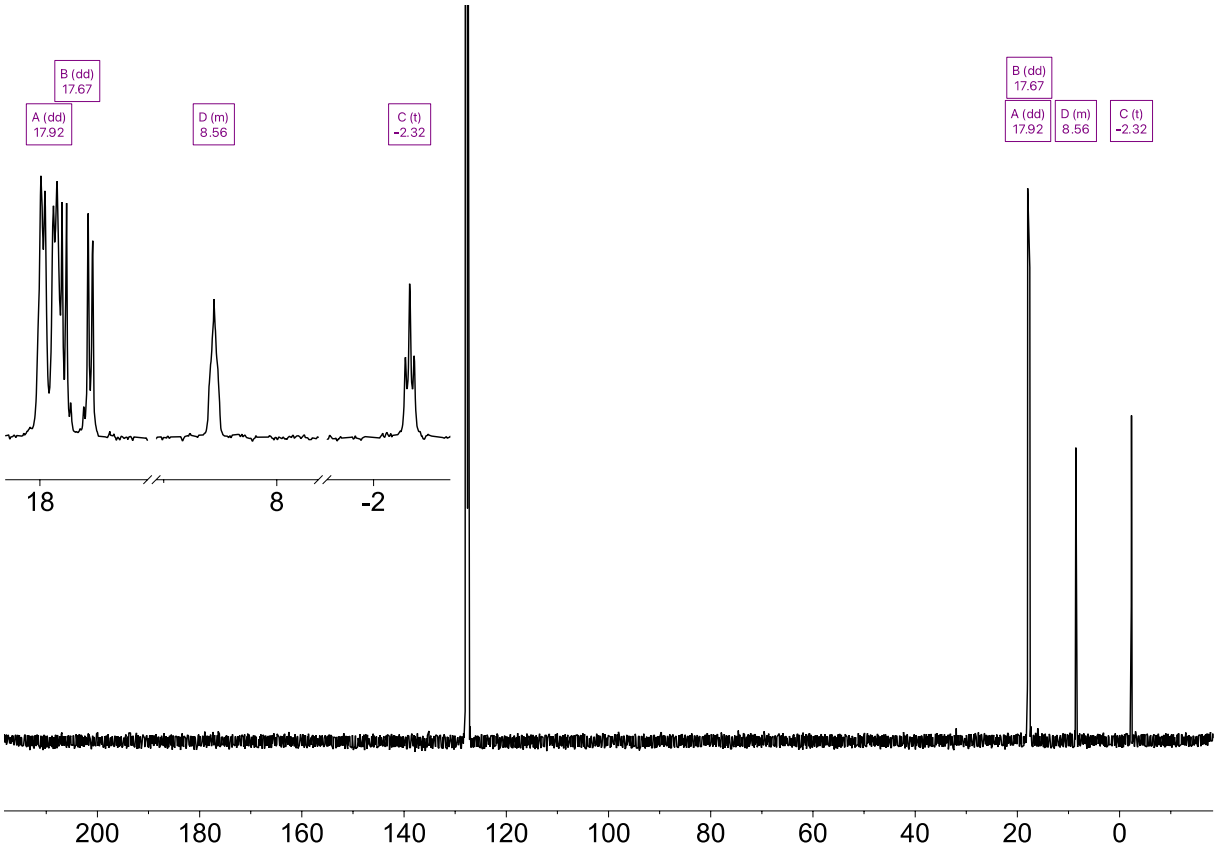

Figure S109: $^{13}C\{^{1}H\}$ NMR spectrum of Bis[BisPhos] in C_6D_6 at 298 K, 125 MHz.

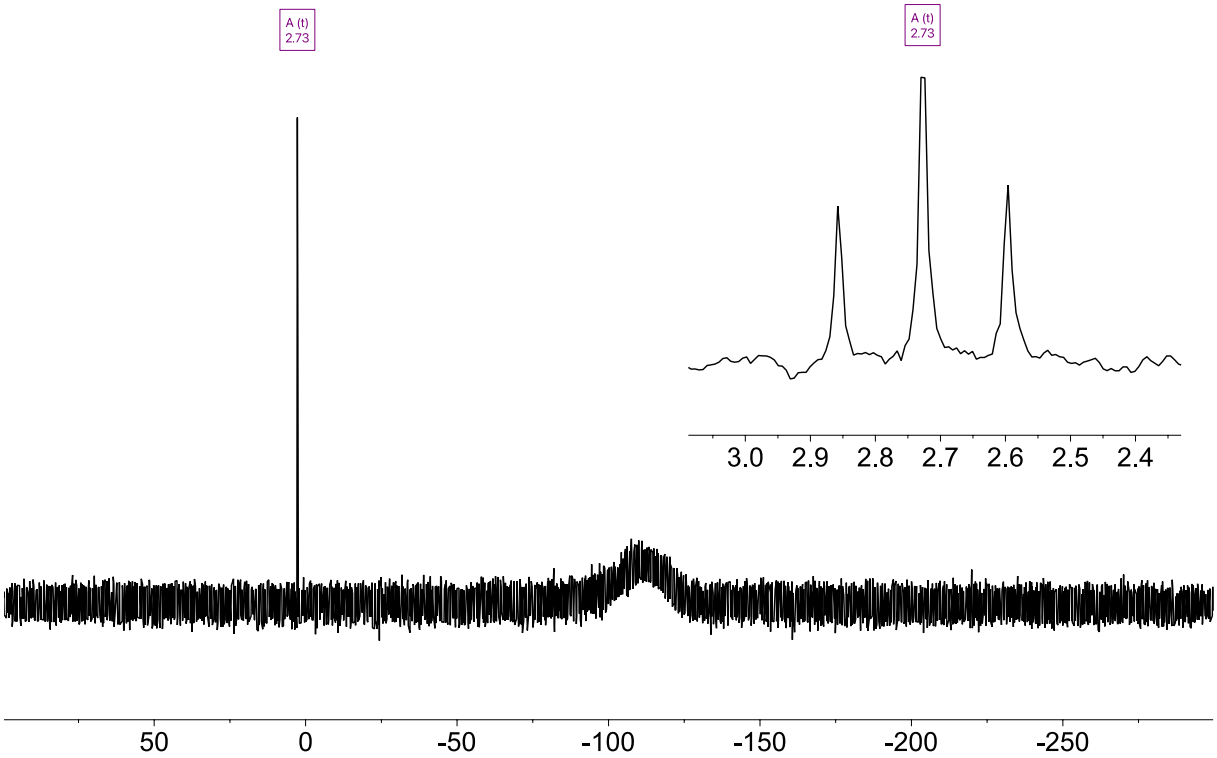

Figure S110: $^{29}Si\{^{1}H\}$ NMR spectrum of Bis[BisPhos] in C_6D_6 at 298 K, 99 MHz.

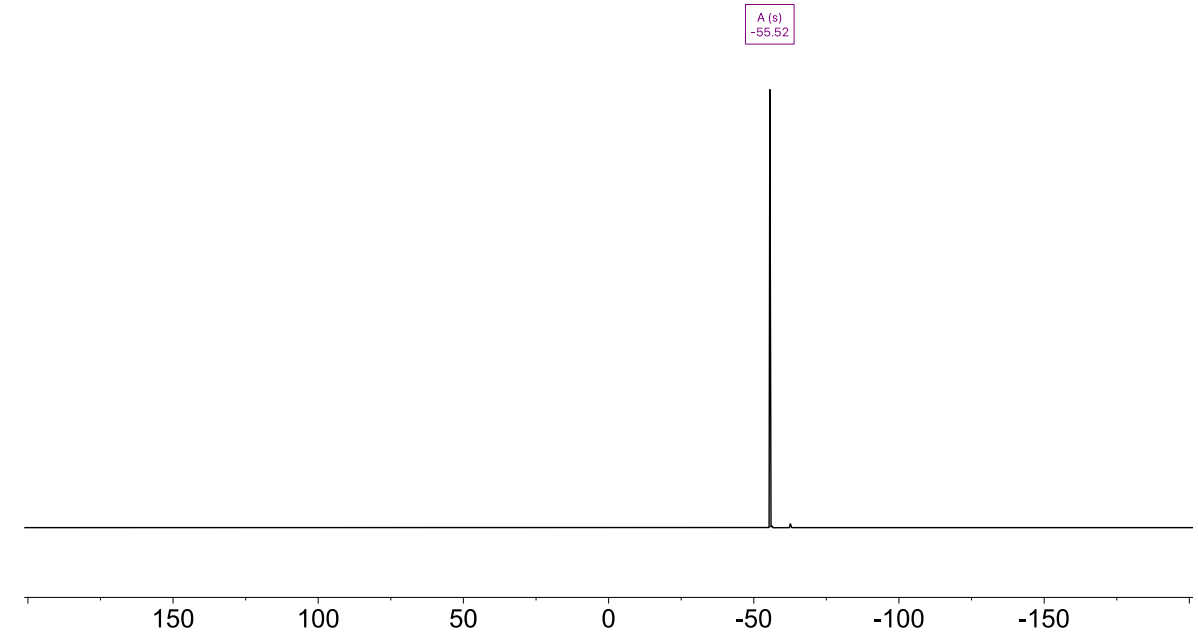

Figure S111: $^{31}P\{^{1}H\}$ NMR spectrum of Bis[BisPhos] in C_6D_6 at 298 K, 202 MHz.

Adduct 9·2Bis[BisPhos]

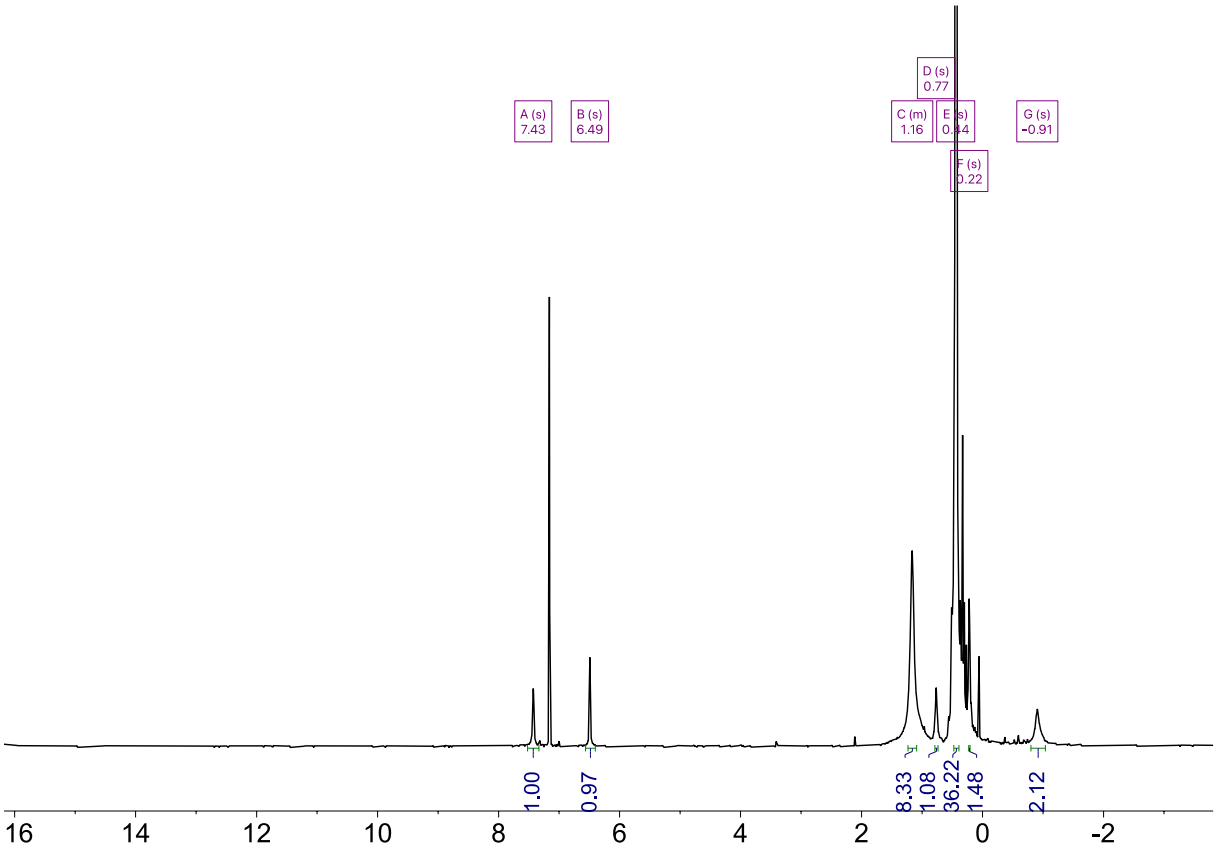

Figure S112: ^{1}H NMR spectrum of **9**·2Bis[BisPhos] in C_6D_6 at 298 K, 500 MHz.

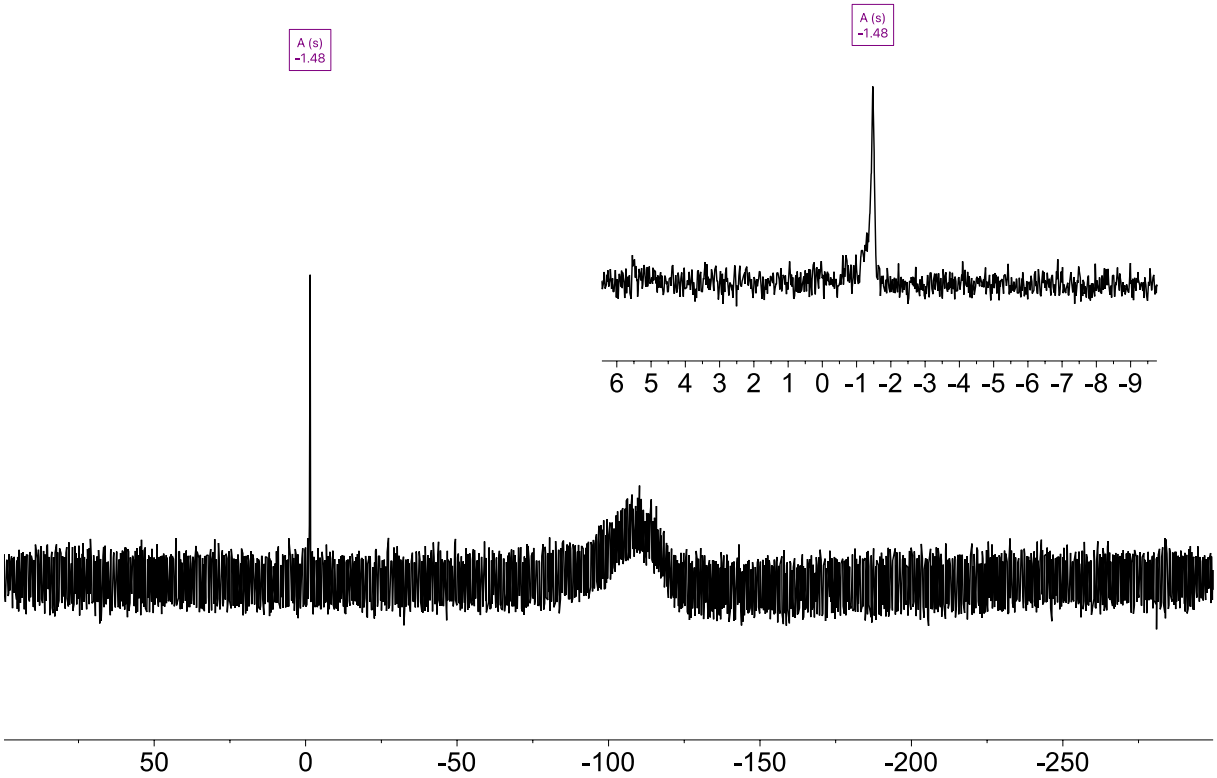

Figure S113: $^{29}Si\{^{1}H\}$ NMR spectrum of **9**·2Bis[BisPhos] in C_6D_6 at 298 K, 99 MHz.

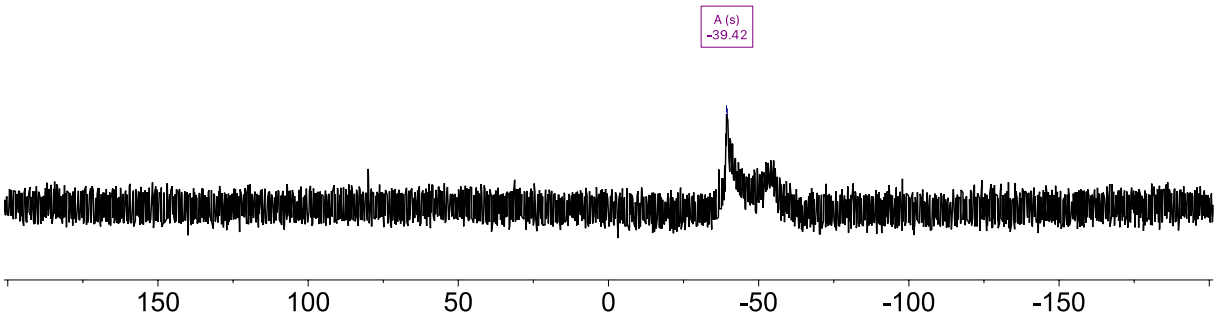

Figure S114: $^{31}P\{^{1}H\}$ NMR spectrum of **9**·2Bis[BisPhos**]** in C_6D_6 at 298 K, 202 MHz.

Adduct **7**·2N-1

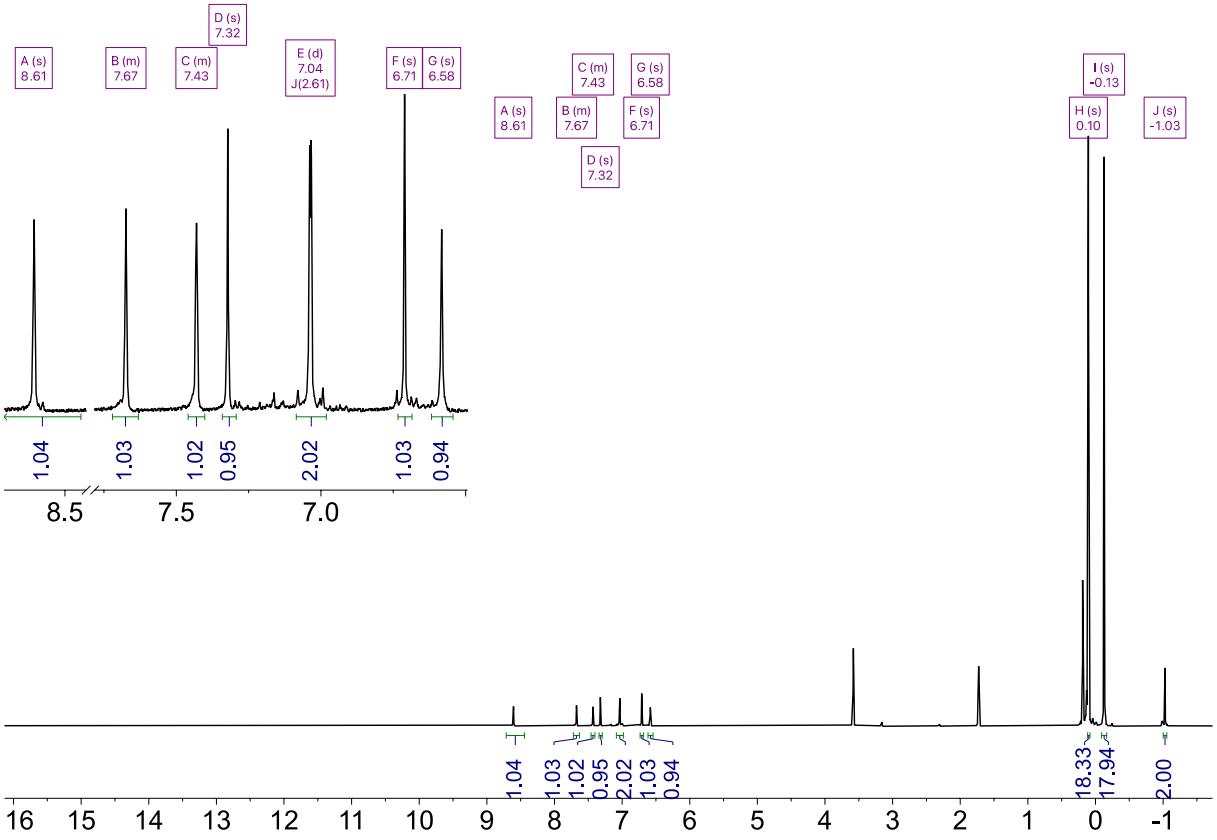

Figure S115: ^{1}H NMR spectrum of **7**·2N-1 in **THF-d$_8$** at 298 K, 500 MHz.

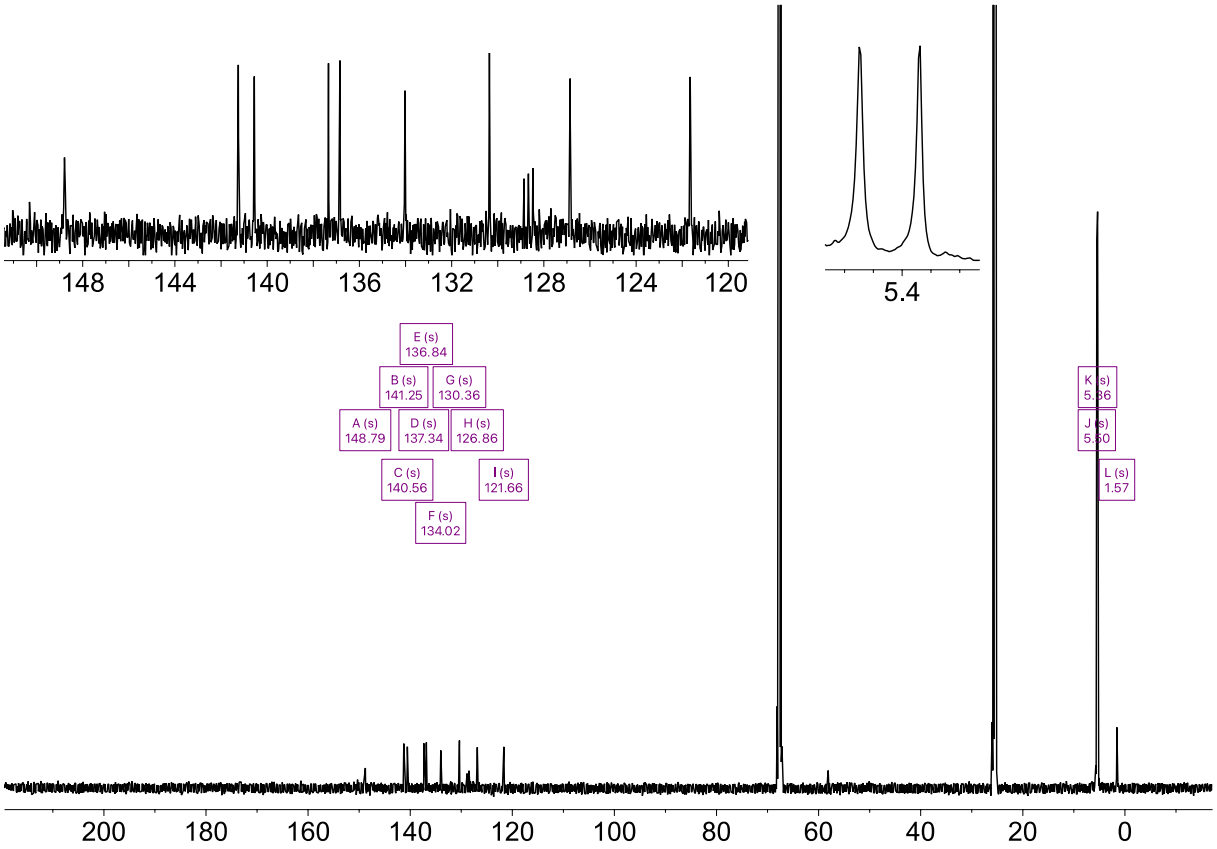

Figure S116: ^{13}C{^{1}H} NMR spectrum of **7**·2N-1 in THF-d$_8$ at 298 K, 125 MHz.

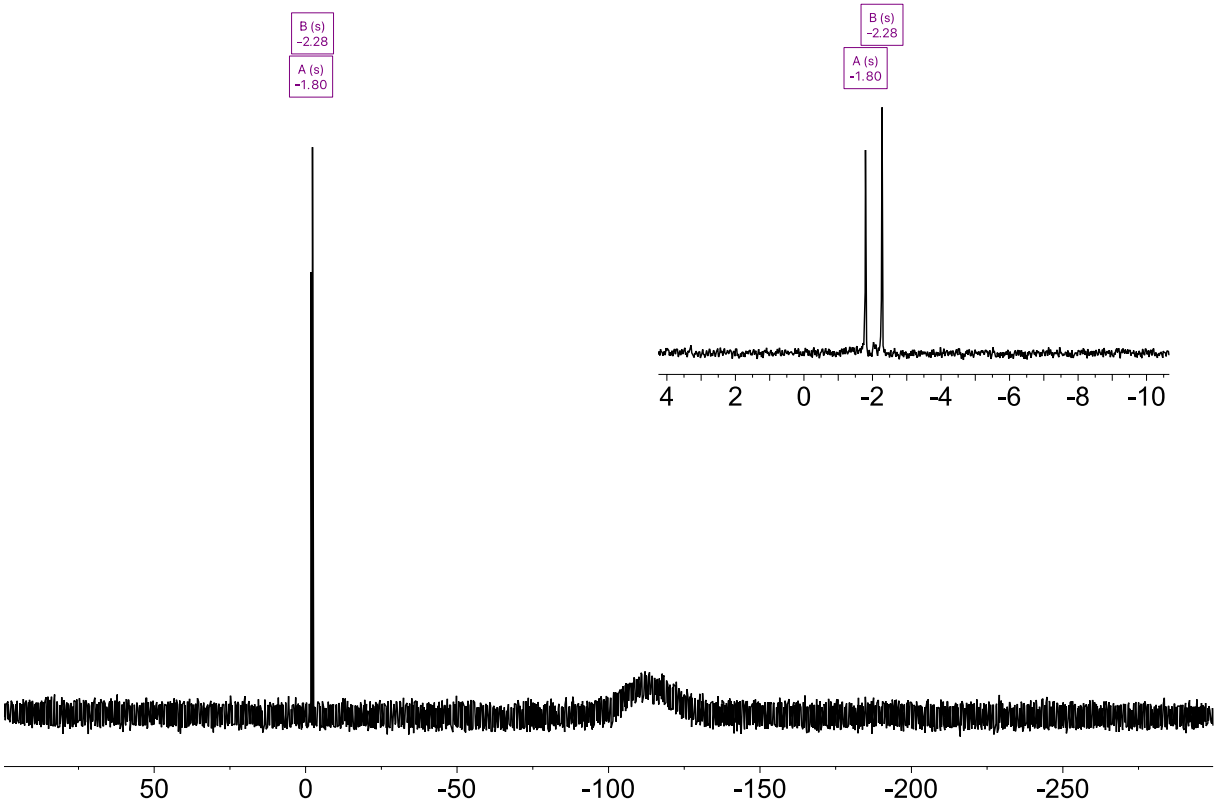

Figure S117: $^{29}Si\{^{1}H\}$ NMR spectrum of **7**·2N-1 in THF-d_8 at 298 K, 99 MHz.

Adduct **9**·2N-1

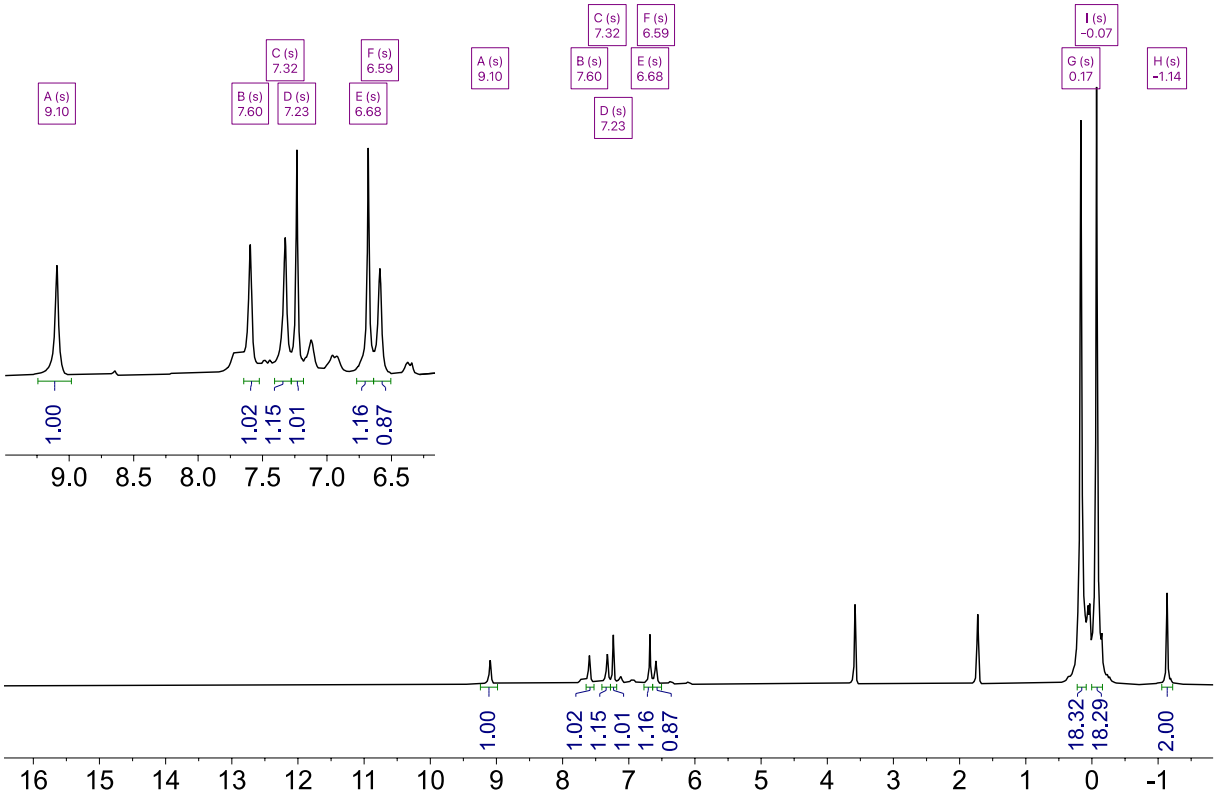

Figure S118: ^{1}H NMR spectrum of **9**·2N-1 in THF-d_8 at 298 K, 500 MHz. Note that the additional signals at 8.0–6.0 ppm come from excess, non-interacting N-1, as can be seen from the resulting cocrystal (Fig. X).

Adduct **7**·2N-2

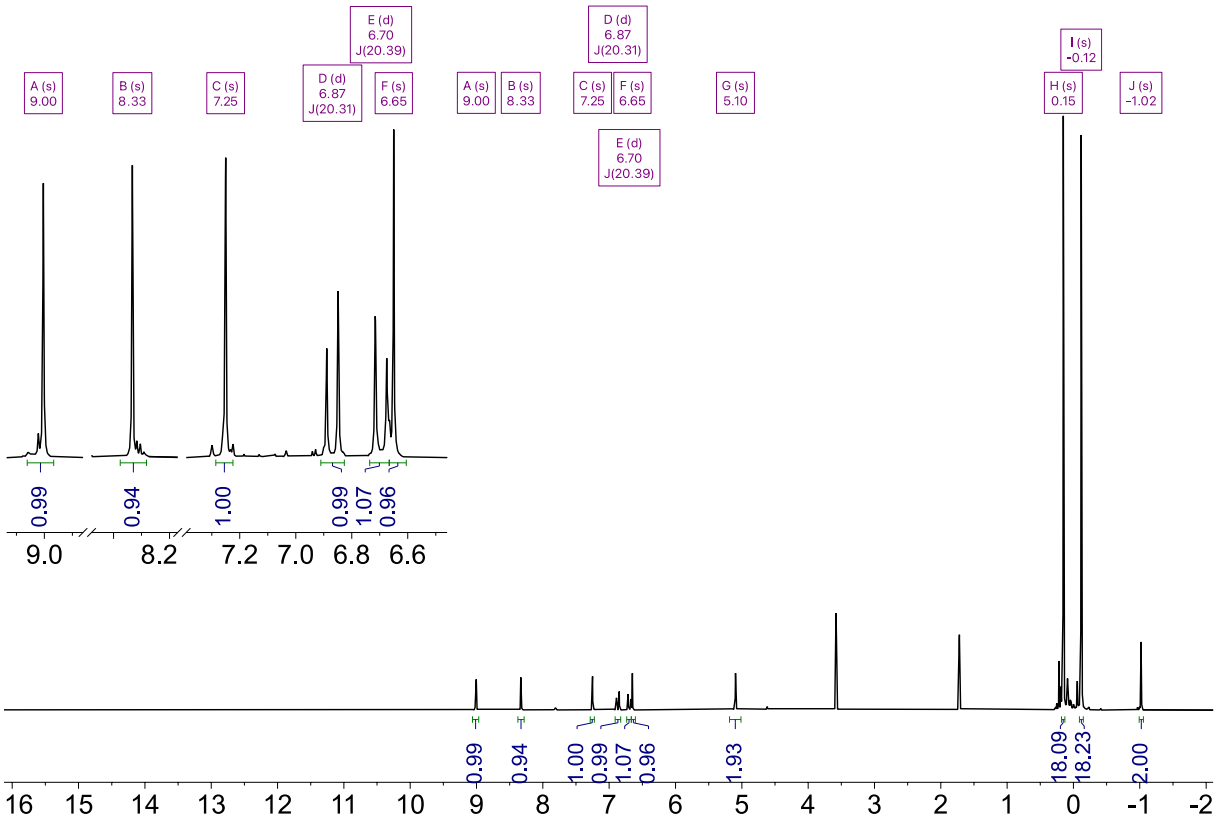

Figure S119: ^{1}H NMR spectrum of **7**·2N-2 in THF-d$_8$ at 298 K, 500 MHz.

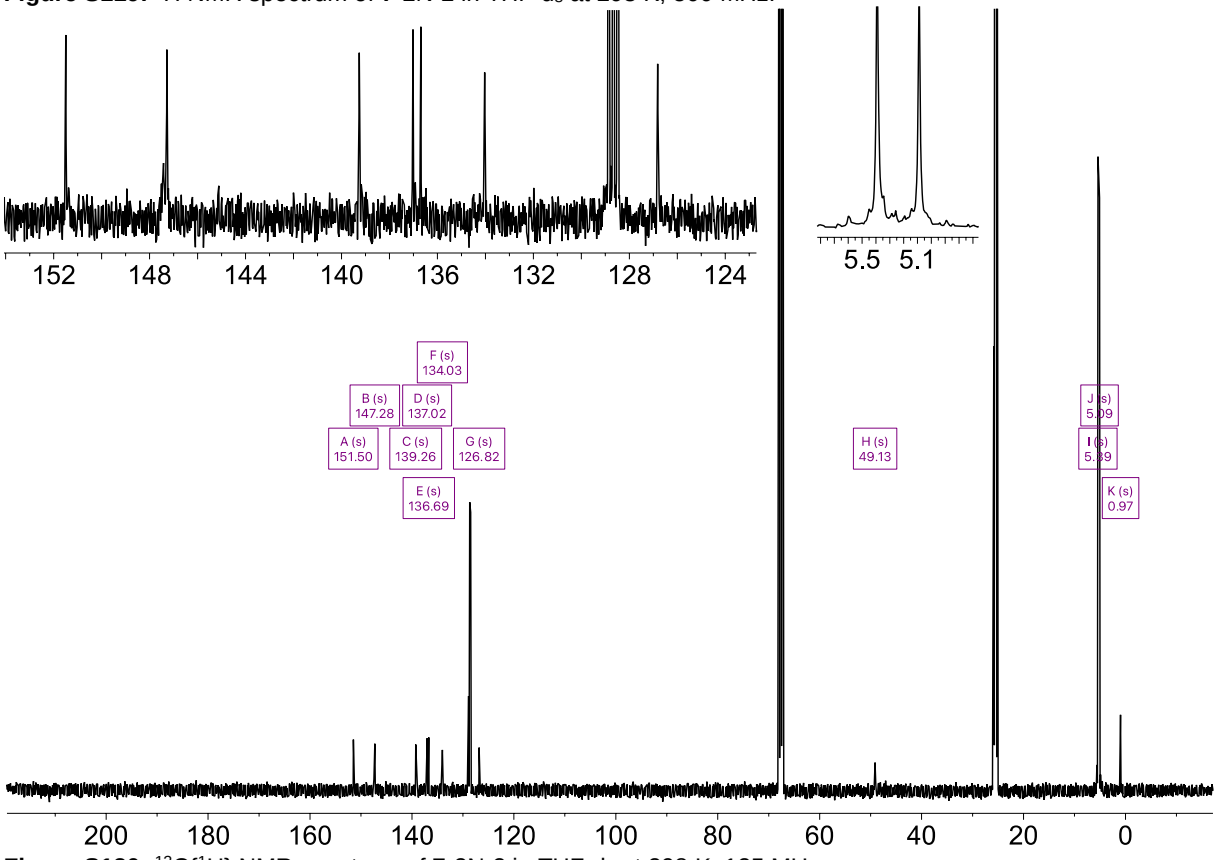

Figure S120: ^{13}C{^{1}H} NMR spectrum of **7**·2N-2 in THF-d$_8$ at 298 K, 125 MHz.

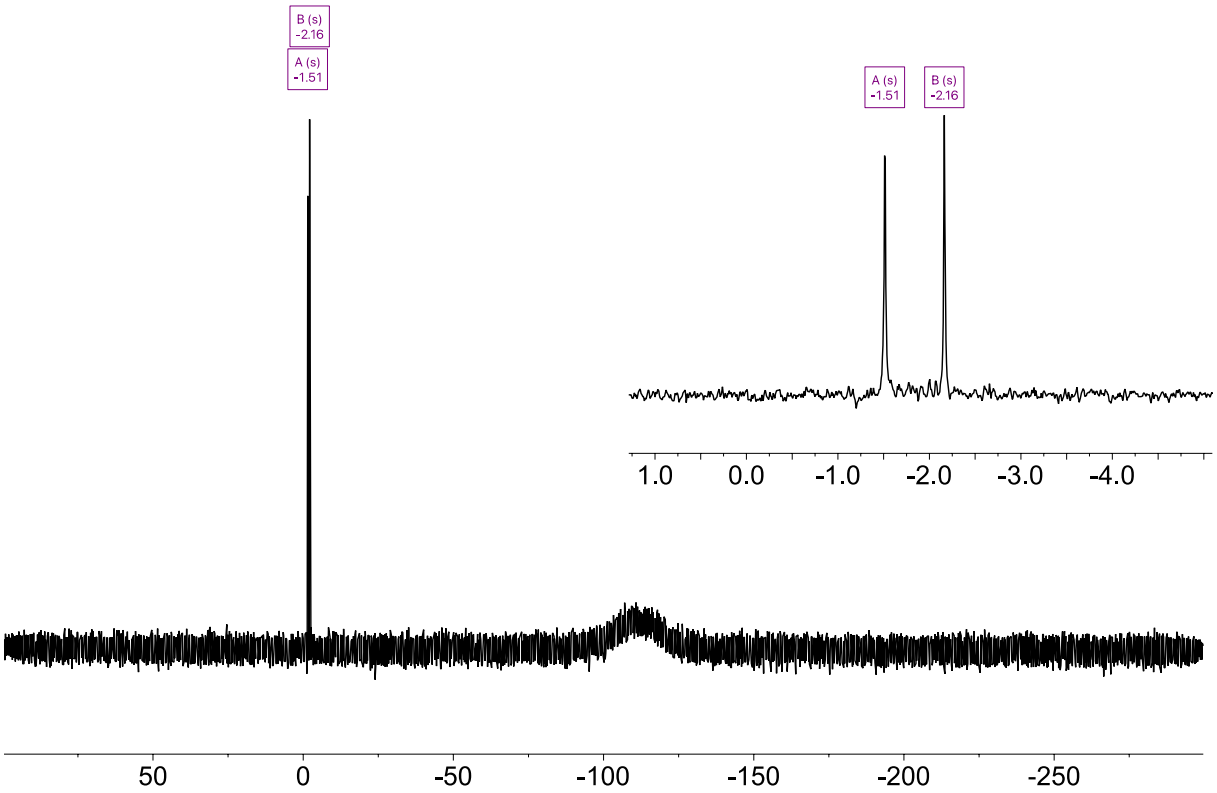

Figure S121: $^{29}Si\{^{1}H\}$ NMR spectrum of **7**·2N-2 in THF-d_8 at 298 K, 99 MHz.

Adduct **8**·2N-2

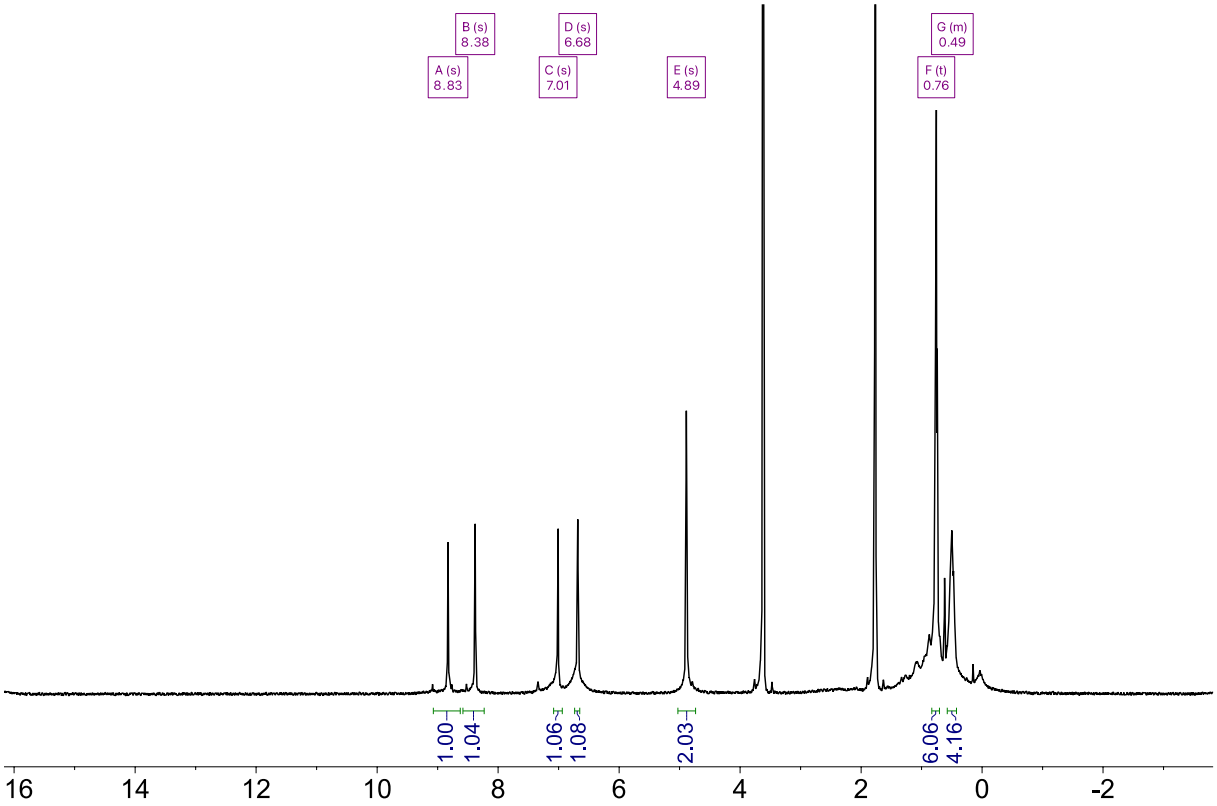

Figure S122: ^{1}H NMR spectrum of **8**·2N-2 in THF-d_8 at 298 K, 500 MHz.

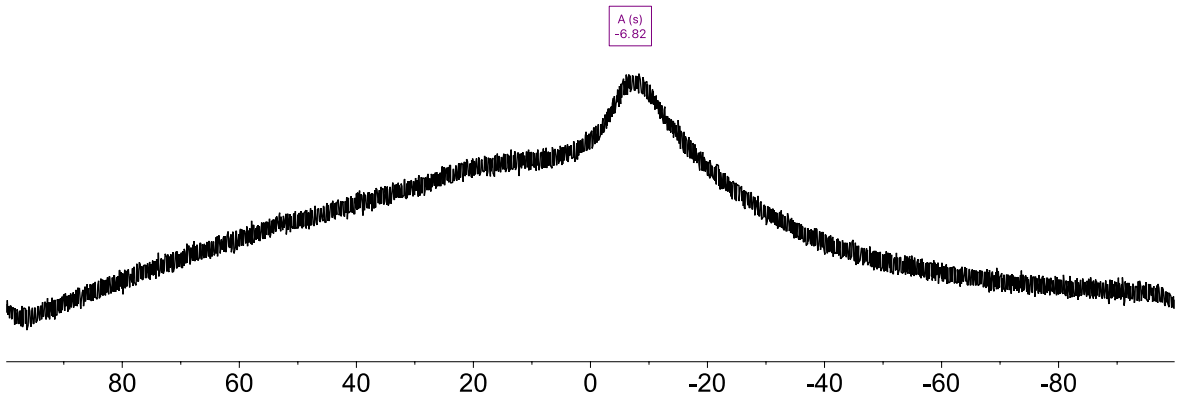

Figure S123: ^{11}B NMR spectrum of **8**·2N-2 in THF-d_8 at 298 K, 160 MHz.

Adduct **9**·2N-2

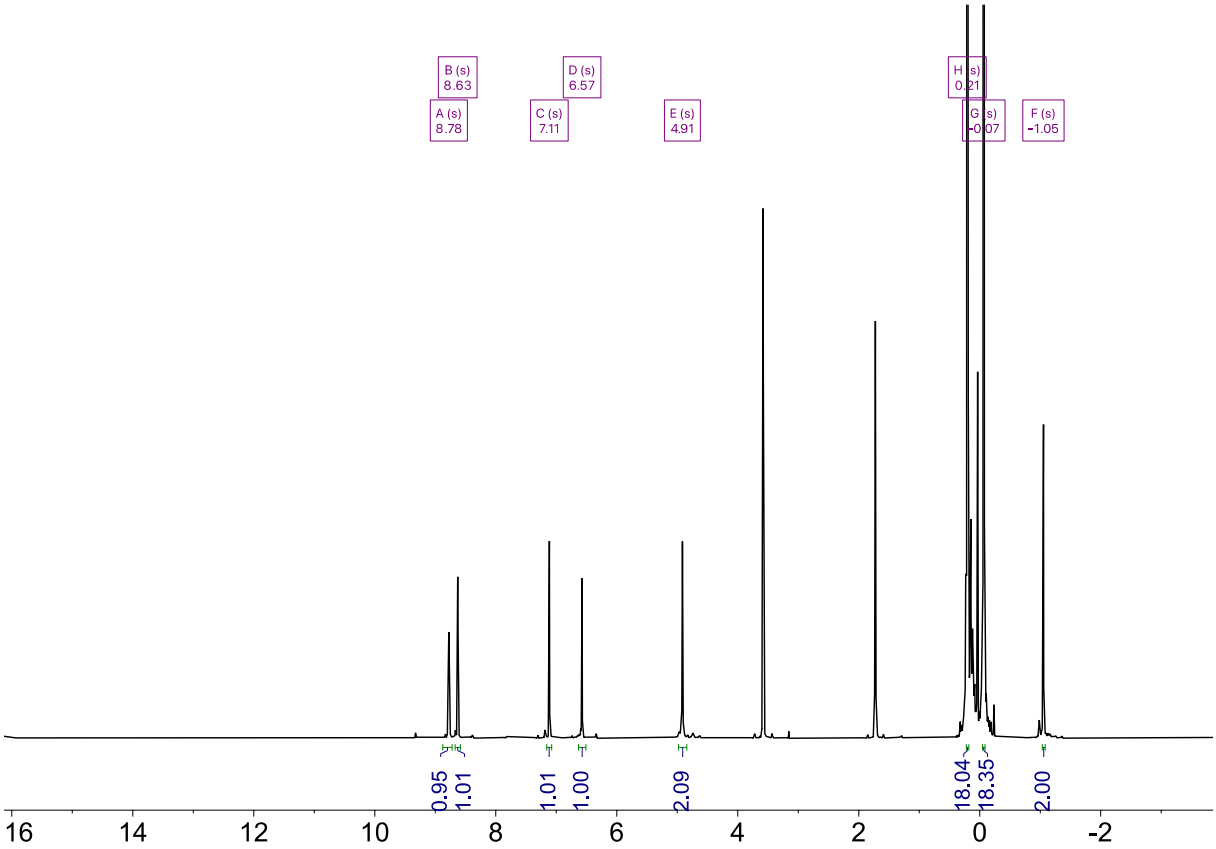

Figure S124: ^{1}H NMR spectrum of **9**·2N-2 in THF-d_8 at 298 K, 500 MHz.

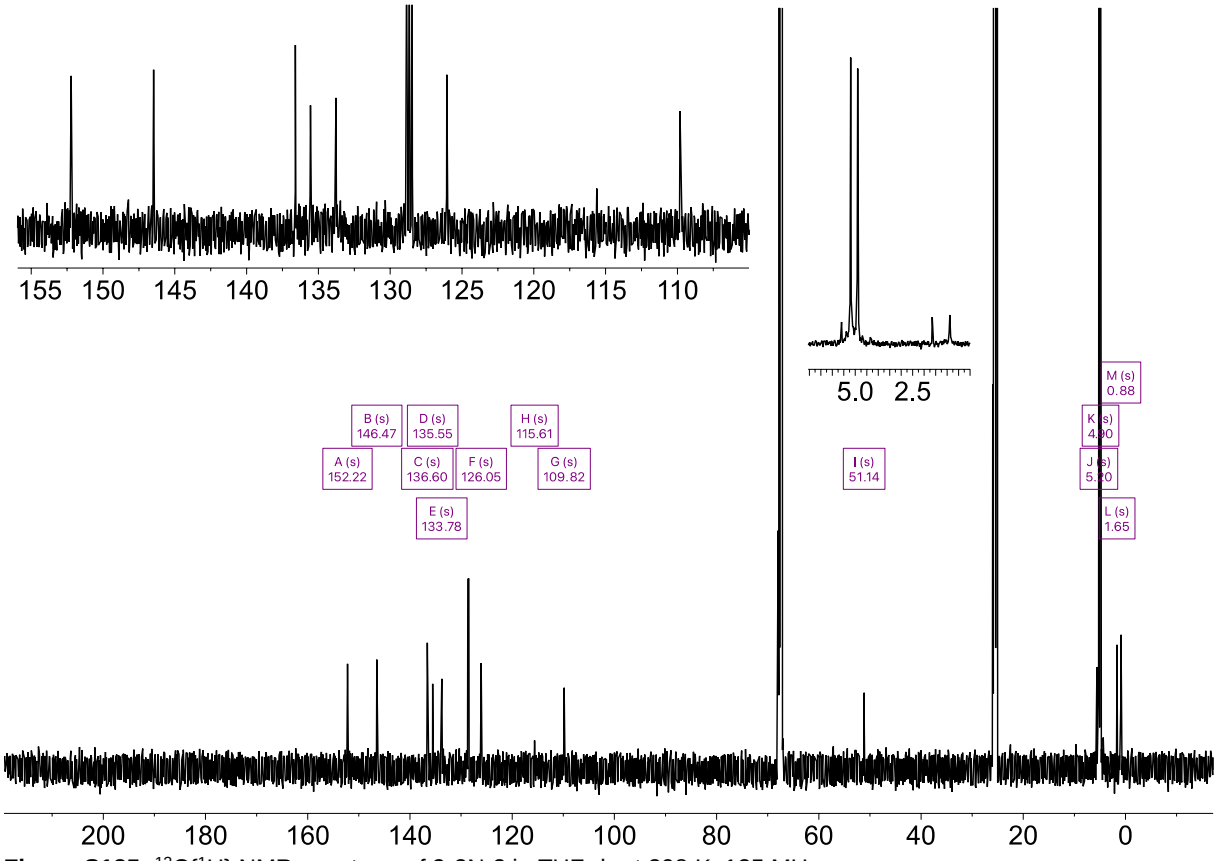

Figure S125: $^{13}C\{^{1}H\}$ NMR spectrum of **9**·2N-2 in THF-d_8 at 298 K, 125 MHz.

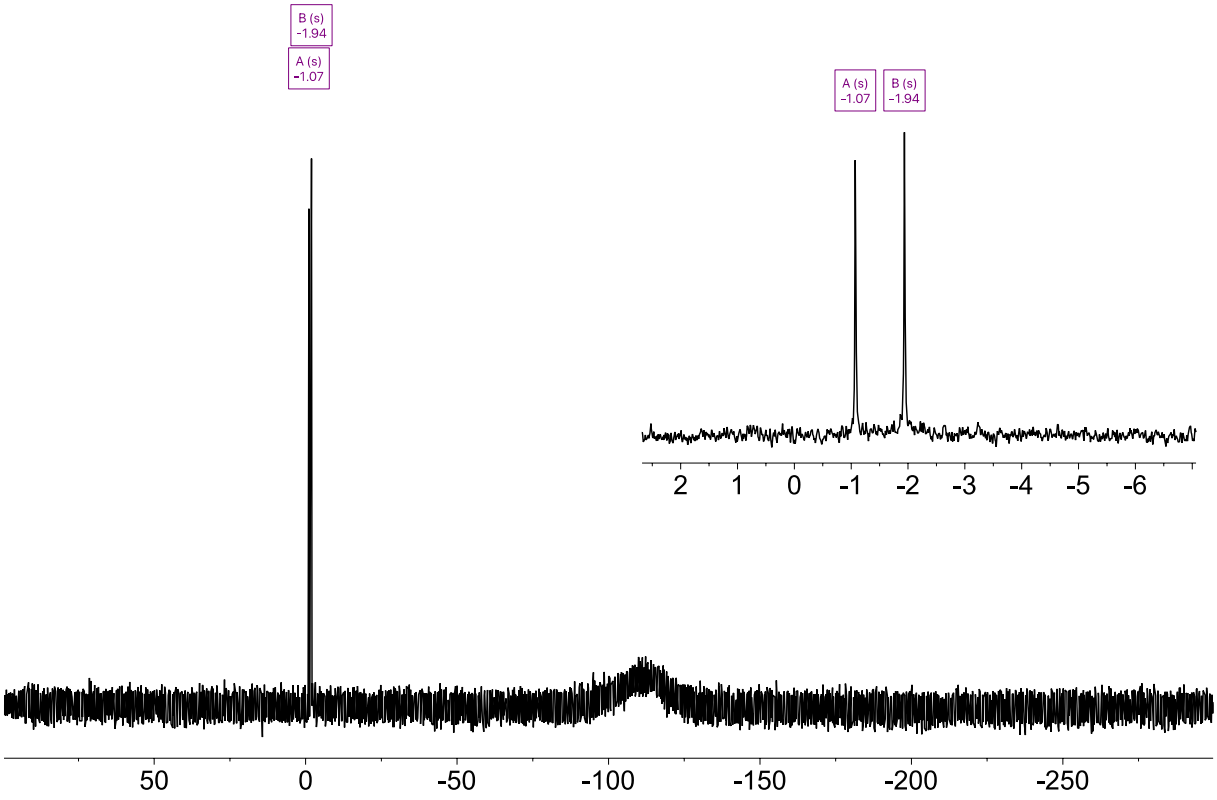

Figure S126: $^{29}Si\{^{1}H\}$ NMR spectrum of **9**·2N-2 in THF-d_8 at 298 K, 99 MHz.

Adduct **7**·2N-4

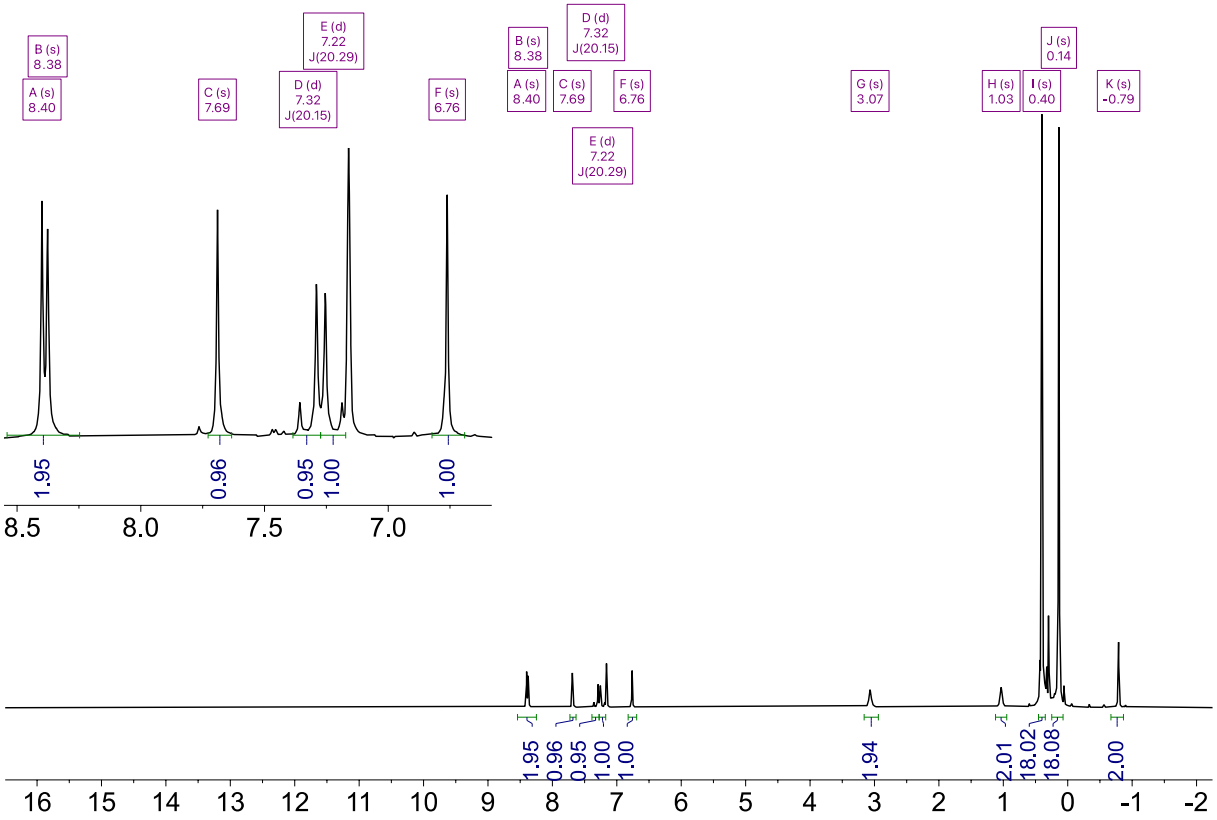

Figure S127: ^{1}H NMR spectrum of **7**·2N-4 in C_6D_6 at 298 K, 500 MHz.

9·2N-4

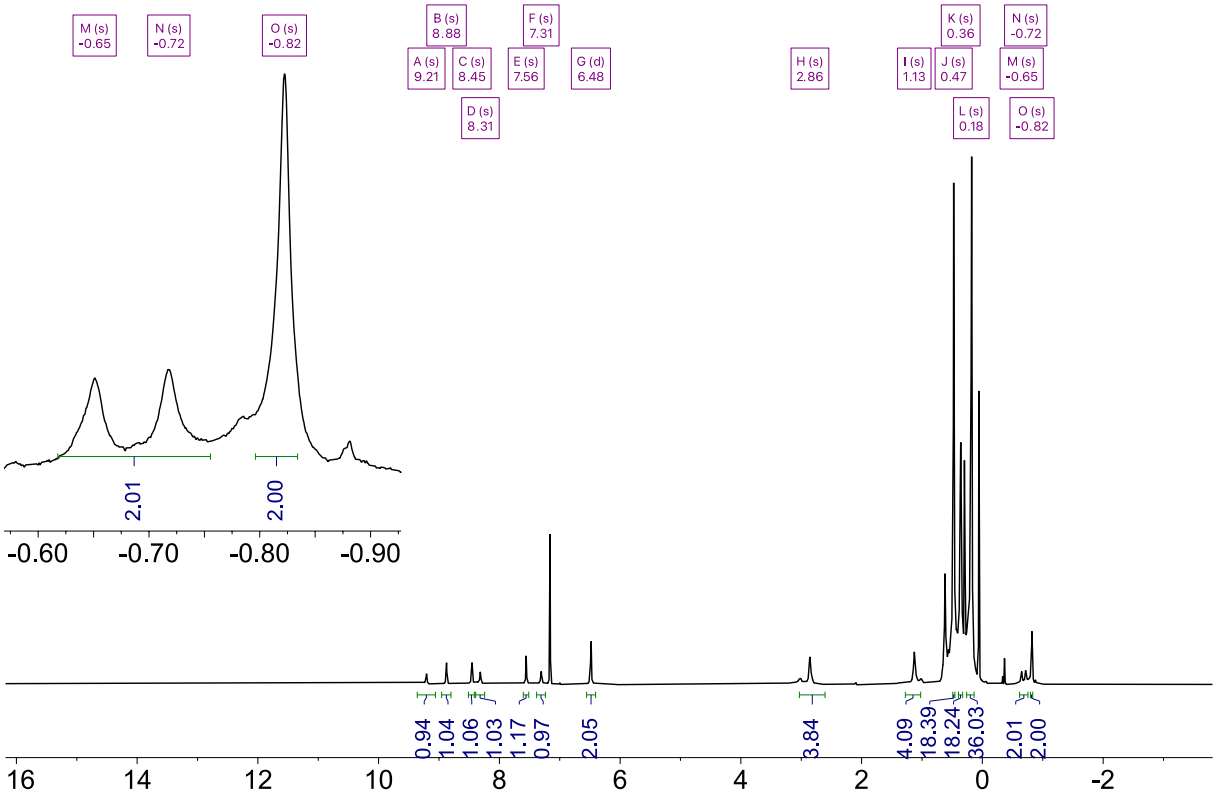

Figure S128: ^{1}H NMR spectrum of **9**·2N-4 in C_6D_6 at 298 K, 500 MHz.

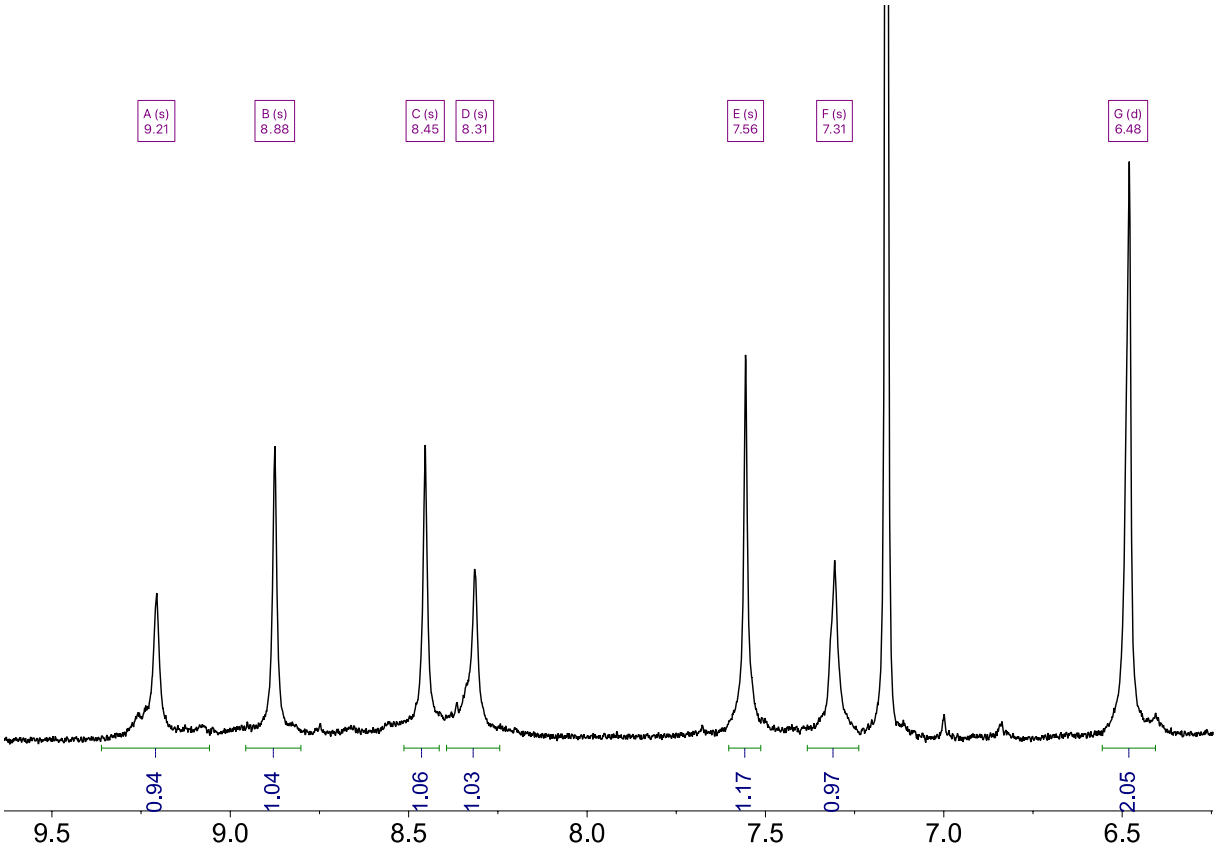

Figure S129: excerpt from the ^{1}H NMR spectrum of **9**·2N-4 in C_6D_6 at 298 K, 500 MHz.

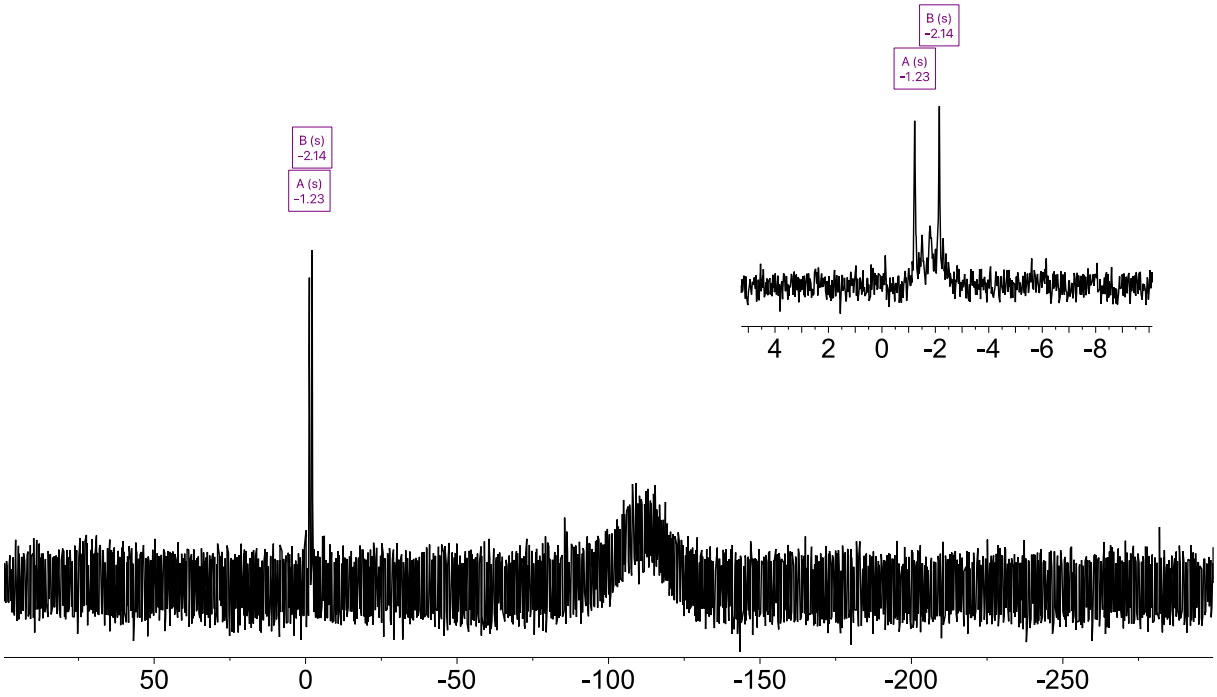

Figure S130: ^{29}Si{^{1}H} NMR spectrum of **9**·2N-4 in C_6D_6 at 298 K, 99 MHz.

Adduct 9·4GBL

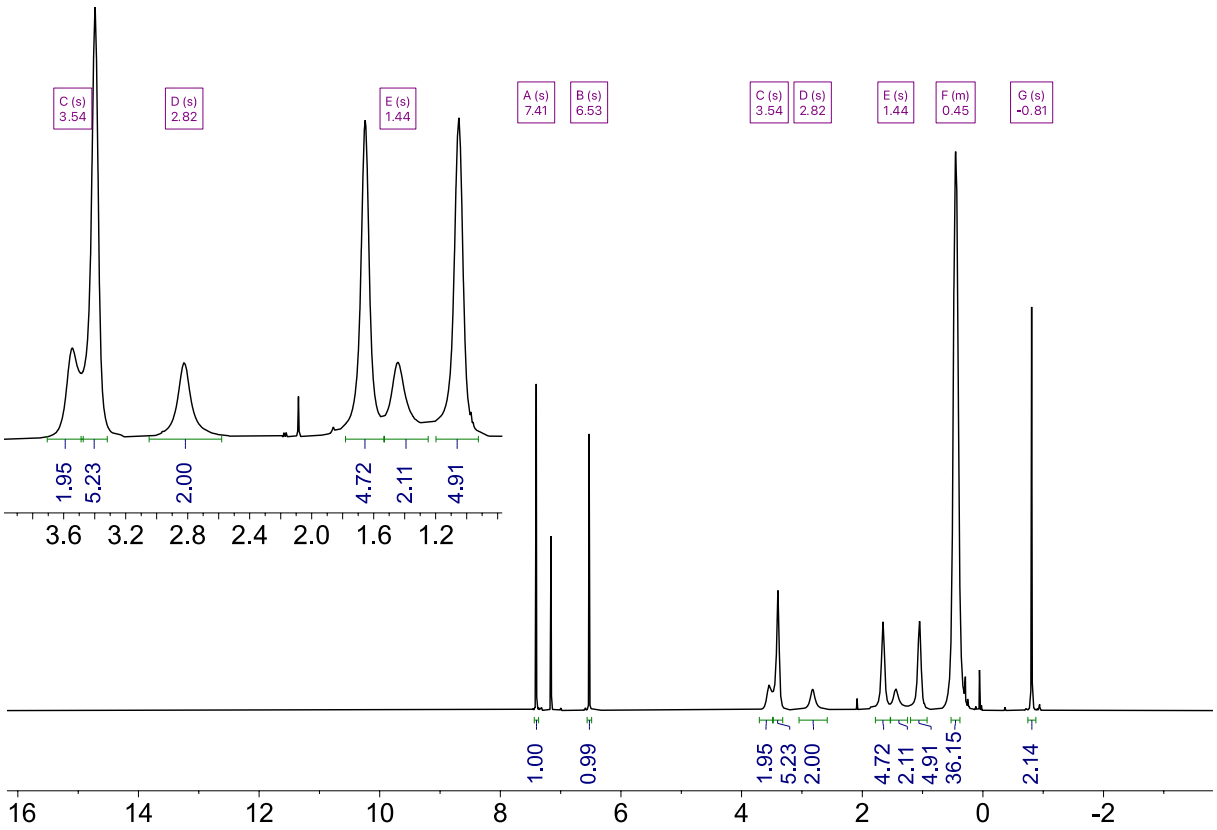

Figure S131: ^{1}H NMR spectrum of **9**·4GBL + ex. GBL in C_6D_6 at 298 K, 500 MHz.

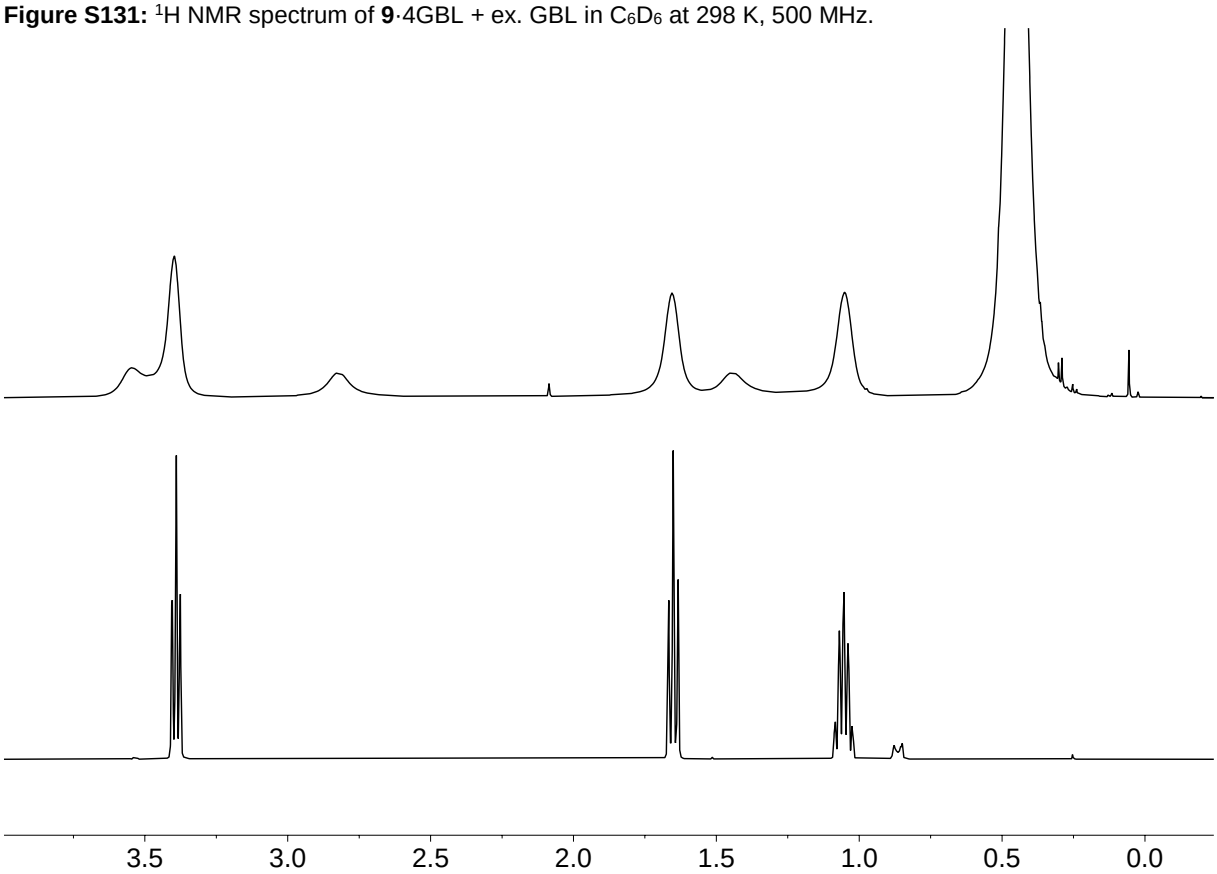

Figure S132: ^{1}H NMR spectra of **9**·4GBL + ex. GBL (above) and GBL in C_6D_6 at 298 K (below), 500 MHz.

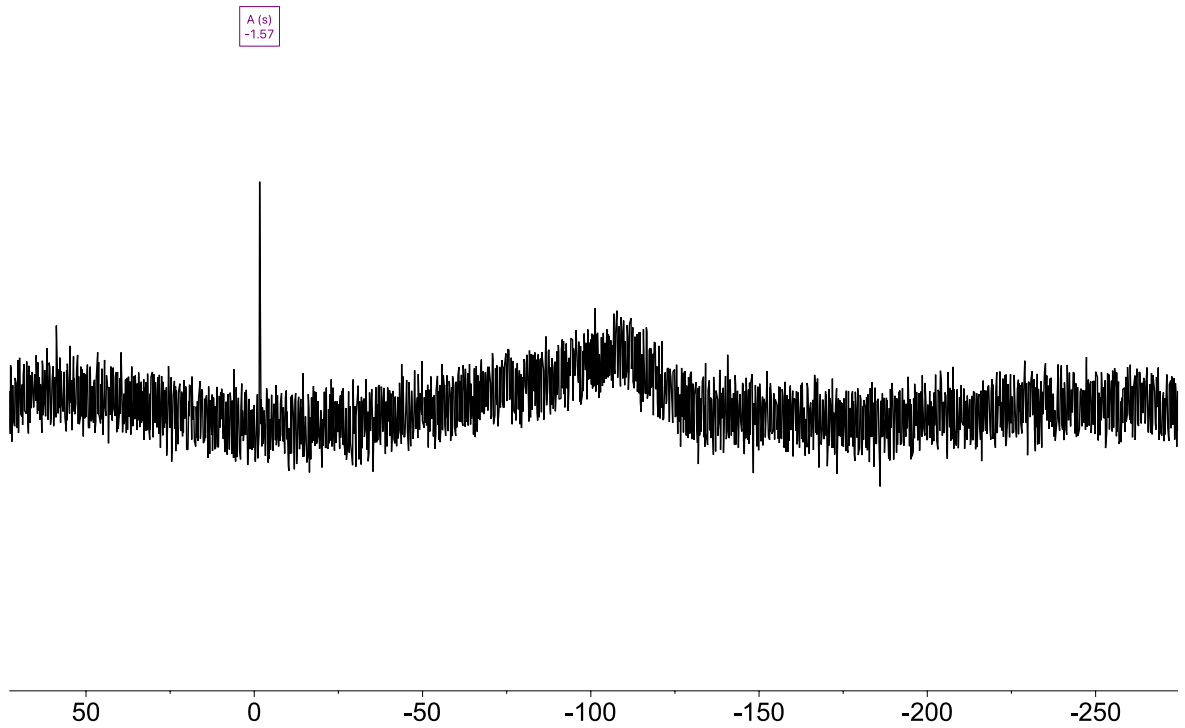

Figure S133: $^{29}Si\{^{1}H\}$ NMR spectrum of **9**·4GBL + ex. GBL in C_6D_6 at 298 K, 99 MHz.

Adduct **7**·4Nico

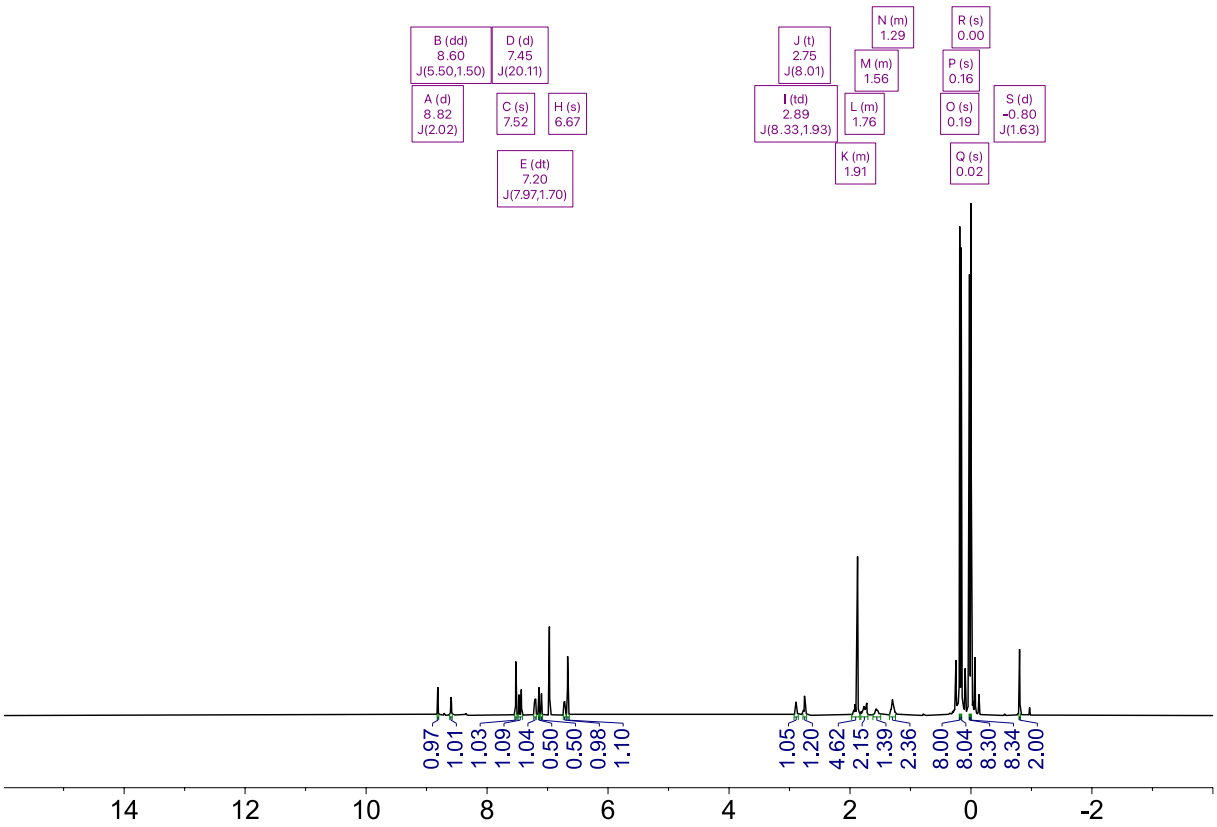

Figure S134: ^{1}H NMR spectrum of **7**·4Nico in C_6D_6 at 298 K, 500 MHz.

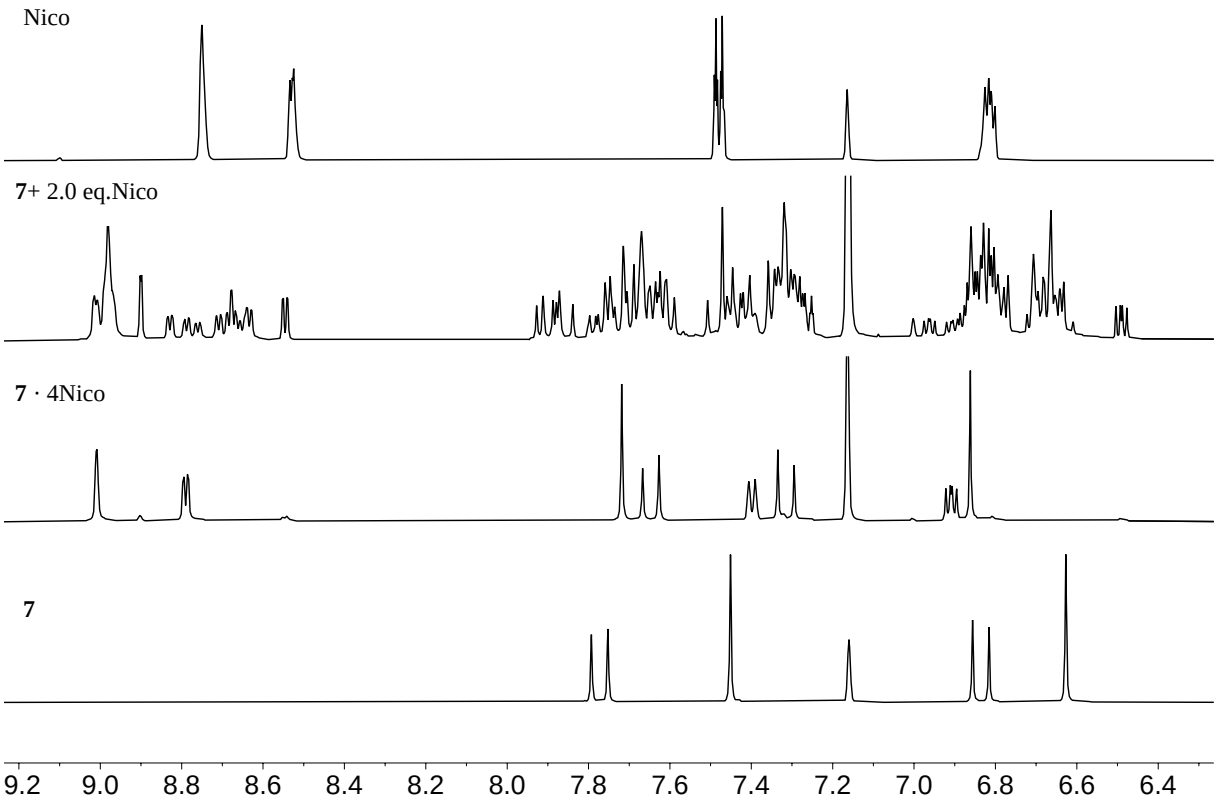

Figure S135: ^{1}H NMR spectra of Nico, **7** + 2.0 eq. Nico, **7**·4Nico and **7** in C_6D_6 at 298 K, 500 MHz.

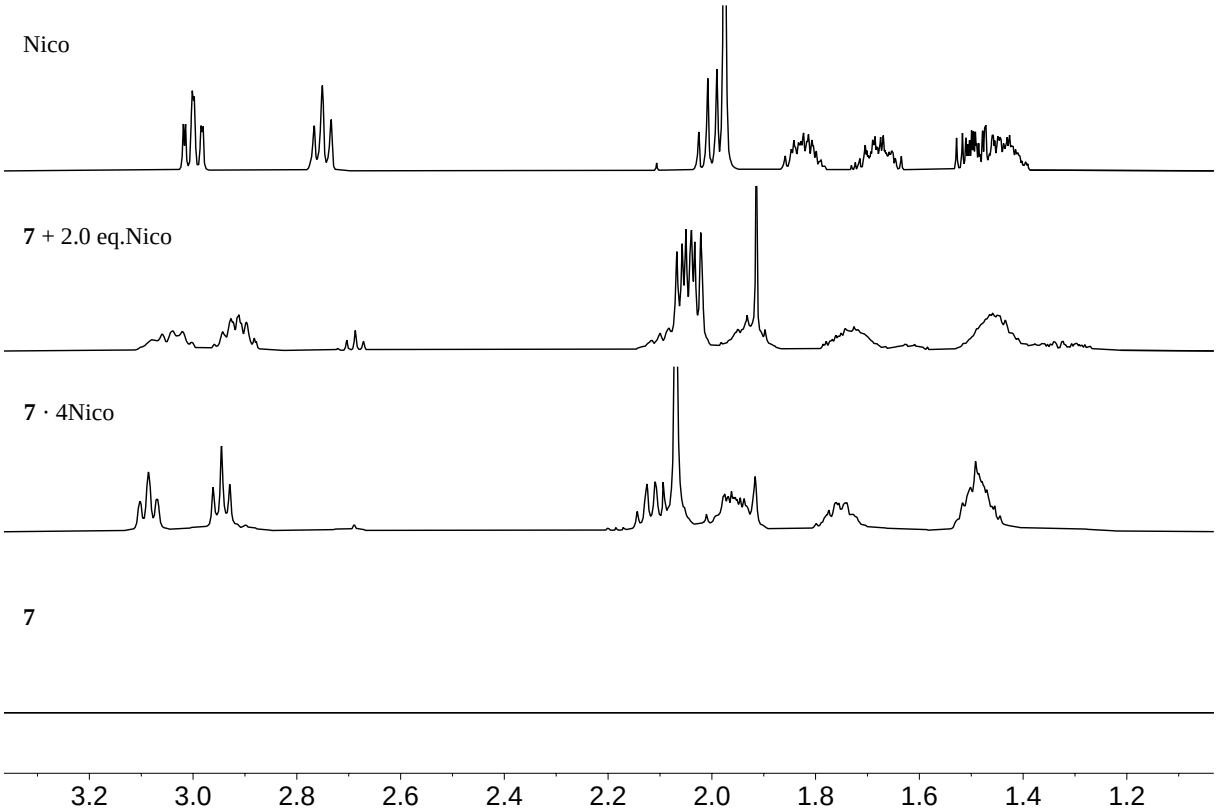

Figure S136: ^{1}H NMR spectra of Nico, **7** + 2.0 eq. Nico, **7**·4Nico and **7** in C_6D_6 at 298 K, 500 MHz.

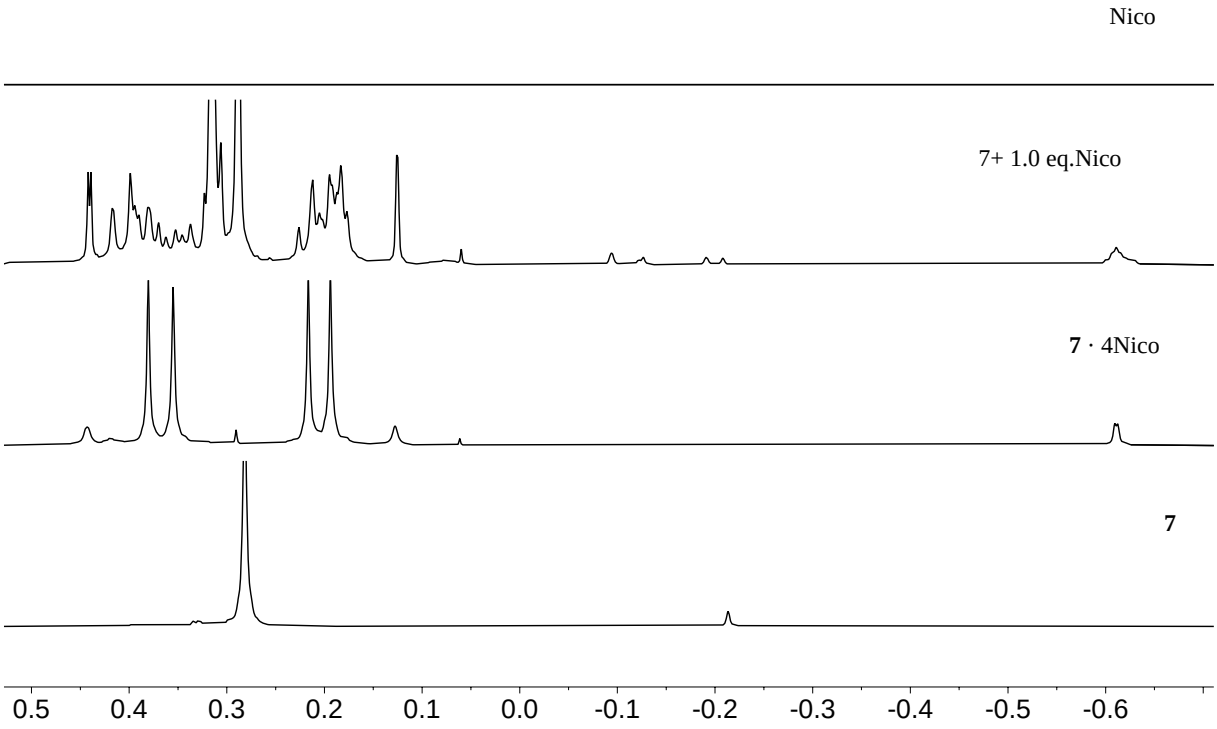

Figure S137: ^{1}H NMR spectra of Nico, **7** + 2.0 eq. Nico, **7**·4Nico and **7** in C_6D_6 at 298 K, 500 MHz.

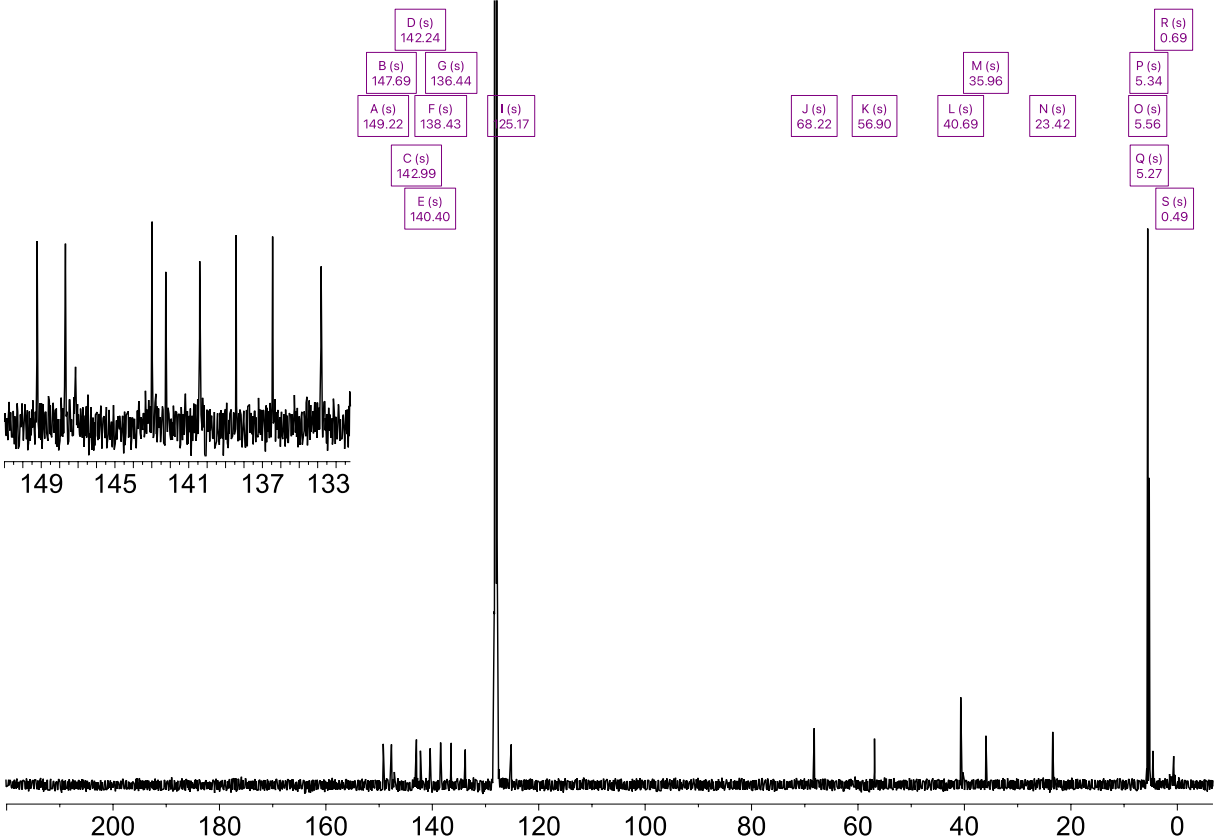

Figure S138: $^{13}C\{^{1}H\}$ NMR spectrum of **7**·4Nico in C_6D_6 at 298 K, 125 MHz.

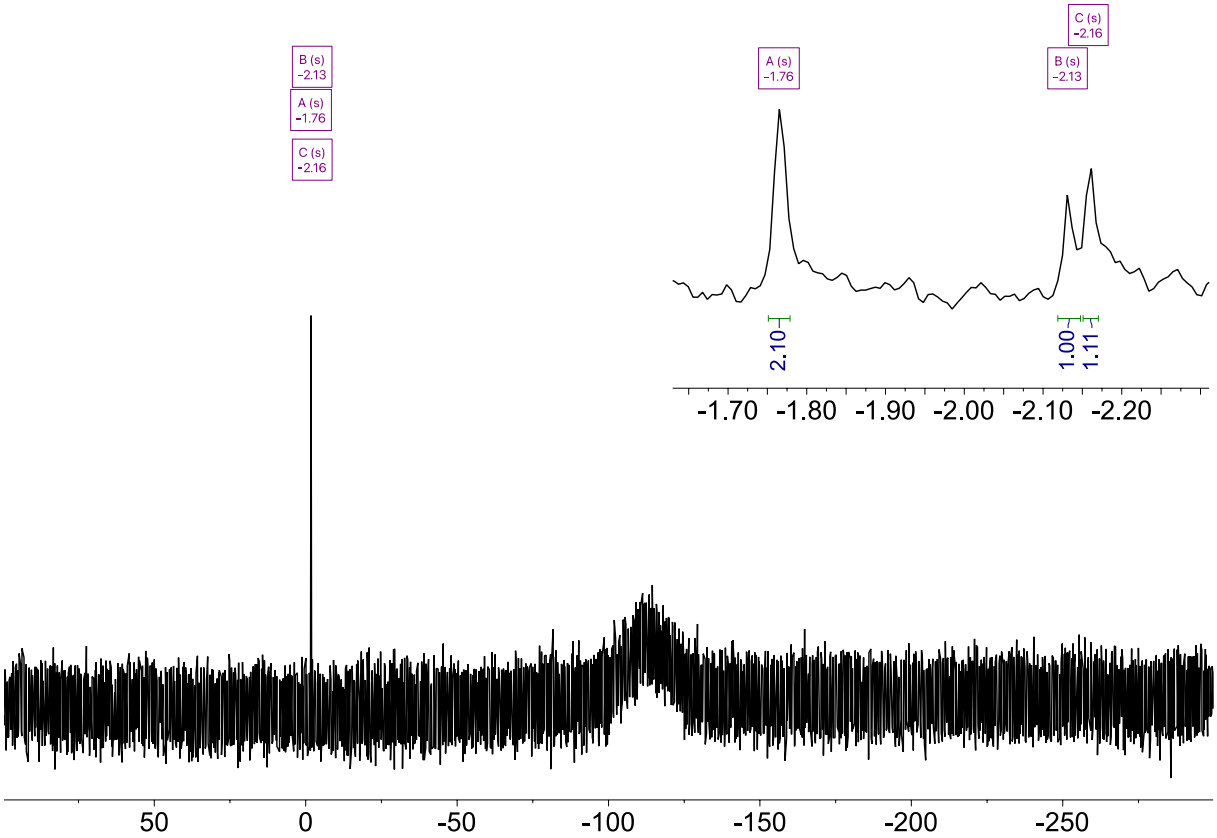

Figure S139: $^{29}Si\{^{1}H\}$ NMR spectrum of **7**·4Nico in C_6D_6 at 298 K, 99 MHz.

Adduct 9·4Nico

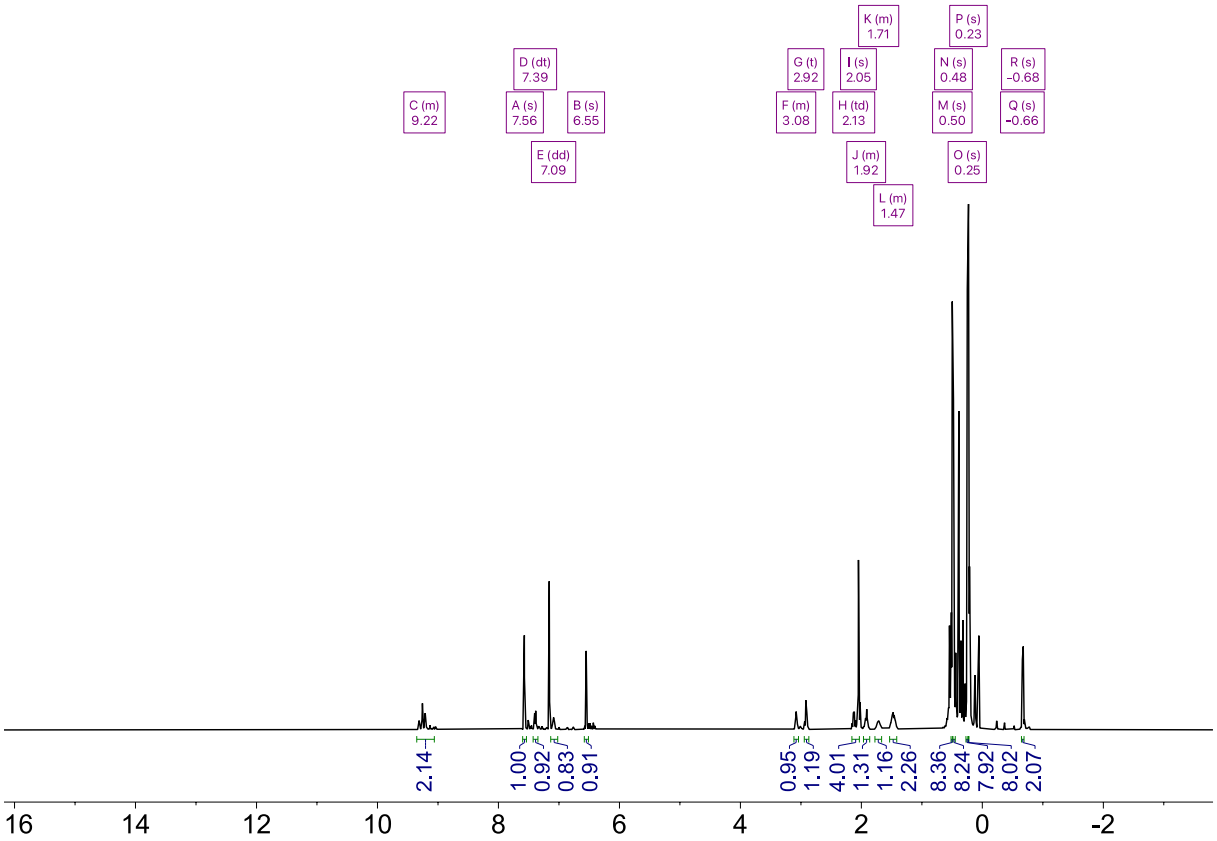

Figure S140: ^{1}H NMR spectrum of **9**·4Nico in C_6D_6 at 298 K, 500 MHz.

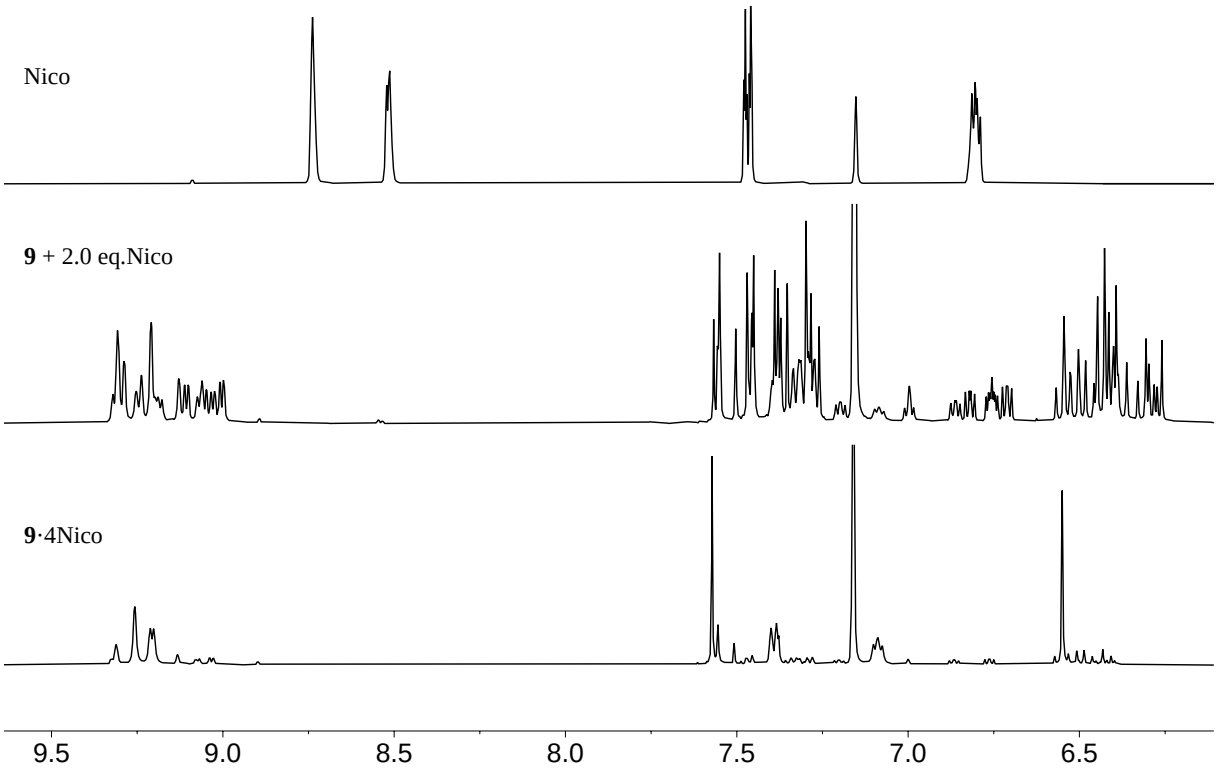

Figure S141: ^{1}H NMR spectra of Nico, **9** + 2.0 eq. Nico and **9**·4Nico in C_6D_6 at 298 K, 500 MHz.

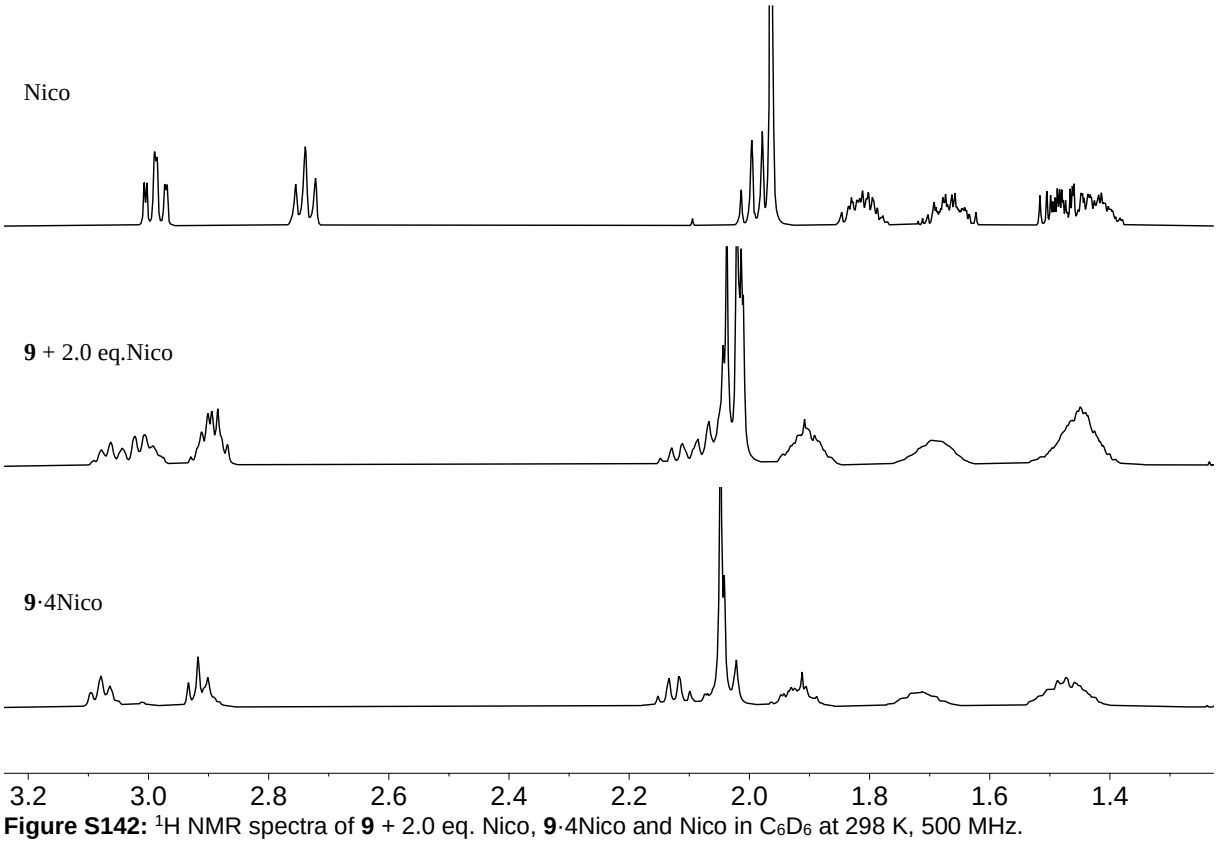

Figure S142: ^{1}H NMR spectra of **9** + 2.0 eq. Nico, **9**·4Nico and Nico in C_6D_6 at 298 K, 500 MHz.

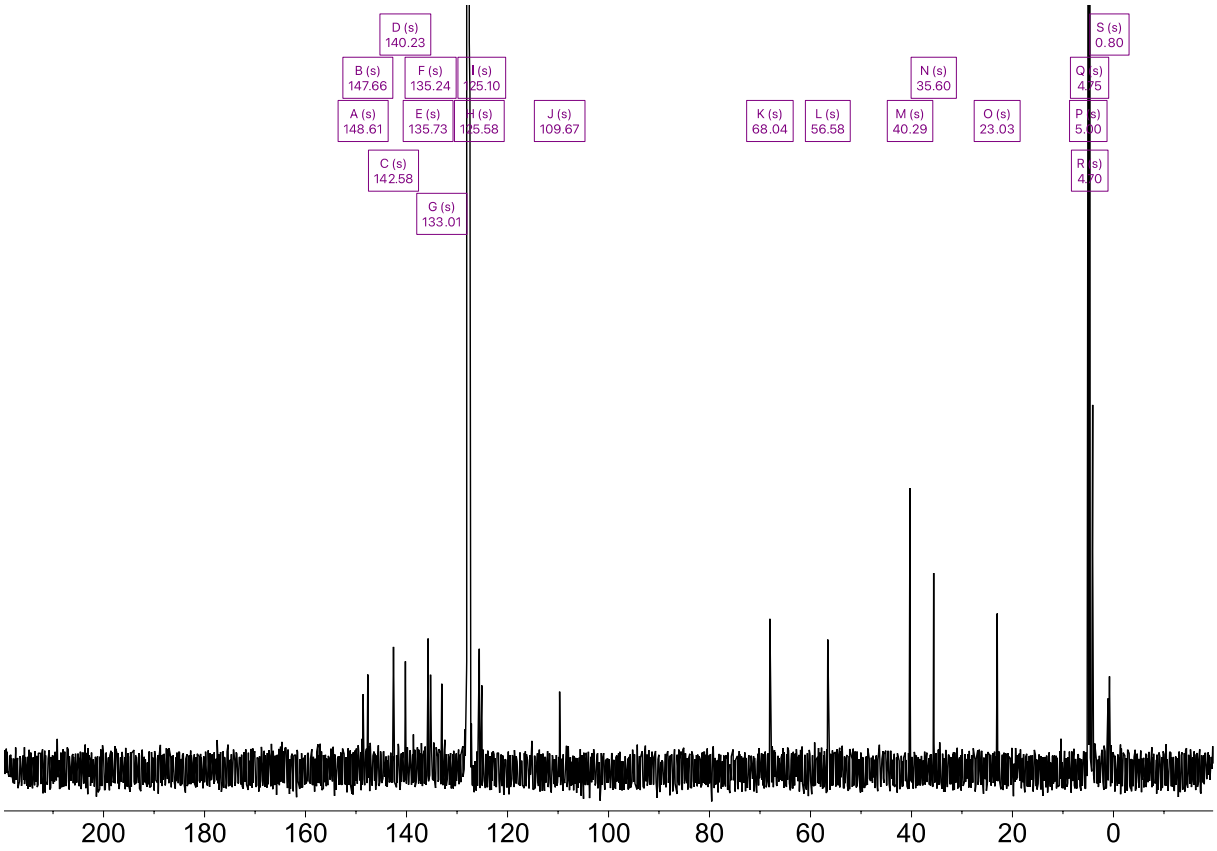

Figure S143: $^{13}C\{^{1}H\}$ NMR spectrum of **9**·4Nico in C_6D_6 at 298 K, 125 MHz.

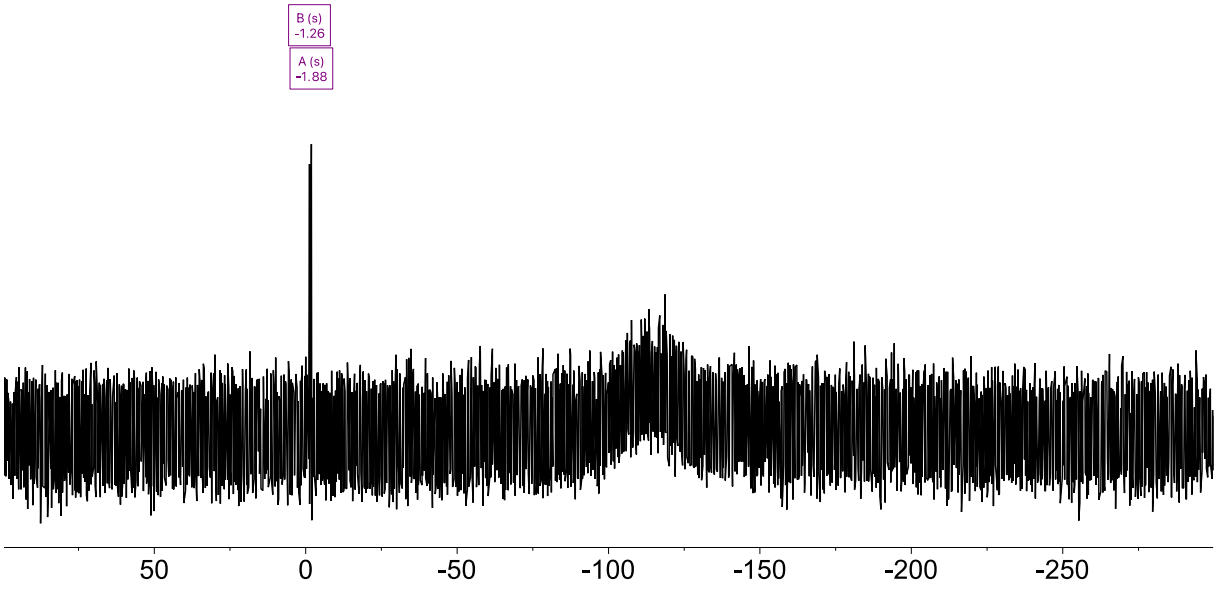

Figure S144: $^{29}Si\{^{1}H\}$ NMR spectrum of **9**·4Nico in C_6D_6 at 298 K, 99 MHz.

Adduct 7 + Theo

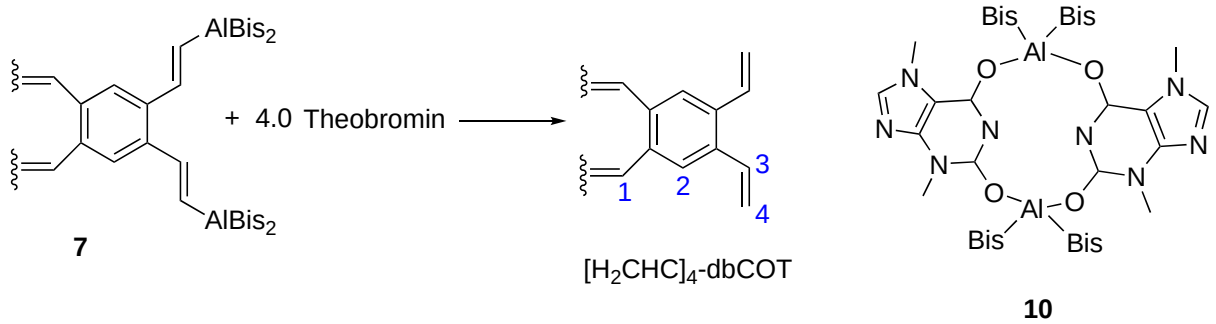

Scheme 2: Reaction of **7** with theobromine leads to substitution of the $AlBis_2$ group with H, forming the tetravinyl $[H_2CHC]_4$-dbCOT and compound **10**.

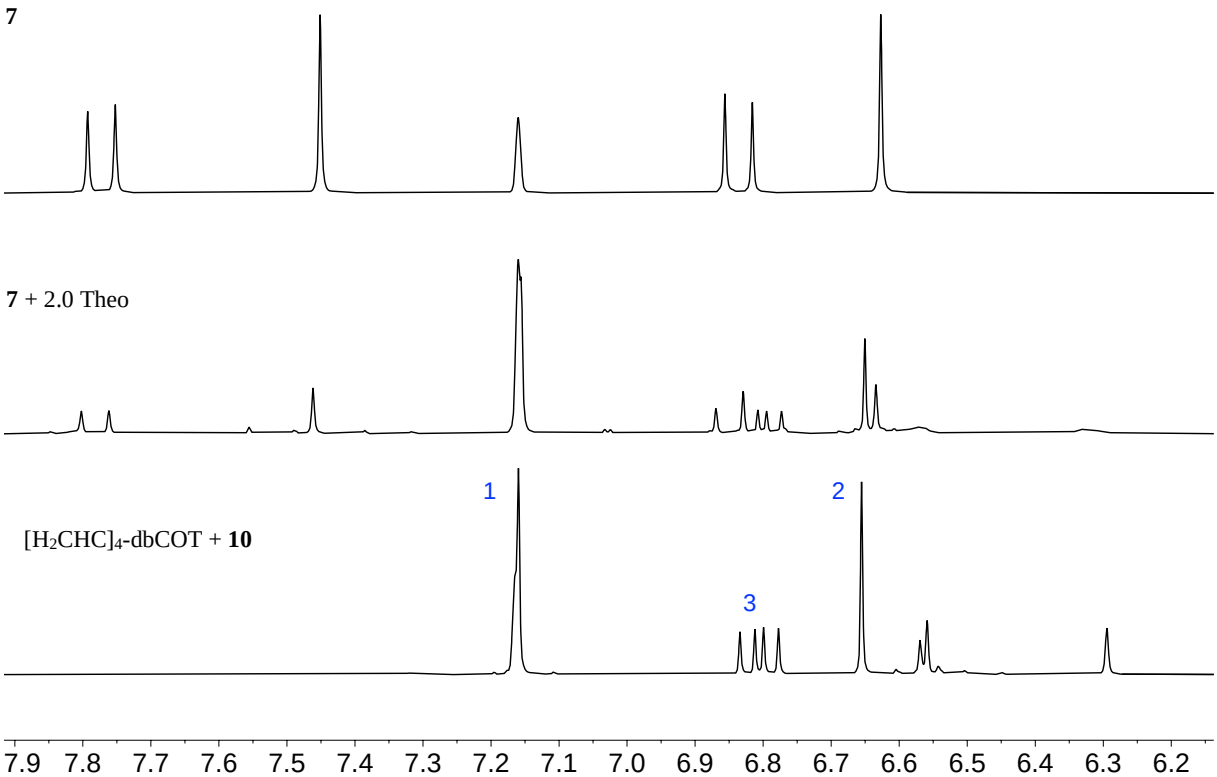

Figure S145: ^1H NMR spectra of **7**, **7** + 2.0 Theobromine and the formed mixer of $[H_2CHC]_4$-dbCOT and **10** in C_6D_6 at 298 K, 500 MHz.

7

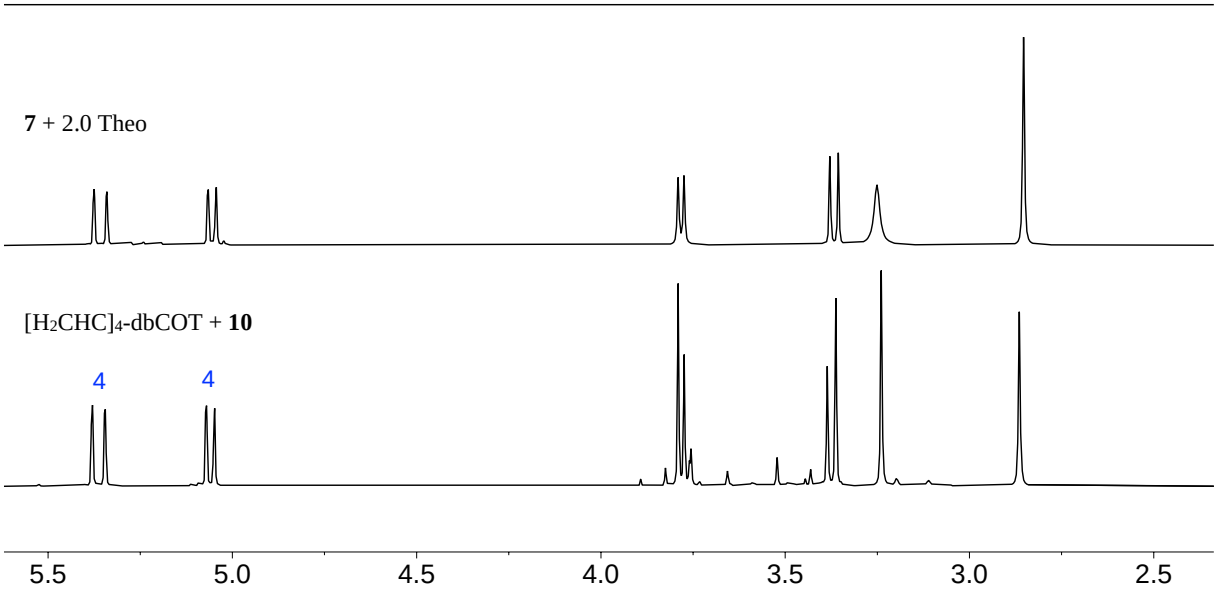

Figure S146: ^{1}H NMR spectra of **7**, **7** + 2.0 Theobromine and the formed mixer of $[H_2CHC]_4$-dbCOT and **10** in C_6D_6 at 298 K, 500 MHz.

Adduct 9 + Theo

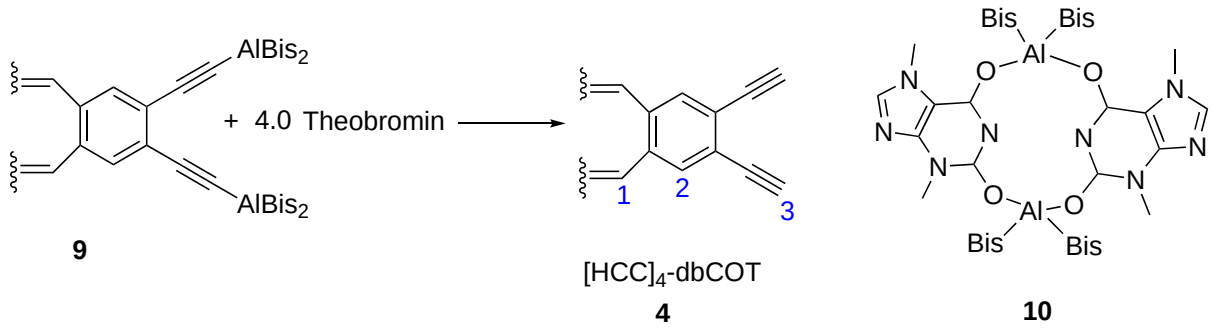

9 [HCC]$_4$-dbCOT **4** **10**

Scheme S147: Reaction of **9** with theobromine leads to substitution of the $AlBis_2$ group with H, forming the tetravinyl $[HCC]_4$-dbCOT **4** and compound **10**.

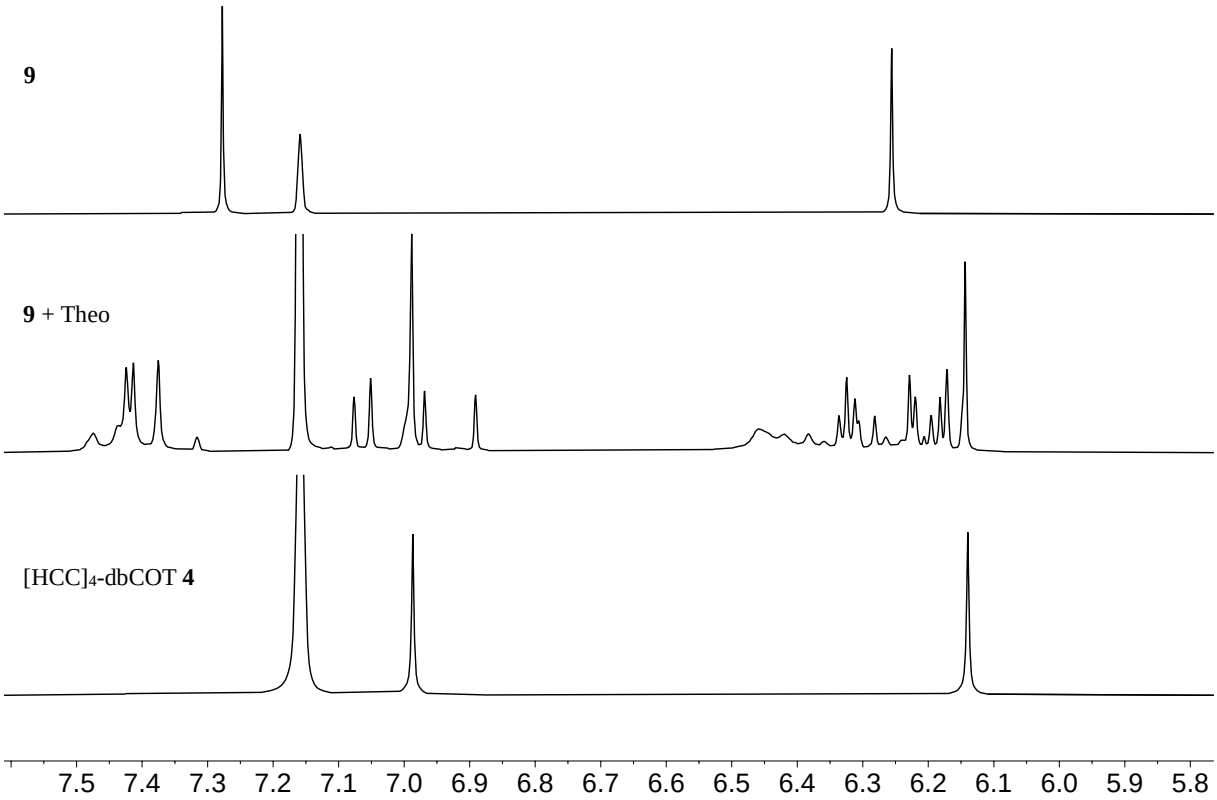

Figure S148: ^{1}H NMR spectra of **9**, **9** + 2.0 Theobromine and [HCC]$_4$-dbCOT **4** in C_6D_6 at 298 K, 500 MHz.

Adduct 7·2Caff

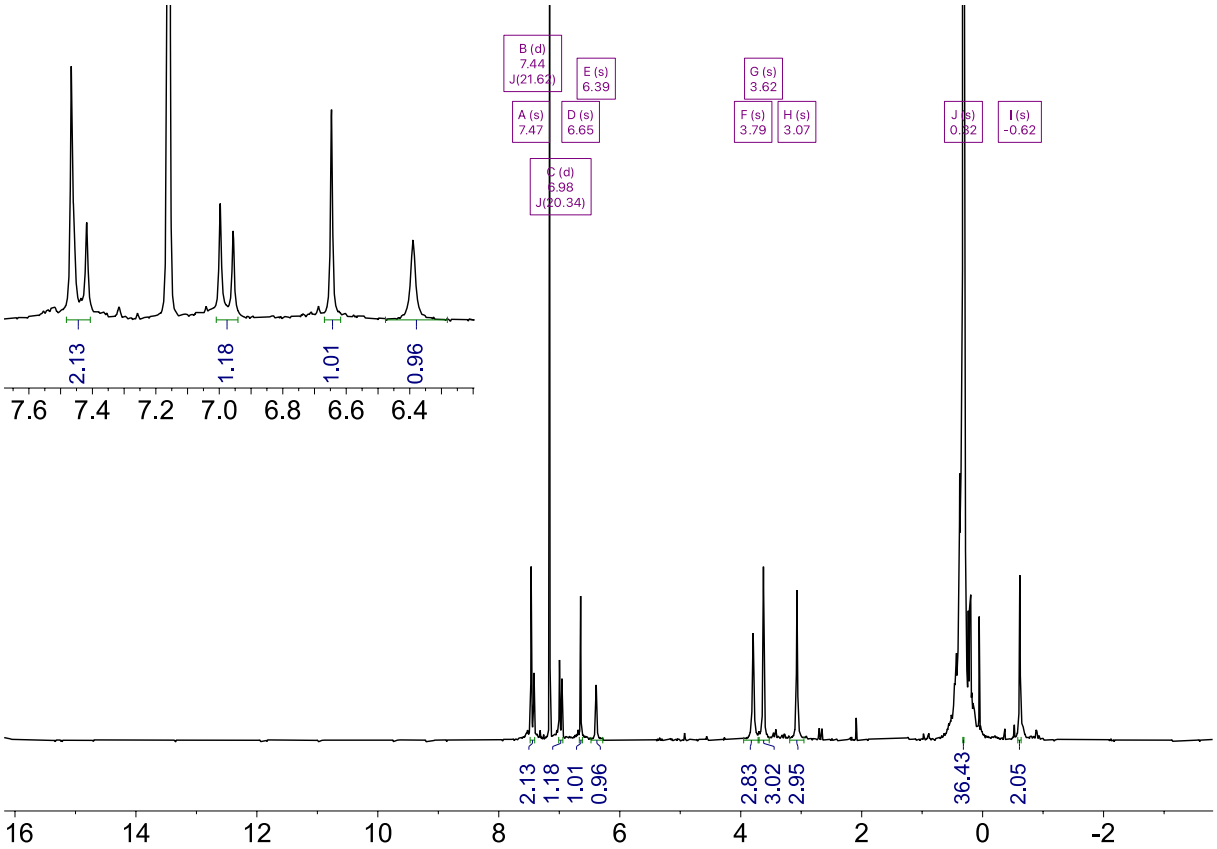

Figure S149: ^{1}H NMR spectrum of **7**·2Caff in C_6D_6 at 298 K, 500 MHz.

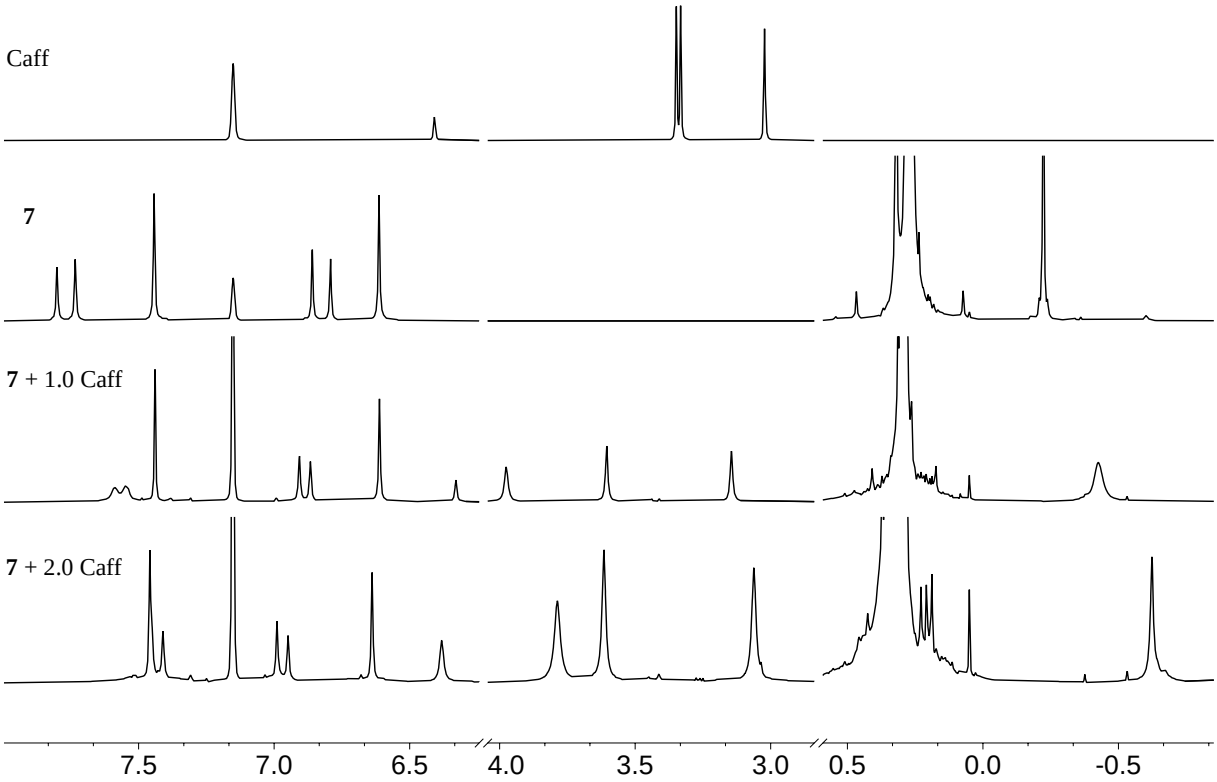

Figure S150: ^{1}H NMR spectra of **7** + different amounts of Caff in C_6D_6 at 298 K, 500 MHz.

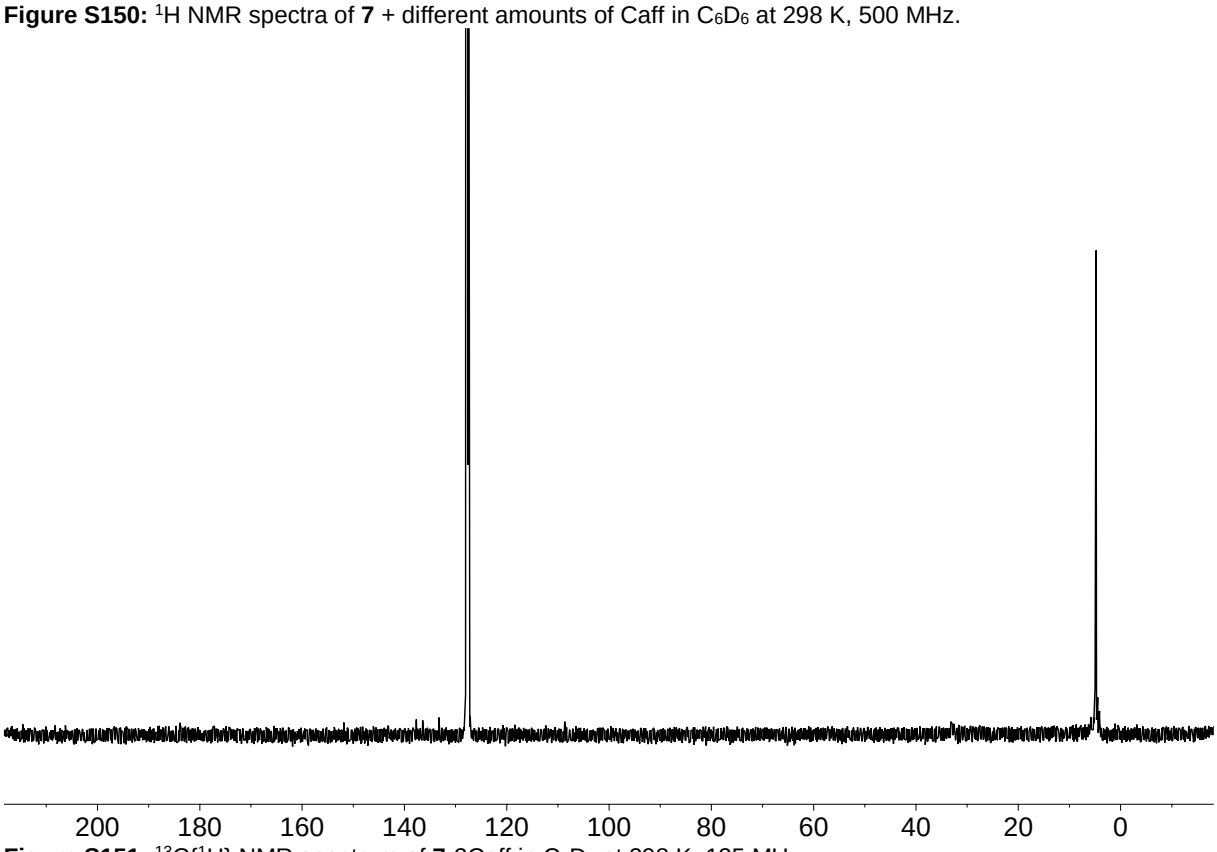

Figure S151: $^{13}C\{^{1}H\}$ NMR spectrum of **7**·2Caff in C_6D_6 at 298 K, 125 MHz.

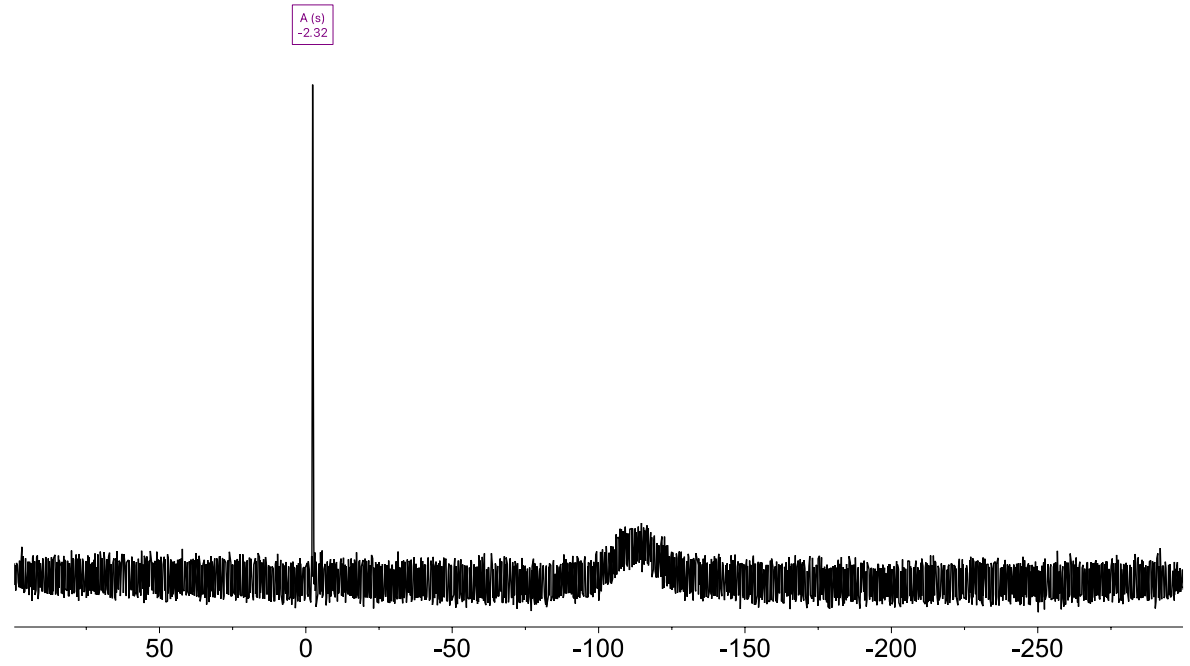

Figure S152: $^{29}Si\{^{1}H\}$ NMR spectrum of **7**·2Caff in C_6D_6 at 298 K, 99 MHz.

Adduct **8**·2Cof / **8**·4Cof

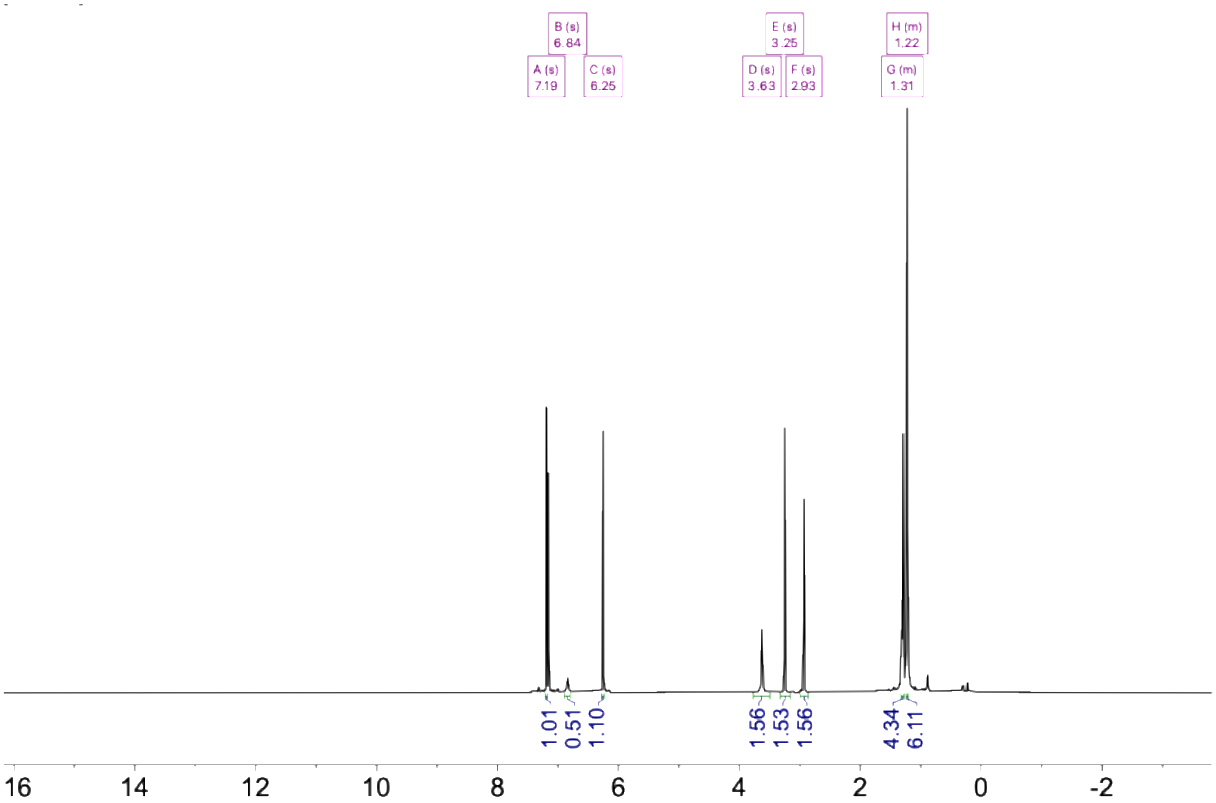

Figure S153: ^{1}H NMR spectrum of **8**·2Caff in C_6D_6 at 298 K, 500 MHz.

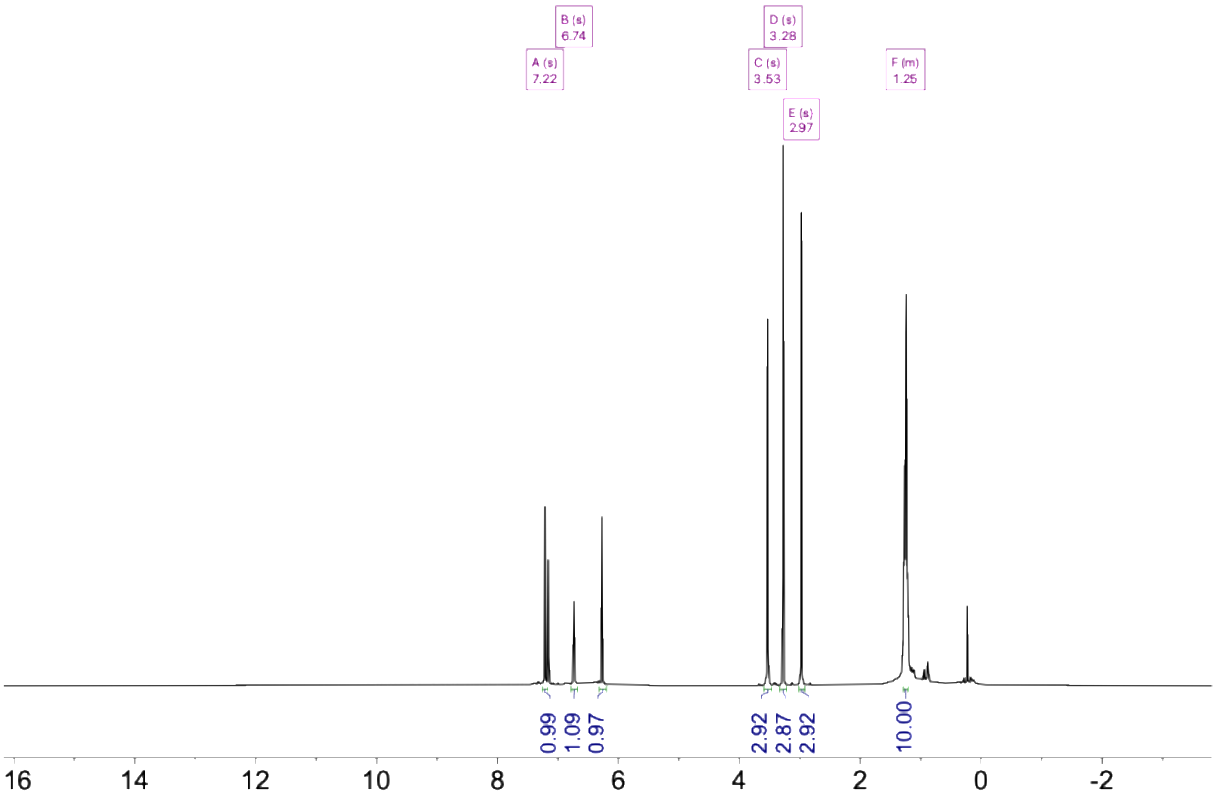

Figure S153: ^{1}H NMR spectrum of **8**·4Caff in C_6D_6 at 298 K, 500 MHz.

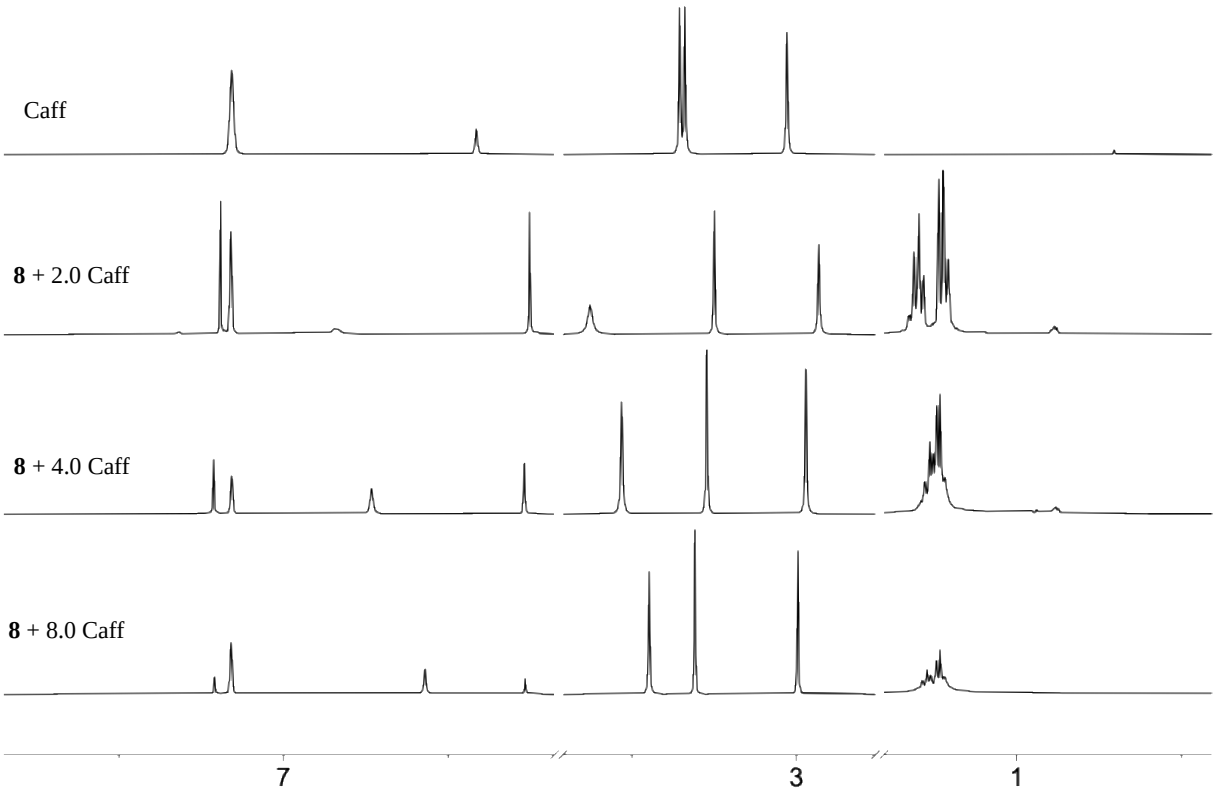

Figure S154: ^{1}H NMR spectra of **8** + different amounts of Caff in C_6D_6 at 298 K, 500 MHz.

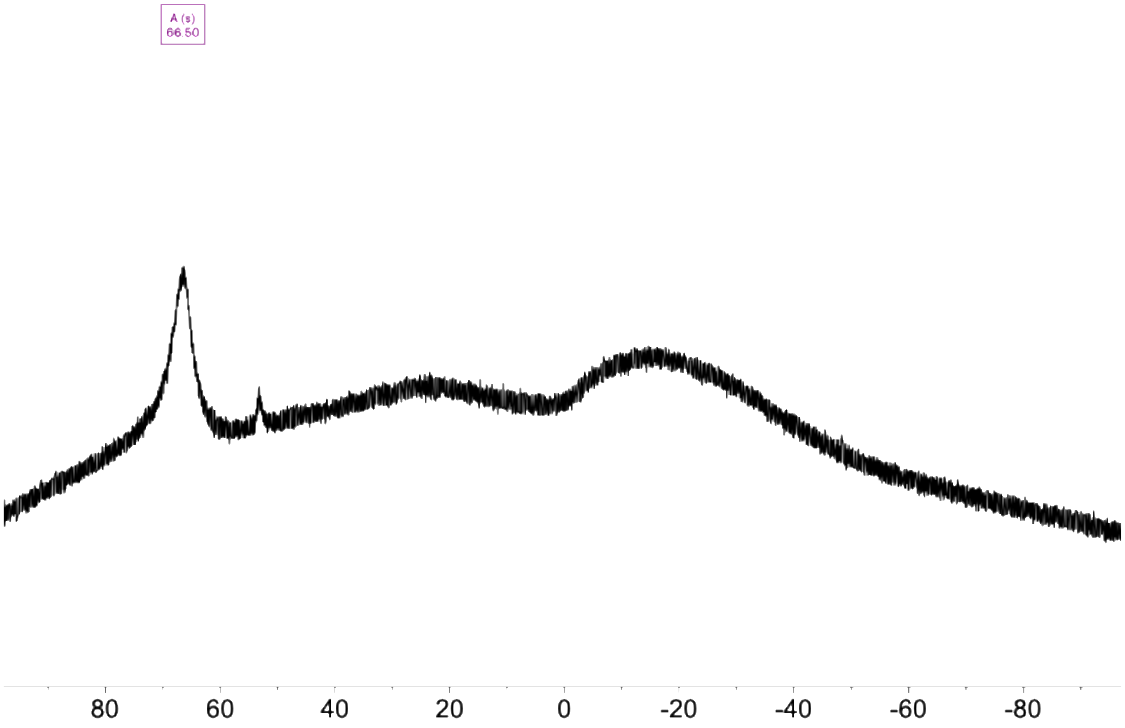

Figure S155: ^{11}B NMR spectrum of **8**·2Caff in C_6D_6 at 298 K, 160 MHz.

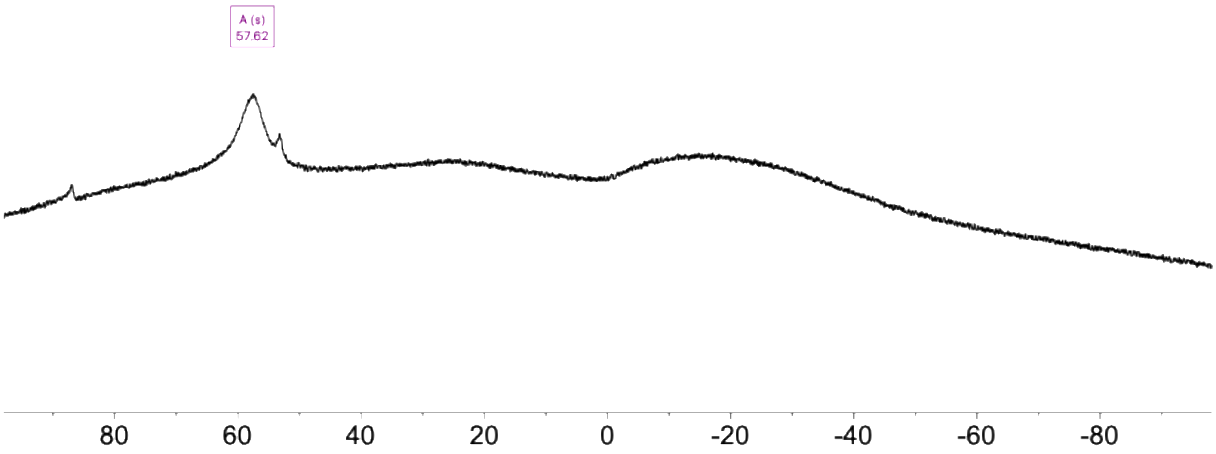

Figure S155: ^{11}B NMR spectrum of **8**·4Caff in C_6D_6 at 298 K, 160 MHz.

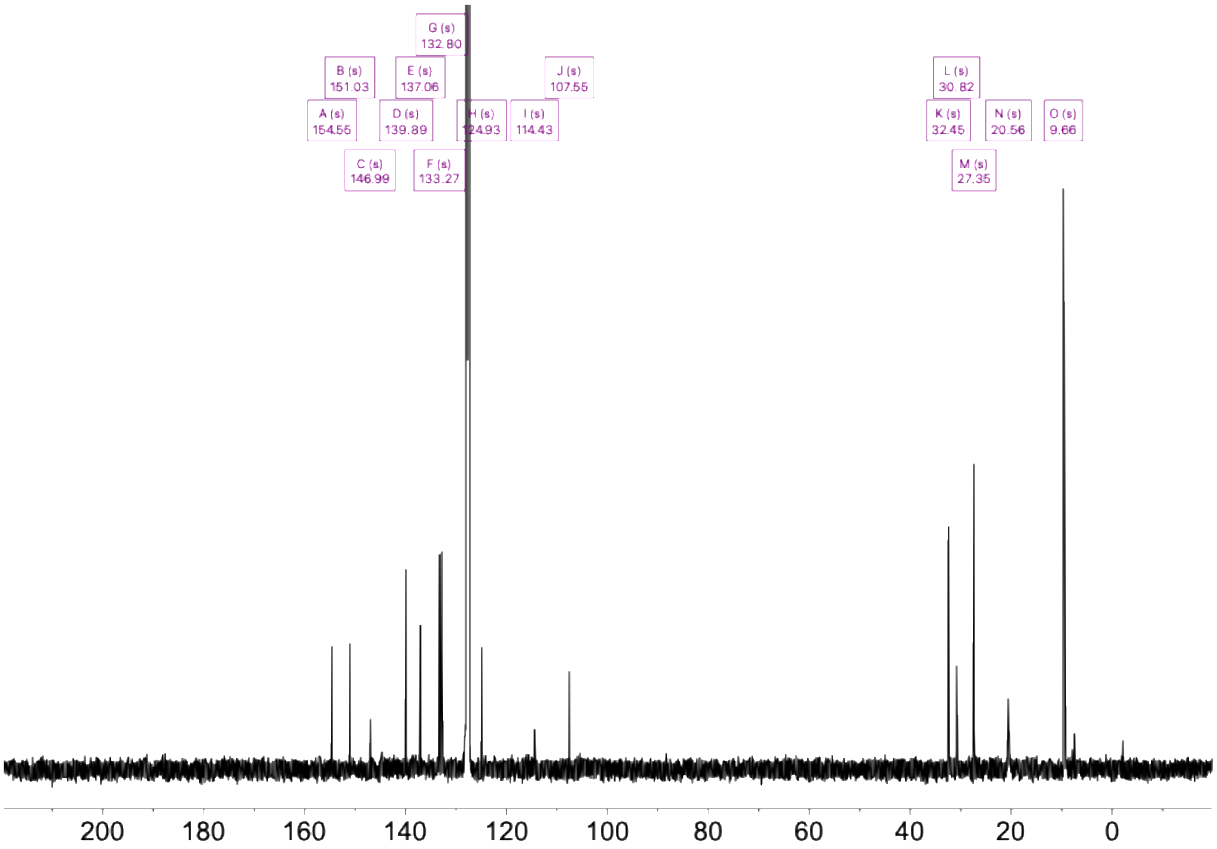

Figure S156: $^{13}C\{^{1}H\}$ NMR spectrum of **8**·2Caff in C_6D_6 at 298 K, 125 MHz.

Adduct **9**·2Cof

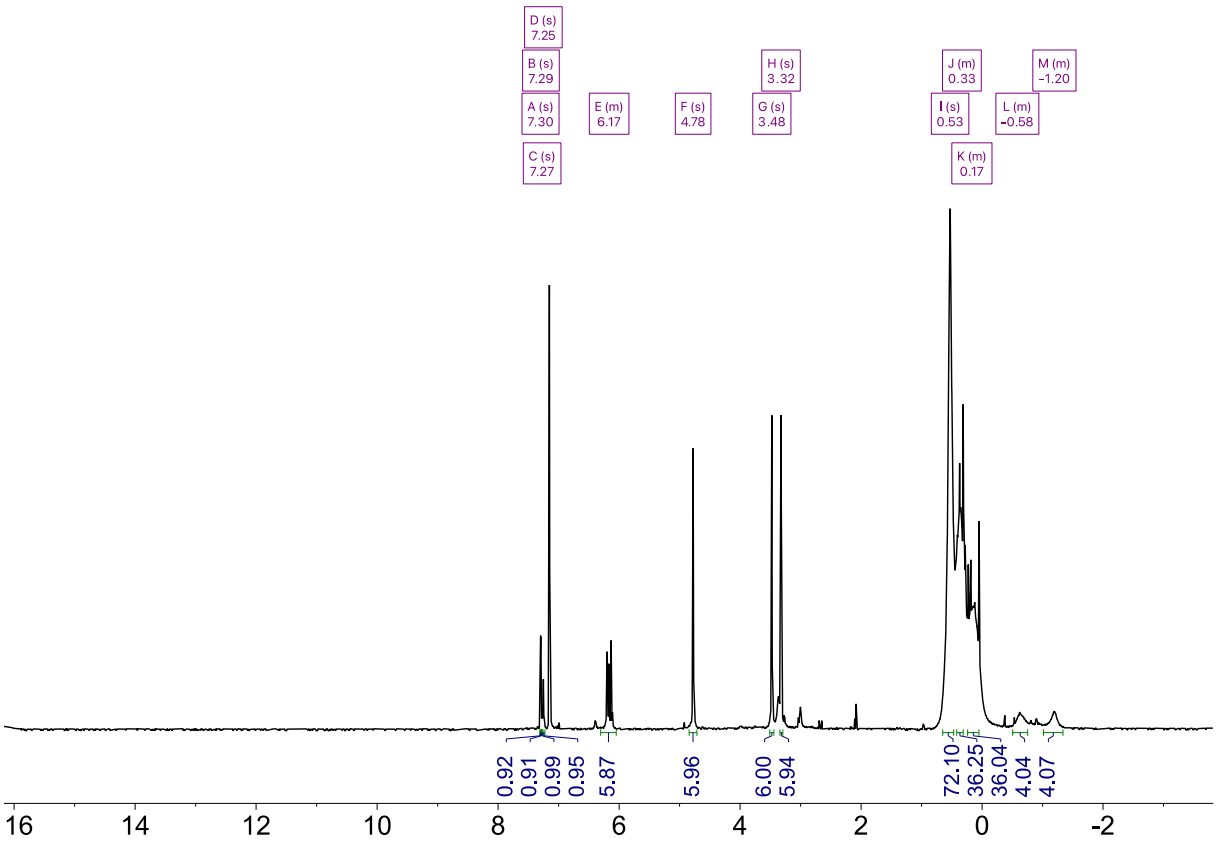

Figure S157: ^{1}H NMR spectrum of **9**·2Caff in C_6D_6 at 298 K, 500 MHz.

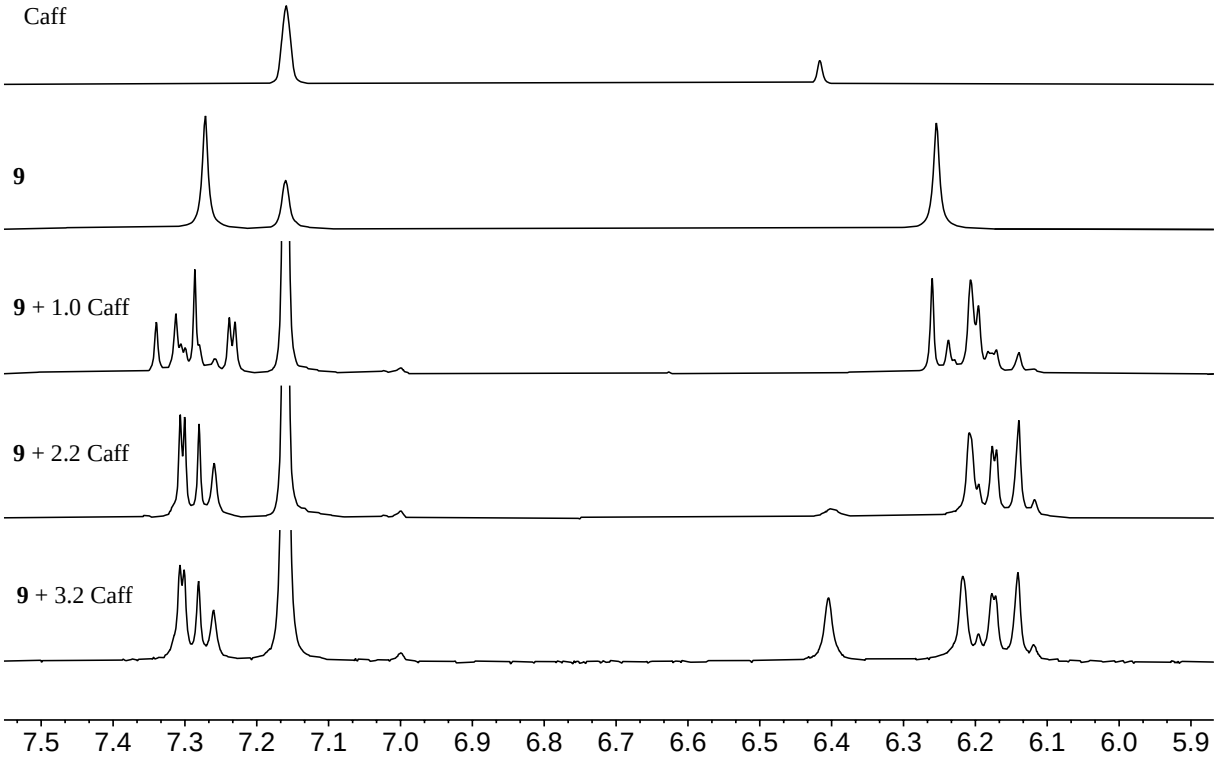

Figure S158: ^{1}H NMR spectra of **9** + different amounts of Caff in C_6D_6 at 298 K, 500 MHz.

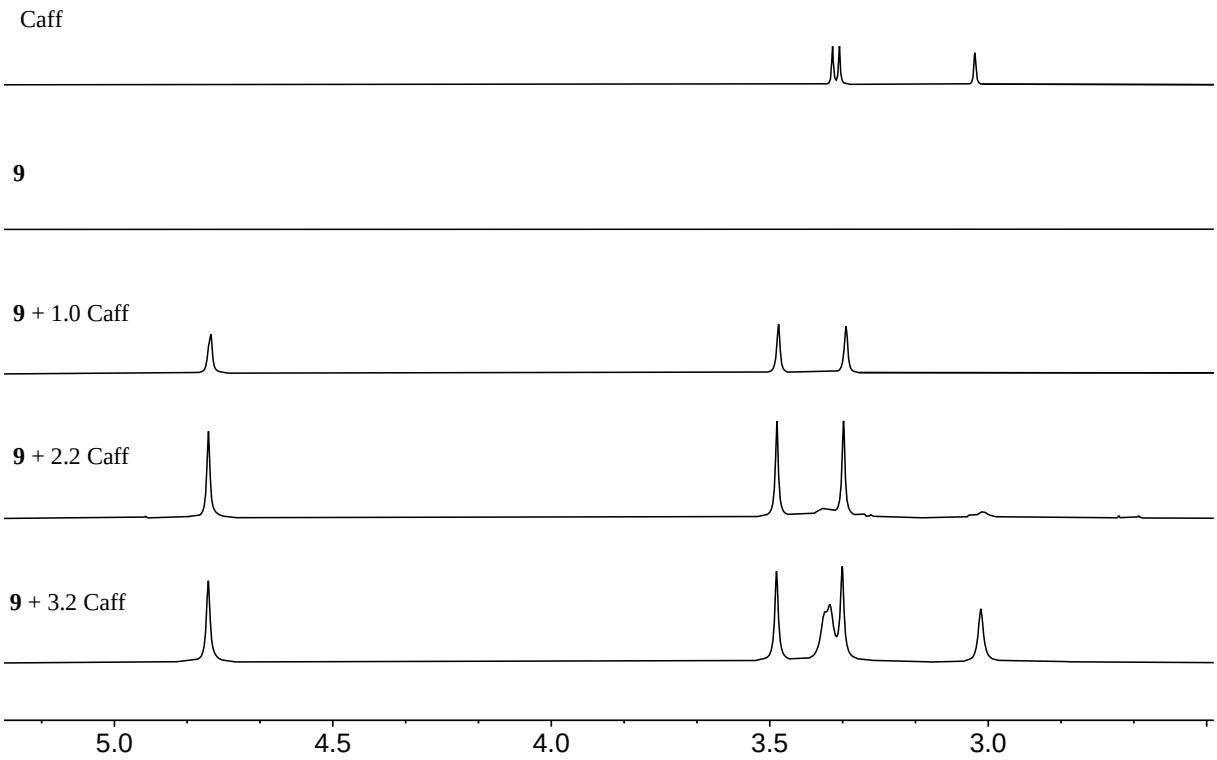

Figure S159: ^{1}H NMR spectra of **9** + different amounts of Caff in C_6D_6 at 298 K, 500 MHz.

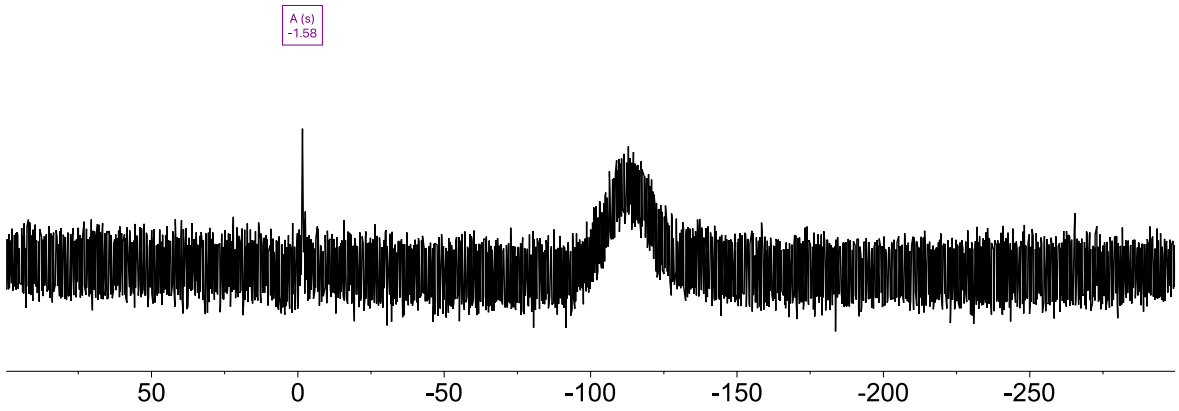

Figure S160: $^{29}Si\{^{1}H\}$ NMR spectrum of **9**·2Caff in C_6D_6 at 298 K, 99 MHz.

Classification of effective Lewis acidity (*eLA*)

To classify the different interactions between PLAs **6**–**9** with the monodentate LBs (THF, ^{t}BuNC, Py, PMe_3, Et_3PO, NMe_3) based on the shifts observed in the NMR spectroscopy, we proceeded as described below:

1. In the first step, only the ^{11}B NMR shifts of the adducts of PLA **8** were analysed. This shift is a measure for the presence of a fourfold coordination at the boron atoms and thus a probe for the strength of the interaction between **8** and the analysed LB. The shifts were sorted according to the strength of the movement (Figure 161a). Initially, the strongest interaction was assigned a value of 1, whereas the free PLA **8** corresponds to a value of 0. The adducts were then assigned values for the strength of their interaction with each other (*eLA*). These values have no deeper meaning for the semi-quantitative analysis and are only used during the creation process of the general overview of effective Lewis acidity (*eLA*). The adduct **8**·4Py was assigned a value of 10 and all other adducts were assigned the corresponding values based on the previously determined relative shifts (sorting between 0 and 1) (Table 3). These values were then be entered into the figure (Figure 161b).

^{11}B NMR Spectra of the Adducts with 8 for calibration

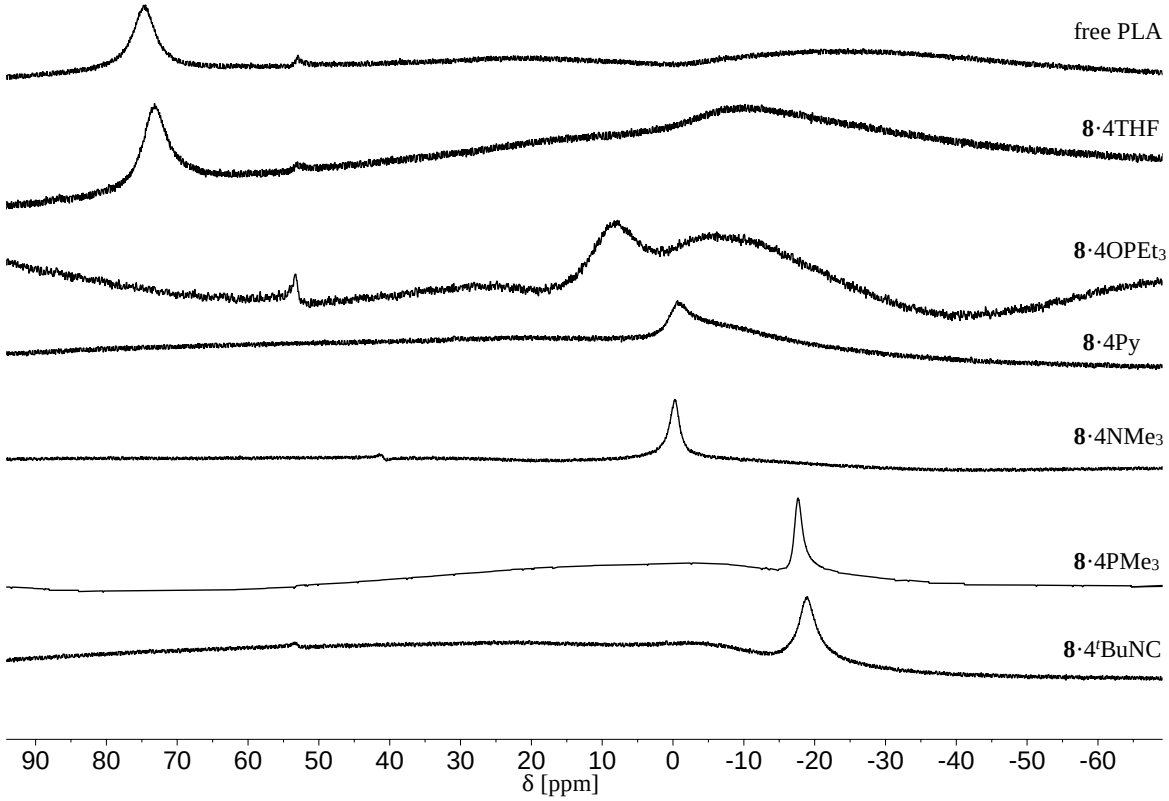

Figure S161a: ^{11}B NMR spectra of **8**·4LB in C_6D_6 at 298 K.

Table 3: Determination of the *eLA* of **8** adducts.

	$\delta(^{11}B)$	shift ($\lvert\delta$[Ad]−δ[free]$\rvert$)	relative shift ($\lvert\delta$[Ad]−δ[free]$\rvert$/ $\lvert\delta$[Ad,Max]−δ[free]$\rvert$)	relative *eLA*
8	74.6	0	0	0
8·4THF	69.7	4.90	0.05	0.65
8·4^{t}BuNC	-18.9	93.5	1.00	12.35
8·4Py	-0.73	75.3	0.81	10.00
8·4PMe_3	-17.6	92.2	0.99	12.23
8·4Et_3PO	8.30	66.3	0.71	8.77
8·4NMe_3	-0.31	74.9	0.81	10.00

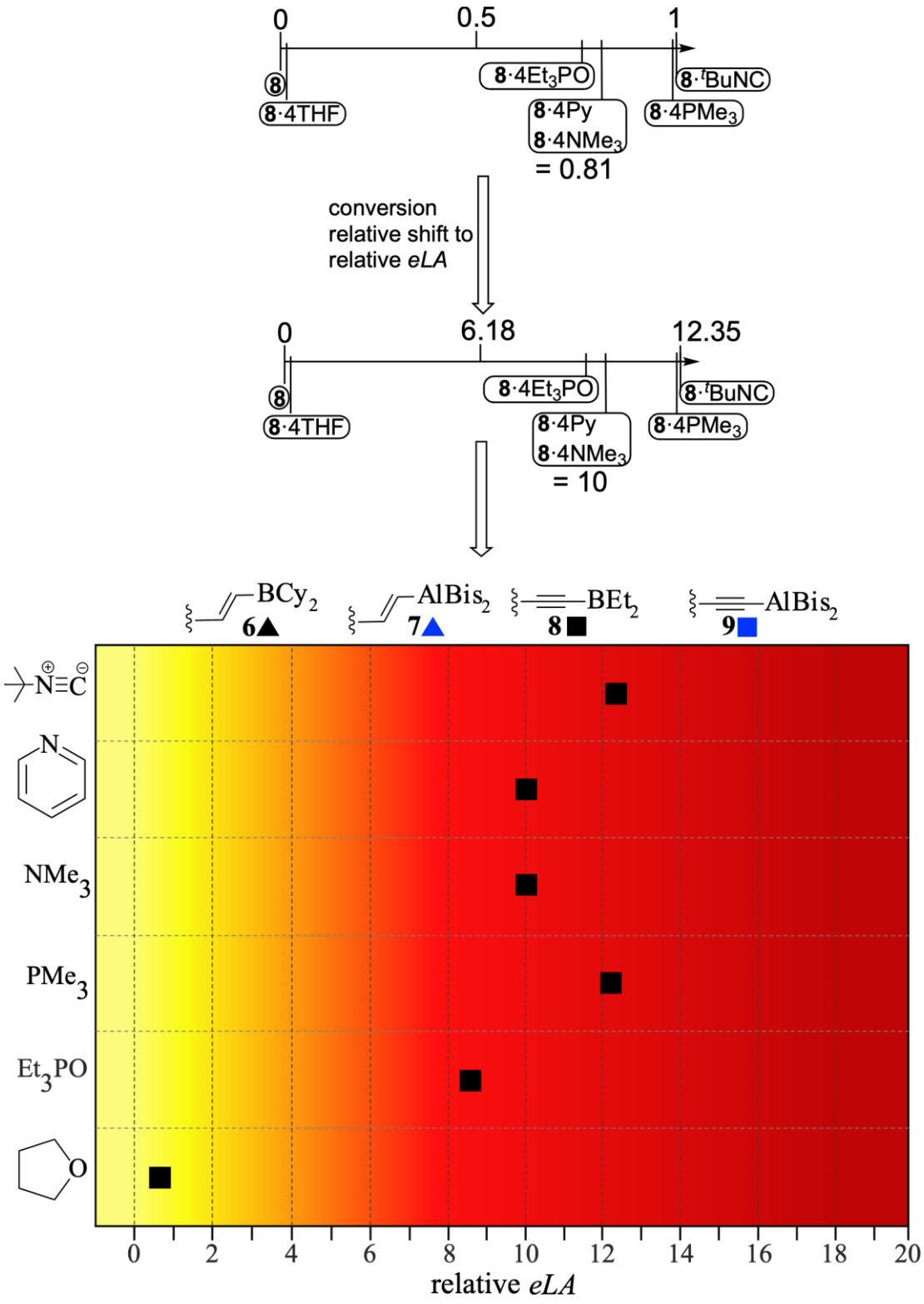

Figure S161b: Illustration of how the semi-quantitative Fig. 3 of the main text was obtained from the relative shifts obtained from NMR data. Here for all **8**·4LB.

2. In the second step, the shift of a signal belonging to the LB was observed during the interaction with the different PLAs. Once the relative ratios had been determined, the interactions could be entered in the figure, whereby the previously determined value for the corresponding adduct with PLA **8** was used for calibration. This is illustrated below for THF where the ^{1}H NMR signal of the THF was considered and for $OPEt_3$ where the ^{31}P NMR signal of the LB was considered.

Adducts with THF

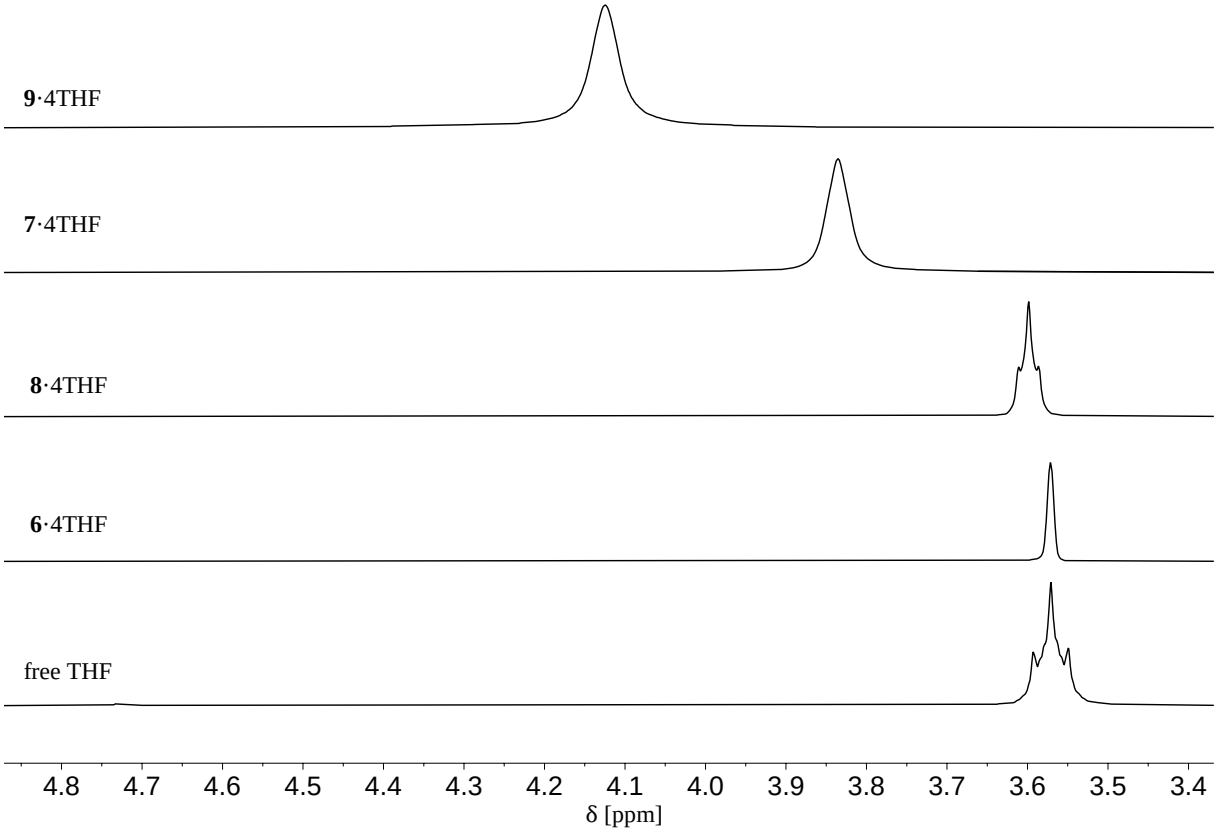

Figure S162a: ^{1}H NMR spectra of **PLA**·4THF in C_6D_6 at 298 K, 500 MHz.

Table 4: Determination of the *eLA* of the THF adducts.

	$\delta(^{1}H)$	shift ($\lvert\delta$[Ad]$-\delta$[free]$\rvert$)	relativ shift ($\lvert\delta$[Ad]$-\delta$[free]$\rvert$/ $\lvert\delta$[Ad,Max]$-\delta$[free]$\rvert$)	relative *eLA*
THF (free)	3.57	0	0	0
9·4THF	4.12	0.55	1.00	11.9
7·4THF	3.84	0.27	0.49	5.86
8·4THF	3.60	0.03	0.05	0.65
6·4THF	3.57	0	0	0

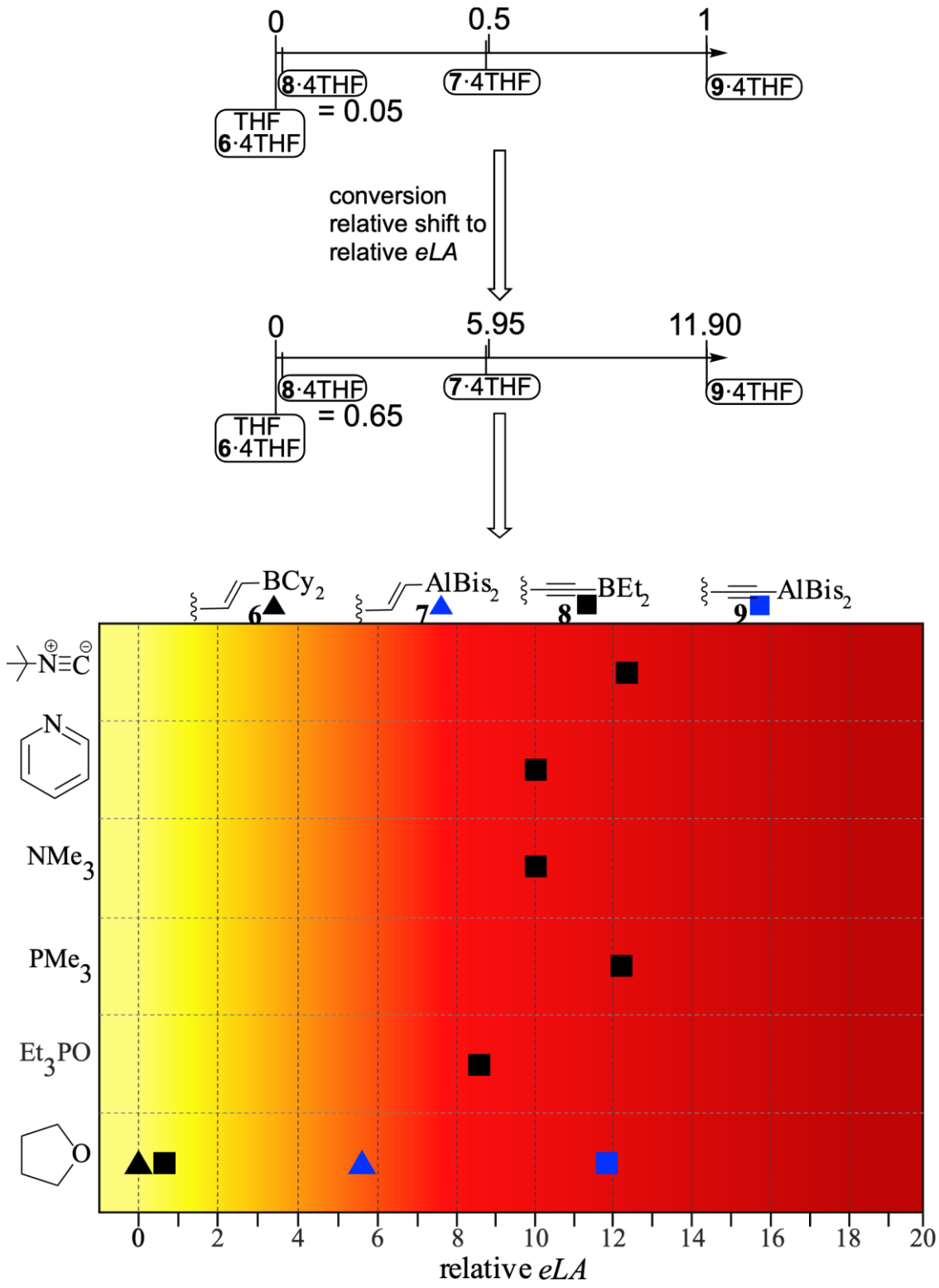

Figure S162b: Illustration of how the semi-quantitative Fig. 3 of the main text was obtained from the relative shifts obtained from NMR data. Here for all **PLA**·4THF.

Adducts with $OPEt_3$

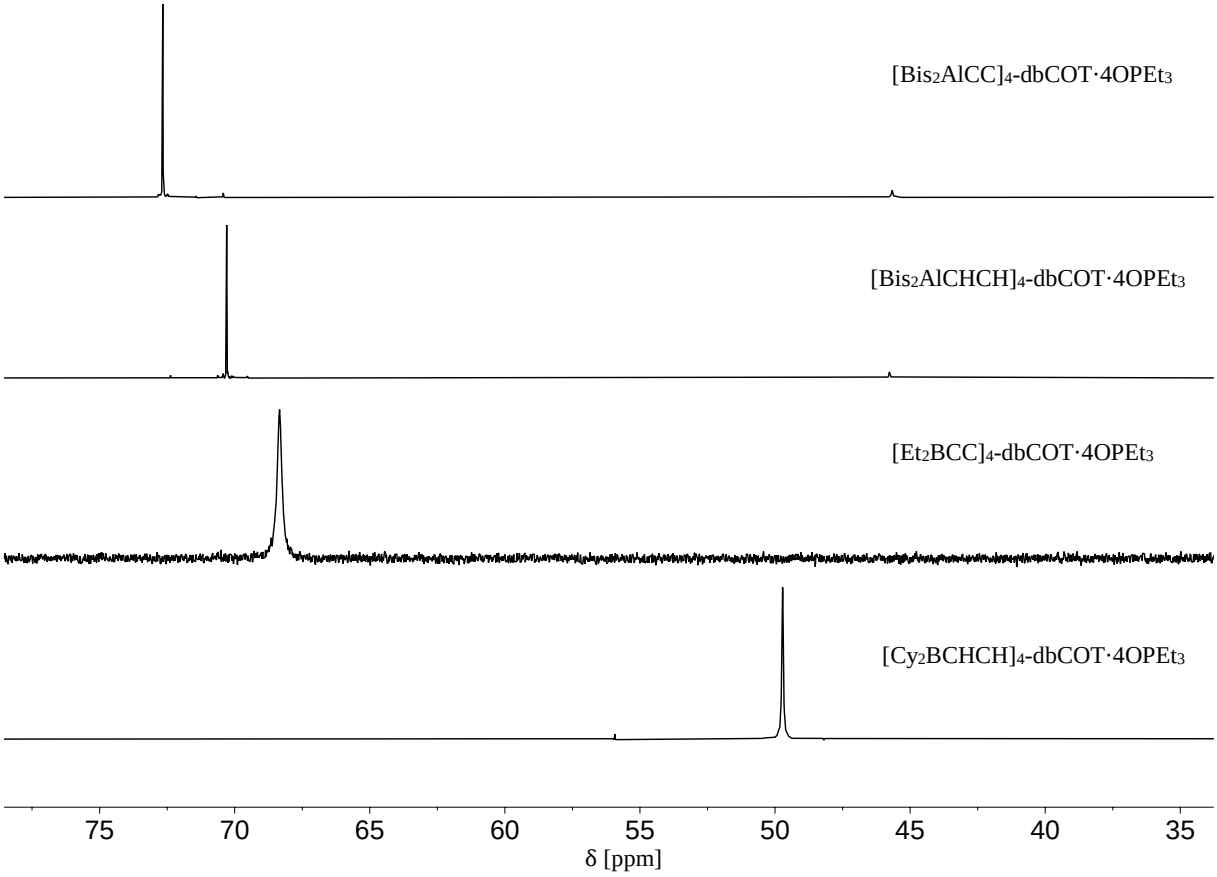

Figure S163a: $^{31}P\{^1H\}$ NMR spectra of PLA·4$OPEt_3$ in C_6D_6 at 298 K, 202 MHz.

Table 5: Determination of the *eLA* of the $OPEt_3$ adducts.

	$\delta(^{31}P)$	shift ($\lvert\delta$[Ad]$-\delta$[free]$\rvert$)	relativ shift ($\lvert\delta$[Ad]$-\delta$[free]$\rvert$/ $\lvert\delta$[Ad,Max]$-\delta$[free]$\rvert$)	relative *eLA*
$OPEt_3$ (free)	45.7	0	0	0
9·4$OPEt_3$	72.7	27.0	1.00	10.44
7·4$OPEt_3$	70,3	24.6	0.91	9.50
8·4$OPEt_3$	68,3	22.6	0.84	8.77
6·4$OPEt_3$	49,7	4.00	0.15	1.57

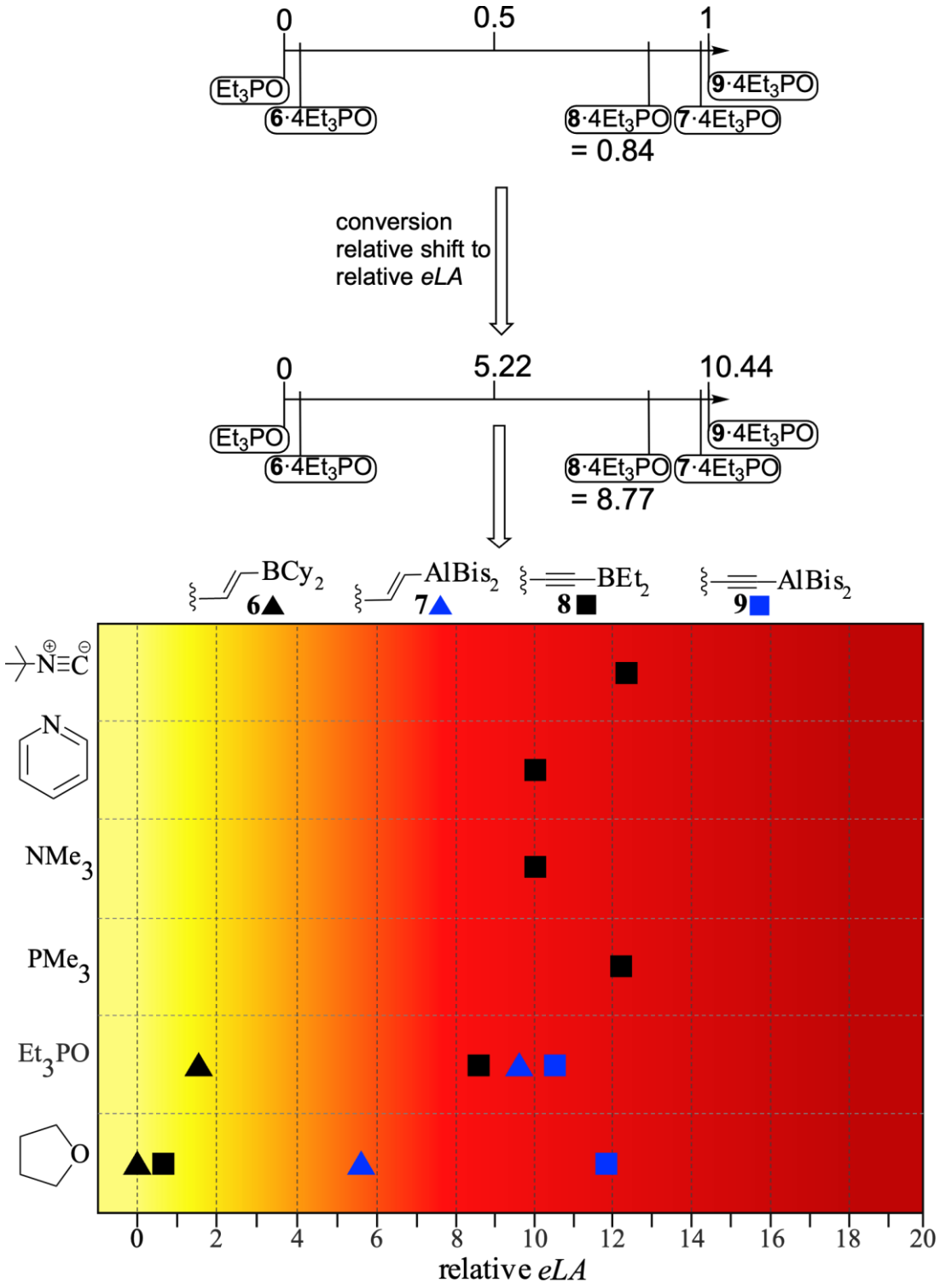

Figure S163b: Illustration of how the semi-quantitative Fig. 3 of the main text was obtained from the relative shifts obtained from NMR data. Here for all **PLA**·4Et_3PO.

3. After proceeding in the same way for the other LBs, the final Fig. 3 shown in the main text was obtained. The numbers of the scale were omitted in this illustration as they have no meaning and only the different shifts of the interactions entered are of significance.

Adducts with Pyridine

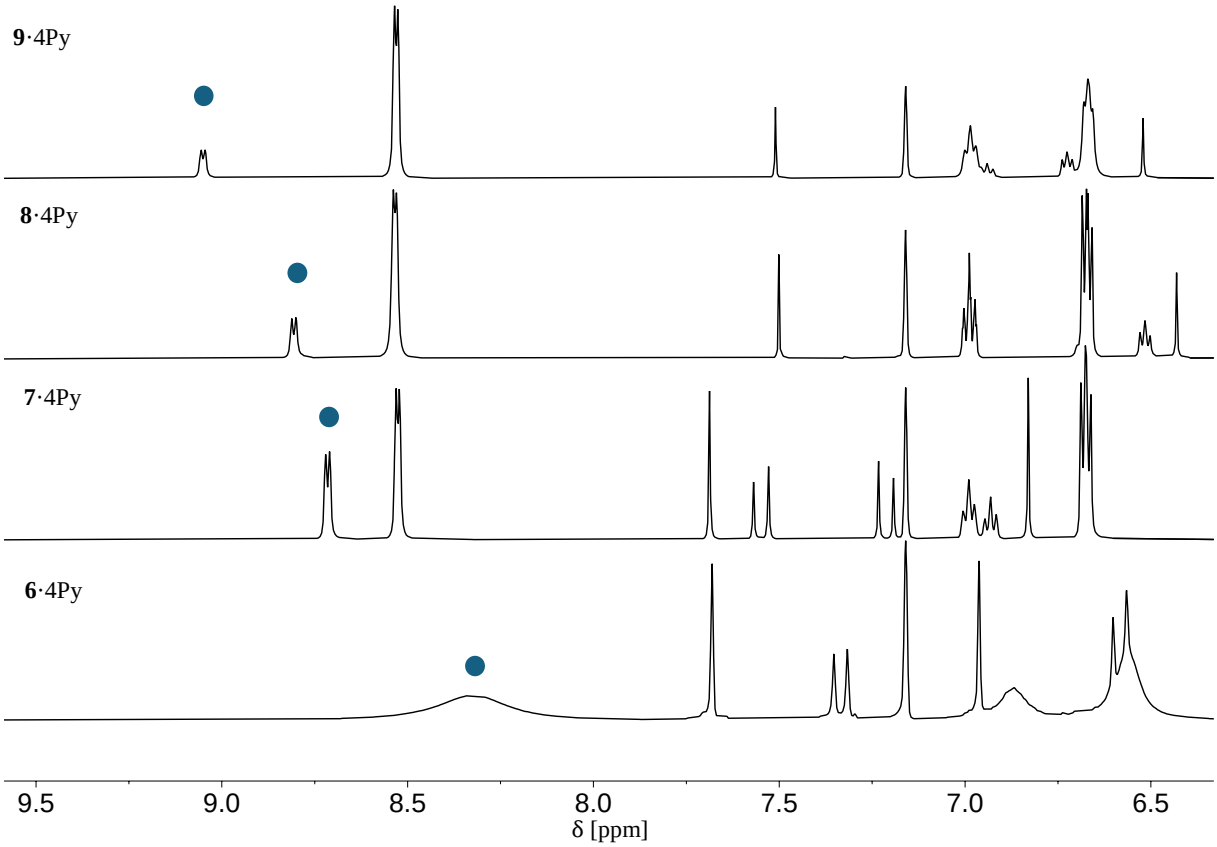

Figure S164: ^{1}H NMR spectra of PLA·4Py in C_6D_6 at 298 K, 500 MHz.

Table 6: Determination of the *eLA* of the pyridine (Py) adducts.

	$\delta(^1H)$	shift ($\lvert\delta$[Ad]$-\delta$[free])	relativ shift ($\lvert\delta$[Ad]$-\delta$[free]$\rvert$/ $\lvert\delta$[Ad,Max]$-\delta$[free]$\rvert$)	relative *eLA*
Py (free)	8.53	0	0	0
9·4Py	9.05	0.52	1.00	19.23
7·4Py	8.70	0.17	0.33	6.35
8·4Py	8.80	0.27	0.52	10.00
6·4Py	8.40	0.13	0.25	4.80

Adducts with PMe_3

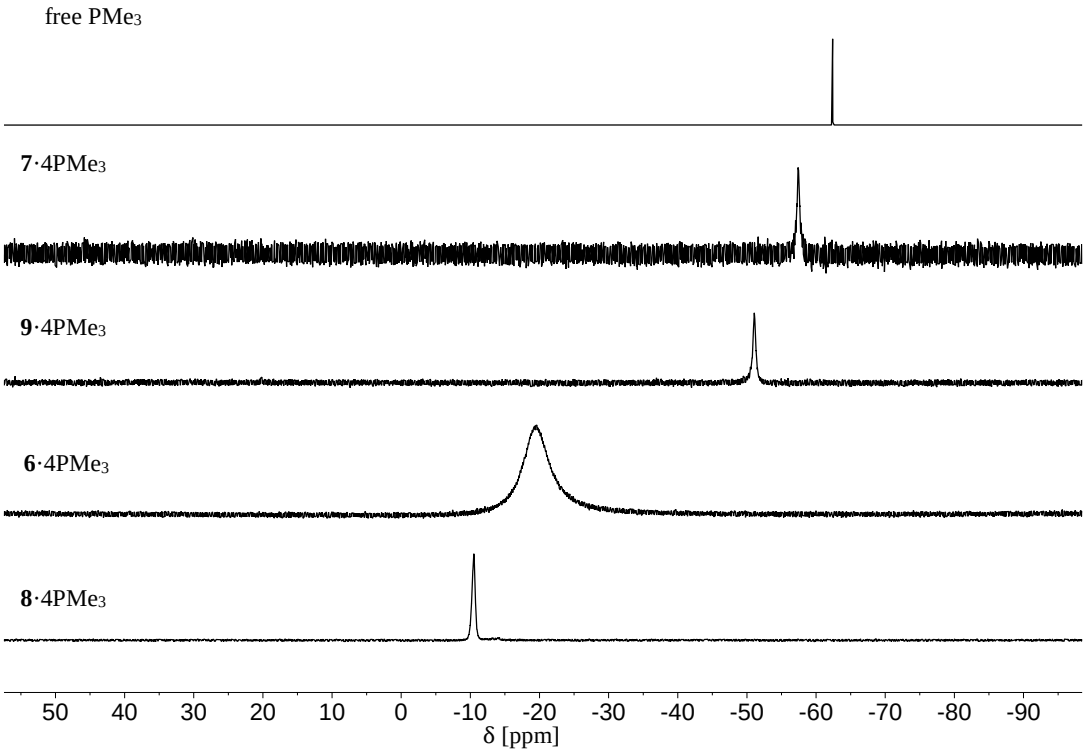

Figure S165: $^{31}P\{^1H\}$ NMR spectra of PLA·4PMe_3 in C_6D_6 at 298 K, 202 MHz.

Table 7: Determination of the *eLA* of the PMe_3 adducts.

	$\delta(^{31}P)$	shift ($\lvert\delta$[Ad]−δ[free]$\rvert$)	relativ shift ($\lvert\delta$[Ad]−δ[free]$\rvert$/ $\lvert\delta$[Ad,Max]−δ[free]$\rvert$)	relative *eLA*
PMe_3 (free)	-62.5	0	0	0
9·4PMe_3	-51.1	11.4	0.22	2.69
7·4PMe_3	-57.5	5.00	0.10	1.22
8·4PMe_3	-10.5	52.0	1	12.23
6·4PMe_3	-19.5	43.0	0.83	10.15

Adducts with NMe_3

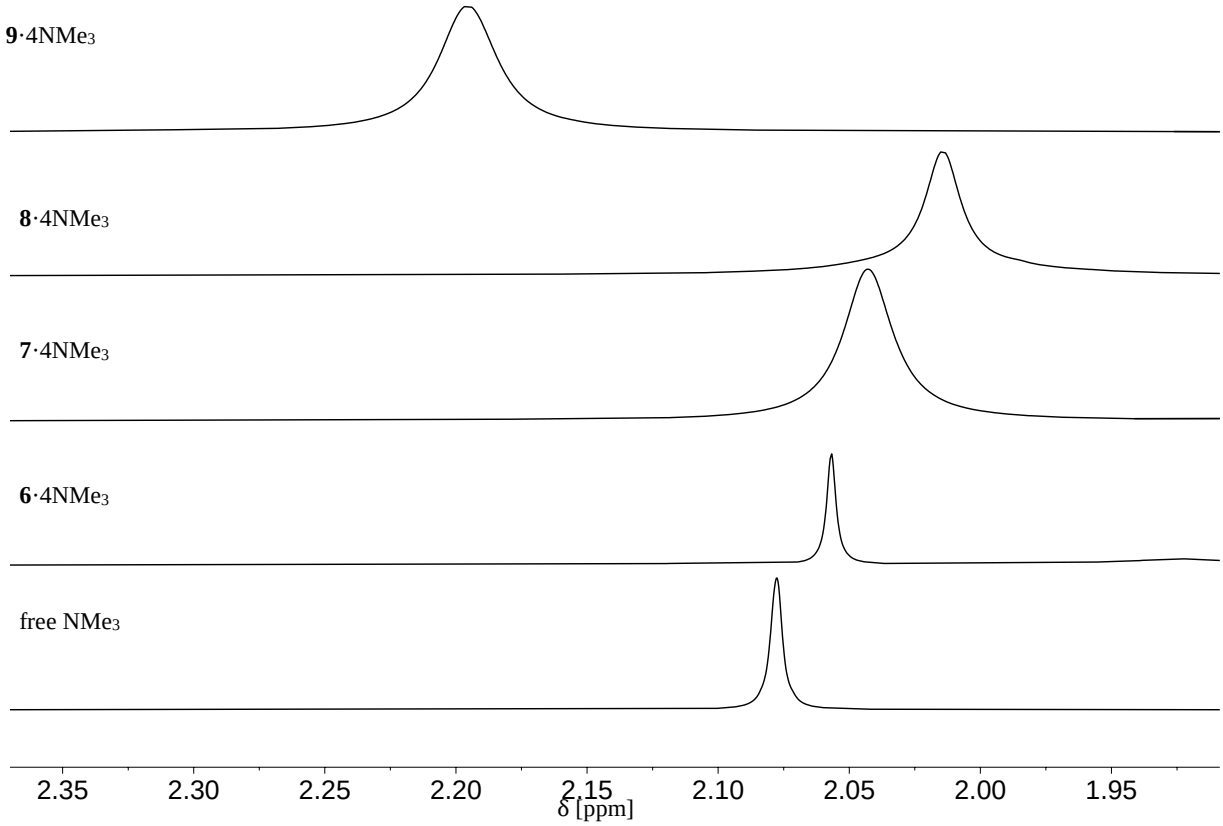

Figure S166: ^1H NMR spectra of PLA·4NMe_3 in C_6D_6 at 298 K, 500 MHz.

Table 8: Determination of the *eLA* of the NMe_3 adducts.

	$\delta(^1H)$	shift (|δ[Ad]−δ[free]|)	relativ shift (|δ[Ad]−δ[free]|/ |δ[Ad,Max]−δ[free]|)	relative *eLA*
NMe_3 (free)	2.08	0	0	0
9·4NMe_3	2.2	0.12	1	17.24
7·4NMe_3	2.04	0.04	0.34	5.86
8·4NMe_3	2.01	0.07	0.58	10.00
6·4NMe_3	2.056	0.024	0.00	0.00

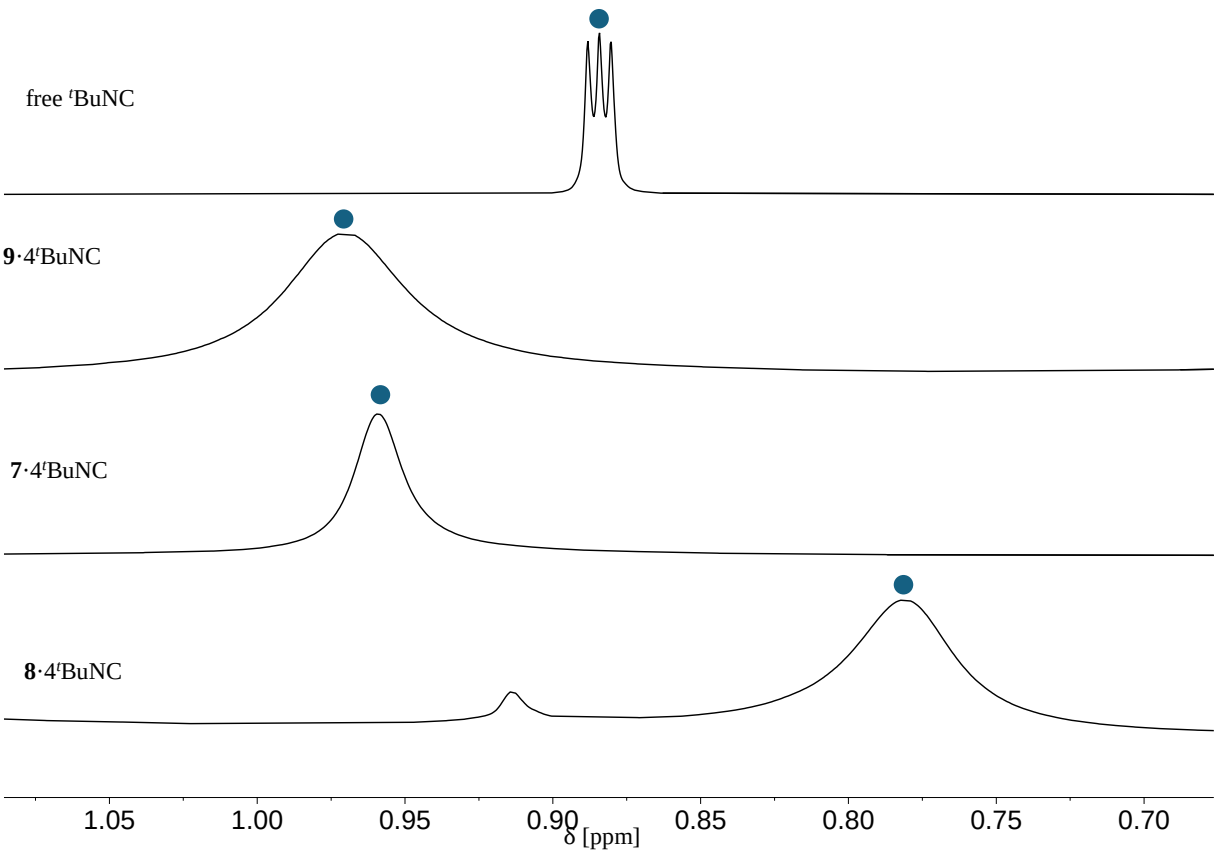

Figure S166: ^{1}H NMR spectra of **PLA**·4^{t}BuNC in C_6D_6 at 298 K, 500 MHz.

Table 5: Determination of the *eLA* of the ^{t}BuNC adducts.

	$\delta(^{1}H)$	shift ($\lvert\delta$[Ad]−δ[free]$\rvert$)	relativ shift ($\lvert\delta$[Ad]−δ[free]$\rvert$/ $\lvert\delta$[Ad,Max]−δ[free]$\rvert$)	relative *eLA*
tBuNC (free)	0.88	0	0	0
9·4^{t}BuNC	0.97	0.09	0.9	11.12
7·4^{t}BuNC	0.95	0.07	0.7	8.65
8·4^{t}BuNC	0.78	0.1	1	12.35
6·4^{t}BuNC	0	0	0	0

Table 3: Determination of the *eLA* of the ^{t}BuNC adducts.

Diffusion NMR measurements

Diffusion NMR experiments were performed on a BRUKER Avance *NEO* 600 FT NMR spectrometer, operating at a ^{1}H resonance frequency of 600.13 MHz. The instrument was equipped with a 5 mm BBO Prodigy cryoprobe with a z-gradient coil providing a maximum gradient strength of 6.57 G cm^{-1} at 10 A. Diffusion data were recorded using the *ledbpgp2s* pulse sequence supplied by the manufacturer. The diffusion coefficients have been corrected according to the diffusion coefficient of H_2O ($2.299 \cdot 10^{-9}$ m^2 s^{-2} at 298 K) reported in the literature.[8] The corresponding proportional factor $D_{H2O,lit.}/D_{H2O,est.}$ was determined on a sample of acetone-d_6 equipped with a capillary containing H_2O. The temperature unit of the instrument was calibrated according to the manufacturer's manual of the instrument using the temperature dependence of the proton chemical shift difference of methanol. To obtain stable temperature conditions, the sample was held in the magnet for at least 1 h at each temperature prior to data collection. Proton diffusion data were collected with 32k data points and a spectral width of 6600 Hz. The relaxation delay was set to 10 s. The diffusion delay time (big Delta, Δ) was set to 50 or 80 ms. The gradient duration time (small delta, δ/2) was adjusted to values between 700 and 1600 µs. The gradient strength within the diffusion experiments was increased linearly in 16 steps. The diffusion data were analyzed using the *T*1/*T*2 module which is part of the BRUKER *TopSpin*® software package. The standard deviation from the experimentally determined gradient strength dependents signal intensities to the fitted decay function was ≤ $1.2 \cdot 10^{-3}$.
DOSY-Plot were also generated with the Bruker *TopSpin*® software.

The hydrodynamic radii were calculated using the Stokes-Einstein equation (eq. 1), and the hydrodynamic volume was calculated using the equation for a spherical volume (eq. 2):[9]

$$D = \frac{k_B T}{c f_s \pi \eta r_H} \quad r_H = \frac{k_B T}{c f_s \pi \eta D} \qquad \text{(eq.1)}$$

$$V_H = \frac{3}{4}\pi r_H^3 \qquad \text{(eq. 2)}$$

D = diffusion constant
k_B = Boltzmann constant
T = temperature
c = c-factor for small molecules
f_s = form factor for small molecules
η = viscosity

Since data for deuterated compounds are not available, the dynamic viscosity of the protonated solvents have been used instead.

The *c*-factor was calculated according to Chen *et al.* (eq. 3):[10]

$$c = \frac{6}{1+0.695\left(\frac{r_{solvent}}{r_{solute}}\right)^{2.234}} \qquad \text{(eq. 3)}$$

$r_{solvent}$ = van der Waals-radius of the solvent
r_{solute} = van der Waals-radius of the solute

Van der Waals-radii of molecules have been calculated using a method reported by Abraham et *al*. (eq. 4).

$$V_{vdW}\,[\text{Å}] = \sum all\ atom\ contributions\ - 5.92 N_b\ - 14.7 R_A\ - 3.8 R_{NR} \qquad \text{(eq. 4)}$$

N_b = number of bonds
R_A = number of aromatic rings
R_{NR} = number of non-aromatic rings

Table S10 Atom contributions used for van der Waals-radii calculations.

Atom	r_{vdW} [Å]	V_{vdW} [Å]
H	1.10	5.58
C	1.70	20.58
P	1.80	13.74
N	1.55	15.59
Al	1.84	26.09
Si	2.10	38.79

Samples for DOSY NMR measurements were freshly prepared by dissolving **6**, **7** and BisPhos and in $CDCl_3$. The adducts were also freshly prepared by adding the appropriate amount of base to the solutions of the PLAs. The exact stoichiometric ratio of host to guest was determined by integrating the host and guest signals in the ^{1}H NMR spectrum prior to the measurement.

Table S11. Values for the corrected diffusion coefficients (D_{corr}), hydrodynamic radii (r_H) and hydrodynamic volume (V_H) from DOSY measurements for different adducts. The data for the host and guest are determined via ^{1}H DOSY NMR.

compound molar ratio (host/guest)	D_{corr}/ 10^{-10} m^2s^{-1} host/guest	r_H / Å host/ guest	V_H/ Å^3 host/guest
6 (1/0)	4.88	8.34	2427
BisPhos (0/1)	12.10	3.97	262
6·2BisPhos (1/2)	3.51/3.57	11.2/11.0	5858/5552

Table S12. Values for the corrected diffusion coefficients (D_{corr}), hydrodynamic radii (r_H) and hydrodynamic volume (V_H) from DOSY measurements for different adducts. The data for the host and guest are determined via ^{1}H DOSY NMR.

compound molar ratio (host/guest)	D_{corr}/ 10^{-10} m^2s^{-1} host/guest free guest	r_H / Å host/ guest free guest	V_H/ Å^3 host/guest free guest
7 at 293 K	3.71	9.54	3637
7 at 323 K	5.93	9.88	4043
7·4Py at 293 K ex. Py	3.20/3.29 17.70	11.0/10.7 3.13	5539/5097 129
7·4Py at 293 K ex Py	5.47/15.9 24.9	10.4/5.65 3.62	4729/756 198

X-Ray Diffraction

Suitable crystals were obtained from saturated solutions as mentioned in the experimental section for the corresponding compounds. The crystals were selected, coated with paratoneN oil, mounted on a glass fiber and transferred onto the goniometer of diffractometer. Using Olex2,[11] the structures were solved with the ShelXT[12] structure solution program using Intrinsic Phasing and refined with the ShelXL[13] refinement package using Least Squares minimization or refined with the olex2.refine[14] refinement package using Gauss-Newton minimization. All experimental data are listed in Table S13–S18.

CCDC 2404657 – 2404671 and 2404643 – 2404656 contain the supplementary crystallographic data for this paper. These data can be obtained free of charge from The Cambridge Crystallographic Data Centre via www.ccdc.cam.ac.uk/structures.

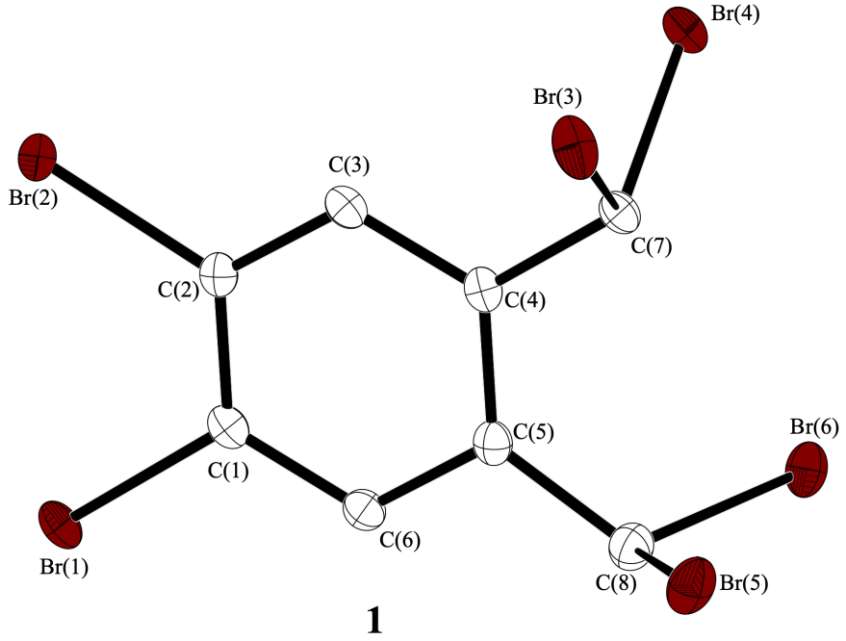

Figure S168. Molecular structure of **1** in the crystalline state. Displacement ellipsoids drawn at the 40% probability level. H atoms are omitted for clarity. Selected distances [Å] and angles [°]: Br(1)–C(1) 1.880(3), C(1)–C(2) 1.391(4), C(2)–Br(2) 1.877(3), C(2)–C(3) 1.389(4), C(4)–C(7) 1.495(4), C(7)–Br(3) , C(7)–Br(4) 1.951(3), Br(1)–C(1)–C(2) 121.7(2), C(4)–C(7)–Br(3) 111.9(2), Br(3)–C(7)–Br(4) 108.09(14).

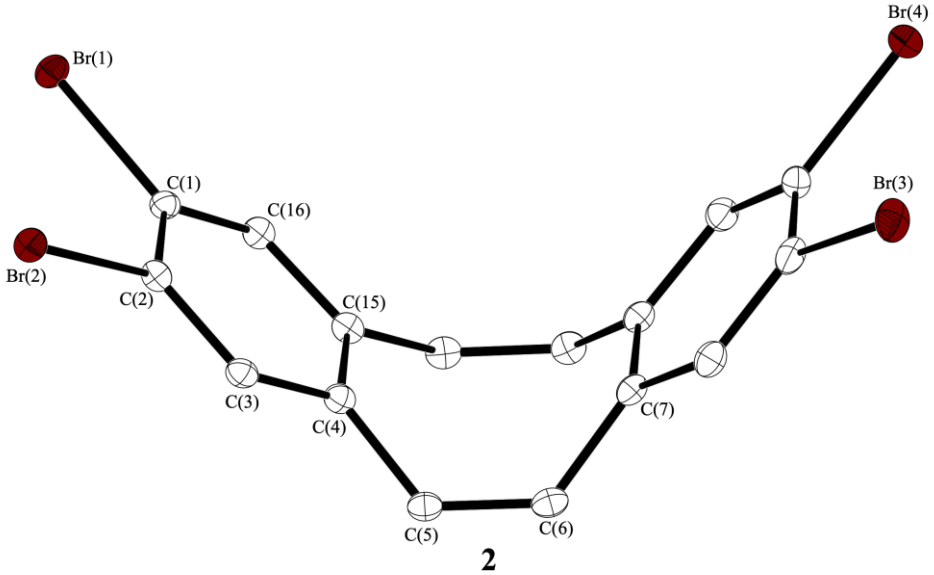

Figure S169. Molecular structure of **2** in the crystalline state. Displacement ellipsoids drawn at the 40% probability level. H atoms are omitted for clarity. Selected distances [Å] and angles [°]: Br(1)–C(1) 1.883(2), C(1)–C(2) 1.385(2), C(2)–Br(2) 1.890(2), C(2)–C(3) 1.386(2), C(3)–C(4) 1.397(2), C(5)–C(6) 1.328(3), C(6)–C(7) 1.475(3), C(4)–C(15) 1.395(2), Br(1)–C(1)–C(2) 121.81(13), C(1)–C(2)–C(3) 120.02(16), C(3)–C(4)–C(5) 117.43(15), C(15)–C(4)–C(5) 123.22(15), θ 44.1(1)/44.7(1).

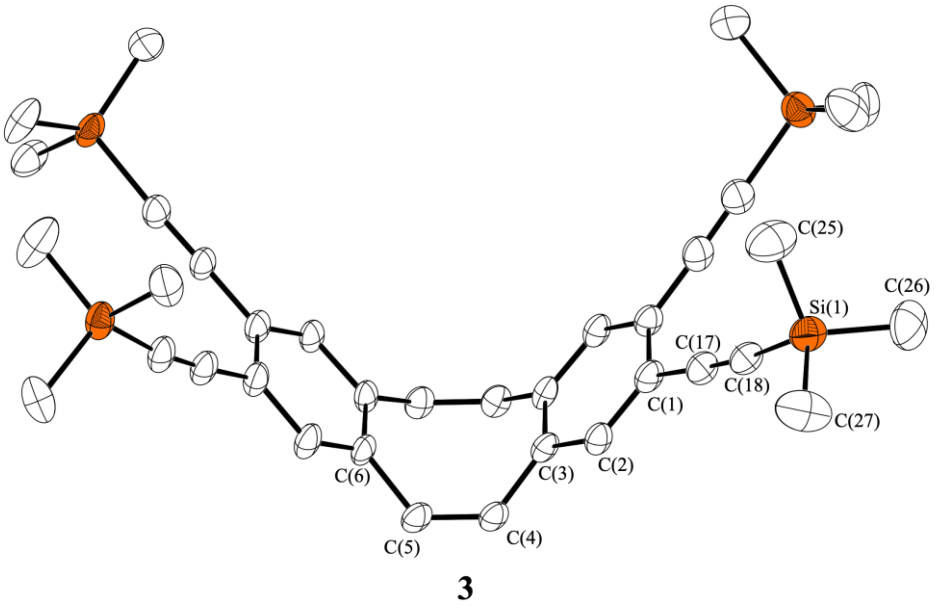

Figure S170. Molecular structure of **3** in the crystalline state. Displacement ellipsoids drawn at the 40% probability level. Minor occupied disordered atoms and H atoms are omitted for clarity. Selected distances [Å] and angles [°]: Si(1)–C(18) 1.826(6), Si(1)–C(25) 1.850(7), C(18)–C(17) 1.219(7), C(17)–C(1) 1.439(7), C(1)–C(2) 1.390(7), C(2)–C(3) 1.400(6), C(3)–C(4) 1.481(6), C(4)–C(5) 1.327(7), C(25)–Si(1)–C(18) 106.3(3), Si(1)–C(18)–C(17) 174.1(5), C(18)–C(17)–C(1) 177.7(5), C(17)–C(1)–C(2) 121.1(4), C(1)–C(2)–C(3) 122.5(4), C(3)–C(4)–C(5) 127.4(4), θ 44.2(4)/42.9(4).

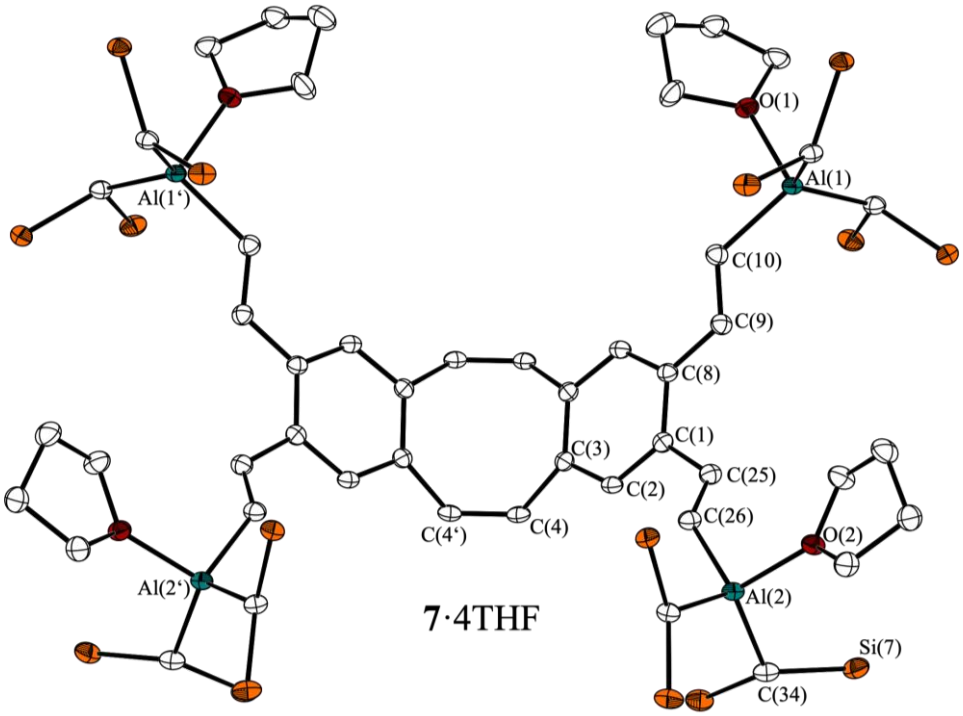

Figure S171. Molecular structure of **7**·4THF in the crystalline state. Displacement ellipsoids drawn at the 40% probability level. Minor occupied disordered atoms, methyl groups and H atoms are omitted for clarity. Selected distances [Å] and angles [°]: Al(1)···Al(2) 8.334(1), Al(1)···Al(1') 11.875(2), Al(2)···Al(2') 10.231(2), Al(1)–O(1) 1.962(2), Al(2)–O(2) 1.940(2), Al(1)–C(10) 1.981(3), C(10)–C(9) 1.340(4), C(9)–C(8) 1.477(3), C(8)–C(1) 1.409(3), C(1)–C(25) 1.482(3), C(25)–C(26) 1.334(4), C(26)–Al(2) 1.984(3), Al(2)–C(34) 2.001(3), C(1)–C(2) 1.395(3), C(2)–C(3) 1.398(3), C(3)–C(4) 1.477(3), C(4)–C(4') 1.329(5), O(1)–Al(1)–C(10) 97.14(10), Al(1)–C(10)–C(9) 128.6(2), C(10)–C(9)–C(8) 126.1(2), C(9)–C(8)–C(1) 122.5(2), C(1)–C(25)–C(26) 123.7(2), C(25)–C(26)–Al(2) 137.5(2), C(26)–Al(2)–O(2) 104.13(10), C(26)–Al(2)–C(34)110.28(11), C(1)–C(2)–C(3) 123.4(2), C(3)–C(4)–C(4') 127.42(13), θ 42.0(1). Symmetry code *x*, 3/2–*y*, +*z*.

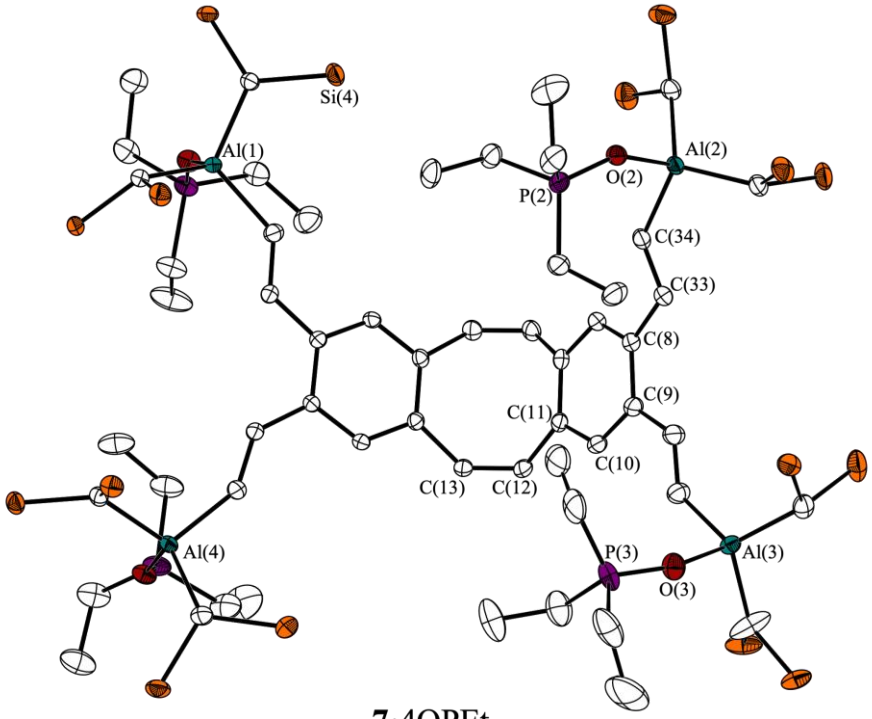

$7 \cdot 4OPEt_3$

Figure S172. Molecular structure of **7**·4OPEt$_3$ in the crystalline state. Displacement ellipsoids drawn at the 40% probability level. Minor occupied disordered atoms, methyl groups and H atoms are omitted for clarity. Selected distances [Å] and angles [°]: Al(1)···Al(2) 10.598(1), Al(3)···Al(2) 8.369(1), .Al(1)–O(1) 1.870(1), Al(2)–O(2) 1.858(1), Al(3)–O(3) 1.856(1), Al(4)–O(4) 1.861(1), O(2)–P(2) 1.523(1), Al(2)–C(34) 1.997(2), C(34)–C(33) 1.341(2), C(33)–C(8) 1.487(2), C(9)–C(10) 1.400(2), C(10)–C(11) 1.395(2), C(11)–C(12) 1.480(2), C(12)–C(13) 1.336(2), P(2)–O(2)–Al(2) 144.94(7), O(2)–Al(2)–C(34) 100.31(6), Al(2)–C(34)–C(33) 133.82(12), C(34)–C(33)–C(8) 123.90(14), C(33)–C(8)–C(9) 124.37(13), C(8)–C(9)–C(10) 117.74(14), C(10)–C(11)–C(12) 117.07(13), C(11)–C(12)–C(13) 128.89(13), θ 40.2(1)/40.8(1).

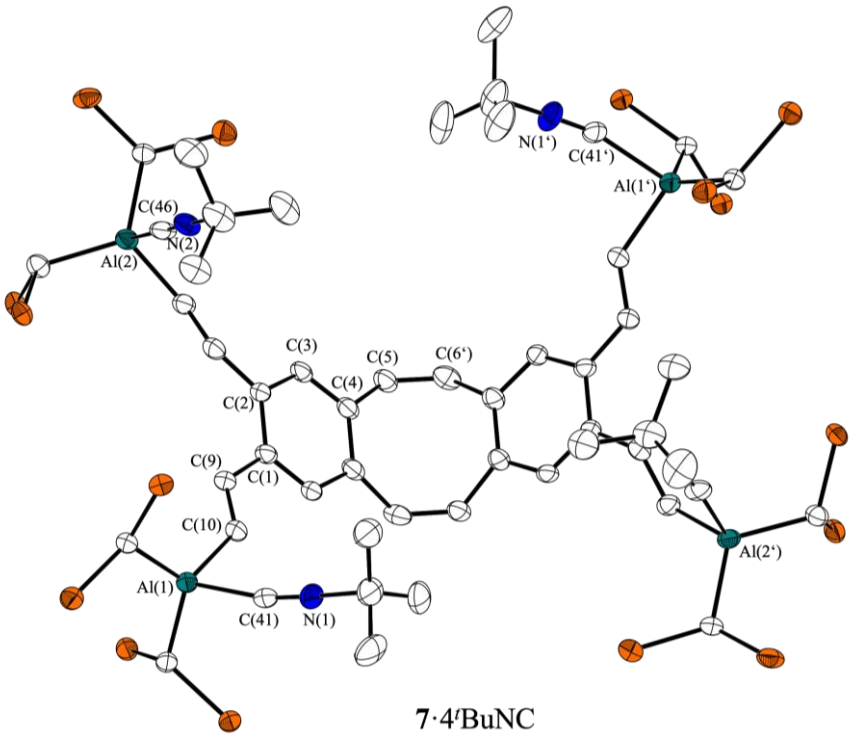

$7 \cdot 4^t BuNC$

Figure S173. Molecular structure of **7**·4^{t}BuNC in the crystalline state. Displacement ellipsoids drawn at the 20% probability level. Minor occupied disordered atoms, methyl groups on Bis and H atoms are omitted for clarity. Selected distances [Å] and angles [°]: Al(1)···Al(2) 8.063(2), Al(1)···Al(2') 11.804(2), Al(1)–C(41) 2.152(6), C(41)–N(1) 1.151(7), Al(2)–C(46) 2.083(6), C(46)–N(2) 1.157(7), Al(1)–C(10) 1.974(5), C(10)–C(9) 1.338(7), C(9)–C(1) 1.469(7), C(1)–C(2) 1.417(7), C(2)–C(3) 1.401(7), C(3)–C(4) 1.380(8), C(4)–C(5) 1.478(7), C(5)–C(6') 1.329(8), N(1)–C(41)–Al(1) 167.2(5), C(41)–Al(1)–C(10) 91.9(2), Al(1)–C(10)–C(9) 135.2(4), C(10)–C(9)–C(1) 126.8(5), θ 41.6(3). Symmetry code 3/2–*x*, 3/2–*y*, +*z*.

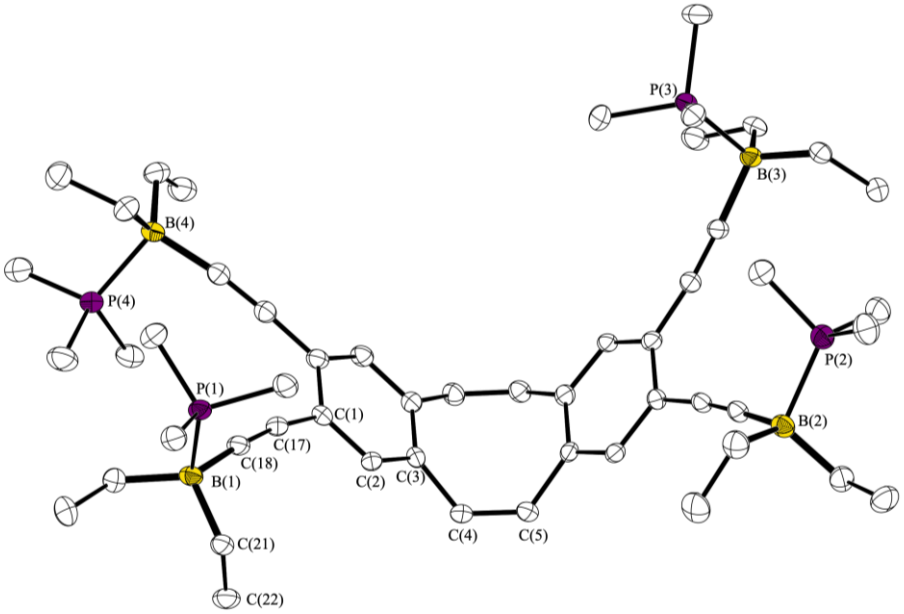

8·4PMe$_3$

Figure S174. Molecular structure of **8**·4PMe$_3$ in the crystalline state. Displacement ellipsoids drawn at the 40% probability level. Minor occupied disordered atoms and H atoms are omitted for clarity. Selected distances [Å] and angles [°]: B(1)···B(2) 11.969(11), B(1)···B(4) 6.295(11), B(2)···B(3) 6.643(11), B(3)···B(4) 12.147(11), B(1)–P(1) 1.966(8), B(2)–P(2) 1.993(8), B(1)–C(21) 1.627(9), B(1)–C(18) 1.596(9), C(18)–C(17) 1.234(9), C(17)–C(1) 1.426(9), C(1)–C(2) 1.382(9), C(2)–C(3) 1.407(9), C(3)–C(4) 1.478(9), C(4)–C(5) 1.329(9), P(1)–B(1)–C(18) 101.5(5), B(1)–C(18)–C(17) 175.5(6), C(18)–C(17)–C(1) 170.7(7), C(2)–C(3)–C(4) 118.2(5), C(3)–C(4)–C(5) 127.2(6), θ 43.6(5)/45.7(5).

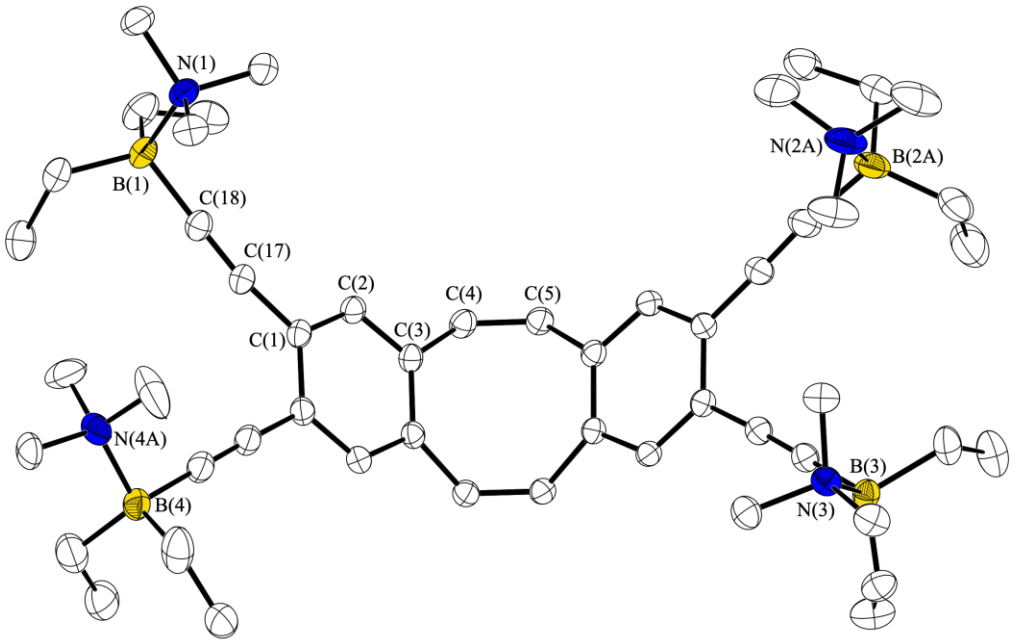

8·4NMe$_3$

Figure S175. Molecular structure of **8**·4NMe$_3$ in the crystalline state. Displacement ellipsoids drawn at the 40% probability level. Minor occupied disordered atoms and H atoms are omitted for clarity. Selected distances [Å] and angles [°]:B(1)···B(2A) 12.654(9), B(1)···B(4) 6.585(4), B(2A)···B(3) 6.020(7), B(3)···B(4) 12.646(4), B(1)–N(1) 1.690(4), B(2A)–N(2A) 1.762(10), B(1)–C(18) 1.590(4), C(18)–C(17) 1.209(3), C(17)–C(1) 1.430(3), C(1)–C(2) 1.402(3), C(2)–C(3) 1.393(3), C(3)–C(4) 1.479(3), C(4)–C(5) 1.332(3), N(1)–B(1)–C(18) 104.63(19), B(1)–C(18)–C(17) 173.5(3), C(18)–C(17)–C(1) 168.5(3), C(2)–C(3)–C(4) 116.0(2), C(3)–C(4)–C(5) 128.7(2), θ 41.8(2)/42.0(2).

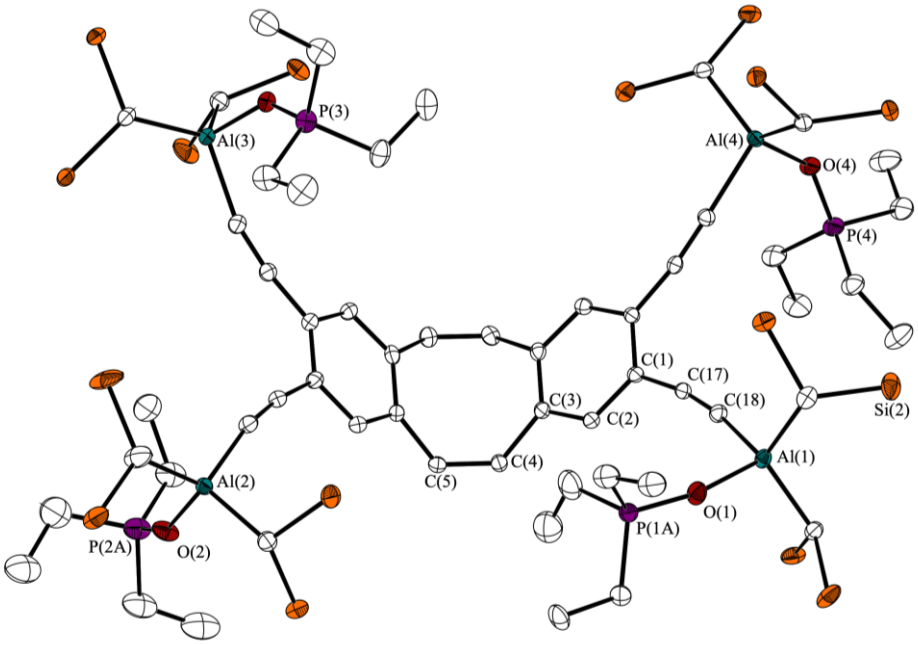

$\mathbf{9}\cdot 4OPEt_3$

Figure S176. Molecular structure of **9**·4OPEt$_3$ in the crystalline state. Displacement ellipsoids drawn at the 40% probability level. Minor occupied disordered atoms, methyl groups and H atoms are omitted for clarity. Selected distances [Å] and angles [°]: Al(1)···Al(2) 11.961(1), Al(1)···Al(4) 7.809(1) , Al(2)···Al(3) 8.200(1), Al(3)···Al(4) 11.746(1), Al(1)–O(1) 1.839(2), Al(2)–O(2) 1.845(3), Al(3)–O(3) 1.853(2), Al(4)–O(4) 1.833(2), O(1)–P(1A) 1.546(4), Al(1)–C(18) 1.977(3), C(18)–C(17) 1.209(4), C(17)–C(1) 1.441(4), C(1)–C(2) 1.395(4), C(2)–C(3) 1.393(4), C(3)–C(4) 1.474(4), C(4)–C(5) 1.329(4), P(1A)–O(1)–Al(1) 158.5(2), O(1)–Al(1)–C(18) 100.41(12), Al(1)–C(18)–C(17) 170.4(3), C(18)–C(17)–C(1) 169.7(3), C(1)–C(2)–C(3) 123.5(3), C(3)–C(4)–C(5) 128.3(3), θ 42.5(3)/42.0(3).

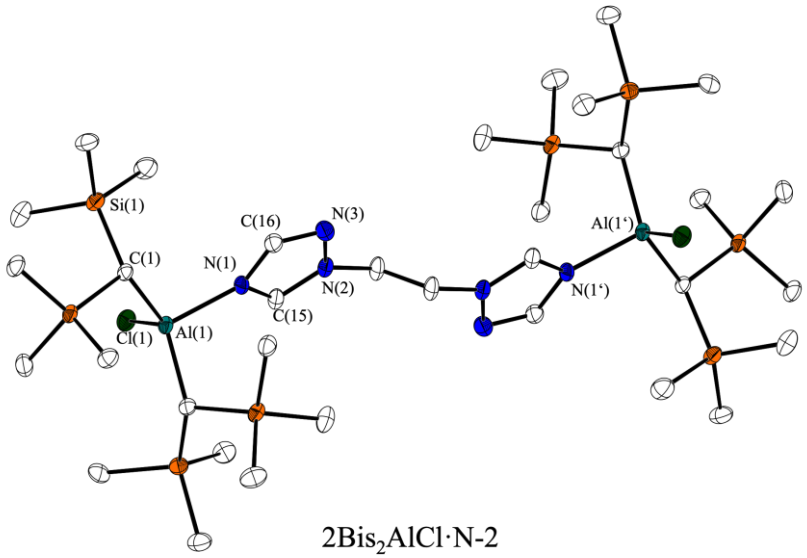

$2Bis_2AlCl\cdot N\text{-}2$

Figure S177. Molecular structure of 2Bis$_2$AlCl·N-2 in the crystalline state. Displacement ellipsoids drawn at the 40% probability level. H atoms are omitted for clarity. Selected distances [Å] and angles [°]: Al(1)···Al(1') 11.610(2), N(1)···N(1') 7.885(7), Al(1)–N(1) 1.992(4), Al(1)–Cl(1) 2.195(2), Al(1)–C(1) 1.972(4), N(1)–C(16) 1.368(6), C(16)–N(3) 1.310(6), N(3)–N(2) 1.361(6), N(2)–C(15) 1.327(6), C(15)–N(1) 1.328(6), C(1)–Al(1)–N(1) 106.42(16), C(1)–Al(1)–Cl(1) 112.34(13).

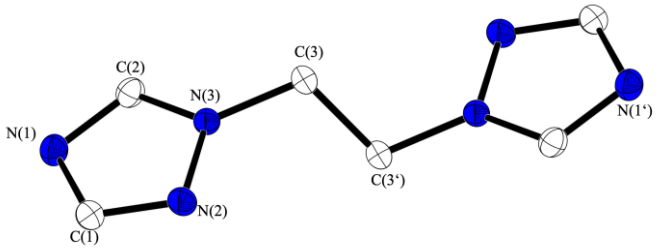

N-2

Figure S178. Molecular structure of N-2 in the crystalline state. Displacement ellipsoids drawn at the 40% probability level. Minor occupied disordered atoms and H atoms are omitted for clarity. Selected distances [Å] and angles [°]: N(1)···N(1’) 7.964(2), N(1)–C(1) 1.360(1), N(1)–C(2) 1.324(1), C(1)–N(2) 1.326(1), N(2)–N(3) 1.361(1), N(3)–C(2) 1.337(1).

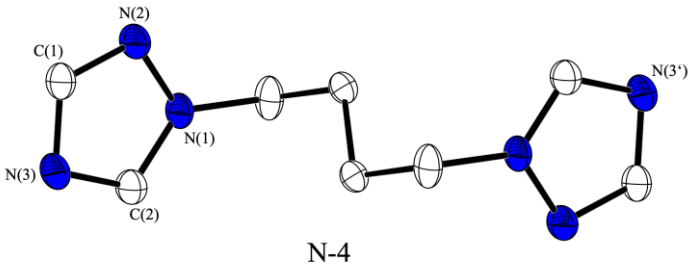

N-4

Figure S179. Molecular structure of N-4 in the crystalline state. Displacement ellipsoids drawn at the 40% probability level. Minor occupied disordered atoms and H atoms are omitted for clarity. Selected distances [Å] and angles [°]: N(3)···N(3’) 8.709(2), N(3)–C(1) 1.356(1), N(3)–C(2) 1.327(1), N(1)–C(2) 1.336(1), N(1)–N(2) 1.354(1).

Table S13. Crystal data for **1–5**.

	1	**2**[a]	**3**[b]	**4**[c]	**5**
Empirical formula	$C_8H_4Br_6$	$C_{16}H_8Br_4$	$C_{36}H_{44}Si_4$	$C_{24}H_{12}$	$C_{36}H_{44}Sn_4$
M [g mol^{-1}]	579.57	519.86	589.07	300.34	951.47
T [K]	100.0(1)	100.0(1)	100.0(1)	100.0(1)	100.0(1)
Crystal system	triclinic	triclinic	orthorhombic	orthorhombic	triclinic
Space group	$P\bar{1}$	$P\bar{1}$	$P2_12_12_1$	$Pnn2$	$P\bar{1}$
a [Å]	7.13408(18)	6.9133(2)	9.3866(2)	26.6836(8)	9.9875(2)
b [Å]	8.45003(17)	7.8228(2)	13.3745(3)	7.1664(3)	13.6226(3)
c [Å]	10.6972(3)	13.9754(4)	29.0130(9)	4.14195(14)	16.6728(3)
α [°]	99.3131(19)	88.282(2)	90	90	66.188(2)
β [°]	94.748(2)	80.067(2)	90	90	74.143(2)
γ [°]	92.1076(18)	84.765(2)	90	90	70.467(2)
V [Å^3]	633.35(3)	741.30(4)	3642.32(16)	792.05(5)	1930.59(8)
Z	2	2	4	2	2
ρ_{calc} [g cm^{-3}]	3.039	2.329	1.074	1.259	1.637
μ [mm^{-1}]	18.977	10.843	1.663	0.547	2.578
F(000) [e]	524	488	1264	312	920
Size [mm]	0.1×0.05×0.03	0.17×0.15×0.02	0.36×0.02×0.02	0.37×0.08×0.05	0.22×0.17×0.15
λ [Å]	0.71073 (Mo Kα)	0.71073 (Mo Kα)	1.54184 (Cu Kα)	1.54184 (Cu Kα)	0.71073 (Mo Kα)
2θ range [°]	5.716 to 60.146	2.958 to 68.958	6.092 to 134.12	6.626 to 152.55	5.302 to 65.61
hkl range	$-10 \le h \le 10$ $-11 \le k \le 11$ $-15 \le l \le 15$	$-10 \le h \le 10$ $-12 \le k \le 12$ $-22 \le l \le 22$	$-11 \le h \le 10$ $-15 \le k \le 15$ $-34 \le l \le 34$	$-33 \le h \le 33$ $-8 \le k \le 7$ $-5 \le l \le 5$	$-14 \le h \le 14$ $-20 \le k \le 20$ $-25 \le l \le 24$
Ref. collected	37562	39618	122950	11289	70956
Independent ref.	3701	6030	6496	1646	13260
$R_{int.}$ / R_{sigma}	0.0552 / 0.0224	0.0379 / 0.0235	0.1894 / 0.0595	0.0480 / 0.0208	0.0309 / 0.0254
Refl. with $I > 2\sigma(I)$.	3314	5048	5380	1599	11445
Data/restraints/param.	3701/0/127	6030/0/213	6496/0/417	1646/1/110	13260/0/373
GoF on F^2	1.060	1.077	1.040	1.108	1.047
R_1 / ωR_2 [$I>2\sigma(I)$]	0.0254 / 0.0596	0.0244 / 0.0537	0.0553 / 0.1361	0.0718 / 0.1651	0.0266 / 0.0558
R_{int} (all data) /ωR_2	0.0300 / 0.0624	0.0339 / 0.0570	0.0709 / 0.1511	0.0730 / 0.1656	0.0351 / 0.0596
ρ_{fin} (max/min) [e Å^{-3}]	2.24/–1.31	0.69/–0.58	0.33/–0.38	0.37/–0.29	1.50/–1.08
Flack parameter	-	-	-0.05(2)	0(8)	-
CCDC	2404657	2404658	2404659	2404660	2404661

[a] Hydrogens were refined isotropically. [b] Disorder of two $SiMe_3$ groups over two sites with ratio 59:41 [c] Absolute structure cannot be determined reliably.

Table S14. Crystal data for **6**, **6**·4PMe_3, [**6**·2BisPhos]$_2$, **7**·4Py and **9**·4Py.

	6[a]	**6**·4PMe_3[b]	[**6**·2BisPhos]$_2$ [c]	**7**·4Py[d]	**9**·4Py [e]
Empirical formula	$C_{78}H_{110}B_4$	$C_{104}H_{180}B_4O_5P_4$	$C_{236}H_{356}B_8P_8Si_4$	$C_{115}H_{203}Al_4N_7Si_{16}$	$C_{109}H_{201}Al_4N_4Si_{16}$
M [g mol^{-1}]	1090.89	1677.59	3639.79	2241.19	2125.09
T [K]	100.1(1)	100.0(1)	100.0(1)	100.0(2)	100.0(1)
Crystal system	triclinic	monoclinic	monoclinic	orthorhombic	monoclinic
Space group	$P\bar{1}$	$P2_1/c$	$P2_1/n$	$Pnma$	$P2_1/c$
a [Å]	17.9240(5)	24.1726(4)	21.3482(2)	35.9270(6)	21.55741(13)
b [Å]	22.5027(4)	14.6669(2)	19.6426(2)	40.0455(7)	34.3831(2)
c [Å]	26.8769(6)	29.3276(5)	27.6990(3)	9.63551(18)	18.76010(13)
α [°]	102.681(2)	90	90	90	90
β [°]	100.038(2)	95.512(2)	107.4257(11)	90	99.6928(6)
γ [°]	104.561(2)	90	90	90	90
V [Å^3]	9929.4(4)	10349.6(3)	11082.0(2)	13862.8(4)	13706.67(16)
Z	6	4	2	4	4
ρ_{calc} [g cm^{-3}]	1.095	1.077	1.091	1.074	1.030
μ [mm^{-1}]	0.438	1.031	1.168	1.964	1.956
F(000) [e]	3588	3696	3976	4872	4636
Size [mm]	0.376×0.08×0.036	0.21×0.12×0.05	0.3×0.17×0.09	0.2×0.09×0.04	0.41×0.223×0.166
λ [Å]	1.54184 (Cu Kα)	1.54184 (Cu Kα)	1.54184 (Cu Kα)	1.54184 (Cu Kα)	1.54184 (Cu Kα)
2θ range [°]	5.252 to 153.986	6.056 to 151.624	5.606 to 153.07	5.392 to 153.288	4.888 to 152.92
hkl range	$-22 \le h \le 22$ $-28 \le k \le 19$ $-31 \le l \le 33$	$-29 \le h \le 28$ $-18 \le k \le 8$ $-30 \le l \le 36$	$-22 \le h \le 26$ $-24 \le k \le 21$ $-34 \le l \le 33$	$-45 \le h \le 33$ $-49 \le k \le 49$ $-12 \le l \le 11$	$-27 \le h \le 24$ $-43 \le k \le 40$ $-23 \le l \le 23$
Ref. collected	89498	51376	98309	87005	107190
Independent ref.	40743	21145	23029	14658	28514
$R_{int.}$ / R_{sigma}	0.0472 / 0.0614	0.0464 / 0.0580	0.0467 / 0.0342]	0.0459 / 0.0265]	0.0303 / 0.0277
Refl. with $I > 2\sigma(I)$.	26764	13033	19481	12036	25654
Data/restraints/param.	40743/1246/2646	21145/288/921	23029/230/1096	14658/336/858	28514/528/1396
GoF on F^2	1.029	1.059	1.039	1.022	1.015
R_1 / ωR_2 [$I>2\sigma(I)$]	0.0936 / 0.2539	0.0853 / 0.2353	0.0539 / 0.1480	0.0630 / 0.1762	0.0356 / 0.0917
R_{int} (all data) /ωR_2	0.1260 / 0.2912	0.1189 / 0.2611	0.0621 / 0.1544	0.0738 / 0.1866	0.0401 / 0.0952
ρ_{fin} (max/min) [e Å^{-3}]	0.70/–0.34	0.71/–0.37	0.60/–0.63	0.65/–0.50	0.44/–0.48
CCDC	2404662	2404663	2404664	2404665	2404666

[a] Disorder of C19 in ratio 93:7, C40 to C44 54:46, C112 and C113 60:40, C117 to C130, B7 60:40, C140 to C144 91:9, C164 and C165 89:11, C170, C171, and C174 83:17, C177 and C182 83:17, C184 71:29, C197 to C202 75:25, C211 to C213 and C216 81:19.
[b] A solvent mask was calculated and 802 electrons were found in a volume of 3188 A^3 in 1 void per unit cell. This is consistent with the presence of 5 THF per formula unit which account for 800 electrons per unit cell. Disorder of one trimethylphosphane group (P1; C31-33) over two sites; ratio 62 (labelled "A"):38 (labelled "B"). Partial disorder of one cyclohexyl group (C26-30) over two sites; ratio 62 (labelled "A"):38 (labelled "B").
[c] Disorder of Si1, C76, and C77 over two sites in ratio 90:10. The solvent benzene beside this group is disordered in the same ratio and could not be squeezed due to the short distance. Disorder of two cyclohexyl-groups over two sites in ratio 71:29 and 53:47. Suitable

restraints were applied for disordered atoms. Highly disordered benzene were squezzed. A solvent mask was calculated and 520 electrons were found in a volume of 2356 A^3 in 1 void per unit cell. This is consistent with the presence of 6[C_6H_6] per asymmetric unit which account for 504 electrons per unit cell.
[d] Disorder of C1, Si1, Si2, C3 to C7 over two sites in ratio 64:36; C11 62:38; Si4, C12 to C14 54:46; C30, Si6 C35, C36 60:40; C39, C40 54:46; Si8, C41 to C43 58:42; C44 to C48 51:49. Pyridine as solvent molecules was highly disordered, therefore a solvent mask was calculated and 492 electrons were found in a volume of 2166 A^3 in 1 void per unit cell. This is consistent with the presence of 1.5[C_5H_5N] per asymmetric unit which account for 504 electrons per unit cell.
[e] Disorder of Si9, Si10, C61 to C67 in ratio 82:18, disorder of Si13, Si14, C82 to C88 in ratio 84:16, disorder of hexane over two sites in ratio 87:13. A disordered hexane molecule on an inversion center was squeezed using the Olex2 routine. A solvent mask was calculated and 108 electrons were found in a volume of 1452 A^3 in 8 voids per unit cell. This is consistent with the presence of 0.5[C_6H_{14}] per asymmetric unit which account for 100 electrons per unit cell.

Table S15. Crystal data for **9**·2N-1, **9**·2N-2, **7**·2N-2, **7**·2N-4 and 2Bis$_2$AlCl·N-2.

	9·2N-1[a]	**9**·2N-2[b]	**7**·2N-2[c]	**7**·2N-4[d]	2Bis$_2$AlCl·N-2[e]
Empirical formula	$C_{141}H_{264}Al_4N_{12}O_{10}Si_{16}$	$C_{134}H_{218}Al_4N_{12}Si_{16}$	$C_{110}H_{196}Al_4F_6N_{12}Si_{16}$	$C_{98.5}H_{194.5}Al_4Cl_{7.5}N_{12}Si_{16}$	$C_{34}H_{84}Al_2Cl_2N_6Si_8$
M [g mol^{-1}]	2844.99	2554.55	2358.14	2370.38	926.65
T [K]	100.0(1)	100.0(1)	100.0(1)	100.0(1)	100.0(1)
Crystal system	monoclinic	monoclinic	triclinic	monoclinic	triclinic
Space group	$P2_1/c$	$C2/c$	$P\bar{1}$	Cc	$P\bar{1}$
a [Å]	43.2023(4)	25.3030(2)	9.8394(7)	42.130(4)	9.2499(7)
b [Å]	13.88810(10)	19.75400(10)	19.1246(13)	9.7827(7)	9.4721(5)
c [Å]	28.5687(4)	33.3226(2)	20.8145(12)	34.113(2)	15.9824(14)
α [°]	90	90	113.328(6)	90	91.255(6)
β [°]	100.5650(10)	109.8660(10)	103.196(5)	100.078(7)	96.736(7)
γ [°]	90	90	90.955(6)	90	105.164(6)
V [Å^3]	16850.6(3)	15664.6(2)	3476.4(4)	13842.4(18)	1340.20(18)
Z	4	4	1	4	1
ρ_{calc} [g cm^{-3}]	1.121	1.083	1.126	1.137	1.148
μ [mm^{-1}]	1.765	1.804	2.056	3.302	3.345
F(000) [e]	6200	5528	1270	5092	502
Size [mm]	0.236×0.143×0.049	0.3×0.22×0.21	0.336×0.069×0.026	0.17×0.05×0.03	0.125×0.092×0.02
λ [Å]	1.54184 (Cu Kα)	1.54184 (Cu Kα)	1.54184 (Cu Kα)	1.54184 (Cu Kα)	1.54184 (Cu Kα)
2θ range [°]	6.244 to 153.944	5.64 to 151.706	5.068 to 133.198	5.262 to 133.2	9.69 to 144.736
	$-54 \le h \le 54$	$-31 \le h \le 30$	$-11 \le h \le 11$	$-49 \le h \le 50$	$-11 \le h \le 11$
hkl range	$-17 \le k \le 17$	$-24 \le k \le 24$	$-22 \le k \le 22$	$-11 \le k \le 11$	$-11 \le k \le 11$
	$-29 \le l \le 35$	$-41 \le l \le 41$	$-24 \le l \le 24$	$-40 \le l \le 40$	$-19 \le l \le 17$
Ref. collected	535296	175515	95080	113723	11032
Independent ref.	34929	16257	36525	22774	7107
$R_{int.}$ / R_{sigma}	0.1248 / 0.0434	0.0523 / 0.0203	0.0772 / 0.1415	0.2832 / 0.2017	0.0608 / 0.0646
Refl. with $I > 2\sigma(I)$.	25740	15190	24272	11712	5596
Data/restraints/param.	34929/75/1719	16257/210/827	36525/120/1238	22774/1/1201	7107/0/248
GoF on F^2	1.040	1.053	0.953	0.934	1.035
R_1 / ωR_2 [$I>2\sigma(I)$]	0.0557 / 0.1508	0.0359 / 0.0936	0.0684 / 0.1726	0.0791 / 0.1504	0.0556 / 0.1521
R_{int} (all data) /ωR_2	0.0772 / 0.1678	0.0383 / 0.0957	0.0977 / 0.1902	0.1518 / 0.1882	0.0677 / 0.1568
ρ_{fin} (max/min) [e Å^{-3}]	0.59/–0.61	0.67/–0.32	0.46/–0.41	0.30/–0.30	0.63/–0.41
Flack parameter	-	-	0.03(3)	0.49(4)	-
CCDC	2404667	2404668	2404669	2404670	2404671

[a] Disorder of Si9, Si10 and bound methyl groups over two sites in ratio 81:19, disorder of Si11 and bound methyl groups over two sites in ratio 67:33, disorder of C93 and C94 over two sites in ratio 75:25, disorder of a bis(imidazol-1-yl)methane over two sites in ratio 78:22, disorder of one oxygen atom of a THF solvent molecule over two sites in ratio 82:18 and disorder of one carbon atom of a THF in ratio 82:18. Suitable restraints were applied for disordered atoms. Four highly disordered THF could not be refined reasonable, therefore a solvent mask was calculated and 640 electrons were found in a volume of 2504 A^3 in 3 voids per unit cell. This is consistent with the presence of 4[C_4H_8O] per asymmetric unit which account for 640 electrons per unit cell. High R_{int} value was caused by ice rings.
[b] Disorder of one benzene molecule over two sites; ratio: 71 (labelled "A"):29 (labelled "B").
[c] Highly disordered $C_6H_4F_2$ could not refined reliably, therefore a solvent mask was calculated with Platon and 116 electrons were found in a volume of 481 A^3 in 1 void per unit cell. This is consistent with the presence of 2[$C_6H_4F_2$] per asymmetric unit (here also unit cell) which account for 58 electrons per unit cell.
[d] A solvent mask was calculated and 604 electrons were found in a volume of 2380 A^3 in 4 voids per unit cell. This is consistent with the presence of 2.5 [$CHCl_3$] per formula unit which account for 580 electrons per unit cell. Refined as inversion twin.
[e] Twinned crystal, ratio 60:40, component 2 rotated by 179.97° around [0.00 -0.00 1.00] (reciprocal) or [0.22 0.09 0.97] (direct).

Table S16. Crystal data for N-4, N-2, [**9**·2N-4]$_n$, **9**·2Caff and [**9**·Bis[BisPhos]]$_n$.

	N-4[a]	N-2	[**9**·2N-4]$_n$[b]	**9**·2Caff[c]	[**9**·Bis[BisPhos]]$_n$[d]
Empirical formula	$C_8H_{12}N_6$	$C_6H_8N_6$	$C_{126}H_{214}Al_4N_{12}Si_{16}$	$C_{132}H_{216}Al_4N_8O_4Si_{16}$	$C_{138}H_{244}Al_4P_4Si_{18}$
M [g mol^{-1}]	192.225	164.18	2454.44	2536.48	2640.74
T [K]	100.0(1)	100.0(1)	100.0(1)	100.0(1)	100.0(1)
Crystal system	monoclinic	monoclinic	triclinic	tetragonal	triclinic
Space group	$P2_1/c$	$P2_1/n$	$P\bar{1}$	$I4cm$	$P\bar{1}$
a [Å]	7.8206(5)	4.7347(2)	15.1799(7)	26.73631(13)	14.2011(2)
b [Å]	8.9850(4)	7.2592(2)	23.1708(10)	26.73631(13)	23.4448(3)
c [Å]	7.0437(4)	10.7281(3)	23.7413(15)	21.28192(12)	25.4314(3)
α [°]	90	90	77.585(4)	90	97.7820(10)
β [°]	106.387(6)	95.375(3)	73.191(5)	90	97.2980(10)
γ [°]	90	90	77.542(4)	90	90.5900(10)
V [Å^3]	474.84(5)	367.10(2)	7700.8(7)	15212.96(18)	8317.98(19)
Z	2	2	2	4	2
ρ_{calc} [g cm^{-3}]	1.344	1.485	1.059	1.107	1.054
μ [mm^{-1}]	0.743	0.862	1.817	1.867	2.174
F(000) [e]	204.698	172	2660	5488	2872
Size [mm]	0.26×0.15×0.12	0.32×0.12×0.09	0.14×0.07×0.06	0.358×0.116×0.111	0.46×0.24×0.23
λ [Å]	1.54184 (Cu Kα)	1.54184 (Cu Kα)	1.54184 (Cu Kα)	1.54184 (Cu Kα)	1.54184 (Cu Kα)
2θ range [°]	11.8 to 151.68	14.754 to 151.838	6.026 to 152.466	6.612 to 151.584	4.826 to 151.68
hkl range	−9 ≤ *h* ≤ 9 −11 ≤ *k* ≤ 11 −8 ≤ *l* ≤ 8	−5 ≤ *h* ≤ 5 −9 ≤ *k* ≤ 9 −13 ≤ *l* ≤ 13	−18 ≤ *h* ≤ 19 −26 ≤ *k* ≤ 29 −29 ≤ *l* ≤ 29	−33 ≤ h ≤ 33 −33 ≤ k ≤ 33 −26 ≤ l ≤ 26	−17 ≤ *h* ≤ 17 −29 ≤ *k* ≤ 28 −31 ≤ *l* ≤ 31
Ref. collected	6330	3035	107150	223990	159989
Independent ref.	969	749	31157	8172	34109
$R_{int.}$ / R_{sigma}	0.0325 / 0.0141]	0.0177 / 0.0124	0.1690 / 0.1694]	0.0788 / 0.0182	0.0509 / 0.0358
Refl. with $I > 2\sigma(I)$.	922	717	14750	7892	28907
Data/restraints/param.	969/0/105	749/0/55	31157/0/1309	8172/73/539	34109/1370/1861
GoF on F^2	1.909	1.049	0.958	1.042	1.017
R_1 / ωR_2 [$I>2\sigma(I)$]	0.0253 / 0.0675	0.0295 / 0.0704	0.0786 / 0.1662	0.0354 / 0.0960	0.0413 / 0.1087
R_{int} (all data) /ωR_2	0.0260 / 0.0678	0.0311 / 0.0718	0.1627 / 0.2107	0.0369 / 0.0976	0.0502 / 0.1162
ρ_{fin} (max/min) [e Å^{-3}]	0.17/−0.14	0.27/−0.23	0.54/−0.43	0.23/−0.28	0.75/−0.43
Flack parameter	-	-	-	0.007(7)	-
CCDC	2404643	2404644	2404645	2404646	2404647

[a] Disorder of C4 over two sites; ratio: 68 (labelled "A"):32 (labelled "B").
[b] A solvent mask was calculated and 243 electrons were found in a volume of 1495 A^3 in 6 voids per unit cell. This is consistent with the presence of 3 benzene solvent molecules per unit cell which account for 252 electrons.
[c] Disorder of the caffeine and one AlBis group with ratio 1:1.
[d] The disordered benzene solvent molecules were constrained to a hexagonal geometry, restraints (SIMU and RIGU) were applied for the disordered atoms.

Table S17. Crystal data for **9**·2BisPhos, **7**·4^{t}BuNC, **8**·4PMe$_3$, **7**·4THF and **9**·4PMe$_3$.

	9·2BisPhos[a]	**7**·4^{t}BuNC[b]	**8**·4PMe$_3$	**7**·4THF[c]	**9**·4PMe$_3$[d]
Empirical formula	$C_{114}H_{216}Al_4F_6P_4Si_{18}$	$C_{106}H_{210}Al_4N_4Si_{16}$	$C_{52}H_{84}B_4P_4$	$C_{132}H_{236}Al_4O_4Si_{16}$	$C_{92}H_{196}Al_4P_4Si_{16}$
M [g mol^{-1}]	2438.28	2098.13	876.31	2444.55	1983.72
T [K]	100.0(1)	100.0(1)	100.0(1)	100.0(1)	100.0(1)
Crystal system	orthorhombic	orthorhombic	triclinic	orthorhombic	orthorhombic
Space group	*Pbca*	*Pccn*	$P\bar{1}$	*Pnma*	*Pccn*
a [Å]	19.64530(10)	17.7903(10)	12.9123(18)	17.7399(2)	38.7753(7)
b [Å]	34.5792(2)	40.887(2)	14.957(2)	39.8645(6)	18.9790(3)
c [Å]	43.5996(2)	19.4511(13)	15.1509(18)	21.7277(3)	17.5374(5)
α [°]	90	90	76.937(11)	90	90
β [°]	90	90	87.373(11)	90	90
γ [°]	90	90	76.947(13)	90	90
V [Å^3]	29618.0(3)	14148.5(14)	2776.8(7)	15365.7(4)	12906.1(5)
Z	8	4	2	4	4
ρ_{calc} [g cm^{-3}]	1.094	0.985	1.048	1.057	1.021
μ [mm^{-1}]	2.464	1.887	1.470	1.813	2.489
F(000) [e]	10544	4600	952	5344	4336
Size [mm]	0.24×0.13×0.08	0.393×0.014×0.013	0.18×0.12×0.05	0.34×0.068×0.012	0.39×0.14×0.07
λ [Å]	1.54184 (Cu Kα)	1.54184 (Cu Kα)	1.54184 (Cu Kα)	1.54184 (Cu Kα)	1.54184 (Cu Kα)
2θ range [°]	5.112 to 152.228	7.072 to 133.2	5.988 to 133.2	6.432 to 151.816	5.184 to 151.716
hkl range	–24 ≤ *h* ≤ 24 –43 ≤ *k* ≤ 43 –54 ≤ *l* ≤ 54	–21 ≤ *h* ≤ 21 –39 ≤ *k* ≤ 48 –21 ≤ *l* ≤ 23	–14 ≤ *h* ≤ 15 –17 ≤ *k* ≤ 17 –17 ≤ *l* ≤ 18	–22 ≤ *h* ≤ 21 –49 ≤ *k* ≤ 45 –25 ≤ *l* ≤ 27	–48 ≤ *h* ≤ 39 –23 ≤ *k* ≤ 20 –21 ≤ *l* ≤ 21
Ref. collected	592270	51844	17674	53322	55357
Independent ref.	30819	12487	9553	16068	13235
$R_{int.}$ / R_{sigma}	0.0792 / 0.0258	0.1631 / 0.1210	0.1307 / 0.2087	0.0669 / 0.0626	0.0367 / 0.0311
Refl. with $I > 2\sigma(I)$.	26245	5610	3999	12006	9535
Data/restraints/param.	30819/0/1303	12487/303/706	9553/0/561	16068/253/813	13235/478/669
GoF on F^2	1.084	0.981	0.953	1.073	1.026
R_1 / ωR_2 [$I>2\sigma(I)$]	0.0518 / 0.1168	0.0798 / 0.1893	0.0864 / 0.1957	0.0554 / 0.1332	0.0928 / 0.2692
R_{int} (all data) /ωR_2	0.0609 / 0.1215	0.1653 / 0.2495	0.1860 / 0.2629	0.0799 / 0.1470	0.1180 / 0.2966
ρ_{fin} (max/min) [e Å^{-3}]	0.78/–0.46	0.28/–0.25	0.53/–0.35	0.58/–0.27	0.95/–0.47
CCDC	2404648	2404649	2404650	2404651	2404652

[a] A solvent mask was calculated and 456 electrons were found in a volume of 3320 A^3 in 2 voids per unit cell. This is consistent with the presence of 1[$C_6F_2H_4$] per formula unit which account for 464 electrons per unit cell.

[b] Weak diffracting crystal. Disorder of two Bis-groups and both t-Butyl-group over two sites with a ratio of 62:33, .76:24, and 58:42. Displacement parameters were restrained of the disordered parts. Highly disordered benzene was removed, therefore a solvent mask was calculated and 164 electrons were found in a volume of 1576 A^3 in 2 voids per unit cell. This is consistent with the presence of 1[C_6H_6] per asymmetric unit which account for 168 electrons per unit cell.
[c] Disorder of two benzene on a mirror plane. One in a 50:50 ratio, one unsymetrically 56:44. The disordered benzene molecules were treated as regular hexagones.
[d] Disorder of two trimethylsilyl groups (Si2, C15-17; Si4, C22-24) and one trimethylphosphane (P1, C41-43) unit over two sites; ratio 78 (labelled "A"):22 (labelled "B"). Disorder of one trimethylsilyl group (Si3, C19-21) over two sites; ratio 51 (labelled "A"):49 (labelled "B").

Table S18. Crystal data for **9**·4OPEt$_3$, **7**·4OPEt$_3$, **8**·4NMe$_3$ and **10**.

	9·4OPEt$_3$[a]	**7**·4OPEt$_3$[b]	**8**·4NMe$_3$[c]	**10**[d]
Empirical formula	$C_{116}H_{230}Al_4O_4P_4Si_{16}$	$C_{128}H_{252}Al_4O_4P_4Si_{16}$	$C_{58}H_{90}B_4N_4$	$C_{48}H_{96}Al_2N_8O_4Si_8$
M [g mol^{-1}]	2370.23	2536.52	886.57	1128.00
T [K]	100.0(1)	100.0(1)	100.0(1)	100.00(10)
Crystal system	triclinic	monoclinic	monoclinic	monoclinic
Space group	$P\bar{1}$	$P2_1/n$	$P2_1/n$	$I2/a$
a [Å]	16.0702(5)	21.79900(10)	15.1733(5)	21.3970(4)
b [Å]	21.6556(6)	22.28150(10)	18.1744(4)	15.32913(18)
c [Å]	22.9947(7)	33.2789(2)	20.5659(6)	21.2535(4)
α [°]	103.010(2)	90	90	90
β [°]	106.293(3)	99.25	93.872(2)	111.019(2)
γ [°]	92.842(2)	90	90	90
V [Å^3]	7429.3(4)	15953.80(14)	5658.4(3)	6507.3(2)
Z	2	4	4	4
ρ_{calc} [g cm^{-3}]	1.060	1.056	1.041	1.151
μ [mm^{-1}]	2.254	2.126	0.433	2.162
F(000) [e]	2588.0	5552.0	1944.0	2440.0
Size [mm]	0.12×0.08×0.05	0.26×0.2×0.14	0.23×0.18×0.1	0.143×0.135×0.132
λ [Å]	1.54184 (Cu Kα)	1.54184 (Cu Kα)	1.54184 (Cu Kα)	1.54184 (Cu Kα)
2θ range [°]	5.118 to 152.042	4.792 to 152.04	6.496 to 152.404	7.27 to 152.074
hkl range	–18 ≤ *h* ≤ 20 –20 ≤ *k* ≤ 26 –28 ≤ *l* ≤ 28	–27 ≤ *h* ≤ 27 –28 ≤ *k* ≤ 27 –41 ≤ *l* ≤ 40	–16 ≤ *h* ≤ 18 –22 ≤ *k* ≤ 15 –25 ≤ *l* ≤ 25	–26 ≤ *h* ≤ 26 –19 ≤ *k* ≤ 19 –26 ≤ *l* ≤ 26
Ref. collected	56630	451055	41019	58185
Independent ref.	29935	33218	11657	6735
$R_{int.}$ / R_{sigma}	0.0587 / 0.0892	0.0462 / 0.0169	0.0333 / 0.0304	0.0499 / 0.0209
Refl. with $I > 2\sigma(I)$.	19129	30044	8667	6482
Data/restraints/param.	29935/1883/1751	33218/742/1570	11657/542/751	6735/447/345
GoF on F^2	1.016	1.043	1.033	1.057
R_1 / ωR_2 [$I>2\sigma(I)$]	0.0597 / 0.1365	0.0396 / 0.1024	0.0812 / 0.2261	0.0351 / 0.0869
R_{int} (all data) /ωR_2	0.1051 / 0.1596	0.0436 / 0.1059	0.1031 / 0.2481	0.0362 / 0.0876
ρ_{fin} (max/min) [e Å^{-3}]	0.88/–0.84	0.93/–1.14	0.56/–0.42	0.34/–0.46
CCDC	2404653	2404654	2404655	2404656

[a] (Partial) Disorder of four trimethylsilyl groups (Si5, C36-38; Si6, C39-41; C55-57; C59) over two sites; ratio 86 (labelled "A"):14 (labelled "B"). (Partial) Disorder of two trimethylsilyl groups (Si7, C43-45; C46/48; Si9, C52-54), and one ethyl group (C98) over two sites; ratio 75 (labelled "A"):25 (labelled "B"). (Partial) Disorder of one methyl group (C25), two triethylphosphane units (P1, C81-86; P2, C87-92), and one ethyl group (C94) over two sites; ratio 61 (labelled "A"):39 (labelled "B"). Disorder of one benzene molecule over two sites; ratio 52 (labelled C111-116):48 (labelled C117-122).
[b] A solvent mask was calculated and 334 electrons were found in a volume of 1842 A^3 in 3 voids per unit cell. This is consistent with the presence of 2[C_6H_6] per formula unit which account for 336 electrons per unit cell. Disorder of two triethylphosphane units (P1; C81-86 and P3; C93-98) over two sites; ratio 75 (labelled "A"):25 (labelled "B"). Disorder of one trimethylsilyl group (Si17; C59-61) over two sites; ratio 86 (labelled "A"):14 (labelled "B"). Disorder of one trimethylsilyl group (Si18; C62-64) over two sites; ratio 57 (labelled "A"):43 (labelled "B").
[c] Disorder of one diethylborane unit (B2; C25-28), one ethyl group (C37/38) and two trimethylamine units (N2; C44-46 and N4; C50-52) over two sites; ratio 73 (labelled "A"):27 (labelled "B").
[d] Disorder of N2, N3, C17 to C21 over two sites, ratio 59:41. Electron density of a highly disordered benzene on an inversion center was removed, a solvent mask was calculated and 172 electrons were found in a volume of 840 A^3 in 2 voids per unit cell. This is consistent with the presence of 1[C_6H_6] per asymmetric unit which account for 168 electrons per unit cell.

Quantum Chemical Calculations

The fluoride and hydride ion affinities were calculated as described by Greb et al. using the trimethylsilyl compounds Me_3SiY (Y = H, F) as a reference system (see equations 1 to 3).[15,16]

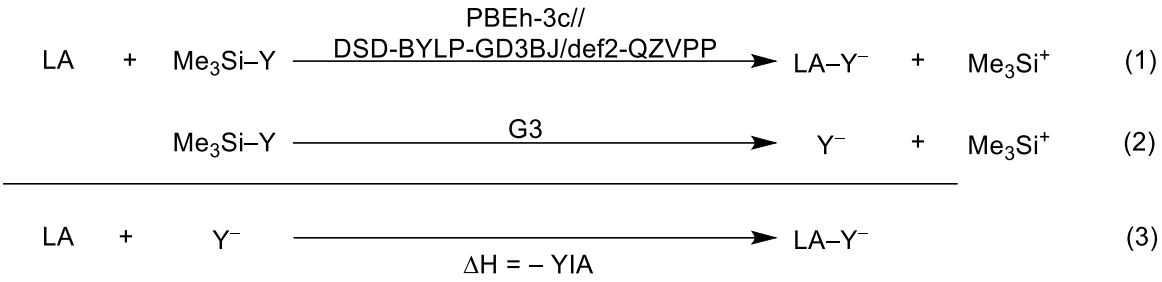

$$LA + Me_3Si{-}Y \xrightarrow{\text{PBEh-3c// DSD-BYLP-GD3BJ/def2-QZVPP}} LA{-}Y^- + Me_3Si^+ \quad (1)$$

$$Me_3Si{-}Y \xrightarrow{\text{G3}} Y^- + Me_3Si^+ \quad (2)$$

$$LA + Y^- \xrightarrow{\Delta H = -\,YIA} LA{-}Y^- \quad (3)$$

The starting geometries were taken from X-ray diffraction solid-state structures of similar compounds or built in Molden (Version 6.9).[17,18] After optimization with the xtb suite,[19–23] the composite method PBEh-3c[24–28] was used in geometry optimization and vibrational analysis with Orca 5.0.2.[29–32] A single point calculation was performed at the DSD-BLYP-GD3BJ/def2-QZVPP[27–29,34–36] level of theory. The resulting electronic energies were used in conjunction with the enthalpy corrections computed with the PBEh-3c functional.

The data used in the calculation of the reaction enthalpies Δ*H* of equation (1) is shown in Table S19. The reaction enthalpy of reaction 2 was taken from [15] and [16] for the FIA and HIA, respectively (Y = F: 952.5 kJ mol^{-1}, Y = H: 924.0 kJ mol^{-1}) The Cartesian coordinates, vibrational frequencies and thermochemistry data of all computed structures can be found below.

Table S19 The total correction to the electronic energy and thermal enthalpy correction calculated at the PBEh-3c/def2-mSVP level of theory as well as the electronic energy at the DSD-BLYP-GD3BJ/def2-QZVPP level of theory and the resulting enthalpy used in the ion affinity calculations for vinyl and alkinyl boranes and alanes and the reference methylsilyl compounds.

molecule	total correction to the electronic energy[a]	thermal enthalpy correction[a]	electronic energy[b]	enthalpy[c]
	E_h	E_h	E_h	E_h
Me_3Si^+	0.11999543	0.00094421	−408.6884403	−408.5675007
Me_3SiF	0.12525114	0.00094421	−508.8756246	−508.7494293
Me_3SiH	0.12992418	0.00094421	−409.5707650	−409.4398966
$BCy_2(CHCHPh)$	0.48189703	0.00094421	−803.7855384	−803.3026971
$BCy_2(CHCHPh)F^-$	0.48306242	0.00094421	−903.7232099	−903.2392032
$BCy_2(CHCHPh)H^-$	0.48794467	0.00094421	−804.4290700	−803.9401811
$BCy_2(CCPh)$	0.45785601	0.00094421	−802.5572795	−802.0984793
$BCy_2(CCPh)F^-$	0.45986470	0.00094421	−902.4979673	−902.0371584
$BCy_2(CCPh)H^-$	0.46485816	0.00094421	−803.2078235	−802.7420211
$AlBis_2(CHCHPh)$	0.66453990	0.00094421	−2264.435370	−2263.769886
$AlBis_2(CHCHPh)F^-$	0.66732343	0.00094421	−2364.422592	−2363.754325
$AlBis_2(CHCHPh)H^-$	0.67030138	0.00094421	−2265.093693	−2264.422448
$AlBis_2(CCPh)$	0.64096482	0.00094421	−2263.216301	−2262.574392
$AlBis_2(CCPh)F^-$	0.64406470	0.00094421	−2363.205892	−2362.560883
$AlBis_2(CCPh)H^-$	0.64716495	0.00094421	−2263.878175	−2263.230066

[a] PBEh-3c/def2-mSVP. [b] DSD-BLYP-GD3BJ/def2-QZVPP. [c] enthalpy = electronic energy + total correction to electronic energy + thermal enthalpy correction.

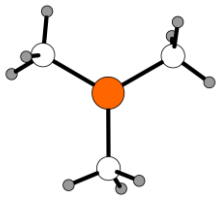

Figure S180 Molecular structure of the trimethylsilyl cation obtained from geometry optimization at the PBEh-3c/def2-mSVP level of theory.

Table S20 Cartesian coordinates, single point energy, total energy correction, thermal enthalpy correction and the lowest six vibrational frequencies of the trimethylsilyl cation obtained from geometry optimization at the PBEh-3c/def2-mSVP level of theory.

13

Si	0.00169298884142	0.00219149920043	0.00225229522111
C	-0.01809664911285	0.08457319752151	1.83243171289599
C	1.58571501597604	-0.21156924637930	-0.89321191715483
C	-1.56614316186418	0.13018428177607	-0.93721459726517
H	0.29602488856262	-0.87709453365897	2.25370691973838
H	0.70893736302007	0.81519693521776	2.19798547476705
H	-0.99742314165342	0.32720252847685	2.24152661487483
H	2.45733250346840	-0.20050529280345	-0.24124567740824
H	1.70566464705683	0.56669723463338	-1.65310653933420
H	1.58108387557640	-1.15838158970722	-1.44415827504514
H	-1.98697300779035	1.13565206331389	-0.82241929704880
H	-1.44649909799954	-0.06342376595598	-2.00193803538716
H	-2.32131622408144	-0.55072331163497	-0.53460967885380

FINAL SINGLE POINT ENERGY −408.351382556903 E_h
Total correction 0.11999543 E_h 75.30 kcal/mol
Thermal Enthalpy correction 0.00094421 E_h 0.59 kcal/mol

6:	49.04 cm^{-1}
7:	57.42 cm^{-1}
8:	83.73 cm^{-1}
9:	214.47 cm^{-1}
10:	215.76 cm^{-1}
11:	226.99 cm^{-1}
12:	619.87 cm^{-1}

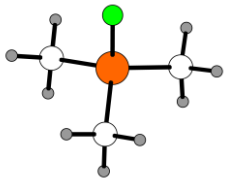

Figure S181 Molecular structure of fluorotrimethylsilane obtained from geometry optimization at the PBEh-3c/def2-mSVP level of theory.

Table S21 Cartesian coordinates, single point energy, total energy correction, thermal enthalpy correction and the lowest six vibrational frequencies of fluorotrimethylsilane obtained from geometry optimization at the PBEh-3c/def2-mSVP level of theory.

14

C	0.03662105665423	-0.03523801688346	-0.17538148787472
Si	0.03064982884630	0.03158053836643	1.69511706058501
C	1.77363938100141	0.08880335686097	2.37465813929369
H	0.47775840306540	0.86863858093747	-0.59968968270960
H	-0.97256320474998	-0.12307350385386	-0.57979626182936
H	2.29119735874715	0.99032149726981	2.04074674718589
H	2.36751871852157	-0.76427364565116	2.04395740209272
H	0.61361974111215	-0.88262629491271	-0.54792724838659
H	1.78672691280764	0.09495559626539	3.46533546986283
C	-0.98818756536749	1.47306901601342	2.31783106839705
H	-0.99569777373151	1.52512071750260	3.40722799841028

H	-0.58998942442273	2.42113636060402	1.95140909834630
H	-2.02517711217487	1.40920989589586	1.98550528901627
F	-0.67036232030927	-1.33770609841479	2.23299140761020

FINAL SINGLE POINT ENERGY −508.373308349128 E_h
Total correction 0.12525114 E_h 78.60 kcal/mol
Thermal Enthalpy correction 0.00094421 E_h 0.59 kcal/mol

6: 137.42 cm^{-1}
7: 156.86 cm^{-1}
8: 157.25 cm^{-1}
9: 189.16 cm^{-1}
10: 191.69 cm^{-1}
11: 234.14 cm^{-1}
12: 282.44 cm^{-1}

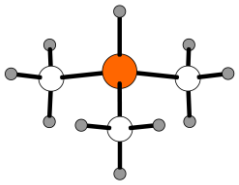

Figure S182 Molecular structure of trimethylsilane obtained from geometry optimization at the PBEh-3c/def2-mSVP level of theory.

Table S22 Cartesian coordinates, single point energy, total energy correction, thermal enthalpy correction and the lowest six vibrational frequencies of trimethylsilane obtained from geometry optimization at the PBEh-3c/def2-mSVP level of theory.

14

Si	-0.23349589900508	0.40350795902128	-0.16419544984231
C	-0.24586283009867	0.42585469204371	1.72013089415167
C	1.53890620446238	0.42503724048086	-0.80447747769337
C	-1.13775575477283	-1.12077223964220	-0.80491123079958
H	-0.93578564348628	1.62041272935378	-0.66165030359415
H	-1.26325756011492	0.43085777077588	2.11290839044487
H	0.25932642375511	-0.44993746499040	2.13060554010608
H	0.26057599800422	1.30888213814796	2.11182318882628
H	1.57046618872549	0.42867816967166	-1.89481783792848
H	2.07792685287747	1.30826622910888	-0.45947076179175
H	2.09467451374064	-0.45042982973513	-0.46452255737185
H	-1.15774960315809	-1.14341407766586	-1.89522220908163
H	-0.65626086370999	-2.04007059247705	-0.46763721738412
H	-2.17170802721945	-1.14687252409336	-0.45856286804167

FINAL SINGLE POINT ENERGY −409.240407934120 E_h
Total correction 0.12992418 E_h 81.53 kcal/mol
Thermal Enthalpy correction 0.00094421 E_h 0.59 kcal/mol

6: 149.30 cm^{-1}
7: 162.98 cm^{-1}
8: 163.66 cm^{-1}
9: 201.51 cm^{-1}
10: 201.97 cm^{-1}
11: 239.54 cm^{-1}
12: 630.35 cm^{-1}

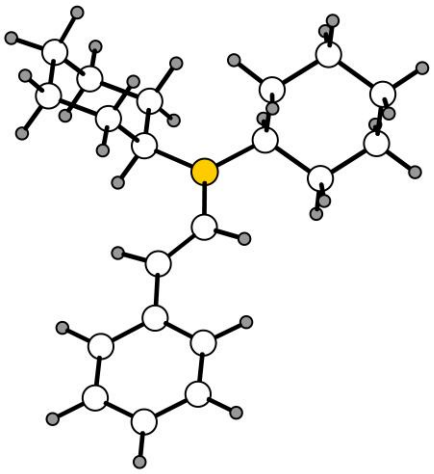

Figure S183 Molecular structure of (*E*)-dicyclohexyl(styryl)borane obtained from geometry optimization at the PBEh-3c/def2-mSVP level of theory.

Table S23 Cartesian coordinates, single point energy, total energy correction, thermal enthalpy correction and the lowest six vibrational frequencies of (*E*)-dicyclohexyl(styryl)borane obtained from geometry optimization at the PBEh-3c/def2-mSVP level of theory.

50
Coordinates from ORCA-job maxi_bcy2_chchph_pbeh-3c_def2-msvp

C	-2.74851290833650	-3.87846267821375	0.34889414371720
C	-2.91081548611289	-3.22102721885344	-1.01640623218517
C	-2.60003637409908	-1.72916635458850	-0.95372670057732
C	-1.19935238598178	-1.45177657825332	-0.39986525319375
C	-1.04336144892104	-2.12634578926216	0.97901837383451
C	-1.35992842339057	-3.61832545373343	0.92228259217513
B	-0.78576970751991	0.08166758749174	-0.32443338348260
C	-1.87742987850939	1.22733150430588	-0.37855540459838
C	-2.46086080898379	1.37272400727871	1.04448939887890
C	-3.56353557480947	2.42704905369561	1.09861860748419
C	-3.08624512988142	3.77201598085019	0.56338319344764
C	-2.51581334020827	3.63481423396152	-0.84373788709512
C	-1.40249605642736	2.59348179418759	-0.88338093877523
C	0.70393273340979	0.46982894828661	-0.10270005477376
C	1.73585467899569	-0.37467401434012	-0.26690184580740
C	3.16250682167847	-0.08217040047387	-0.13383962932416
C	4.07623688811275	-1.13446100234245	-0.21286017950055
C	5.43785912161544	-0.91408992266961	-0.08371214214079
C	5.91385709784473	0.37148592103005	0.12117998069950
C	5.01809418987244	1.43122555747198	0.19609766571992
C	3.65968598472828	1.20814160566811	0.06955598422450
H	2.97969975944631	2.04845950682720	0.11924127263271
H	1.52118631134405	-1.40651853906092	-0.53535954136953
H	6.12699246735624	-1.74585448990856	-0.14576850554774
H	0.94245659775608	1.49685827491878	0.16531819297421
H	-2.70896452623843	0.91080465160389	-1.02259743465510
H	-0.48334835482940	-1.95551461285342	-1.06903861666324
H	-1.66188658316220	1.65051478973305	1.74268354256995
H	-2.85416299632631	0.41565278309469	1.39856247889855
H	-1.00710530706975	2.50433790232889	-1.89893806958630
H	-0.57085199756200	2.95244871868545	-0.26710375432422
H	-2.71203795574327	-1.28789761041445	-1.94802657444607
H	-3.34927581967932	-1.23968865766832	-0.32033580449220
H	-1.71638296087005	-1.64626925695258	1.69943928056877
H	-0.03373619839557	-1.97273044937125	1.36580281178998
H	-3.92673536015178	2.53460490133250	2.12412065469194
H	-4.41545755347062	2.08219409889354	0.50279116929763
H	-2.14514031508593	4.60028694631685	-1.19739847726727
H	-3.31480668982489	3.33930020084777	-1.53277777143405
H	-2.23571967228889	-3.70163388969641	-1.73357581070164
H	-3.92371256020560	-3.38070445634019	-1.39507488965223
H	-0.61144343232819	-4.11821661059283	0.29721483956367

H	-1.27209445067413	-4.05678627315967	1.91968926262674
H	-3.90506031032447	4.49543060314232	0.57640003361455
H	-2.31152059079351	4.17042328336454	1.22788545430389
H	-3.50235396920147	-3.47563719459049	1.03405995877658
H	-2.93701496089505	-4.95263099539685	0.28116362431051
H	3.70996172128880	-2.14143212276308	-0.37443416260742
H	6.97652264639400	0.55016244633013	0.21819286247053
H	5.38406801795925	2.43788849625209	0.34945154932953

FINAL SINGLE POINT ENERGY −802.697377786147 E_h
Total correction 0.48189703 E_h 302.39 kcal/mol
Thermal Enthalpy correction 0.00094421 E_h 0.59 kcal/mol

6: 17.52 cm^{-1}
7: 20.48 cm^{-1}
8: 38.27 cm^{-1}
9: 51.73 cm^{-1}
10: 53.67 cm^{-1}
11: 70.83 cm^{-1}
12: 89.32 cm^{-1}

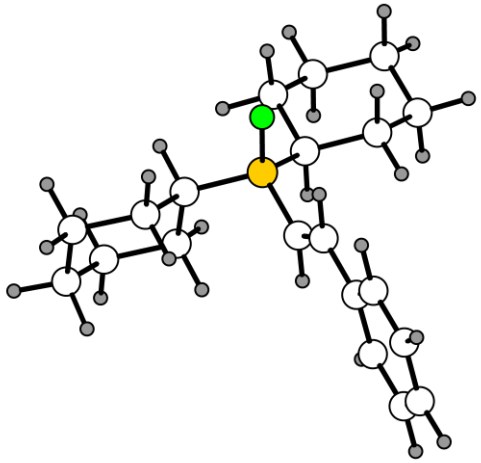

Figure S184 Molecular structure of (*E*)-dicyclohexylfluoro(styryl)borate obtained from geometry optimization at the PBEh-3c/def2-mSVP level of theory.

Table S24 Cartesian coordinates, single point energy, total energy correction, thermal enthalpy correction and the lowest six vibrational frequencies of (*E*)-dicyclohexylfluoro(styryl)borate obtained from geometry optimization at the PBEh-3c/def2-mSVP level of theory.

51
Coordinates from ORCA-job maxi_bcy2_chchph_f-_pbeh-3c_def2-msvp

C	3.28859794689662	1.13841960402064	-0.21950195968109
C	1.81190266339190	1.16650655449912	0.18392132053289
C	1.25246752946992	2.57501292178864	-0.03854282920905
C	2.07119849230836	3.66330397376622	0.65400100903023
C	3.53465635901835	3.61116840956325	0.22970370291300
C	4.12214030531688	2.22287840700940	0.46337313717361
B	0.90814078248766	0.00769714622865	-0.57832571237915
C	1.52127608231176	-1.51320541290374	-0.35004797152439
C	1.77398997315738	-1.87989096175798	1.11405072463531
C	2.35692129906262	-3.28292964143662	1.28502026150538
C	1.47685166584202	-4.33777306404732	0.62214063556160
C	1.22921456394909	-3.99995567748049	-0.84436975113685
C	0.65090254349531	-2.59395472682008	-0.99775978505021
C	-0.59956147947299	0.07331165384676	0.00949928936553
C	-1.71747040977123	0.31966853857812	-0.68823699060218
C	-3.09103875301304	0.38480661980229	-0.18868670554785
C	-4.14977153672821	0.51385489462097	-1.09557373448155
C	-5.46945152787685	0.57632325112685	-0.67756253103553
C	-5.78060569312334	0.51450229263770	0.67275912377246
C	-4.74462948808243	0.39180027678573	1.59166243417327
C	-3.42867011819735	0.33083499930806	1.17035633444868

H	-3.92166845968183	0.56197667442789	-2.15425817017007
H	-1.61893648225772	0.48280541028249	-1.75883259118607
H	-4.96647352257235	0.34770309405822	2.65139602327247
H	-0.72040696602200	-0.10327959033715	1.08315976191859
H	2.49919697670356	-1.54840418578440	-0.86000635487202
H	1.77015830076041	0.98182648097360	1.27141166931057
H	0.83379111551193	-1.82270830797391	1.67857760081683
H	2.44601893765197	-1.15384777898977	1.58153637745134
H	0.50514653620995	-2.36642037693998	-2.05648901648545
H	-0.35000625216629	-2.57028959264381	-0.54941145045687
H	0.21416091068224	2.62194342824239	0.30139352168991
H	1.22021127316252	2.78542020008560	-1.11390873029508
H	3.36561416372577	1.26128975839722	-1.30644040103370
H	3.72561884418369	0.15972459313010	0.00159404173153
H	2.49582019909136	-3.52071639771082	2.34583549063054
H	3.35417035090971	-3.31274674673149	0.83004395394322
H	0.56463743627482	-4.74641734352125	-1.29377024564168
H	2.17762493217458	-4.06287434170330	-1.39201677768176
H	2.00921269122116	3.52589442784486	1.74068643652620
H	1.65529344794933	4.65566173939907	0.44628488060305
H	4.15216644671129	2.02589386686252	1.54217649168502
H	5.16135392081538	2.19089855011420	0.11655494549100
H	1.92531151760309	-5.33206666974725	0.72239878537467
H	0.51398103077932	-4.37866005382100	1.14531787345462
H	3.60548478398438	3.85425388384881	-0.83723961542774
H	4.11979130991223	4.37142360567263	0.75858486951741
H	-2.64024161185736	0.24558561727143	1.90728764521232
H	-6.80959937830698	0.56433582520978	1.00573392062735
H	-6.25993984286761	0.67440355580418	-1.41226379057934
F	0.88241525057104	0.28070418594295	-2.00056424799097

FINAL SINGLE POINT ENERGY	−902.467427783343 E_h	
Total correction	0.48306242 E_h	303.13 kcal/mol
Thermal Enthalpy correction	0.00094421 E_h	0.59 kcal/mol

6:	17.17 cm^{-1}
7:	26.93 cm^{-1}
8:	43.53 cm^{-1}
9:	54.14 cm^{-1}
10:	55.16 cm^{-1}
11:	76.58 cm^{-1}
12:	87.31 cm^{-1}

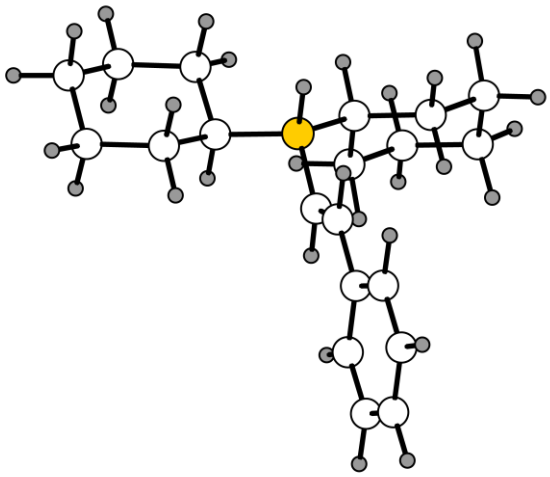

Figure S185 Molecular structure of (*E*)-dicyclohexyl(styryl)hydroborate obtained from geometry optimization at the PBEh-3c/def2-mSVP level of theory.

Table S25 Cartesian coordinates, single point energy, total energy correction, thermal enthalpy correction and the lowest six vibrational frequencies of (*E*)-dicyclohexyl(styryl)hydroborate obtained from geometry optimization at the PBEh-3c/def2-mSVP level of theory.

51
Coordinates from ORCA-job maxi_bcy2_chchph_h-_pbeh-3c_def2-msvp

C	-3.40077791273418	-0.44945761290594	1.07735747399980
C	-3.03900559116614	-0.48299788968786	-0.27642369320265
C	-4.08000371474117	-0.62898753207425	-1.20173972574664
C	-5.40448333282429	-0.72828184605908	-0.80672130809211
C	-5.73953168313793	-0.68703886483175	0.53867765525482
C	-4.72176186048619	-0.54725160549720	1.47549577091520
C	-1.66050067156373	-0.37602531583350	-0.75307074848136
C	-0.54938152237996	-0.13672635582068	-0.03850301033986
B	0.95093595141791	-0.00951638786239	-0.61826950415793
C	1.91052564007642	-1.15053025985270	0.09559017522318
C	1.41507705200220	-2.56542342666401	-0.21352759841138
C	2.29853363816999	-3.66659360453240	0.37184783359210
C	3.74750618601489	-3.51283405070146	-0.07911837654465
C	4.27473093753453	-2.12102705694392	0.25421425052886
C	3.37550551505821	-1.03006098763960	-0.32776463337057
C	1.51526326675678	1.53005944981757	-0.39511522788702
C	1.74036118789114	1.92657669741583	1.06581008421612
C	2.27968392773996	3.34907809607494	1.22078173323660
C	1.37243349835642	4.36512478141713	0.53323386611918
C	1.14886949480831	3.99988115554888	-0.93108275507662
C	0.62161917183727	2.57231113197184	-1.06943300572869
H	-2.62706231558763	-0.34796615461816	1.82762311509757
H	-1.54435008424241	-0.49629447361764	-1.82853859416424
H	-6.17989687285699	-0.83850246276511	-1.55573849751471
H	-0.69022410122314	-0.01053343405490	1.04195669121231
H	1.87868529248358	-1.03407367147170	1.19416989433133
H	2.49649645724661	1.59211549799389	-0.89508516885380
H	1.36316451574008	-2.68635173778747	-1.30308421748590
H	0.38767617841455	-2.68738198786736	0.14103334144117
H	3.77359970548112	-0.04990662012280	-0.04857284227032
H	3.42912894212952	-1.07166992418743	-1.42374330545297
H	2.42712936830865	1.22408267630803	1.54872376904297
H	0.79569022805221	1.84885892191093	1.62039264125850
H	-0.38650356613870	2.52012744617988	-0.64022037498222
H	0.50200026130813	2.31613889282022	-2.12626457009834
H	1.92103207391795	-4.65811925797309	0.09693410456924
H	2.25945932020060	-3.61579758944016	1.46699970726863
H	5.30376222139766	-2.01152296056590	-0.10745721638296
H	4.31878425799809	-2.00806322730505	1.34443467036724
H	3.27949013942633	3.40294874889550	0.77316144401402
H	2.40224846391824	3.60997216466812	2.27837823623282
H	2.09988988316288	4.08819004423865	-1.47079894750851
H	0.46368054697348	4.71818950995629	-1.39556131302410
H	4.37993858364840	-4.28507380299812	0.37244722910322
H	3.80264833412196	-3.66347872188305	-1.16390392164414
H	0.40421680396376	4.38268024750910	1.04779719191851
H	1.78765874756996	5.37496981867442	0.62228182610961
H	-3.83343072133888	-0.66068020509277	-2.25700462357475
H	-6.77238517489902	-0.76461544348121	0.85393763926740
H	-4.96227550500863	-0.51689074897979	2.53168884218542
H	0.92657304950118	-0.23250817498276	-1.83771163400934

FINAL SINGLE POINT ENERGY −803.338075390389 E_h
Total correction 0.48794467 E_h 306.19 kcal/mol
Thermal Enthalpy correction 0.00094421 E_h 0.59 kcal/mol

6: 16.88 cm^{-1}
7: 25.92 cm^{-1}
8: 40.19 cm^{-1}
9: 52.01 cm^{-1}
10: 54.03 cm^{-1}
11: 73.46 cm^{-1}
12: 81.06 cm^{-1}

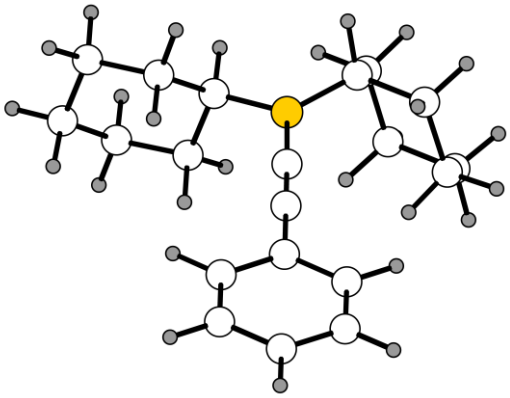

Figure S186 Molecular structure of dicyclohexyl(phenylethynyl)borane obtained from geometry optimization at the PBEh-3c/def2-mSVP level of theory.

Table S26 Cartesian coordinates, single point energy, total energy correction, thermal enthalpy correction and the lowest six vibrational frequencies of dicyclohexyl(phenylethynyl)borane obtained from geometry optimization at the PBEh-3c/def2-mSVP level of theory.

48
Coordinates from ORCA-job maxi_bcy2_ccph_pbeh-3c_def2-msvp

B	1.18598588606624	-0.30397895137179	0.58621581900926
C	2.10598876033894	0.96610709660721	0.38431567263701
C	1.59235159247231	2.18372965905071	1.16739689380783
C	2.20100535756457	1.31387774393120	-1.11373971926008
C	3.05370380882855	2.55647490298413	-1.35481265613155
C	2.54141376292586	3.75027300176108	-0.55782356518477
C	2.44982918148330	3.42125274571659	0.92772257231658
H	3.12417849810234	0.74891792773739	0.73551351005555
H	2.61311816393175	0.47237562157521	-1.67796945760776
H	1.19380100370340	1.48212941410921	-1.51161928432947
H	3.07292333908147	2.79321872774619	-2.42173771664930
H	2.04208874512506	4.27212352689624	1.47962260574122
H	3.18603987556352	4.61787773990198	-0.71802855550525
H	1.54836459585787	4.02957296425285	-0.92650786769655
H	3.45625430404195	3.25055821502036	1.32572506639551
H	1.55790516760791	1.95856407772156	2.23723109855343
H	0.55987520222466	2.39409921616818	0.86962191667201
C	1.77477991087888	-1.69859024215350	1.03949701378681
C	3.02981868418906	-2.12346536638457	0.26242143336588
C	2.67552836285132	-2.63181003593334	-1.13161163660717
C	1.67626108467478	-3.78073950955582	-1.06448837766072
C	0.42862656569559	-3.38594523913483	-0.28223319079245
C	0.78103576197768	-2.86132686825421	1.10621830074257
H	2.09820740729178	-1.46517403474729	2.06971177857545
H	3.53822231077142	-2.92614374896339	0.80894236526079
H	3.74848446207086	-1.30310156114633	0.19403001864789
H	2.24942786431465	-1.81499390958513	-1.72614098892114
H	3.58056738627259	-2.94850768671404	-1.65620279729200
H	2.15332071983146	-4.64005735937530	-0.57987754077161
H	1.40566278183802	-4.10716827810505	-2.07157547644426
H	-0.11845344700379	-2.61476014881571	-0.83470773056773
H	-0.24883048667177	-4.23961866864174	-0.19849841714622
H	-0.12752006304792	-2.55533223957060	1.62993606351404
H	1.21452297397017	-3.67918982313718	1.69412767707664
C	-0.31162757369343	-0.11303198919347	0.41706291137607
C	-1.50587214818994	0.05740005014584	0.27998546578191
H	4.08919116443451	2.34538378660899	-1.06654507789669
C	-2.90215646956850	0.26314104520596	0.12416087898875
C	-3.41487184677341	1.55817469129837	0.00435166308881
C	-4.77614538095330	1.75933549119525	-0.13845945014074
C	-5.64123275955742	0.67393361359845	-0.16758300619674
C	-5.14095341666755	-0.61608912279003	-0.05248969829208
C	-3.78084112650148	-0.82349560146482	0.09473173635142
H	-2.73467746221822	2.39889696007056	0.02739696176790
H	-5.16471185595848	2.76496952868955	-0.22736997443974

H	-6.70549258462092	0.83341892499664	-0.27939704569085
H	-5.81413367838210	-1.46253661005310	-0.07552587472229
H	-3.38405084457425	-1.82550538679846	0.18801723763383

FINAL SINGLE POINT ENERGY −801.460164451553 E_h
Total correction 0.45785601 E_h 287.31 kcal/mol
Thermal Enthalpy correction 0.00094421 E_h 0.59 kcal/mol

6: 19.30 cm^{-1}
7: 19.79 cm^{-1}
8: 24.14 cm^{-1}
9: 30.14 cm^{-1}
10: 49.01 cm^{-1}
11: 73.62 cm^{-1}
12: 100.78 cm^{-1}

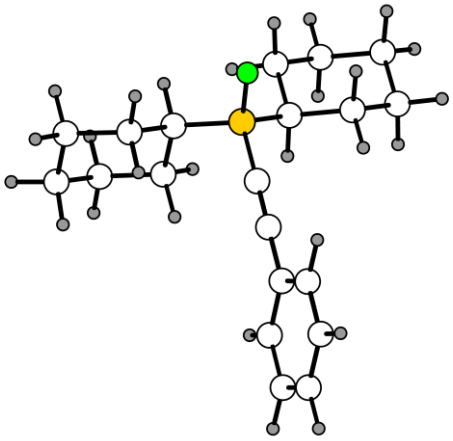

Figure S187 Molecular structure of dicyclohexylfluoro(phenylethynyl)borate obtained from geometry optimization at the PBEh-3c/def2-mSVP level of theory.

Table S27 Cartesian coordinates, single point energy, total energy correction, thermal enthalpy correction and the lowest six vibrational frequencies of dicyclohexylfluoro(phenylethynyl)borate obtained from geometry optimization at the PBEh-3c/def2-mSVP level of theory.

49
Coordinates from ORCA-job maxi_bcy2_ccph_f-_pbeh-3c_def2-msvp

C	3.93708336151376	1.02796972508904	1.02553537898707
C	3.07740105082837	0.49950032500153	0.05293232684197
C	3.62922645950918	0.16094216155061	-1.19023024063840
C	4.97707824365656	0.34518976167341	-1.44719642440478
C	5.81599784688542	0.87072867152768	-0.47318795972914
C	5.28449655191474	1.20984731622707	0.76417511994996
C	1.69668733057879	0.31413363756328	0.31552726833295
C	0.51162817899149	0.15891943516137	0.54261401961511
B	-1.06473616318578	-0.05717112554245	0.77691118153625
C	-1.45739107496681	-1.59262681216682	0.32886771905064
C	-0.71408872579776	-2.65677252684135	1.14011237725651
C	-1.11649112962710	-4.07999335700944	0.75698282872792
C	-0.91792204865286	-4.32834315772453	-0.73464838637639
C	-1.65910135239673	-3.28600613420858	-1.56585381492065
C	-1.26441591812388	-1.86538730305483	-1.16376805303767
C	-1.86148104252435	1.08922397472491	-0.10324983164485
C	-1.51937023108257	2.50923707257095	0.35568763029848
C	-2.24511856383839	3.58802049266836	-0.44588695090999
C	-3.75520303326386	3.37812405202991	-0.41025462532906
C	-4.12107116583168	1.97686525865092	-0.88795218163353
C	-3.38098683623649	0.90139094897462	-0.09307336533948
H	-1.52994339527514	1.00634801217484	-1.15128908505580
H	-3.64430183209422	-0.08306842466113	-0.49168387545727
H	-3.73744633097393	0.91257169043886	0.94367186374187
H	-5.20520043182706	1.82851648292097	-0.82775558130988
H	-1.99526782016723	4.58685623480504	-0.07111748374019
H	-4.26753816359753	4.13650153140022	-1.01213245263306
H	-4.10939341091882	3.50913629236058	0.61921046227744

H	-1.90515493136674	3.55456532290665	-1.48805154126519
H	-0.43878463045530	2.66343282073150	0.29454136365286
H	-1.78283670793896	2.62019743457198	1.41398785346825
H	-2.53114884420432	-1.72262208793530	0.54509974368281
H	-0.88546336305558	-2.49822059132155	2.20732400306458
H	0.36575578233897	-2.53852358446415	0.98592077119650
H	-0.54950461316714	-4.81581931448970	1.33809931775809
H	-2.17291206680906	-4.23567702872362	1.00807854726094
H	-1.24116834239187	-5.33910667339561	-1.00612779395331
H	0.15249143243972	-4.27310063293234	-0.96478720315132
H	-1.47310533133193	-3.45357074413931	-2.63262045551194
H	-2.73839651317331	-3.41326683457718	-1.41741241298892
H	-0.21277037896710	-1.69725473320987	-1.42873796064619
H	-1.84060415620605	-1.15086828447250	-1.75909681118788
H	-3.85485069570358	1.88296114367199	-1.94803884480594
H	2.97791564355500	-0.24991996029579	-1.95033408670733
H	5.37704107670647	0.07505567644301	-2.41701690098201
H	6.86968654341086	1.01470352972217	-0.67568987033377
H	5.92625632327226	1.62111669135038	1.53387535043208
H	3.52539581030669	1.29376876305187	1.99006860194719
F	-1.35153616755515	0.11538174030230	2.17857976951445

FINAL SINGLE POINT ENERGY −901.234891030346 E_h
Total correction 0.45986470 E_h 288.57 kcal/mol
Thermal Enthalpy correction 0.00094421 E_h 0.59 kcal/mol

6: 7.66 cm^{-1}
7: 24.00 cm^{-1}
8: 30.86 cm^{-1}
9: 50.80 cm^{-1}
10: 56.45 cm^{-1}
11: 75.39 cm^{-1}
12: 93.27 cm^{-1}

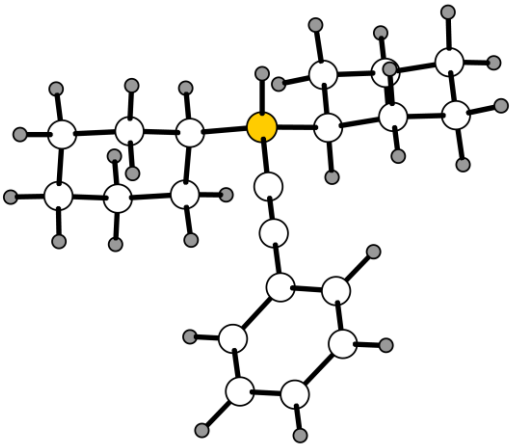

Figure S188 Molecular structure of dicyclohexyl(phenylethynyl)hydroborate obtained from geometry optimization at the PBEh-3c/def2-mSVP level of theory.

Table S28 Cartesian coordinates, single point energy, total energy correction, thermal enthalpy correction and the lowest six vibrational frequencies of dicyclohexyl(phenylethynyl)hydroborate obtained from geometry optimization at the PBEh-3c/def2-mSVP level of theory.

49
Coordinates from ORCA-job maxi_bcy2_ccph_h-_pbeh-3c_def2-msvp

C	3.64332189620539	1.72030649560068	0.53671731333250
C	3.02069601030693	0.52630257928801	0.14359127029794
C	3.81434986489832	-0.43888332900367	-0.49346366332659
C	5.16215915769800	-0.22004150118416	-0.72220454021797
C	5.76252227937856	0.96816283043046	-0.32635667465810
C	4.99083256327646	1.93580313298091	0.30395173211143
C	1.64187928282467	0.30540536836475	0.38152615636761
C	0.45460286999438	0.12834001097493	0.59258825740309
B	-1.09721203661854	-0.09942529956347	0.83443591174614
C	-1.51998012241002	-1.62075857757741	0.36835192187976
C	-0.74190252939022	-2.70176884742873	1.11986790563336
C	-1.15555875717919	-4.11924836895536	0.72601854614319
C	-1.03086063678324	-4.33314381243914	-0.77927539990161
C	-1.81384995701642	-3.27500055639985	-1.55071857292875
C	-1.39897215242716	-1.86318518051771	-1.13680180578594
C	-1.93865305182366	1.09021314252770	0.05886974730998
C	-1.58337086385035	2.47716558924806	0.59770002236008
C	-2.36512706085431	3.60728482771335	-0.06953838793597
C	-3.86881815206026	3.37510463092103	0.03670039935130
C	-4.25162026925224	2.00648903311013	-0.51772803353839
C	-3.45170694132897	0.88596313518053	0.14666049995244
H	-1.66987024455657	1.08491898879601	-1.01116360555323
H	-3.73273897126956	-0.07091445344245	-0.30329842325615
H	-3.74050866054487	0.81481959099946	1.20368921131804
H	-5.32831301969415	1.84034587382775	-0.39785856876934
H	-2.10302061852221	4.57623112826093	0.37032233046671
H	-4.42165251627325	4.16779378188873	-0.47911042842666
H	-4.16511409106268	3.42935506420083	1.09133285559408
H	-2.08633758466033	3.66481187688458	-1.12861368146062
H	-0.50949323907019	2.64858004977432	0.48607134607972
H	-1.77971040063415	2.49799496528971	1.67762754308448
H	-2.58111142938176	-1.75760035051653	0.63472649813517
H	-0.86811545155575	-2.55931445078950	2.19715939242608
H	0.33028222397433	-2.57518693592333	0.92531859043617
H	-0.55801888890592	-4.86562623658429	1.26159014487350
H	-2.19789042397753	-4.28603570837821	1.02464094475635
H	-1.36426142589888	-5.33923265804474	-1.05611269651573
H	0.02667946914295	-4.26904832919985	-1.06162797829190
H	-1.68192085280043	-3.42163564573005	-2.62874514782671
H	-2.88417957675442	-3.40732572393024	-1.35010468562954
H	-0.36045710164725	-1.68842791071753	-1.44614489700361
H	-2.00027316460031	-1.13320979015537	-1.68773196472406
H	-4.05710285766911	1.99267578803826	-1.59705526065153
H	3.34937700841325	-1.36501596110561	-0.80482530560247
H	5.75019539539613	-0.98436093288096	-1.21596590959999
H	6.81635087901870	1.13799564756532	-0.50733752092520
H	5.44385233293389	2.86835968682257	0.61851879441724
H	3.04545019840551	2.47604805488519	1.02884219869945
H	-1.30532221879351	0.00890759889395	2.04697832455426

FINAL SINGLE POINT ENERGY −802.109036368859 E_h
Total correction 0.46485816 E_h 291.70 kcal/mol
Thermal Enthalpy correction 0.00094421 E_h 0.59 kcal/mol

6: 2.77 cm^{-1}
7: 21.89 cm^{-1}
8: 32.26 cm^{-1}
9: 50.18 cm^{-1}
10: 54.01 cm^{-1}
11: 73.41 cm^{-1}
12: 97.76 cm^{-1}

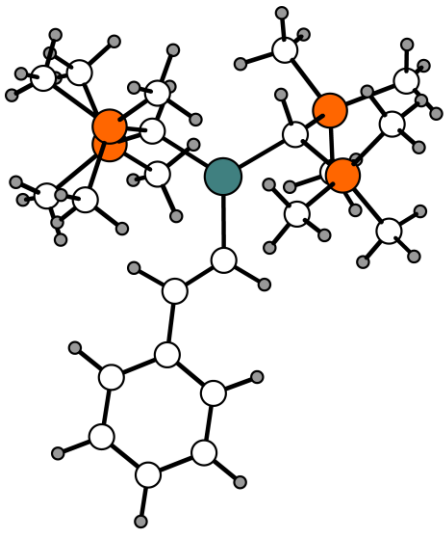

Figure S189 Molecular structure of (*E*)-bis(bis(trimethylsilyl)methyl)(styryl)aluminum obtained from geometry optimization at the PBEh-3c/def2-mSVP level of theory.

Table S29 Cartesian coordinates, single point energy, total energy correction, thermal enthalpy correction and the lowest six vibrational frequencies of (*E*)-bis(bis(trimethylsilyl)methyl)(styryl)aluminum obtained from geometry optimization at the PBEh-3c/def2-mSVP level of theory.

72
Coordinates from ORCA-job maxi_albis2_chchph_pbeh-3c_def2-msvp

C	-5.77324910458079	3.12409017749273	0.09786523443906
C	-4.56039557824865	3.73184282530980	0.39915319604058
C	-3.38804557969857	2.99856804183567	0.38411696326067
C	-3.39995437671626	1.63897737829423	0.06606367575371
C	-4.62595661584059	1.04304363708792	-0.23174714948188
C	-5.80244934017575	1.77484191908309	-0.21806265289719
C	-2.18829217612527	0.81471732506441	0.02369929350839
C	-0.91178579177639	1.18715204439453	0.20789164581235
Al	0.55239869001651	-0.07501308511073	-0.00810054753490
C	2.39408576264195	0.56928711513848	-0.15079083846990
Si	2.51219863921110	2.16422067844760	-1.13610345032782
C	4.22872893058047	2.35445477931631	-1.90154140087779
C	0.24960671833122	-2.00441908425702	-0.10930541316813
Si	-0.76557776170794	-2.74685165170512	1.29051365552904
C	-0.03333772130589	-4.42818284222871	1.74578720771870
Si	-0.16712274278906	-2.58025559296834	-1.84644688977832
C	-1.74509661259159	-1.79228474820387	-2.51891733337245
C	1.25456829165151	-2.09155053245600	-2.99642452657818
C	-0.33958143026990	-4.46020521180082	-1.94720093928526
C	-2.58994905703600	-2.99706355594189	0.86206316688561
C	-0.68707430732188	-1.66440196594381	2.84025261073265
Si	3.18659677168781	0.58093826966061	1.55178841106743
C	4.85683124724465	1.46467502539851	1.60326308983982
C	3.48395560908824	-1.20696673123107	2.09385362379342
C	2.04032038769714	1.39949343674831	2.81450256050115
C	2.15361553474658	3.67973365988689	-0.06614516364480
C	1.27035562278937	2.15522788484686	-2.56512911280859
H	1.26904457134485	-2.39518957817432	0.05034324866608
H	1.08401144005951	-2.44827232930606	-4.01390523566394
H	2.20298273218120	-2.51502042314261	-2.65980513273474
H	1.38957786796113	-1.00908912020209	-3.05728379923696
H	0.56430438435303	-4.96010939347757	-1.59423625750701
H	-0.50507449852066	-4.78063888991674	-2.97772807873829
H	-1.17281239400698	-4.83987301919154	-1.35403846611879
H	-1.67346342985091	-0.70439346972003	-2.57923895507254
H	-2.62137610512764	-2.02862672745361	-1.91347018423818
H	-1.94479380603148	-2.15578200463944	-3.52882847625120
H	-3.11178047806781	-2.05907339967269	0.66988228866425
H	-3.10042162502377	-3.47567851087042	1.70014584796295
H	-2.73227731305739	-3.63946636962615	-0.00815310933259

H	-1.24348072661525	-2.11836981974795	3.66281481452912
H	-1.11186091865932	-0.67142739535391	2.67674425503364
H	0.33979632492898	-1.53268156033599	3.19129571377094
H	-0.07090434848229	-5.12878835252011	0.91070707554233
H	-0.56793225177422	-4.88347085052849	2.58151233042412
H	1.01305764905367	-4.33437285312709	2.04417626747403
H	-0.72909026415700	2.24047278679578	0.42061599884081
H	2.92409682772284	-0.20506993904833	-0.72727580866982
H	-2.39066746197458	-0.22908610045900	-0.20629387218170
H	2.55694181542461	-1.78215642828828	2.14977624449640
H	3.95154939688801	-1.25285806376804	3.07893561253337
H	4.14378896957011	-1.72772218486588	1.39723488112837
H	2.52965794543126	1.47421846238915	3.78779032574317
H	1.11438836652029	0.84080476478483	2.97393962954781
H	1.75742589669406	2.41025115542347	2.51778524954198
H	4.78076020026759	2.52406621829991	1.35452913777312
H	5.56544834123039	1.01598966968578	0.90501671630198
H	5.29545921369576	1.39874816178354	2.60087011740203
H	2.15684621192417	4.58534563446575	-0.67565688954427
H	2.89997340320237	3.81851925939000	0.71741063415831
H	1.17820273039104	3.62324793778323	0.41989841626997
H	1.38491380287871	3.04254687516030	-3.19153782218664
H	0.23303986995227	2.13921779116470	-2.22325404284323
H	1.41468010385553	1.29059107803957	-3.21731496769897
H	4.29172295988598	3.26288816075629	-2.50394723052614
H	4.46405874138028	1.51491693920341	-2.55841704467156
H	5.01406310401158	2.40739883079090	-1.14718675989047
H	-4.65456401953644	-0.01096868427250	-0.48360354530546
H	-4.53128762944661	4.78466782481834	0.64747205922827
H	-6.74095617243792	1.29115674423480	-0.45481500172311
H	-6.68836959487230	3.70116123472977	0.11085796746091
H	-2.45350527876871	3.48972298815075	0.62320741608429

FINAL SINGLE POINT ENERGY −2262.420164596219 E_h
Total correction 0.66453990 E_h 417.00 kcal/mol
Thermal Enthalpy correction 0.00094421 E_h 0.59 kcal/mol

6: 15.19 cm^{-1}
7: 18.25 cm^{-1}
8: 23.07 cm^{-1}
9: 28.22 cm^{-1}
10: 34.09 cm^{-1}
11: 43.95 cm^{-1}
12: 56.62 cm^{-1}

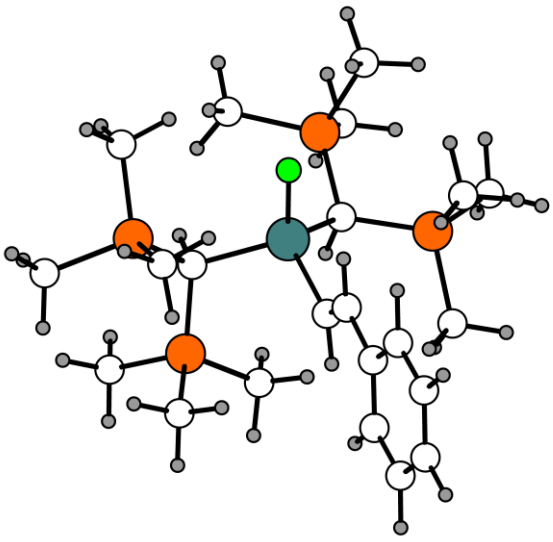

Figure S190 Molecular structure of (*E*)-bis(bis(trimethylsilyl)methyl)fluoro(styryl)aluminate obtained from geometry optimization at the PBEh-3c/def2-mSVP level of theory.

Table S30 Cartesian coordinates, single point energy, total energy correction, thermal enthalpy correction and the lowest six vibrational frequencies of (*E*)-bis(bis(trimethylsilyl)methyl)fluoro(styryl)aluminate obtained from geometry optimization at the PBEh-3c/def2-mSVP level of theory.

73

Coordinates from ORCA-job maxi_albis2_chchph_f-_pbeh-3c_def2-msvp

C	-6.63553052904528	-0.62653255590969	-0.02772608103228
C	-6.11142709912528	-0.89418242926174	1.22767455259776
C	-4.74530501875395	-0.80603003444768	1.44613475440980
C	-3.86040308498483	-0.45481033689377	0.42377115617953
C	-4.40946828790418	-0.18175550252212	-0.83330823961602
C	-5.77209180177799	-0.26733201166170	-1.05580052639705
C	-2.41959354091089	-0.38373282508582	0.70680983626833
C	-1.42040282483508	-0.20013364165338	-0.16806697648983
Al	0.51737906751574	-0.04065459155887	0.34171069767551
C	1.14467237471172	1.82435719075978	-0.16795204541892
Si	0.51553731928770	2.33356919938525	-1.83965520483043
C	-1.24798953057652	3.02678967735935	-1.78333000560654
C	1.70411105524118	-1.46334784114079	-0.49802098779501
Si	3.32631094835676	-1.62258557402764	0.40124078222778
C	4.07197066860848	0.03456018581863	0.94331048399072
Si	0.77662465961990	-3.06589069750717	-0.71223863688431
C	-0.42800131363992	-2.95092931348547	-2.17191234368813
C	1.88291644781908	-4.56729360007264	-1.11422874707149
C	-0.21351803511923	-3.55189535084955	0.82418267566891
C	4.67822251026741	-2.40260547221049	-0.69144779421007
C	3.18144314536608	-2.66305083231075	1.97734283048036
F	0.57670997773794	-0.25447822064436	2.03595227370937
Si	0.80741576857467	3.03235207313740	1.21131385684361
C	1.97800507073470	2.75794799853768	2.67639654324043
C	-0.95921780323639	2.91413388758592	1.87742047933754
C	1.07527288879516	4.85779489123641	0.72082355200435
C	0.52441886565682	0.91698316363026	-3.10625375001454
C	1.60931371995619	3.66940254145087	-2.64176112538591
H	1.93864529090629	-1.09782903390886	-1.50966903324686
H	2.46853356923496	-4.40573630878431	-2.02149067398310
H	1.27302658614983	-5.46052317251952	-1.27035988295781
H	2.58572112046382	-4.79077746791717	-0.30981572096147
H	-0.65521561342446	-4.54432183285118	0.70617085356046
H	-1.02409954814734	-2.84469983672749	0.99844931138363
H	0.40563381312414	-3.56618642389036	1.72190802562343
H	-1.22064930307142	-2.23015820508638	-1.97069275310620
H	-0.90391746867936	-3.91428312874700	-2.36896097389357
H	0.08094175112713	-2.64126629136970	-3.08734599910625
H	5.63249958026520	-2.45186464919146	-0.16124452220382
H	4.83908543860379	-1.80720767936586	-1.59318859388421
H	4.42672759762821	-3.41336154106318	-1.01295006671652
H	4.12534445822628	-2.67122795097874	2.52700406149626
H	2.91013168463036	-3.70145252148192	1.77851129243142
H	2.41685606724948	-2.24031730882183	2.63021858498540
H	4.22560823051573	0.71406747230515	0.10273729655598
H	5.04487252032586	-0.12533091010982	1.41522874410299
H	3.43535931636524	0.54605118305971	1.66469731549167
H	-1.73705187359983	-0.09536515457863	-1.21000848535702
H	2.23818182737336	1.75704475358943	-0.26560291279402
H	-2.17410534831608	-0.50894055836084	1.76062084397713
H	-1.71390215222051	3.02409707358393	1.09827376469806
H	-1.13959036903446	3.69010176185749	2.62576376864117
H	-1.12897148049697	1.94772551627760	2.35163139829545
H	0.93068504786571	5.51039703751118	1.58551724940082
H	0.38749269026398	5.19432470571449	-0.05743465366197
H	2.08960388615134	5.02630927086684	0.35234351300217
H	3.02420358123313	2.88437873110402	2.39003416444433
H	1.86012503035676	1.75229761035763	3.07882585204633
H	1.76940909489103	3.46885512857883	3.47947042897350
H	1.53963582222099	0.55349404470102	-3.27962492047680
H	0.13427498156005	1.25842837688600	-4.06823501256961
H	-0.07257096443106	0.05919630691660	-2.79468116672701
H	2.64599164654649	3.33164207684144	-2.70995761829012

H	1.60957230873218	4.60004258541000	-2.07334976356397
H	1.27617078973299	3.90057148152217	-3.65648231960928
H	-1.30279590167064	3.93370748669601	-1.17858673879627
H	-1.94658955653096	2.30986898333438	-1.34954633478127
H	-1.60397032949431	3.27931612983684	-2.78456785270731
H	-3.75718270908289	0.10805104629964	-1.64760171425721
H	-6.76853460444429	-1.17261906957902	2.04239041350288
H	-6.16659535435297	-0.04782497601441	-2.04039237346038
H	-7.70158509613247	-0.69229217850591	-0.20413121851653
H	-4.34559454355436	-1.01707526505474	2.43128798882205

FINAL SINGLE POINT ENERGY	−2362.238018592796 E_h	
Total correction	0.66732343 E_h	418.75 kcal/mol
Thermal Enthalpy correction	0.00094421 E_h	0.59 kcal/mol

6:	9.87 cm^{-1}
7:	19.64 cm^{-1}
8:	21.12 cm^{-1}
9:	35.17 cm^{-1}
10:	41.09 cm^{-1}
11:	51.24 cm^{-1}
12:	64.70 cm^{-1}

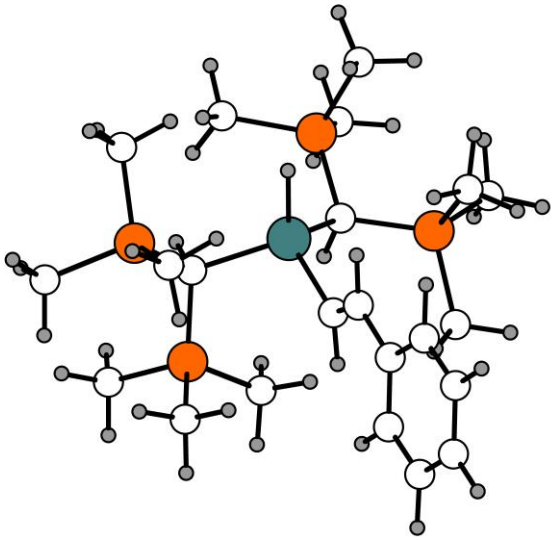

Figure S191 Molecular structure of (*E*)-bis(bis(trimethylsilyl)methyl)(styryl)aluminumhydride obtained from geometry optimization at the PBEh-3c/def2-mSVP level of theory.

Table S31 Cartesian coordinates, single point energy, total energy correction, thermal enthalpy correction and the lowest six vibrational frequencies of (*E*)-bis(bis(trimethylsilyl)methyl)(styryl)aluminiumhydride obtained from geometry optimization at the PBEh-3c/def2-mSVP level of theory.

73
Coordinates from ORCA-job maxi_albis2_chchph_h-_pbeh-3c_def2-msvp

C	6.56970168233806	-0.73117179052531	0.21461711498008
C	5.67879786796374	-0.24284768899732	1.16280990618263
C	4.33186671632791	-0.12661406269241	0.86921615249626
C	3.82714401973441	-0.49797104677308	-0.38134127899311
C	4.74006786082168	-0.97609731046199	-1.32477069218973
C	6.09012660937126	-1.09638928179855	-1.03396277714640
C	2.40327691560791	-0.40174875455142	-0.73396925094454
C	1.37146294836483	-0.16508278502975	0.08807543860125
Al	-0.55155635995693	-0.01442509650596	-0.49088471755839
C	-1.20340227999826	1.85307073048269	0.05727641457544
Si	-0.59213142644045	2.36702991113030	1.73258717994078
C	1.16941218922491	3.07110246312260	1.68708931323574
C	-1.72937285421499	-1.46176322688287	0.36269664642643
Si	-3.31564944914753	-1.65427832135353	-0.58745772982604
C	-4.09473143428024	-0.00232806324259	-1.09914059769926
Si	-0.77344941758525	-3.04010159456874	0.61528640120848
C	-1.85360457564386	-4.55226667750678	1.04812325690972
C	0.20895748269426	-3.56195987785375	-0.91910475597708
C	0.43064524367515	-2.87497555245249	2.07104183555582
C	-4.68742033250570	-2.51796735123328	0.41469780388100
C	-3.05741567732013	-2.63948395452071	-2.18524384674208
H	-0.59088589894422	-0.19400052999823	-2.10755183275063
Si	-0.84774865157882	3.04222849749179	-1.33073383289171
C	-1.98168381141018	2.71708269252905	-2.81600176409604
C	0.93215865251796	2.91616364014532	-1.96303720704989
C	-1.13442127175710	4.87576368542080	-0.88534092501375
C	-0.60626097652751	0.95226151580512	3.00150071469618
C	-1.69434605059035	3.70801557858477	2.51758076834839
H	-1.99333316192171	-1.09080380672235	1.36521153765499
H	0.98412684524940	-4.28505706183103	-0.65565676288741
H	0.70121496942522	-2.71124140932551	-1.38966712389745
H	-0.43212476957782	-4.02406616339015	-1.67173760342213
H	-0.07749825870368	-2.51223327898139	2.96726025646572
H	1.23862417772256	-2.18056431952186	1.84255783708960
H	0.88396416057984	-3.83778280208554	2.31800378207648
H	-2.46128921178793	-4.37332522467800	1.93754548516275
H	-1.23448711704412	-5.43158336437800	1.24107869184257
H	-2.53738123775433	-4.80780091552950	0.23639313636370
H	-4.42189340412912	-3.53406711887296	0.70604076976572
H	-5.61781379550149	-2.56937018974622	-0.15628308925253
H	-4.90198093766905	-1.96587501925923	1.33278176466737
H	-2.23755272639057	-2.20225702279794	-2.75773156073836
H	-3.95216231472203	-2.61819829003158	-2.81085165143379
H	-2.80935586538612	-3.68641168163055	-1.99987216239982
H	-4.33885404030526	0.61751417950988	-0.23375850323863
H	-5.02309856727296	-0.17254485496173	-1.65005470388895
H	-3.43175124075033	0.57864824976849	-1.74004901694241
H	1.64648901021814	-0.03290872381650	1.13883756423433
H	-2.29786132912567	1.77963307222707	0.13692610944327
H	2.20250632254869	-0.56224123249219	-1.79325372472661
H	1.11859834346988	1.93264858236259	-2.39609979620308
H	1.67441177716305	3.06202802671127	-1.17797705809923
H	1.11804863483184	3.66354783801682	-2.73857880901853
H	-0.97306764433770	5.51937739412903	-1.75340053592267
H	-0.46910178045207	5.22498129603003	-0.09316118871466
H	-2.15803882285042	5.04163782057463	-0.54172565517676
H	-3.03457110193997	2.86718029189060	-2.56837152736646
H	-1.86362382665157	1.69003570372454	-3.16377049975264
H	-1.74111693688528	3.38336775378703	-3.64766855897388
H	-0.00602217099295	0.09711107840741	2.68879033318019
H	-1.62156594347771	0.58458676158427	3.16521290016973
H	-0.22293282388561	1.28877493715426	3.96773685996935
H	-2.73211552848383	3.37192476511709	2.57624639583461

H	-1.68842413990569	4.63462644842154	1.94229402130156
H	-1.37259816201284	3.94678551092991	3.53413604692042
H	1.21766980487017	3.99385410336359	1.10580737429586
H	1.87080073290785	2.36961220071877	1.23296061281425
H	1.52947481762819	3.29961845854567	2.69267638495727
H	4.37499416835566	-1.26439259804155	-2.30383076356211
H	6.03931249611280	0.05545055965037	2.13965923058342
H	6.77011690474332	-1.47592351001322	-1.78672003347221
H	7.62330367781190	-0.82087023191118	0.44660766720100
H	3.65690770693879	0.26684875402965	1.61888750733664

FINAL SINGLE POINT ENERGY −2263.076430544720 E_h
Total correction 0.67030138 E_h 420.62 kcal/mol
Thermal Enthalpy correction 0.00094421 E_h 0.59 kcal/mol

6: 12.99 cm^{-1}
7: 18.91 cm^{-1}
8: 20.36 cm^{-1}
9: 35.46 cm^{-1}
10: 39.96 cm^{-1}
11: 42.97 cm^{-1}
12: 55.20 cm^{-1}

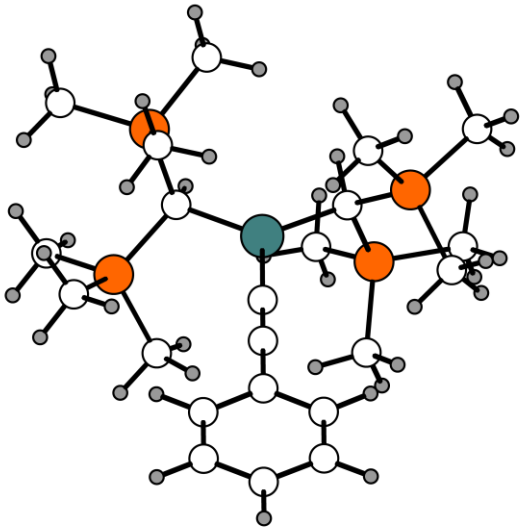

Figure S192 Molecular structure of bis(bis(trimethylsilyl)methyl)(phenylethynyl)aluminum obtained from geometry optimization at the PBEh-3c/def2-mSVP level of theory.

Table S32 Cartesian coordinates, single point energy, total energy correction, thermal enthalpy correction and the lowest six vibrational frequencies of bis(bis(trimethylsilyl)methyl)(phenylethynyl)aluminum obtained from geometry optimization at the PBEh-3c/def2-mSVP level of theory.

70
Coordinates from ORCA-job maxi_albis2_ccph_pbeh-3c_def2-msvp

C	-6.63542515803470	0.05918845880718	0.00388860289298
C	-5.92870024514266	1.25118176958878	-0.07604965426660
C	-4.54483228725981	1.24098470656793	-0.07645346634668
C	-3.85006979313782	0.03137225625404	0.00300165232611
C	-4.56873713819044	-1.16408699788862	0.08296700349248
C	-5.95254016803596	-1.14666607254919	0.08345722094651
C	-2.42806779473523	0.01754962985181	0.00229565934588
C	-1.21147321488088	0.00613204050409	0.00201492804425
Al	0.70151083052263	-0.00703907541578	-0.00006781802496
C	1.61823833155073	-1.71930360274209	0.09605157089009
Si	1.88479045317155	-2.37008905856203	-1.64859998917517
C	2.50190739777753	-4.15367223942220	-1.69130538273305
C	1.63927917104459	1.69374656188305	-0.09710485285577
Si	0.82667524383427	2.87285239688261	-1.31702073788075
C	2.06664608018753	4.16322434056571	-1.92250955536803
Si	1.91595687701057	2.34168993960075	1.64694179515656
C	3.20571241489416	1.23488019004764	2.47672524222168
C	2.56067207636276	4.11564653090162	1.68641564066622
C	0.32594641443824	2.26220436487063	2.66319193414496
C	-0.65986318120749	3.74562581551542	-0.55013967331497
C	0.23439308347152	1.92360491411583	-2.84408092332222
Si	0.79170736605697	-2.88937047799016	1.31528953569665
C	-0.70536329051502	-3.74339335135961	0.54786510557439
C	0.21233567640840	-1.93419095268601	2.84366223348641
C	2.01559687049397	-4.19627643129616	1.91810302036798
C	0.29618937080708	-2.26454009919701	-2.66468007323293
C	3.19061074494618	-1.28258961834253	-2.47859465084686
H	2.64335880364051	1.46564608693405	-0.48773656140940
H	1.83214376497830	4.83059649343635	1.30114293534728
H	3.46943143371643	4.22335611329694	1.09228942914999
H	2.79942432088896	4.41634624542622	2.70835158964435
H	0.50012829734493	2.63530587646668	3.67452084558304
H	-0.06499922126745	1.24687340664477	2.76652569673395
H	-0.47296548259079	2.86281865291375	2.22704172279250
H	2.89017497861699	0.18890972918567	2.50100476248194
H	3.39380452622419	1.53761648510503	3.50832862983366
H	4.16013577250746	1.26878847638456	1.94813559080757
H	-1.39032140007481	3.02460124496440	-0.17911185313191
H	-1.16132937332311	4.37540561472909	-1.28737530640453
H	-0.37710799108306	4.38866694332584	0.28502635672870
H	-0.13931126182990	2.60535222433890	-3.61092288181419
H	-0.58092097607201	1.23378045106373	-2.61307612140695
H	1.04181455789257	1.34619092981121	-3.30125201193366
H	2.40263338723630	4.82364625651105	-1.12292463355648
H	1.62632644611812	4.78919585304353	-2.70110015439704
H	2.95273722864028	3.69050341936098	-2.35009522909005
H	2.62498950728434	-1.50249758470047	0.48624772196170
H	-0.59535708603583	-1.23461208787822	2.61507940070950
H	1.02744992762299	-1.36646611774831	3.29930478849671
H	-0.16767298982352	-2.61183428664717	3.61107002876158
H	2.34153871480066	-4.85991941429948	1.11704661586554
H	1.56811459201135	-4.81765453623017	2.69633566074893
H	2.90865935288792	-3.73650980338473	2.34527337839219
H	-1.21587643493285	-4.36518216147482	1.28567706355356
H	-0.43070425492794	-4.39172762386495	-0.28594011375832
H	-1.42590325032283	-3.01320287055002	0.17534837705926
H	-0.51382107876084	-2.84894578129130	-2.22695998665455
H	0.46341550929353	-2.64342059558260	-3.67503007189908
H	-0.07552231430394	-1.24230069128164	-2.77094284920491
H	4.14356269235615	-1.32751802151926	-1.94817420783414
H	2.88876100240501	-0.23266184608628	-2.50608870726151
H	3.37647736868941	-1.59035528862073	-3.50910620770803
H	3.41043968284851	-4.27677950007121	-1.09979370798417

H	2.73333735990569	-4.45618478069414	-2.71439511613432
H	1.76341383502922	-4.85806641347480	-1.30556531417715
H	-3.98961940565592	2.16741863151748	-0.13922836674823
H	-6.50075973295528	-2.07722505154592	0.14583342146779
H	-4.03206507662295	-2.10139140470121	0.14530133290546
H	-7.71729234244987	0.07004774790788	0.00424088871188
H	-6.45825172774554	2.19251315787360	-0.13804517501361

FINAL SINGLE POINT ENERGY −2261.190978987607 E_h
Total correction 0.64096482 E_h 402.21 kcal/mol
Thermal Enthalpy correction 0.00094421 E_h 0.59 kcal/mol

6: 13.79 cm^{-1}
7: 15.52 cm^{-1}
8: 18.84 cm^{-1}
9: 25.60 cm^{-1}
10: 35.95 cm^{-1}
11: 38.49 cm^{-1}
12: 50.00 cm^{-1}

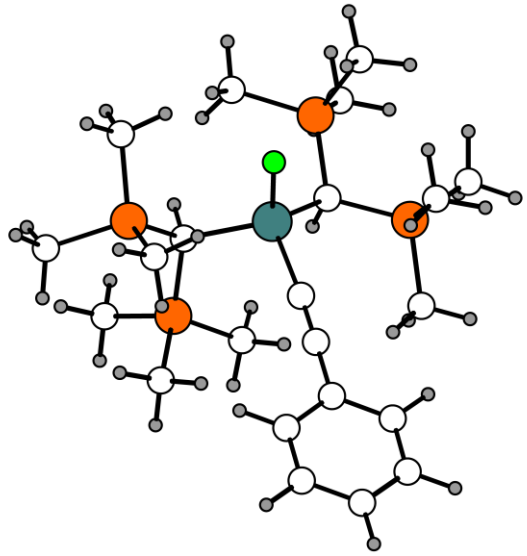

Figure S193 Molecular structure of bis(bis(trimethylsilyl)methyl)fluoro(phenylethynyl)aluminate obtained from geometry optimization at the PBEh-3c/def2-mSVP level of theory.

Table S33 Cartesian coordinates, single point energy, total energy correction, thermal enthalpy correction and the lowest six vibrational frequencies of bis(bis(trimethylsilyl)methyl)fluoro(phenylethynyl)aluminate obtained from geometry optimization at the PBEh-3c/def2-mSVP level of theory.

71

Coordinates from ORCA-job maxi_albis2_ccph_f-_pbeh-3c_def2-msvp

C	6.82165702192241	-1.06206937894132	-0.46876949839830
C	5.99007028233613	-2.16076397090215	-0.29849292512236
C	4.61391150039550	-2.00818560183632	-0.31873798191274
C	4.03862902559939	-0.74757090083583	-0.51091404118995
C	4.88707192279261	0.35218005691475	-0.68092806902290
C	6.26213175913794	0.19421250400113	-0.65955205393642
C	2.62795009423347	-0.57926222477091	-0.53346659048824
C	1.42162680947334	-0.40962193932893	-0.54791944103340
Al	-0.52463609164310	-0.01277892984987	-0.59547495044892
C	-0.76775163928674	1.83666343394199	0.17657470640351
Si	-0.46947031455072	3.13451001849751	-1.12816495181094
C	1.13821255269097	2.83654663474077	-2.07942659904418
C	-1.63845732204971	-1.41578310063776	0.33588649807290
Si	-3.40752203074545	-1.34427533013839	-0.24185429202025
C	-4.59859881593023	-2.09209972728222	1.04261531446104
Si	-0.84871689626853	-3.10148210143502	0.23095639081071
C	0.59021184709010	-3.23602419459925	1.45462393285658
C	-2.01568759700840	-4.53980534885170	0.68852613409262
C	-0.19757913161614	-3.49169497974532	-1.50216878407410
C	-3.68095109762811	-2.25462305912408	-1.88087653858345
C	-4.05371479869698	0.42018206885498	-0.50425609158568
F	-0.95477866678604	-0.03026257415041	-2.24124066778887
Si	0.16215217254766	2.09258308950432	1.76752033918558
C	-0.67126666025793	3.43055081974934	2.83509465148233
C	1.96708366186767	2.60513966448601	1.50699658076212
C	0.19823876599751	0.54564250069096	2.86480762704713
C	-1.89105847504161	3.19327037556785	-2.37824804639884
C	-0.37653335788369	4.91091749234931	-0.43841018201508
H	-1.64380890413574	-1.14305461348210	1.40158090570145
H	-1.48255355558618	-5.49287843916665	0.64497051982683
H	-2.87008347806024	-4.61509731915823	0.01404266742282
H	-2.40901406012685	-4.43190244489793	1.70147107015802
H	0.17220076161440	-4.51852859198849	-1.55786458031784
H	0.62195584320900	-2.82663478692160	-1.77708413440364
H	-0.97387021930014	-3.37594162852303	-2.25961373198951
H	1.36676611306248	-2.50752036891269	1.22023541751514
H	1.04103215602586	-4.23116353984798	1.43157421150382
H	0.25943565626167	-3.04901904558183	2.47856211516608
H	-4.70986484446494	-2.12988663148672	-2.22593433367049
H	-3.48893530771730	-3.32643099293924	-1.81073146278132
H	-3.02035112780457	-1.84869994561013	-2.64814046074271
H	-3.99408565586216	1.01564705713258	0.40904327871027
H	-5.10342790538472	0.39595042151776	-0.80790323540567
H	-3.49808551094828	0.94877847122497	-1.27913896134433
H	-5.63717323473055	-2.01163507090901	0.71235954369467
H	-4.52053646143258	-1.56693201851845	1.99725238674629
H	-4.39482136172742	-3.14564347961302	1.23579752632289
H	-1.83463722271275	1.90172696473716	0.43930834457810
H	2.06308110902530	3.54122560149046	0.95484936369076
H	2.49666983468080	1.83211612008727	0.94890958075654
H	2.47609446930595	2.73316841136575	2.46482577775433
H	0.72008439796489	0.74867864407591	3.80332195695763
H	0.70989463959572	-0.28564185036545	2.37744259688108
H	-0.80881691815475	0.20853437900734	3.11858244446229
H	-0.16913437101137	3.54705919664156	3.79853186898636
H	-1.71124236433144	3.16655785980017	3.04061013980226
H	-0.67651975698061	4.40471168046145	2.34503243418155
H	-1.97191975164197	2.25153073326849	-2.91985493231734
H	-1.73998123531463	3.99318678318138	-3.10695135229486
H	-2.84748492379970	3.37721857897024	-1.88360944377018
H	0.44493787801220	5.05482746596525	0.26536557613437
H	-1.29887237354782	5.18016590232551	0.08110300552990
H	-0.23920128913021	5.63082053327679	-1.24923742289994

H	1.34401810459138	3.65789283968113	-2.77018223270804
H	1.08452646733114	1.91512286359298	-2.65982169964194
H	1.99329762879823	2.73967745492887	-1.40935348012682
H	3.96421147702737	-2.86329795933976	-0.18601483181546
H	6.90117012233777	1.05794237324576	-0.79347834878827
H	7.89714254083896	-1.18406555642440	-0.45325640045065
H	6.41667562987476	-3.14469448021643	-0.14930062150870
H	4.44900258365775	1.33003263105492	-0.83200153580562

FINAL SINGLE POINT ENERGY −2361.012471471899 E_h
Total correction 0.64406470 E_h 404.16 kcal/mol
Thermal Enthalpy correction 0.00094421 E_h 0.59 kcal/mol

6: 12.72 cm^{-1}
7: 18.31 cm^{-1}
8: 22.60 cm^{-1}
9: 33.32 cm^{-1}
10: 41.79 cm^{-1}
11: 45.99 cm^{-1}
12: 63.33 cm^{-1}

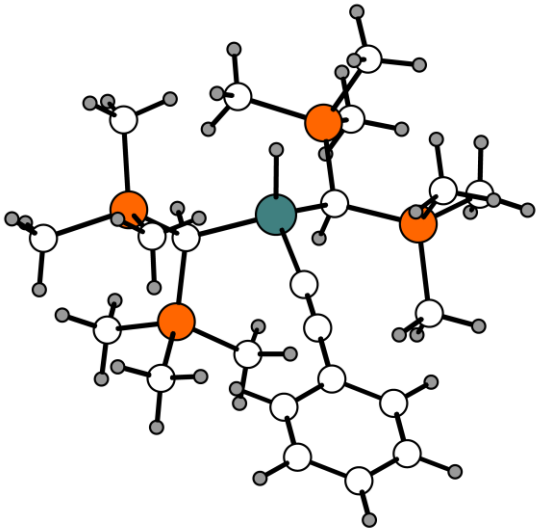

Figure S194 Molecular structure of bis(bis(trimethylsilyl)methyl)(phenylethynyl)aluminumhydride obtained from geometry optimization at the PBEh-3c/def2-mSVP level of theory.

Table S34 Cartesian coordinates, single point energy, total energy correction, thermal enthalpy correction and the lowest six vibrational frequencies of bis(bis(trimethylsilyl)methyl)(phenylethynyl)aluminiumhydride obtained from geometry optimization at the PBEh-3c/def2-mSVP level of theory.

71
Coordinates from ORCA-job maxi_albis2_ccph_h-_pbeh-3c_def2-msvp

C	-6.62018143845424	0.91914855869196	-0.17517354092087
C	-6.04621139857912	-0.32271351293040	-0.41200640441892
C	-4.67127467374027	-0.45230965934137	-0.50536263687307
C	-3.83586269965688	0.66164026628071	-0.36214187597805
C	-4.42602176370372	1.90759116851383	-0.12341637108469
C	-5.80213912800670	2.03169997196919	-0.03152787003294
C	-2.42495219498480	0.52008564651784	-0.45071152587830
C	-1.21691938127254	0.36676222550454	-0.50748156054176
Al	0.73208332992922	-0.01597444954449	-0.63166833618657
C	0.99018054170998	-1.87000589439552	0.16601157289707
Si	0.67723613376338	-3.14525840477830	-1.15266400863378
C	-0.96093439910775	-2.86006217448880	-2.05492668835284
C	1.84128736089330	1.38172488106189	0.34648236820182
Si	3.59854621478824	1.33651208889509	-0.25948418756097
C	4.81965941292051	2.08271178077592	0.99705958544444
Si	1.03472288187999	3.06009269992402	0.29017328422041
C	0.35132973987792	3.47565845316262	-1.42577465893079
C	-0.38477713780421	3.15965700982723	1.53964312357652
C	2.19542701459973	4.50360216934124	0.74966199338390

C	3.81621785058562	2.26366107503795	-1.89908984758341
C	4.24940643427218	-0.42062767226216	-0.56164752310924
H	1.12502516577491	0.00574301229382	-2.20446019110698
Si	0.09011643488495	-2.14241269419142	1.76984129844616
C	0.95422805413737	-3.48411180113016	2.80981274580836
C	-1.71268660083912	-2.67637678597702	1.53435771029298
C	0.05361115921695	-0.60984269946250	2.88545534018381
C	2.05939101110953	-3.12578398008845	-2.44852311432275
C	0.63366399807039	-4.93930530350925	-0.50718492463987
H	1.85385996943945	1.07575002978130	1.40272176244829
H	-0.84534368005225	4.15061553470486	1.54216494359301
H	-0.03622766568391	2.95664762861816	2.55453230393681
H	-1.15774385236670	2.42796210699331	1.30323085879655
H	1.64820333667964	5.44971140236269	0.74792635748445
H	3.02650437947425	4.60871683756303	0.05029715822208
H	2.62226892054468	4.37448993252682	1.74636119931016
H	-0.45581424873241	2.79675921768273	-1.70436586143946
H	1.12088827019385	3.39582575207126	-2.19476307158545
H	-0.04359835145656	4.49418975285604	-1.45424786093640
H	3.12104296817646	1.87347394387998	-2.64473081332109
H	4.82898681650541	2.13481757690838	-2.28724466200167
H	3.63569483911160	3.33592564109207	-1.80777126007647
H	4.21685325083112	-1.02656527986067	0.34603544474805
H	5.28939244724788	-0.38940862158833	-0.89624418770771
H	3.67212332836338	-0.94336148493533	-1.32533191596332
H	5.85035524015094	2.00255937591244	0.64292449589136
H	4.76299310471619	1.55632910084571	1.95248894632573
H	4.61967357257898	3.13582804843625	1.19612215376109
H	2.06340972992825	-1.92743288198482	0.40261447620643
H	-2.25771707304613	-1.91181616121738	0.97972322361476
H	-2.20802268953943	-2.80534770374490	2.49930057387755
H	-1.80548070206251	-3.61680418638629	0.98882473382125
H	-0.46209125208366	-0.82697043393328	3.82425310233854
H	-0.46400058481683	0.22369591700885	2.40893119466825
H	1.06043068073467	-0.27104778429691	3.13787694480886
H	0.99050082565462	-4.44381001767603	2.29278148130754
H	0.45012041687590	-3.64216656145765	3.76637261510593
H	1.98505794641426	-3.19640003348530	3.02944494304848
H	1.88344066512245	-3.87203290304595	-3.22675270697325
H	3.03115387518588	-3.34230226782210	-1.99902441387353
H	2.12384814533813	-2.14725215238949	-2.92574739619335
H	1.57157788692731	-5.20580149431779	-0.01486672542546
H	0.48482935922828	-5.64521751603060	-1.32811214092954
H	-0.16818195433128	-5.10638776003752	0.21415236777336
H	-1.12026141520256	-3.61850575845822	-2.82524332608159
H	-0.98142648415236	-1.88145054737832	-2.53604292936374
H	-1.81055244078647	-2.89537692755019	-1.37159047341453
H	-4.22271378233481	-1.41943010625883	-0.69089150520340
H	-6.23963349651864	3.00456750322030	0.15456886902568
H	-7.69560984205180	1.01894816061729	-0.10233296881869
H	-6.67400923584661	-1.19775226604745	-0.52457391287781
H	-3.78752527262358	2.77376343212403	-0.00925449632724

FINAL SINGLE POINT ENERGY		−2261.851713871672 E_h	
Total correction		0.64716495 E_h	406.10 kcal/mol
Thermal Enthalpy correction	...	0.00094421 E_h	0.59 kcal/mol

7:	18.18 cm^{-1}
8:	24.32 cm^{-1}
9:	34.17 cm^{-1}
10:	41.29 cm^{-1}
11:	45.11 cm^{-1}
12:	63.16 cm^{-1}

References

1 C. Sánchez-Sánchez, A. Nicolaï, F. Rossel, J. Cai, J. Liu, X. Feng, K. Müllen, P. Ruffieux, R. Fasel and V. Meunier, *J. Am. Chem. Soc.*, 2017, **139**, 17617–17623.
2 M. G. Moloney, Ed., *Category 1, Organometallics: Compounds of Group 14 (Ge, Sn, Pb)*, Georg Thieme Verlag, Stuttgart, 2003.
3 T. Chen and K. Altmann, *Chem. – Eur. J.*, 2015, **21**, 8403–8407.
4 W. Uhl, L. Cuypers, R. Graupner, J. Molter, A. Vester and B. Neumüller, *Z. Anorg. Allg. Chem.*, 2001, **627**, 607–614.
5 M. Zaidlewicz, in *Encyclopedia of Reagents for Organic Synthesis*, ed. John Wiley & Sons, Ltd, John Wiley & Sons, Ltd, Chichester, UK, 2001, p. rc089.
6 H. H. Karsch and A. Appelt, *Z. Naturforsch.*, 1983, **38B**, 1399–1405.
7 Y.-Y. Liu, J. Li, J.-F. Ma, J.-C. Ma and J. Yang, *CrystEngComm*, 2012, **14**, 169–177.
8 W. S. Price, H. Ide and Y. Arata, *J. Phys. Chem. A*, 1999, **103**, 448–450.
9 A. Macchioni, G. Ciancaleoni, C. Zuccaccia and D. Zuccaccia, *Chem. Soc. Rev.*, 2008, **37**, 479–489.
10 H. C. Chen and S. H. Chen, *J. Phys. Chem.*, 1984, **88**, 5118–5121.
11 O. V. Dolomanov, L. J. Bourhis, R. J. Gildea, J. A. K. Howard and H. Puschmann, *J. Appl. Crystallogr.*, 2009, **42**, 339–341.
12 G. M. Sheldrick, *Acta Crystallogr. Sect. C*, 2015, **71**, 3–8.
13 G. M. Sheldrick, *Acta Crystallogr. Sect. A*, 2008, **64**, 112–122.
14 L. J. Bourhis, O. V. Dolomanov, R. J. Gildea, J. A. K. Howard and H. Puschmann, *Acta Crystallogr. Sect. Found. Adv.*, 2015, **71**, 59–75.
15 P. Erdmann, J. Leitner, J. Schwarz and L. Greb, *ChemPhysChem*, 2020, **21**, 987–994.
16 P. Erdmann and L. Greb, *ChemPhysChem*, 2021, **22**, 935–943.
17 G. Schaftenaar, J. H. Noordik, *J. Comput.-Aided Mol. Des.* 2000, **14**, 123.
18 G. Schaftenaar, E. Vlieg, G. Vriend, *J. Comput.-Aided Mol. Des.* 2017, **31**, 789.
19 S. Grimme, C. Bannwarth, P. Shushkov, *J. Chem. Theory Comput.*, 2017, **13**, 1989–2009.
20 C. Bannwarth, S. Ehlert, S. Grimme, *J. Chem. Theory Comput.*, 2019, **15**, 1652–1671.
21 C. Bannwarth, E. Caldeweyher, S. Ehlert, A. Hansen, P. Pracht, J. Seibert, S. Spicher, S. Grimme, *Wiley Interdiscip. Rev.: Comput. Mol. Sci.* 2021, **11**, e1493.
22 S. Grimme, *J. Chem. Theory Comput.*, 2019, **15**, 2847–2862.
23 P. Pracht, F. Bohle, S. Grimme, *Phys. Chem. Chem. Phys.*, 2020, **22**, 7169–7192.
24 S. Grimme, J. G. Brandenburg, C. Bannwarth, A. Hansen, *J. Chem. Phys.* 2015, **143**, 54107.
25 H. Kruse, S. Grimme, *J. Chem. Phys.*, 2012, **136**, 154101.
26 S. Grimme, S. Ehrlich, L. Goerigk, *J. Comput. Chem.* 2011, **32**, 1456.
27 S. Grimme, J. Antony, S. Ehrlich, H. Krieg, *J. Chem. Phys.* 2010, **132**, 154104.
28 F. Weigend, *Phys. Chem. Chem. Phys.* 2006, **8**, 1057.
29 F. Neese, *Wiley Interdiscip. Rev. Comput. Mol. Sci.*, 2012, **2**, 73–78.
30 F. Neese, *Wiley Interdiscip. Rev. Comput. Mol. Sci.*, 2017, **8**, e1327.
31 F. Neese, F. Wennmohs, U. Becker, C. Riplinger, *J. Chem. Phys.*, 2020, **152**, 224108.
32 F. Neese, *Wiley Interdiscip. Rev.: Comput. Mol. Sci.*, 2022, **12**, e1606.
33 S. Kozuch, D. Gruzman, J. M. L. Martin, *J. Phys. Chem. C* 2010, **114**, 20801.
34 F. Weigend, R. Ahlrichs, *Phys. Chem. Chem. Phys.* 2005, **7**, 3297.
35 A. Hellweg, C. Hättig, S. Höfener, W. Klopper, *Theor. Chem. Acc.* 2007, **117**, 587.